Potential of human PON2 as an anti-Pseudomonal therapy

by

Naseem Mohammad Ali

School of Medicine

Submitted in fulfilment of the requirements for the

Doctor of Philosophy (Medical Studies)

University of Tasmania June, 2015

DECLARATION OF ORIGINALITY

This thesis contains no material which has been accepted for a degree or diploma by the University or any other institution, except by way of background information and duly acknowledged in the thesis, and to the best of my knowledge and belief no material previously published or written by another person except where due acknowledgement is made in the text of the thesis, nor does the thesis contain any material that infringes copyright.

Signature Date - 02/11/15

AUTHORITY OF ACCESS

This thesis may be made available for loan. Copying and communication of any part of this thesis is prohibited for two years from the date this statement was signed; after that time limited copying and communication is permitted in accordance with the Copyright Act 1968.

Signature Date - 02-11-15

STATEMENT OF ETHICAL CONDUCT

The research associated with this thesis abides by the international and Australian codes on human and animal experimentation, the guidelines by the Australian Government's Office of the Gene Technology Regulator and the rulings of the Safety, Ethics and Institutional Biosafety Committees of the University

ABSTRACT

Cystic Fibrosis (CF) is the most common life-limiting single gene disorder in Caucasian populations. CF results from mutations in the gene encoding the CF transmembrane conductance regulator (CFTR) protein, which leads to accumulation of thick and sticky mucus in the airways of people with CF, ultimately dampening immune clearance of potential respiratory pathogens. In fact, chronic airway infection by the opportunistic bacterial pathogen *Pseudomonas aeruginosa* is the major cause of mortality and morbidity in individuals with CF. The ability of *P. aeruginosa* to chronically infect the airways of people with CF stems, in part at least, from its remarkable capacity to grow as complex multi-cellular communities called biofilms, which offer protection from host immune responses and eradication by conventional antibiotics. Biofilm formation by *P. aeruginosa* is co-ordinated by a cell density-dependent signalling system called quorum sensing (QS). While *P. aeruginosa* has multiple QS systems, the major system involves the diffusible signalling molecule *N*-3-oxo-dodecanoyl-*L*-homoserine lactone (C12HSL). C12HSL not only acts an important biofilm signalling molecule but also regulates bacterial virulence factor production. In addition, C12HSL has gene modulatory and cytotoxic effects in host cells. Collectively, these properties have stimulated much research interest in developing novel antimicrobial therapies that specifically target QS.

The present study investigated the potential of using the human enzyme, Paraoxonase-2 (PON2), to target and inhibit biofilm formation by, and virulence of, *P. aeruginosa*. Human PON2 is usually produced intracellularly and has previously been demonstrated to have highly specific hydrolytic activity towards C12HSL, and thereby seems to represent an innate mechanism by which host cells might attempt to counter *P. aeruginosa* QS, and hence infection by this organism. Here, it was hypothesized that the virulence of, and biofilm-formation by, *P. aeruginosa* could be diminished by manipulating human PON2 (hPON2) levels, either by augmenting native PON2 expression, or by supplementing lactonase activity using a recombinant form of human PON2 (rhPON2) exogenously. Thus, the aim of the first part of this thesis was to determine the gene modulatory and cytotoxic effects of C12HSL on airway epithelia, and investigate the regulation of PON2 expression in mammalian cells. The second part of this thesis was aimed at producing rhPON2 and investigating whether exogenously supplied rhPON2 could disrupt *P. aeruginosa* QS, and thereby increase its susceptibility to the clinically relevant antibiotic tobramycin.

C12HSL was found to alter gene expression in cultured airway epithelial cells, even at low concentrations. This included the down-regulation of genes involved in immune signalling and the unfolded protein response. C12HSL also induced apoptosis and affected epithelial cell viability and metabolic activity in a concentration dependent manner. The results also show that while C12HSL itself did not significantly alter the expression of native *PON2* in airway epithelial cells, PON2 gene expression and PON2 protein levels rapidly increased in response to agonism of the major mammalian C12HSL receptor PPARγ; in turn, these results would seem to link the regulation of human PON2 to a known major regulator of the inflammatory response.

Recombinant hPON2 was able to hydrolyse almost all detectable C12HSL produced in *P. aeruginosa* cultures with no effect on bacterial growth. Treatment of *P. aeruginosa* cultures with rhPON2 tended to decrease expression of all three *P. aeruginosa* QS systems and associated virulence genes. Importantly, rhPON2-dependent hydrolysis of C12HSL during bacterial growth, significantly increased the susceptibility of *P. aeruginosa* cells to the bactericidal effects of the antibiotic tobramycin. In contrast, treatment of *P. aeruginosa* with rhPON2 combined with a high concentration of tobramycin, whilst hydrolysing the C12HSL and increasing bacterial killing by over an order of magnitude, significantly up-regulated the expression levels of a number of important QS and QS-dependent virulence genes of *P. aeruginosa* including, *lasI, lasB* and *algD.* One interpretation of this result is that bacterial cells treated with this combination up-regulate *lasI,* the gene that catalyses C12HSL synthesis, and other virulence encoding genes, presumably due to antibiotic-induced stress, via a C12HSL-independent mechanism.

Taken together, the results of this thesis demonstrate that low-level C12HSL can influence gene expression in human airway cells, and reveal for the first time that native human PON2 expression is regulated via a major mammalian C12HSL receptor. In addition, rhPON2-treatment of *P. aeruginosa* leads to reduction of C12HSL levels and the reduction of bacterial virulence gene expression. The efficacy of rhPON2 in conjunction with antibiotics however, requires further investigation, using lower-concentrations (clinically achievable levels) of antibiotic and antibiotics with alternative mechanisms of action. The results of this thesis strongly support rhON2 being a novel and useful anti-Pseudomonal therapy.

ACKNOWLEDGEMENTS

Firstly, I would like to extend my deepest thanks and gratitude to my supervisory team. They have been the most knowledge, inspiring, insightful and caring team I could have asked for. They have nurtured my growth as a scientist and as a person, providing support beyond what I expected. It was a privilege to work with them. This thesis is as much a testament to their efforts as it is to mine.

I thank my supervisor Louise Roddam for all the help and guidance over the last five to six years. I also thank her for accepting me as a PhD. student, it has been a pleasure and a distinct highlight of my life so far. Her ability to impart wisdom and calm my nerves has been instrumental in helping me to complete this work. I thank my co-supervisors Margaret Cooley, Phoebe Griffin and Mark Ambrose for being available to give advice whenever required, provide an outlet for intellectual debate and their insightful input into my research.

I would also like to thank all the members of the Host Pathogen Interactions group, past and present for their friendship over the years, particularly Joanne Pagnon and Emily Mulcahy. In addition, I need to thank my peers here at the University of Tasmania. I have made many life-long friends during my years as an honours and PhD. student, friendships that I will cherish for a very long time. I thank in particular, Cesar Tovar, Nick Blackburn, Stan Mitew and Emma Cazaly for sharing successes and failures and for the help and advice along the way. You guys, have made my PhD an amazing experience.

Importantly, I need to acknowledge the tireless contribution of my family. My parents and siblings for their support and most importantly my wife, Shahad, for her understanding, love, support and unwavering belief in me even when I found it hard to believe in myself.

I would like to thank the Clifford Craig Medical Research Trust and the Royal Hobart Hospital Research Foundation for funding these studies and finally, I want to acknowledge the Australian government for my IPRS scholarship and the Australian Cystic Fibrosis Research Trust for their studentship grant. Without these scholarships, this degree would not have been feasible for me.

TABLE OF CONTENTS

FIGURES

TABLES

COMMON ABBREVIATIONS

Table i List of commonly used abbreviations	
Abbreviation	**Full form**
µg	Micrograms
µL	Microliter
µM	Micromolar
AHL	Acyl homoserine lactone
C12HSL	*N*-3-oxo-dodecanoyl-*L*-Homoresine Lactone
C4HSl	*N*-butyryl-*L*-Homoserine Lactone
CCCM	Complete cell culture medium
cDNA	Complimentary deoxyribonucleic acid
CF	Cystic fibrosis
CFTR	Cystic fibrosis transmembrane conductance regulator
CFU	Colony forming units
C_T	Cycle threshold
DMEM	Dulbecco's modified eagle medium
DMSO	Dimethylsulfoxide
DNA	Deoxyribonucleic acid
DPBS	Dulbecco's phosphate buffered saline
EDTA	Ethylenediaminetetraacetic acid
ENac	Epithelial sodium channel
EPS	Exopolymeric substance
ER	Endoplasmic reticulum
FBS	Foetal bovine serum
FEV_1	Forced expiratory volume in one second
FITC	Fluorescein isothiocyanate
GW	GW9662
HCl	Hydrochloric acid
IL	interleukin
Kg	Kilogram
KO	Knockout
LB	Lysogeny broth
Log	Logarithmic
LPS	Lipopolysaccharide
MAPK	Mitogen-activated protein kinase
MCS	Multiple cloning site
mg	Milligrams
Mg	milligram
mL	Millilitre
mM	Millimolar
mRNA	Messenger ribonucleic acid
NaOH	Sodium hydroxide
NFκB	Nuclear factor -κB

Abbreviation	Full form
ng	Nanogram
NLR	Nod-like receptor
nM	Nanomolar
PBS	Phosphate buffered saline
PCR	Polymerase chain reaction
PFU	Plaque forming units
PI	Propidium iodide
Pio	Pioglitazone
PON	Paraoxonase
PPAR	Peroxisome proliferator activated receptor
PPRE	PPAR response element
PQS	*Pseudomonas* quinolone signal
qPCR	Quantitative polymerase chain reaction
QS	Quorum sensing
QSI	Quorum sensing inhibition
RG	Rosiglitazone
rhPON2	Recombinant human paraoxonase 2
RNA	Ribonucleic acid
ROS	Reactive oxygen species
RPM	Revolutions per minute
RT-qPCR	Reverse transcription-quantitative polymerase chain reaction
RXR	Retinoid x receptor
S.E.M	Standard error of mean
SDS	Sodium dodecyl sulphate
SDS-PAGE	Sodium dodecyl sulphate polyacrylamide gel electrophoresis
TE	Tris-EDTA buffer
TLR	Toll-like receptor
T3SS	Type three secretion systems
TZD	Thiazolidinediones
UPR	Unfolded protein response
wt	Wild-type
EPS	Exopolymeric substances

CHAPTER ONE – INTRODUCTION AND LITERATURE REVIEW

1.1 CYSTIC FIBROSIS, A LIFE LIMITING DISEASE

Cystic Fibrosis (CF) has been known as a distinct clinical entity since the 1930s and is now recognized as the most common life-limiting monogenic disorder in Caucasian individuals. An estimated 100,000 people globally are affected by CF. The incidence rate of CF varies between countries and people of different ethnicities (summarized in Table 1.1), but CF is most common among people of Northern European descent [1]. In Australia, the figure is approximately 1 in 2500 births. The disease is particularly relevant to Tasmania as Tasmania has the second highest incidence in the world, 1 in 1600 births, second only to Ireland [2, 3].

Table 1.1 Global CF incidence rates. Table shows the estimated incidence of CF in a number of countries, regions or among population demographics.

Country/Region/Population	Estimated Incidence Rate
Australia	1:2500 [4]
Tasmania	1:1600 [4]
People of North European descent	1:3000 [1]
USA	1:3500 [5]
UK	1:2,381 [3, 6]
Canada	1:3608 [7]
Ireland	1:1,353 [2, 3]
Japan	1:350,000 [8]
Sweden	1:5,600 [9]
Denmark	1:4,700 [10]
Finland	1:25,000 [10]
Spain	1:3,750 [11]
Italy	1:4,238 [12]
Greece	1:3,500 [11]
Saudi Arabia	1:4,300 [13]
Chile	1:3,500 [14]
Brazil	1:6,902 [15]
Mexico	1:8,500 [16]
African populations	1:15,000 [17]

CF is a multi-organ disease, primarily affecting the lungs, but also the liver, pancreas and intestine. While the disease severity varies from individual to individual, the average life expectancy of individuals with CF is considerably shorter than that of a healthy individual. Despite a remarkable improvement in life expectancy over the last two decades, a child born in the developed world after the year 2000 with CF is still only expected to live into his/her 50s [6, 18]. The treatment burden is also high for CF patients. They experience frequent hospitalizations because of periodic worsening of lung function (exacerbations) as a result of persistent lung infections. They typically need to take combinations of multiple antibiotics to manage infections and must participate in daily physiotherapy to ease chest congestion. The use of antibiotics has heralded the emergence of antibiotic-resistant strains, and the use of ever higher doses of, and more toxic, antibiotics. This has led to a call for

novel antimicrobial therapies. To this day, there is no cure for the disease, and though there are emerging therapies that small subsets of the CF population benefit from, these come at great financial cost to individuals and healthcare organizations.

Pulmonary failure, a consequence of persistent bacterial lung infections particularly with the Gram-negative pathogen *Pseudomonas aeruginosa*, accounts for 80% of CF related deaths [5]. Infection with *P. aeruginosa* in CF increases the risk of early death by almost three-fold [19]. Despite intense research being focused on easing bacterial lung infections, there are to date no reports of sustained eradication from, or indeed prevention of, bacterial infections in the CF lung [20, 21].

1.1.2 Genetic basis of Cystic Fibrosis

CF is an autosomal recessive genetic disorder, resulting from inherited mutations in the Cystic Fibrosis Transmembrane conductance Regulator (*CFTR*) gene. The protein product of *CFTR* is a cyclic adenosine monophosphate regulated (cAMP) transmembrane chloride ion channel located on the apical membrane of epithelial and blood cells (Figure 1.1). Although CFTR primarily functions as a chloride channel, it also has various regulatory roles including inhibition of the Epithelial Sodium Channel (ENaC) [23], inhibition of Calcium-Activated

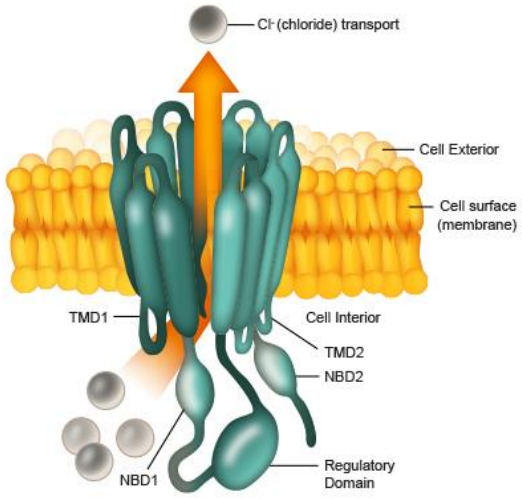

Figure 1.1 Structure of the CFTR protein. Figure shows the structure of the CFTR protein (green), an ATP-binding cassette transporter made up of five domains: the two transmembrane domains (TMD) that form the channel pore in the cell membrane (yellow), the two nucleotide binding domains (NBD) and one regulatory domain. The main function of the CFTR protein is the transport of chloride ions (grey). Figure from CF Education Steering Group (ESG), 2015 [22].

Chloride Channels (CaCC) [1], activation of Outwardly Rectifying Chloride Channel (ORCC) [24], regulation of ATP channels[25] and bicarbonate-chloride exchange [26].

CFTR is located on the long arm of human chromosome 7 [27] and over a thousand distinct mutations of the gene have been reported. For many of the mutations, the majority of which are very rare (only 20 have a allelic frequency >0.1% [28]), the phenotypic effects on the carrier are unknown or have been shown to be non-consequential [29, 30]. Ninety percent of CF patients carry a ΔF508 mutation involving a deletion of phenylalanine at position 508 [31]. While the frequency of the different mutations vary by geographical region , no other single mutation accounts for more than 5% of the global CFTR mutations [32]. Approximately 80% of *CFTR* mutations are associated with CF disease and can be separated into 6 classes of mutations with varying degrees of CFTR function (Figure 1.2) [28].

Mutations in *CFTR* give rise to the clinical manifestations of CF and that are observed in multiple organs. CF pathogenesis is characterized by the accumulation of thick, sticky mucus in organs producing mucin such as the lungs, sinuses, intestine, pancreas and reproductive organs. Clinical diagnosis of CF is partially based on one such manifestation, high sweat salt content due to the absence of functional CFTR in the sweat glands restricting chloride and sodium reabsorption [33]. If a baby has a positive result for CF during newborn screening, (raised levels of immunoreactive trypsinogen as an indirect consequence of *CFTR* mutations), or if a patient shows symptoms of CF, clinical diagnosis is carried out by *CFTR* mutation screening followed by the Gibson and Cooke sweat test when mutation screening identifies heterozygous results, [34, 35].

The most significant clinical effects of CF are observed in the respiratory system and are a consequence of the inability of airways to channel chloride through CFTR. At birth, the lungs of CF infants appear normal. Yet, as early as four months of age, the lungs begin to show signs of infection and inflammation [36]. Infection initiates in early childhood with a progression of organisms including *Staphylococcus aureus, Haemophilus influenzae, Streptococcus pneumoniae* and, most significantly *P. aeruginosa*. Infections in CF are discussed further in section 1.1.4.2.

CFTR is surface-expressed by ciliated epithelial cells in the airway and plays an important role in maintaining the hydrated periciliary mucus layer on the airway surface (airway surface liquid) required for adequate mucociliary clearance. Two main models of sodium and chloride reabsorption attempt to explain the resultant airway dehydration, viscous mucus and impaired mucociliary clearance observed in CF (Figure 1.3)**.** The first, the low-

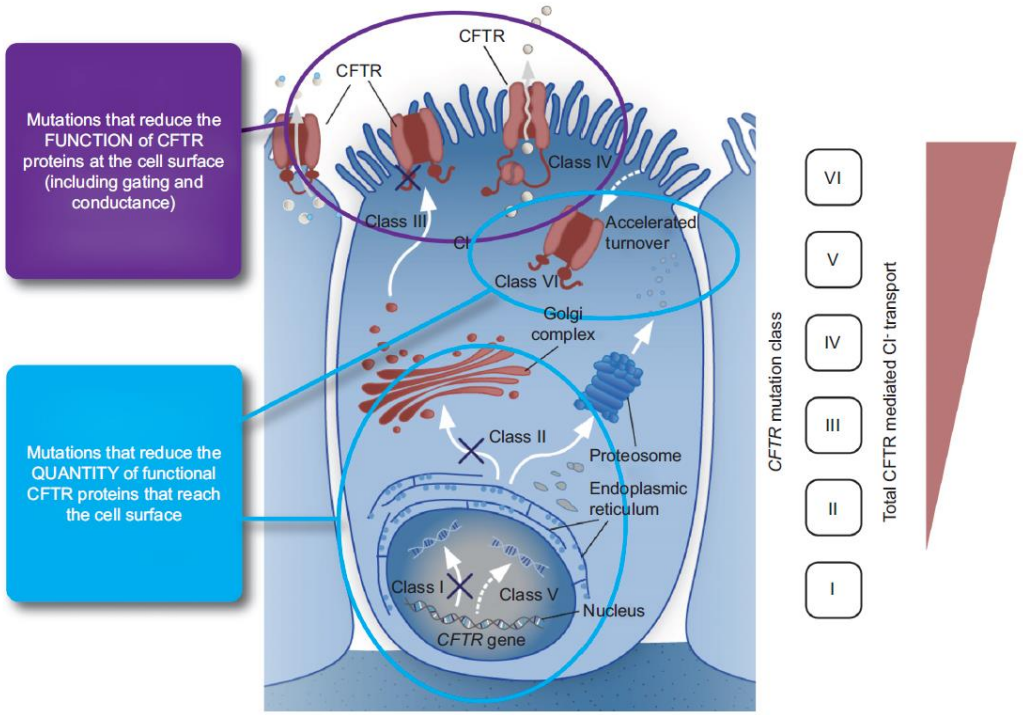

Figure 1.2 CFTR Mutations. Mutations of the *CFTR* gene are categorized into 6 classes. The figure illustrates the mechanisms that differentiate between the 6 classes and the ability of CFTR in individual classes to mediate Cl^- transport. Class I, II and III mutations generally result in a lack of functional CFTR, or CFTR expression/functionality is significantly reduced. Class I CFTR mutations typically result in truncated CFTR or its complete absence as a consequence of premature stop codons, nonsense, or frame-shift mutations and mRNA splicing defects [37]. The deletion of glycine at position 542 (G542X) is a common class I mutation with a premature stop codon. Class II mutations, including the prevalent ΔF508, result in defects in protein folding and maturation, so the proteins are not transported to the apical membrane and are instead prematurely degraded. The phenylalanine deletion in ΔF508 prevents it from being processed into its mature glycosylated form [38]. Class III mutations result in CFTR that is expressed at normal levels and transported to and inserted into the apical membrane but is non-functional. The relatively common G551D mutation, found in 4%–5% of CF patients [5, 39], has defective Cl^- channel gating and is an example of a class III mutation [37]. Class IV mutations are similar to class III mutations in that CFTR is produced at normal levels, but unlike class III mutations, the CFTR displays aberrant and/or reduced function [37]. Class V mutations are the least severe and normally the result of splicing defects; they cause decreased production of functional CFTR. The relatively newly defined class VI mutations produce unstable but functional CFTR at the apical membrane as a result of C-terminal truncation [37, 40]. Figure from Derichs *et al.*, 2013 [41].

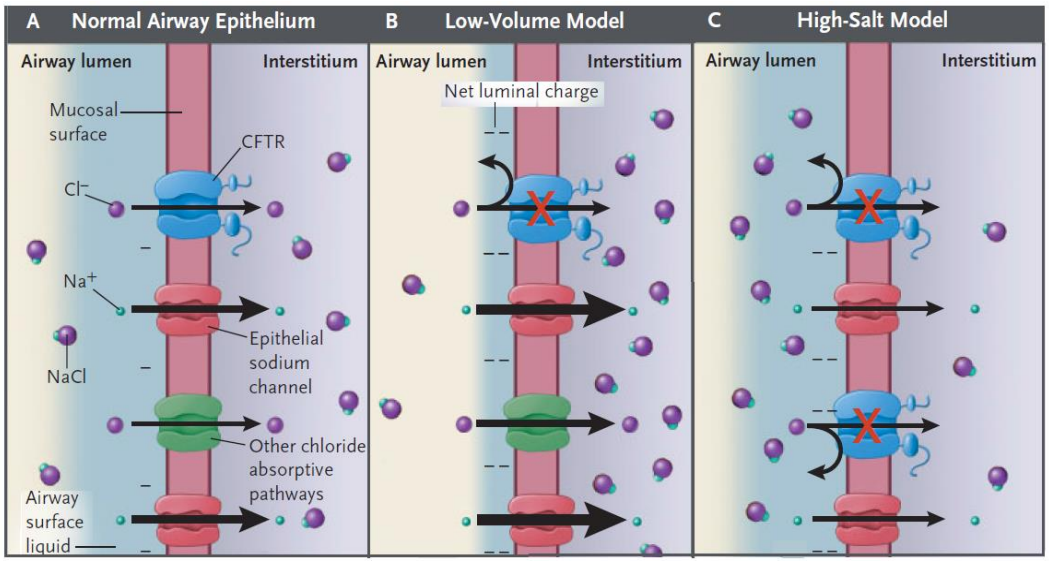

Figure 1.3 Competing models explaining the airway dehydration, viscous mucus and impaired mucociliary clearance in the CF airway. Panel A shows the transport of sodium and chloride ions through CFTR (blue) ENaC (red) and other ion channels (green) on the mucosal surface of healthy airway epithelia, together with the net luminal charge. The other two panels show how the action of these channels and the airway epithelia are affected in CF as explained by the low-volume (Panel B) and high-salt (Panel C) models. The low-volume model proposes a loss in regulation of sodium absorption by ENaC because of the absence of functional CFTR [42]. As a consequence, sodium and chloride are hyper-absorbed from the airway lumen and the resulting osmotic imbalance causes absorption of water into the cells, dehydrating the airway lumen. The second model, the high-salt model, postulates that without functional CFTR, sodium and chloride are not reabsorbed into the interstitium, allowing the ions to accumulate in the airway surface liquid [43]. Figure adapted from Rowe *et al.*, 2005 [33].

volume model, proposes that sodium and chloride hyper-absorption from the airway lumen results in an osmotic imbalance that dehydrates the airway lumen. The second model, the high salt model, postulates CFTR-dependent blockage of chloride reabsorption into the airway epithelia, which allows the ions to accumulate in the airway surface liquid [43]. Opinion is divided amongst researchers as to which model better explains the CF phenotype, but both models attribute an important role for the absence of functional CFTR in the development of the CF lung pathology. More importantly, both models also account for the most damaging consequence of the *CFTR* mutation in the airway, accumulation of dehydrated mucus leading to sustained bacterial infection. The low volume model allows for mucus on the epithelium to form plaques with hypoxic niches that can harbour bacteria [42, 44]. The increased airway surface liquid chloride concentrations proposed in the high salt model, in combination with the resulting hyperpolarized epithelia, disrupt the production of innate immunity antimicrobial molecules, enabling bacteria to persist in the lung [43, 45, 46]. It is therefore plausible that a combination of both models may be in effect in the CF airway.

Gastrointestinal complications are the other major pathology associated with CF. Around 15% of CF patients are born with an obstructed ileum and almost 90% will develop pancreatic insufficiency because of defective secretion of digestive enzymes [1]. The thickened secretions in the pancreatic ducts cause blockages, and because of the resulting autolysis, the pancreatic tissue is replaced over time with fatty tissue. The glandular obstruction of bile canaliculi can cause clinically apparent cirrhosis in about 5% of patients [47]. The poor absorption of fat-soluble vitamins can also cause a number of complications including night blindness and bleeding disorders. Without adequate caloric intake and supplementation with fat-soluble vitamins, CF patients would not survive past the first few months. A major consequence of the gastrointestinal complications in CF is the development of CF-related diabetes, with almost 45% of individuals with CF aged above 35 diagnosed with this complication [5].

Almost 99% of adult males with CF are born with a congenital absence of the vas deferens, rendering them infertile [48]. This is frequently observed even in males heterozygous for *CFTR* mutations and who are otherwise asymptomatic [1]. Infertility is less serious in females and although not well understood, fertility complications are attributed to combinations of factors related to the *CFTR* mutation, including the thickening of the cervical mucus [49]. However, improvements in fertility medication and CF nutrition support means that men with CF have options to father children and women can have a healthy pregnancy. In the US, the number of women with CF who have successfully given birth almost doubled between 1997 and 2012 [5].

1.1.3 Cystic Fibrosis therapies

Since the first comprehensive description of CF in the 1930s [50], the search for CF disease-modifying therapies has been ongoing. As understanding of the disease pathophysiology has increased, we have begun to identify potential strategies to address the basic CF defect. Two main methods of addressing the basic CF defect have been identified. The first, gene therapy, involves strategies that modify or correct the abnormal expression of *CFTR.* Gene therapy became the primary focus of many CF researchers after the identification and cloning of the *CFTR* gene [51]. Early attempts at correcting *CFTR* defects were through the administration of *CFTR* DNA directly to the cells, which has up to now been largely unsuccessful. With the advent of the genomics era, gene therapy research has evolved for

the better. Researchers have since identified CF disease-modifying therapies through the use of novel drugs to target and correct defects arising from specific CF mutations. The second method of addressing the basic CF defect involves cell therapy, where live whole cells are administered. Cell therapy, using a variety of stem/progenitor cells and even a tissue-engineered lung may hold some promise, but this form of therapy is still an emerging field and further research is required. Because cell therapy research is in its infancy, the difficulty of transferring genes into the lungs, and the expense associated with large, meaningful clinical trials to test novel disease-modifying therapies, CF research has largely been restricted to further understanding the disease and providing strategies to increase life expectancy and quality of life. As a result of this research, the life expectancy of CF patients has steadily risen over the last 20 years. In the 1980s, the median life expectancy of a CF patient was around 25–30 years [1, 5, 6] but a child born with CF today is expected to live into their 50s [1, 6]. This increase in life expectancy has been coupled with marked improvements in a number of indicators of quality of life including body mass index, lung function and even live birth rates [5]. With the increase in CF patient life expectancy, the discovery of drugs and treatment strategies that improve the quality of life has important implications for health economics and is vital to the lives of people living with CF and their families.

1.1.3.1 Current symptom-targeted CF therapies

Current CF therapies are generally targeted towards preventing malnutrition and treating the lung pathophysiology. A list of common maintenance CF therapies is shown in Table 1.2. Pancreatic enzyme replacement to prevent malnutrition is essential for CF patients, and as for the large number of CF patients who develop pancreatic insufficiency, dietary

Table 1.2 Common maintenance therapy drugs in CF. Adapted from Lubsch, 2007 [52]

Drug	**Dosage**
Gastrointestinal Therapy	
Fat-soluble vitamins	<1 year, 1 mL daily 1 to 3 years, 1 mL, twice daily 4 to 10 years, 1 capsule daily >10 years, 1 capsule, twice daily
Pancreatic enzymes	1000 to 2500 lipase U/kg prior to meal and one half dose prior to each snack
Pulmonary Therapy	
Dornase alpha	2.5 mg inhaled daily
7% hypertonic saline	4 mL inhaled twice daily
Tobramycin	300 mg inhaled twice daily, administered in 28 day cycles
Azithromycin	500 mg, inhaled once every two days

supplementation of fat soluble vitamins is mandatory [6]. Patients who receive adequate nutrition not only have a survival advantage but also have improved lung function [53, 54].

The viscous mucus in the airways is particularly problematic for CF patients and is normally targeted with a number of drugs. The thick mucus contains large quantities of extracellular DNA and this is countered with aerosolized Dornase Alfa, a highly purified solution of recombinant human DNase. Hypertonic saline is administered as a hyper-osmolar agent to hydrate the airway lumen while inhaled β-agonists assist mucociliary clearance [1, 5, 55]. There is, however, limited evidence of the effectiveness of these therapies based on lung function improvement. Patients are also required on an almost daily basis to supplement these drugs with chest physiotherapy and the use of mechanical clearance devices to drain the tenacious airway mucus.

Aggressive antibiotic therapy is the cornerstone of current CF therapy. Acute management in response to pulmonary exacerbation, particularly as a result of *P. aeruginosa* infection, involves combination high-dose intravenous antibiotic therapy to provide synergistic antimicrobial activity and to slow development of resistance. The combinations are individualized based on the microbial flora of the patient. As part of the daily maintenance therapies to keep chronic infections at bay, patients also receive inhaled tobramycin and azithromycin at regular intervals, tobramycin in 28 day cycles, and azithromycin on alternate days. [1, 52]. For patients with end-stage lung disease, the last resort is lung transplantation. For certain patients, this has the potential to vastly improve their quality of life, but deciding who gets transplants is contentious, and the availability of lungs limited. Some of the issues pertaining to CF lung transplantation are further elucidated in a recent review by Braun and Merlo [56].

There is considerable research being carried out on treatment of the symptoms of CF with the aim of improving the quality of and extending life. Treating specific symptoms will improve the chances of patients surviving long enough that a gene-targeted therapy may become available. The use of antibiotics to treat long-term infections has however, increased the levels of antibiotic resistance in individuals with CF. Consequently, the development of novel antimicrobial therapies has become an important area of CF research.

1.1.3.2 Gene therapy and CFTR modulation on the horizon

An increased understanding of CF disease and its associated genetics has allowed the discovery of a number of promising *CFTR* modulators specific to individual genetic mutations. Gentamicin, shown to be able to allow ribosomes to read through premature

mRNA stop codons (class I mutations), was the first such molecule, and caused small changes in the nasal potential difference, a test used to detect changes in CFTR function [57, 58]. However, this was only observed when doses above safe levels were used that consequently caused adverse side effects such as nephrotoxicity. The compound PTC 124 or Ataluren has had promising results in *in vitro* studies, and has been shown to restore CFTR function to a significant fraction of the normal level in mice with the class I G542X *CFTR* mutation [59]. Phase 2 trials in humans have shown positive changes in chloride transport and increases in lung function as measured by FEV_1 (forced expiratory volume in 1 second) [60, 61]. Phase 3 trials are underway to determine the long-term efficacy and safety of this treatment, but concerns remain about the possibility of malignancies as a consequence of allowing ribosomes to read through native stop codons. So far, the drug seems specific to premature stop codons and could be effective in other diseases where premature stop codons are an issue (e.g., Duchenne Muscular Dystrophy [62].)

The most successful of the recent *CFTR*-modulating compounds is VX-770 or Ivacaftor. This is a CFTR potentiator that increases the opening of CFTR channels, although its mechanisms of action are not completely understood. It has been shown *in vitro* to effectively increase CFTR opening of class III G551D mutations. A trial of Ivacaftor for 96 weeks at 150 mg twice daily in patients with the ΔF508 mutation aged 12 or above showed no significant increase in chloride transport or FEV_1 [63]. When a similar dose was administered to patients with at least one G551D mutation in a randomized, double-blind, placebo-controlled, multicentre trial, marked improvements in disease symptoms were observed. By 48 weeks, 10% vs. 0% increase in FEV1 was observed in Ivacaftor vs. placebo groups. In the Ivacaftor group, increases were also observed in chloride transport, the patients gained more weight, and they scored their quality of life higher. In addition, the number of pulmonary exacerbations was almost halved in that time period for the treated group [64]. Because of these dramatic improvements in CFTR function, Ivacaftor has been approved by the FDA for patients with at least one G551D mutation. Although it was made available to Australian patients under the pharmaceutical benefits scheme in December 2014 [65], it does come at a significant cost: almost $300,000 per year per patient and is needed throughout their lifetime. A significant drawback of Ivacaftor is that it is only effective in individuals with the rare G511D mutation (present only in 4%–5% of CF patients [5, 39]). Another *CFTR* modulator, VX-809 or Lumacaftor, has been shown *in vitro* to correct the folding and processing of CFTR in ΔF508 cell lines and to increase chloride secretions in human bronchial epithelial cells [66]. However, in a phase 2b study, no change in chloride transport, lung function or

exacerbation rate were observed [67]. Given these poor results, the use of Lumacaftor in conjunction with Ivacaftor was studied in a phase 2 study, because Lumacaftor could potentially correct CFTR folding and processing and Ivacaftor could then potentiate the opening of the CFTR. The study found a 7% increase in FEV_1 compared with placebo and a Phase 3 randomized, double blind, placebo controlled, parallel group study is currently being carried out to further establish the efficacy of this combination therapy [68].

There are also drugs that attempt to correct the biochemical defects in CF without influencing CFTR. Moli1901 or Lancovutide attempts to compensate for CFTR by stimulating an alternate chloride channel and has shown promising increases in FEV_1 in early trials [69]. Phase 2b studies were completed in late 2013 but the results are yet to be published. Another drug, Denufosol, which attempts to reduce epithelial sodium reabsorption through ENaC, also showed promising initial results, but phase 3 trials determined that the drug failed to meet its primary endpoint, a significant increase in baseline FEV_1 [70].

With the exception of Ivacaftor, which is limited in its use to only people with the rare G551D mutation, all other CFTR-modulating drugs require further research before they can be successfully applied to individuals with CF. Consequently, the use and development of symptom-targeted drugs and particularly of novel antimicrobial therapies remain essential to treating individuals with CF to enhancing their quality and length of life.

1.1.4 Pathogens in Cystic Fibrosis lung infections

1.1.4.1 Impaired immune response to pathogens in CF

Human lungs process, on average, over 10,000 L of air a day, and are well equipped for coping with the associated barrage of microbes. The ciliated airway epithelial cells and mucus provide a physical barrier to prevent infection. The epithelial cells and closely associated cells involved in the immune system also have specialized receptors that allow them to detect the presence of a diverse multitude of pathogens. Upon detection of pathogens, the host cells, both epithelia and inflammatory cells, respond through a number of mechanisms including inflammation and induction of innate and adaptive immunity. The physical barriers and innate and adaptive immune responses to *P. aeruginosa* in human airways are summarized in Figure 1.4.

The normal immune response to pathogens is impaired in people with CF. A striking feature of the CF airway immune response is excessive inflammation, and is thought to contribute significantly to the declining pulmonary function. Neutrophils and cytokines are known to be found in high concentrations in the airway fluids of individuals with CF, even in young children [71].While the cytokines help in the recruitment of immune cells, the neutrophils themselves produce large quantities of proteases that can digest a diverse range of substrates, including host cell proteins. The excessive neutrophil infiltration of the airways seen in CF overwhelms the airway tissue, with the cleavage of structural proteins resulting in bronchiectasis [72]. Upon cell death the neutrophils release oxygen radicals that further contribute to airway damage [73]. There is also debate about whether the excessive inflammation in the airway is the result of inflammation that is disproportionate to infection, or if there is excessive inflammation independent of airway infections [Reviewed in 74, 75]. Much research has been aimed at understanding the mechanisms that link the CFTR function to modulated inflammation but these mechanisms are yet to be fully described. Regardless of the cause, correction of the inflammatory defects is a potential therapeutic target in individuals with CF.

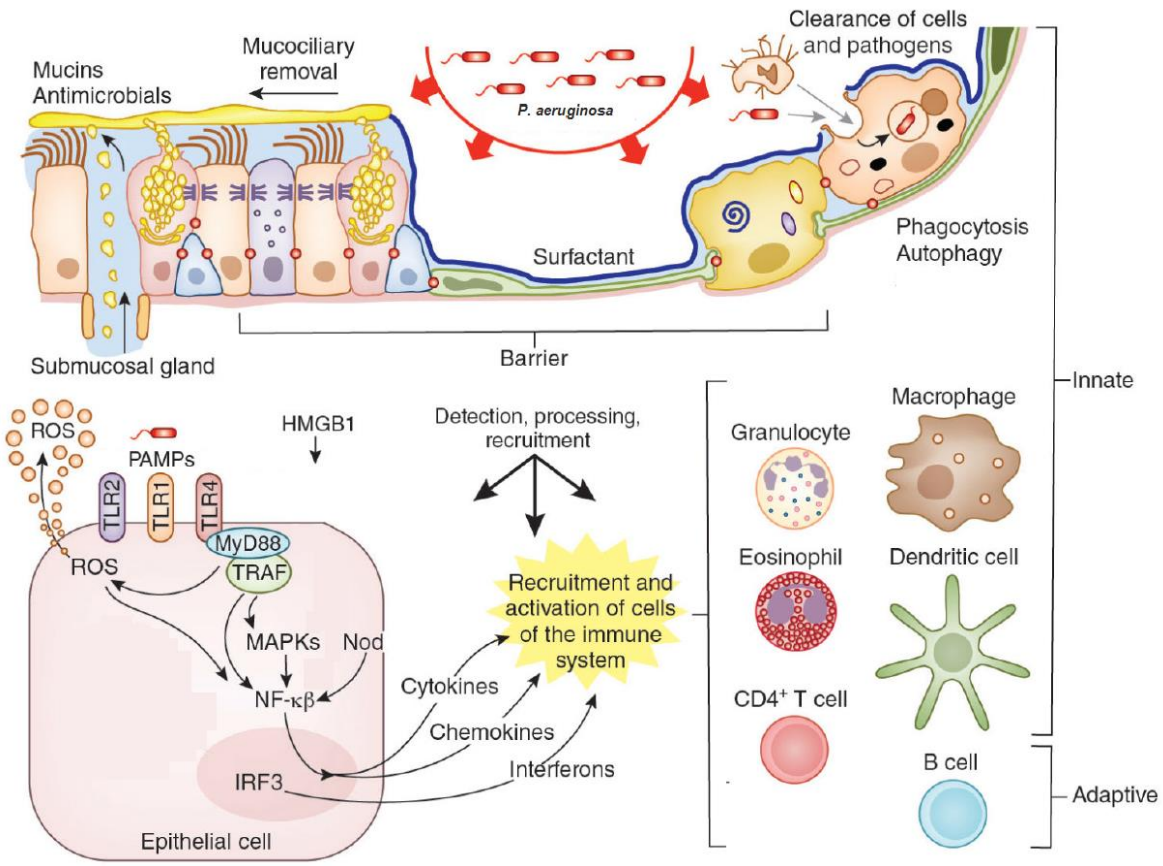

Figure 1.4 Outline of host immune responses to *P. aeruginosa*. The epithelial cells in the airway form a physical barrier to infection and employ various mechanisms to counter infection from pathogens like *P. aeruginosa.* The predominant cell type in the airways, the ciliated epithelial cell, has hair like extensions powered by mitochondria, which beat rhythmically in a unidirectional manner to force particulates out of the lungs, providing a mechanical mechanism to keep the airway free of pathogens. Interspersed among the ciliated epithelial cells are secretory cells producing surfactants and mucins. The surfactants, while playing an important role in maintaining the surface tension of the air-liquid interface and thus preventing the collapse of the airway, are also capable of binding and opsonizing microbial pathogens [76]. The mucins are high molecular weight glycolipids that trap foreign particles, which can then be transported out of the airway by cilia-mediated transport. The inter-cellular junction proteins play an important role in maintaining the structural integrity of the respiratory epithelium [77, 78], making the epithelia less permeable to pathogens and their products. The airway also plays an important role in the initial identification of the pathogen and the regulation of the amplitude of the immune response to the pathogen. The activation of specific pattern recognition receptors (PAMPs)such as Toll-like Receptors (TLRs) and NOD-like receptors (NLRs) by *P. aeruginosa* initiate epithelial cell-intrinsic signalling pathways via nuclear factor κB (NF-κB), mitogen-activated protein kinase (MAPK) and interferon regulatory factors (IRF). This causes the production of various cytokines, chemokines, interferons, reactive oxygen species and antimicrobial proteins that help in the recruitment and activation of the innate and adaptive immune responses and assist in killing the pathogen. Multiple pathways that regulate apoptosis, the unfolded protein response and autophagy are also activated, and these pathways help to integrate the requirements to clear infection with cell survival. Alveolar macrophages are also recruited during infection and play a significant role in sequestering antigen and phagocytising foreign material. Dendritic cells in the basal lamina trigger the adaptive response, bringing B and T-cells into the picture. The degranulation of phagocytic cells also releases antimicrobial cationic molecules such as LL-37 and lactoferrin [79]. Figure adapted from Whitsett and Alenghat, 2015 [78]

1.1.4.2 Cystic Fibrosis lung microbiome and clinical significance

CF lung infections are polymicrobial in nature and the pathogens vary between individuals and over time (Figure 1.5). Infections in CF children tend to be caused by *Staphylococcus aureus* and common airway commensals like *Haemophilus influenzae* [80, 81]. The effects of long-term colonization by *S. aureus* are not considered to be as severe as those of some of the other CF pathogens, but the emergence of particularly virulent strains of Methicillin resistant *S.aureus* (MRSA) is concerning to the CF community [81]. The prevalence of *H. influenza* infection wanes as patients get older and there is contention as to what role, if any, *H. influenzae* plays in pulmonary disease progression. Rosenfield and colleagues have shown that *H. influenzae* can induce inflammation in the airways, but a cross-sectional analysis of 7,010 European CF patients found no association between *H. influenzae* colonization and decreased FEV_1 [81-83].

It is believed that these early infections damage the epithelial surfaces, and in conjunction with the inhibited mucociliary clearance mechanisms of the lungs and the aberrant inflammatory status, prime the airways for infections with opportunistic pathogens. The major pathogen in adult CF patients is *P. aeruginosa.* An estimated 80%–90% of adult CF

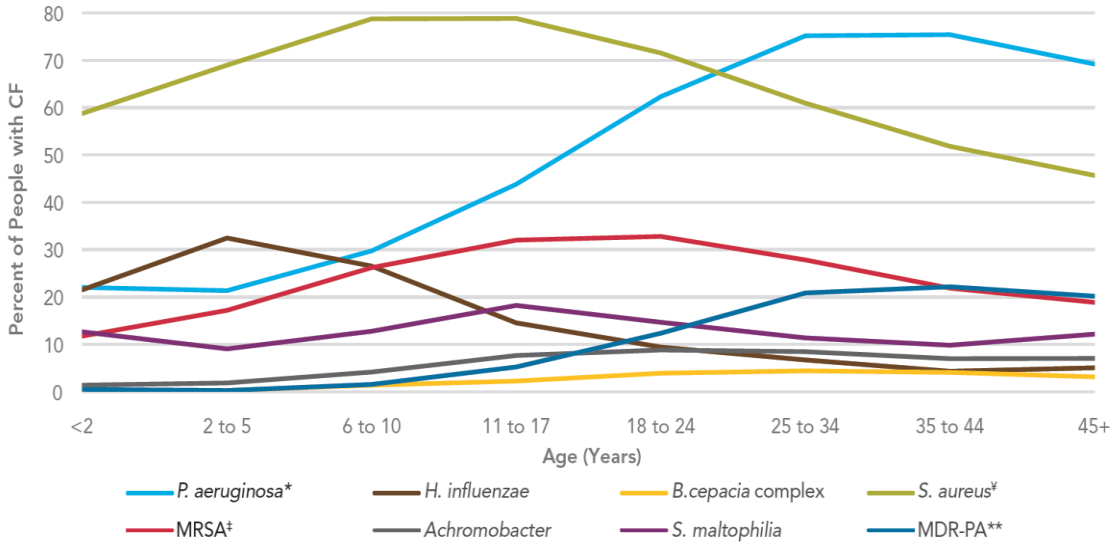

Figure 1.5 Changing microbial ecology of the CF lung. Figure shows the prevalence of prominent CF pathogens in the lungs percentage of American CF patients (2012). * *P.aeruginosa* includes multi-drug resistant *P.aeruginosa* (** MDR-PA), ¥ *S.aureus* includes methicillin-resistant *S.aureus* (‡ MRSA). Figure from Patient Registry Annual Data Report of the US Cystic Fibrosis Foundation, 2012 [5]
.

patients produce respiratory cultures containing *P. aeruginosa,* and infection with *P. aeruginosa* is associated with worse clinical progression of disease [5, 19]. The prevalence of multi-drug resistant *P. aeruginosa* (MDR-PA), has doubled in the US to 9.5% compared with CF respiratory cultures positive for (MDR-PA) in the decade preceding 2012 [5]. Other CF pathogens include *Burkholderia cepacia* complex (Bcc), *Mycobacterium* species, *Pandoraea* species and the nosocomial pathogens *Stenotrophomonas maltophilia* and *Achromobacter xylosoxidan*. The Bcc is a group of related bacteria consisting of a number of species. Despite their low prevalence, approximately 2.6% in the 2012 US CF population, infection with Bcc is linked to rapid decline in lung function and increased mortality, and is sometimes associated with necrotising pneumonia [5, 81, 84, 85]. Recent molecular studies indicate that there is a highly diverse bacterial community within the CF lung, with many different bacterial species, including anaerobes, also present [80, 86].

The most common fungus involved in CF respiratory disease is *Aspergillus fumigatus* [87]. *A. fumigatus* can cause a chronic allergy-associated inflammatory response in some CF patients and invasive infection after lung transplantation, but evidence correlating its prevalence with worse lung function is poor [80, 81]. A number of other fungal and yeast species including *Exophiala (Wangiella) dermatitidis, Scedosporium* species and the yeast species of *Candida* have also been recovered from CF respiratory cultures. Reported incidences vary dramatically from study to study, ranging from as low as 11% to as high as 78%. This is attributed to the use of different culturing methods, but what is clear is that the incidence increases with patient age [80].

Individuals with CF also frequently acquire viral respiratory infections, but surprisingly, these do not occur any more frequently in CF patients than in the healthy population. However, viral respiratory infections in CF are usually more severe, last longer and often cause pulmonary exacerbations that may lead to hospitalization [81, 88, 89]. The most common virus seen in CF is respiratory syncytial virus, followed closely by influenza A and B viruses. Parainfluenza virus, rhinovirus and adenovirus infections are less frequently observed [90]. It is thought that virus infections have little long-term influence on declining lung function [81], but that they may predispose individuals with CF to more pathogenic bacteria such as *P. aeruginosa* [89].

CF patients will typically experience recurrent episodes of pulmonary symptoms called exacerbations, which present as increased respiratory symptoms including cough, pneumothorax, haemoptysis and increased sputum production and airway obstruction.

Quite often, these exacerbations require hospitalization. An increasing number of exacerbations is associated with worse lung function, because the persistent infections cause irreversible break down of the bronchial muscle and elastic tissue. The resulting pulmonary decline leads to eventual respiratory failure [91]

Despite the advances in CF therapies in the last 3 decades and the increased life expectancy and quality of life, microbial infections still cause substantial damage to the CF lung. It remains important to develop our understanding of the mechanisms these microbes utilize to persist in the lung and the interactions among the microbes themselves and between the microbes and host cells, thereby allowing us to improve and refine therapies targeting these infections.

1.2 *PSEUDOMONAS AERUGINOSA*

P. aeruginosa is a ubiquitous Gram-negative rod that is capable of causing severe opportunistic infections in immunocompromised individuals. Its metabolic diversity, overall adaptability and intrinsic ability to develop antibiotic resistance facilitates its survival on a diverse range of natural and artificial environments/surfaces. It is particularly troublesome on medical surfaces such as ventilators, and in the US, it is among the most common nosocomial pathogens and the second most frequently isolated pathogen from patients with ventilator-associated pneumonia [92]. Because it is the major CF pathogen and because of its association with increased clinical deterioration [5, 19], *P. aeruginosa* is the most widely studied pathogen, and eradication/ prevention of *P. aeruginosa* would have important implications for CF research and therapies and other *P. aeruginosa* infections.

1.2.1 Genomic plasticity of *P. aeruginosa*

P. aeruginosa has the largest genome of any disease-causing bacteria, ranging from 6.22 Mb to 6.91 Mb depending on the strain [93]. There are dozens of strains of *P. aeruginosa*, 32 of which had been completely or partially sequenced by late 2012 [92]. The sequencing of a number of strains shows that around 90% of the genomic content is conserved between strains. The remaining 'regions of genomic plasticity' contain genes unique to that strain or to a small subset of strains [94], suggesting that environmental selection pressures play an important role in the evolution of the *P. aeruginosa* genome [93]. Bacteria with higher proportions of regulatory proteins in their genomes are thought to be capable of surviving in diverse environments, and PAO1, the first of the *P. aeruginosa* strains to be sequenced, has 521 genes or nearly 10% of its genome dedicated to encoding regulatory proteins, far higher than most other bacteria [95].

P. aeruginosa displays remarkable metabolic diversity, growing on/in various nutrient-poor environments/surfaces. The PAO1 sequencing identified genes involved in β-oxidation of various carbon compounds and approximately 300 cytoplasmic transport systems [95]. Studies of the *P. aeruginosa* genome have identified numerous other systems important to *P. aeruginosa* pathogenicity and persistence, including virulence factors, intrinsic drug efflux and resistance systems, and protein secretion systems [95]. In summary, its genomic plasticity enhances the potential of *P. aeruginosa* to adapt to, and survive in, a diverse range of environments.

1.2.2. Mechanisms of *P. aeruginosa* pathogenesis

P.aeruginosa has a diverse range of virulence factors and associated mechanisms that contribute to respiratory pathogenesis. What follows is a description of such key virulence factors and pathogenic mechanisms and how they contribute to *P. aeruginosa* infections

1.2.2.1 Flagella and pili

Each *P. aeruginosa* cell has a single polar flagellum and any number of short type IV pili on the cell surface. Flagella are essential for the motility of the bacteria, but they also function as adhesins to epithelial membranes. Flagella mutants have been shown to be less invasive [96], and cause decreased mortality [97] in murine models of *P. aeruginosa* infection. Binding of flagella to the host epithelial cells elicits a potent neutrophilic inflammatory response, which can be detrimental to the airways during chronic infections because of persistent inflammation [98]. Flagella can also elicit a caspase-1-mediated response in host macrophages via the Nod-like receptor (NLR) IPAF [99]. Type IV pili are important adhesins of *P. aeruginosa,* they contribute to its swarming motility and facilitate aggregation of bacteria to form micro-colonies, a strategy that concentrates *P. aeruginosa* and potentially protects it from the host immune response [100, 101].

1.2.2.2 Type 3 secretion systems

P. aeruginosa utilizes type 3 secretion systems (T3SS), where a needle-like structure on the cell surface, closely related to flagella, is used to secrete toxins directly into host cells. The two main *P. aeruginosa* exotoxins transported this way are *exoU* and *exoS*. These exotoxins target host-cell actin cytoskeletal organization, degrading the integrity of the plasma membrane and causing rapid host cell death. Death of the epithelial cells results in the loss of the physical barrier in the airway, aggravating *P. aeruginosa* infection, and is thought to lead to the symptoms observed during bacterial pneumonia, including haemoptysis, bronchiectasis, and necrosis of lung tissue [102].

1.2.2.3 Proteases

P. aeruginosa produces a number or proteases that contribute to persistence in the lung. Alkaline protease and protease IV are both able to degrade host complement proteins, fibronectin, fibrinogen and immunoglobulins [103, 104]. Alkaline protease also helps *P. aeruginosa* to avoid detection by the immune system by interfering with flagella recognition through the host TLR5 [105]. LasA and LasB are elastases produced by *P. aeruginosa*. LasA has low elastolytic activity and is thought to instead enhance LasB activity [106]. LasB,

together with Protease IV, is thought to degrade the lung surfactants that assist in opsonizing bacteria, thus allowing *P. aeruginosa* to evade phagocytosis [104, 107].

1.2.2.4 Lipopolysaccharide

The outer membrane of *P. aeruginosa* is coated with lipopolysaccharide (LPS), a complex glycolipid. *P. aeruginosa* LPS consists of three domains: the membrane bound lipid A that anchors LPS to the membrane, a polysaccharide core and a highly variable glycan polymer known as O-antigen that is exposed on the outer surface. LPS plays an important role in instigating the *P. aeruginosa* immune response and has a role in antigenicity [108]. Lipid A binds to host TLR4 and activates the nuclear factor kappa B (NFκB) pathway that triggers the IL-8 mediated neutrophilic infiltration characteristic of *P. aeruginosa* infections. The O-antigen of the *P. aeruginosa* LPS is responsible for conferring serogroup specificity and it is believed that the polysaccharide nature of *P. aeruginosa* LPS O-antigen is responsible for the strong antibody response towards O-antigen [108].

1.2.2.5 Rhamnolipid

The surfactant rhamnolipid is essential for *P. aeruginosa* swarming motility [109], influences biofilm formation [110] and has antimicrobial activities [111]. Rhamnolipid is also considered to have a role in protecting *P. aeruginosa* biofilms against the host immune system [112] and are classed as virulence factor as they disrupt tight junctions in host cells [113]. Disruption of the epithelia allows infiltration of *P. aeruginosa,* promoting development of infection.

1.2.2.6 Alginate

The production of the exopolysaccharide alginate is important in the colonization by *P. aeruginosa* of medical devices and cell surfaces, particularly in CF [114], and *P. aeruginosa* strains isolated from the CF lung typically overexpress alginate (mucoid variants). Though not essential for the formation of biofilms [115], alginate plays an important role in the maturation of biofilms and helps maintain hydration of bacterial cells in biofilms [116]. Alginate also offers protection by restricting the penetration of antibiotics and host molecules through the biofilm matrix and thus contributes to the pathogenesis of *P. aeruginosa* [117].

1.2.2.7 Other virulence factors

P. aeruginosa colonies have a characteristic blue-green colour resulting from another virulence causing molecule, the pigment pyocyanin. Pyocyanin is capable of disrupting host catalase activity, inhibiting mitochondrial electron transport in the epithelia and causing

oxidative stress in host cells [118]. Other well characterized *P. aeruginosa* virulence factors include pyoverdine, which sequesters iron from the host to help establish infection and support biofilm formation [119, 120], endotoxin A, which can inhibit protein synthesis in host cells [121], hydrogen cyanide, a secondary metabolite that inhibits many host cellular processes [122], and lipases, which can break down opsonising surfactants in the airway [92]. *P. aeruginosa* itself is protected from cyanide as it possesses a cyanide-insensitive oxidase [123].

1.2.2.8 Quorum sensing

An important mechanism that assists in *P. aeruginosa* persistence in the CF lung and contributes significantly to its pathogenesis is quorum sensing (QS). QS is mediated by small diffusible molecules produced by the bacteria that allow the coordination of community-wide activities. Almost a quarter of the expressed *P. aeruginosa* proteome is controlled by QS [124]. In *P. aeruginosa,* QS plays an essential role in the expression and regulation of numerous virulence determinants including, but not limited to, T3SSs, exotoxins, proteases, rhamnolipid, alginate, pyocyanin, pyoverdine, and hydrogen cyanide [Reviewed in 119]. QS also plays an important role in the formation of biofilms. Biofilms essentially envelop the bacterial community in an exopolymeric substance (EPS) matrix (mixture of polysaccharides, extracellular DNA and proteins), protecting it from the host's immune responses and external antimicrobial agents like antibiotics, and facilitates survival of the *P. aeruginosa*. Bacteria enveloped in such biofilms are considered to be up to 1000 times more resistant to antibiotics than those in a planktonic state [125]. QS and biofilm formation is discussed further in section 1.2.4.

1.2.3 *P. aeruginosa* infections in CF

P. aeruginosa infections in CF evolve over-time. Initial *P. aeruginosa* infections occur intermittently during the first decade of life [126]. These infections are usually contracted from the environment, and may be eradicated through the aggressive early use of anti-Pseudomonal antibiotics (median *P. aeruginosa* free period 18–19 months) [127, 128] [127, 128] [127, 128] [127, 128] [127, 128] [127, 128]. However, *P. aeruginosa* generally recurs or persists leading to chronic infection [129]. During chronic infection *P. aeruginosa* is exposed to multiple stresses driving adaption to the lung environment. Mutation resulting in overproduction of alginate is characteristic of these adapted *P. aeruginosa* [116], and mucoidy offers significant protection to the bacteria from antibiotics and the host immune system [117]. The evolution of non-mucoid, and possibly easier to clear, early *P. aeruginosa* infections into the persistent chronic mucoid *P. aeruginosa* is detailed further in Figure 1.6.

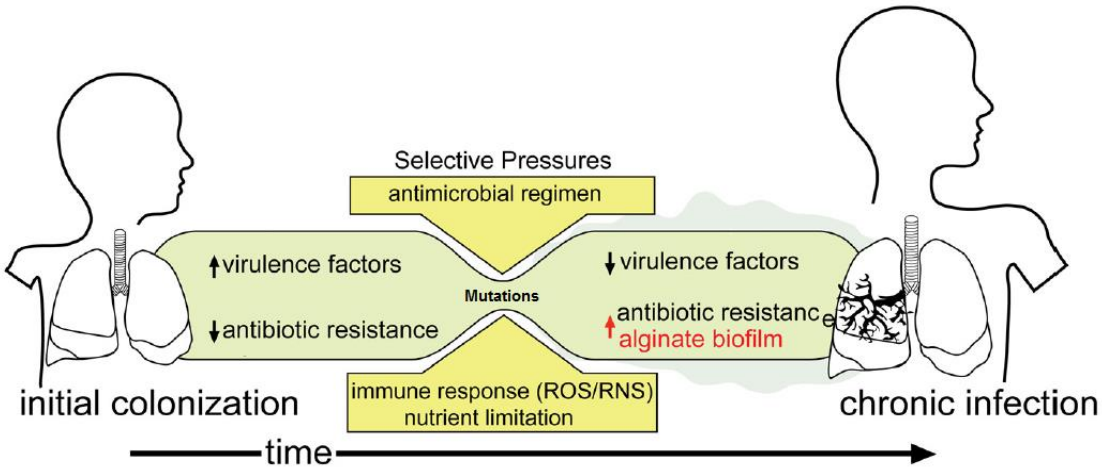

Figure 1.6 Evolution of *P. aeruginosa* infection in the CF lung. Initial colonization of the CF airway by *P. aeruginosa* from environmental sources is intermittent and considered to be more susceptible to anti-Pseudomonal therapies [126, 130]. These early *P. aeruginosa* are exposed to a number of stresses in the airway, including antimicrobials, the immune response, nutrient and iron limitations, and hypoxia [131], and over time the *P. aeruginosa* in the airways develop mutations that allow them to persist in the airways [129]. These mutants typically express reduced levels of acute virulence factors but characteristically overproduce alginate. As a result, the biofilms produced by these mucoid *P. aeruginosa* have increased protection against the host immune response and conventional antibiotics [126], resulting in the chronic infections seen in the CF lung. Figure adapted from Okkotsu *et al*., 2014.[129].

1.2.4 *P. aeruginosa* QS and biofilm formation

1.2.4.1 *P. aeruginosa* QS signalling systems

QS was first described in the 1970s, when researchers discovered that the expression of an endogenous luciferase by *Vibrio fischeri* was population density dependent [132]. We now understand that in a basic QS system (Figure 1.7), a bacterial inducer protein helps synthesize small, diffusible signalling molecules that are released into the extracellular space, and the concentration of the molecule increases in proportion to cell density. A cognate receptor protein, when bound to the signal molecule, functions as a transcriptional regulator of QS-dependent genes including that encoding the inducer protein, thereby allowing the molecule to also regulate its own expression. This biochemical mechanism allows cell density-dependent regulation of community-wide gene expression, and is conserved across many Gram-negative bacteria.

QS in *P. aeruginosa* is a complex system that is used to monitor cell density, regulate virulence factor production, induce biofilm formation and monitor changes in the environment and availability of nutrients. The *P. aeruginosa* quorum signalling system consists of three such QS circuits arranged hierarchically, the Las, Rhl and PQS systems (Figure 1.8). At the top of the *P. aeruginosa* QS hierarchy is the Las system, which produces an acyl homoserine lactone (AHL) signalling molecule *N*-3-oxo-dodecanoyl-*L*-homoserine lactone (C12HSL), a fatty acyl chain linked to a homoserine lactone ring via an amine bond. The lactone rings are derived from *S*-adenosylmethionine, a common co-substrate involved in methyl group transfers, while the variable acyl chains are obtained from the cellular acyl-acyl carrier protein pool [133]. C12HSL production is catalysed by the LasI synthase (inducer) and is recognized by its cognate receptor LasR, a transcriptional regulator. The Las system is directly involved in the regulation of a number of key virulence factors including the expression of alkaline proteases, exotoxins [134] and elastases LasA and LasB [135]. *P. aeruginosa* harbouring *lasR* mutations are avirulent in *in vivo* mouse models of infection [136, 137]. The Las system also regulates the Rhl system, because LasR bound to C12HSL up-regulates the expression of RhlR, the receptor for the Rhl system [138]. The Rhl system synthase RhlI is necessary for the production of another acylated homoserine lactone, *N*-butanoyl-*L*-homoserine lactone (C4HSL) which binds to its cognate receptor RhlR. The Rhl system is involved in the regulation of the T3SS [139] and production of rhamnolipid [135]. Both the Las and Rhl systems are intimately connected to the third QS system, the PQS system. LasR bound to C12HSL is required for synthesis of the PQS system

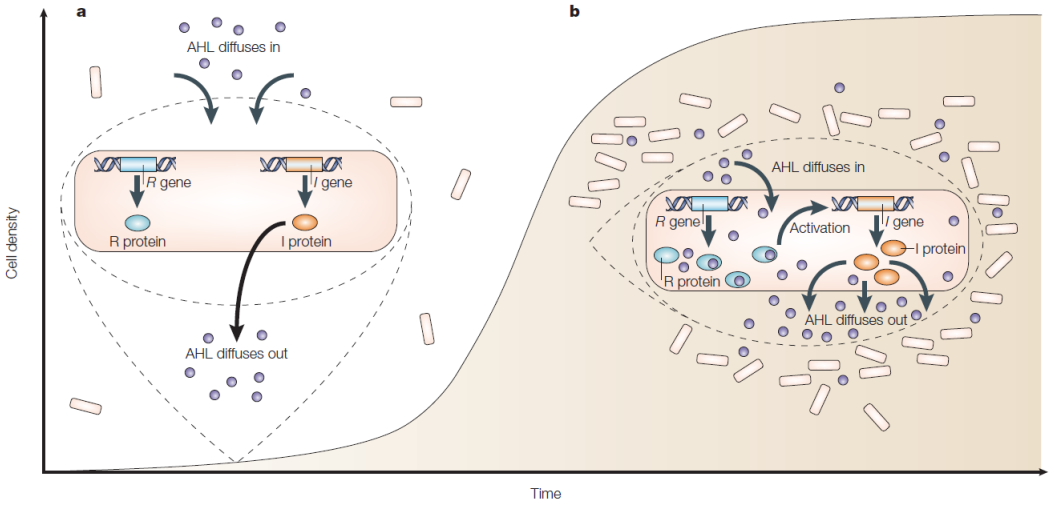

Figure 1.7 The basic quorum signalling system. Figure illustrates a basic QS system involving AHL (purple ball) as the signalling molecule. The bacterial inducer gene produces the inducer (orange oval) protein which helps to produces the small, diffusible signalling molecules (AHL) that diffuse into the extracellular space. As the bacterial population increases, the concentration of the molecule increases outside, and the signal molecule diffuses into surrounding bacteria. Once the concentration is high enough, a bacterial receptor protein (blue oval) modulates gene expression in the individual bacteria, expressing more inducer protein and effecting a population-wide change in gene expression. Figure from Lazdunski *et al.,* 2005. [140].

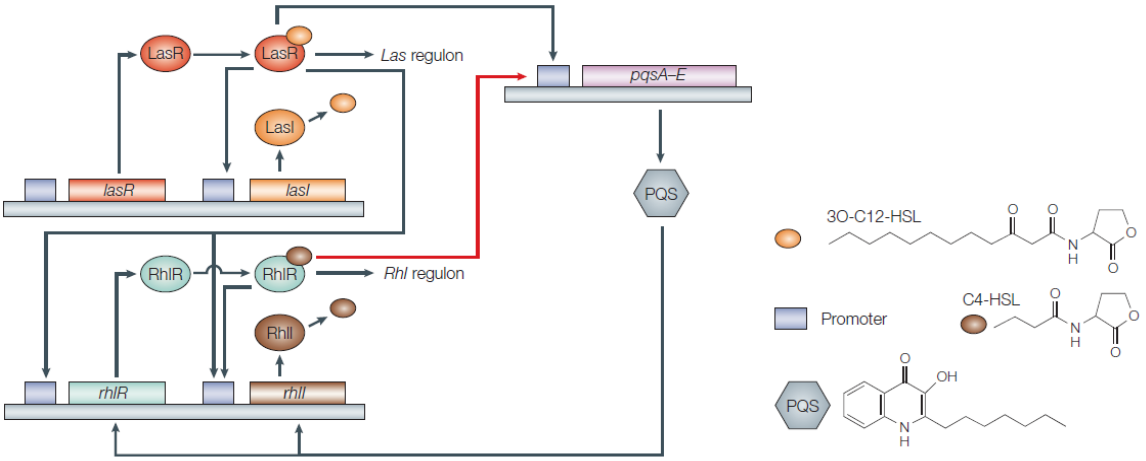

Figure 1.8 The *P. aeruginosa* QS systems are hierarchically arranged. The *P. aeruginosa* QS systems includes three hierarchically arranged circuits. Black arrows represent positive regulation while red arrows indicate negative regulation. At the top of the hierarchy is the Las system, which utilizes the C12HSL signalling molecule and is capable of positively regulating itself and both the Rhl and PQS systems as well as genes in its regulon. The RhlR system utilizes C4HSL as its signalling molecule and regulates genes in the Rhl regulon while also positively regulating itself and negatively regulating the PQS system, which is at the bottom of the hierarchy. Figure adapted from Lazdunski *et al*., 2005 [140].

signalling molecule 2-heptyl-3-hydroxy-4-quinolone or *Pseudomonas* QS (PQS), which in turn influences the transcription of *rhlI and rhlR* [141, 142]. However, RhlR bound to C4HSL inhibits PQS synthesis [141, 142]. PQS plays an important role in the production of pyoverdine. It has been identified that, to keep these systems in check and provide a mechanism whereby a threshold for activation can be created, the quorum signalling control repressor (QscR) controls the timing of and repression of QS [143]. It forms complexes with LasR and RhlR, thereby by repressing *P. aeruginosa* virulence. To ensure that the bacteria does not QS beyond its energetic means, *lasR* and *rhlR* expression are under the control of Vfr, a protein that responds to the metabolic and energy status of the cell [140]. AlgR2, historically thought to regulate alginate biosynthesis, also regulates the QS in a similar way to Vfr [140, 144]. The QS system is further regulated by RsaL, a major Las transcriptional repressor[145], QteE, which prevents accumulation of both LasR and RhlR [146], and QslA, which ensures LasR does not initiate transcription prematurely [147].

1.2.4.2 *P. aeruginosa* biofilms

Biofilms can be defined as bacterial communities that are adherent to each other and/or to interfaces and surfaces while enveloped in extracellular polymeric substances [148]. *P. aeruginosa* biofilms consist of differentiated mushroom- and pillar-like structures composed of an exopolysaccharide matrix consisting of a mixture of polysaccharides, extracellular DNA, lipids and proteins. These structures are interconnected by fluid-filled channels that allow the transfer of nutrients and waste.

In the development of lung infections, planktonic bacteria are ineffective in sustaining chronic infections [149]. Biofilm formation begins with cells attaching to each other and the supporting surface. At this point, the bacteria begin to switch their mode of growth. Bis-(3′-5′,) cyclic dimeric guanosine monophosphate, an intracellular messenger, together with the GAC system, a two component regulatory system, play major roles in the establishment of biofilms [119, 150, 151]. QS plays an equally important role in the formation of biofilms. Davies and colleagues established this when they studied the biofilms formed by *lasI* mutants and found that the *lasI* mutants produced flat biofilms that were sensitive to a biocide agent, while wild-type *P. aeruginosa* formed the normal mushroom-shaped biofilms that were resistant to the biocide agent. These biofilms could be rescued to ones similar to wild-type with the application of exogenous C12HSL [152]. In addition, AHLs have been detected in the lungs of mice infected with *P. aeruginosa* [153]. Singh and colleagues have observed *P. aeruginosa* biofilms in sputum from CF patients and observed that the QS signal ratios in the sputa resembled the QS signal ratios seen in *in vitro* biofilms (almost equal

A

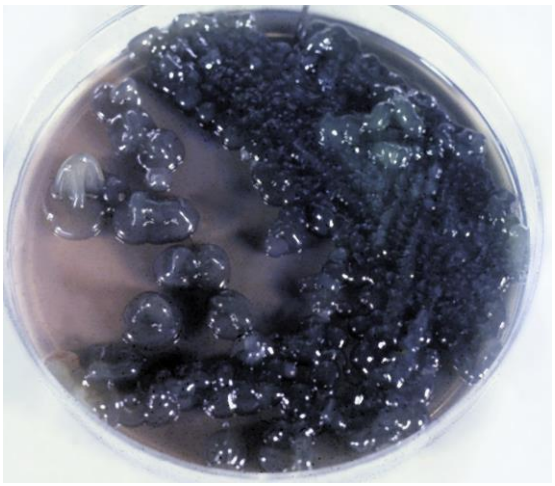

B

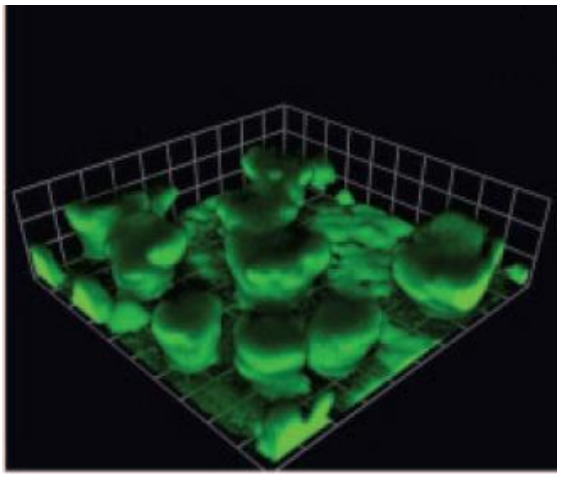

C

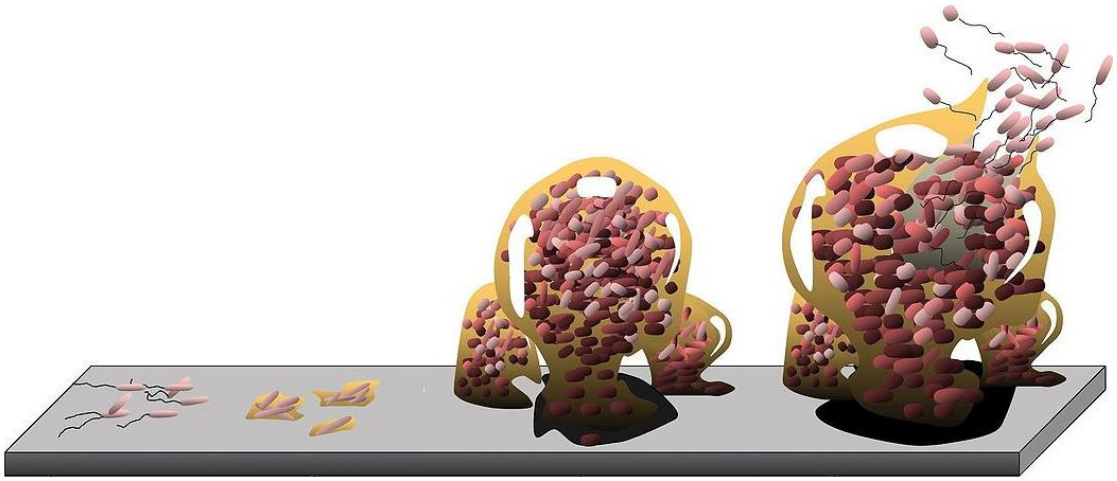

Figure 1.9 The *P. aeruginosa* biofilm. A) Mucoid *P. aeruginosa* strain growing on a MacConkey agar plate over producing alginate. When stored upside down, the material will drip onto the plate lid. Figure from Pritt *et al*., 2007 [154]. B) The characteristic mushroom- and pillar-like structures are shown from a 6 day PAO1 biofilm using confocal scanning laser microscopy. The squares are 61 µM on a side. Figure from Banin *et al*., 2005 [155]. C) Illustration of planktonic biofilm developing into a mature biofilm. The planktonic bacteria on the left begin to attach to each other and a surface. They then switch to a mucoid phenotype and begin to produce the exopolysaccharide matrix. These colonies of bacteria mature into biofilms with fluid-filled channels that support the transport of nutrients and waste. Individual bacteria eventually disperse into the environment and restart the biofilm formation cycle. Figure adapted from Monroe *et al*., 2007[156].

amounts of C12HSL and C4HSL in biofilms and sputa when compared with 3 to 10 times more C12HSL than C4HSL in mid-logarithmic *P.aeruginosa* broth cultures) [157]. QS has also been shown to play roles in the production of Psl, one of the polysaccharides that make up the biofilm EPS [158], and extracellular DNA[159].

Upon irreversible attachment of bacterial cells to each other and the supporting surface, the bacterial cells in the biofilms begin to produce the EPS matrix. The extracellular matrix is comprised of three main types of polysaccharide with varying functions, extracellular DNA, and a collection of proteins. The three main polysaccharides in the *P. aeruginosa* EPS are Psl, Pel and alginate. Psl and Pel are both scaffolding sugars in the EPS, allowing for the initiation of biofilm formation and adhesion of bacteria [160-162]. They also help provide a physical barrier from the host immune response and antibiotics [160, 162]. Mucoid *P. aeruginosa* strains in biofilms in the CF lung typically overproduce the EPS alginate because of mutations in the AlgU operon , the master regulator of alginate biosynthesis [Reviewed in 116]. While not essential for biofilm formation [115], alginate plays significant roles in biofilm structure, protection and maintenance [163, 164] and is believed to offer *P. aeruginosa* the protection it requires to form chronic infections in the CF lung. Extracellular DNA is also a vital component of the EPS matrix, providing structural support and protection against host immunity, and is the most significant pro-inflammatory contributor to the EPS matrix [159, 165-167]. The proteins in the EPS mainly have supporting roles in structure and adhesion [168].

The maturing biofilm develops into the characteristic mushroom- and pillar-like structures supported by the EPS and interspersed with fluid-filled channels that allow for the exchange of nutrients and waste products [169] (Figure 1.9). These structures limit diffusion of oxygen, antibiotics and immune mediators, providing considerable protection to *P. aeruginosa*. *P. aeruginosa* in biofilms are considered to be 1000 times more resistant to antibiotics than their planktonic counterparts [125]. The biofilms also play an important role in the development of antibiotic resistance, as further described in section 1.2.5. Eventually, bacterial cells detach from the biofilm allowing dispersion of *P. aeruginosa* through the environment to form new biofilms

1.2.5 Antibiotic resistance in *P. aeruginosa*

Once *P. aeruginosa* biofilms are established in the airways, they are virtually impossible to clear either by the host immune response or through the use of conventional antibiotics. There are three hypothesized mechanisms for the resistance that biofilms have against antibiotics. Firstly, the thickness of the biofilm prevents the penetration of the antibiotic into the biofilm where it can affect the bacteria, and consequently the bacteria are exposed to sub-inhibitory concentrations, resulting in decreased killing. Secondly, the zones of nutrient depletion and waste accumulation in the biofilms and the generally hypoxic conditions in biofilms inhibit antibiotic activity [170]. Finally, exposure to sub-inhibitory concentrations of antibiotics helps to select for bacteria that are more resistant to the antibiotics [170]. The biofilms also offer protection against the host immune cells. Freshly isolated neutrophils have been shown to be ineffective in phagocytising QS-proficient *P. aeruginosa* biofilms, but effective when exposed to a QS mutant biofilm [112, 171]. One of the ways that biofilms protect against host neutrophils is thought to be through utilizing a 'biofilm shield', where the bipolar rhamnolipid is localized to the biofilm surface and lyses the invading neutrophils [172].

Of particular concern to CF physicians is the increased incidence of antibiotic-resistant *P. aeruginosa.* The prevalence of MDR-PA in the US has doubled from 4.2% in 2002 to 9.5% in 2012 [5], and is thought to be highly associated with the increased use of antibiotics [173]. The increase in resistance rates and the absence of novel therapies have seen physicians resort to the use of older antibiotics, despite their toxicity [174].

P. aeruginosa demonstrates remarkable versatility in its mechanisms for developing resistance to antibiotics. Particularly useful are the two-component regulatory systems (TCSs) [92]. TCSs are comprised of a primitive signal transduction system, where a membrane-bound sensor protein monitors changes in the extracellular environment and then activates a transcriptional regulator to alter gene expression in response to stimulus. TCSs are generally used by bacteria to adapt to their environment, and particular *P. aeruginosa* TCSs such as GAC have been implicated as participating in biofilm formation and antibiotic resistance [119, 175].

Other mechanisms include the horizontal transfer of DNA [176]: the low permeability of the outer membrane of *P. aeruginosa* means that the uptake of small hydrophilic molecules, including particular antibiotics, is restricted [176], membrane efflux (Mex) pumps that

allow it to efflux a broad range of antibiotics including β-lactams [176], and AmpC in the periplasm, a β-lactamase that can efficiently hydrolyse a number of common antibiotics including penicillin [177].

Another issue contributing to antibiotic resistance is the way antibiotics are administered to patients. One such example is that of the commonly used CF antibiotic tobramycin, the use of which results in increased FEV_1 and reduced morbidity [178]. However, translation of *in vitro* microbiological determinations of *P. aeruginosa* inhibitory antibiotic concentrations into clinically achievable concentrations is difficult. Poor penetration of the antibiotic into the bronchial secretions of CF patients impairs its antibiotic activity while increasing the development of antibiotic resistance [179]. Attempts to increase dosages must be balanced with the nephrotoxicity and ototoxicity of the antibiotic [179, 180]. In a study by Smith and colleagues, after 3 months of three times daily 600 mg doses of inhaled tobramycin, the proportion of CF patients with *P. aeruginosa* cultures that have a minimum inhibitory concentration of antibiotic of > 8 μg/mL had increased from 29% to 73%. Thus, care must be taken with the administration of antibiotics to CF patients. Tobramycin, as part of maintenance therapy, is typically administered intermittently (on a monthly basis) to CF patients.

1.2.6 *P. aeruginosa* inter-kingdom signalling

P. aeruginosa QS molecules co-ordinate bacterial virulence, but importantly they are also capable of modifying the immune response of their mammalian hosts in a process termed inter-kingdom signalling. In the CF lung, inter-kingdom signalling further exacerbates the already altered immune signalling. This bipartite attack on the host makes QS an important feature in *P. aeruginosa* pathogenesis. Williams and colleagues demonstrated that both major AHLs produced by *P. aeruginosa* could traverse mammalian cell membranes and, once inside the cell, they retain their biological activity [181]. It is thought that C12HSL enters the cells passively and that the lipophilic nature of the AHLs facilitates their transport across the plasma and nuclear membrane [182, 183].

Once inside the host cells, C12HSL is capable of influencing multiple cellular processes, as summarized in Table 1.3, including modulating multiple aspects of host immunity, inducing apoptosis in a range of cells, modulating calcium transport and inducing the unfolded

Table 1.3 Table of evidence on effects of C12HSL on the mammalian host	
Specific Feature	**Effect**
Immune system	
Peripheral Blood Mononuclear Cells (PBMC)	• Immunosuppressive effect on human PBMC [184, 185] • Influences T-cell cytokine production [186]
Lymphocytes	• Inhibits mitogen-induced lymphocyte proliferation in murine macrophages [187]
NF-κB	• Disrupts NF-κB signalling in murine macrophages, fibroblasts and epithelia [188] • Significant over-representation of differentially expressed genes in the NF-κB pathway in a transcriptome array of human airway epithelial cells treated with C12HSL [189] • Significantly over-represented gene ontology of positive regulation of the NF-κB cascade in a transcriptome array of human airway epithelial cells treated with C12HSL [189]
Tumor necrosis factor alpha (TNF-α)	• Suppress LPS-induced TNF-α secretion in murine macrophages [187, 188, 190] and human macrophages [187] • Significant over-representation of differentially expressed genes in the TNF-α pathway in a transcriptome array of human airway epithelial cells treated with C12HSL [189]
Interleukins (IL) IL-6, IL-8, IL-12	• Increased IL-6 in CF airway epithelial cell lines (*wild-type* and ΔF508) [189] • Influences I*l-6* in murine mast cells [191] • Increase in I*l-6* and I*l-8* gene expression in murine fibroblasts [192] • Increase in *IL6* and *IL8* gene expression in human vascular endothelial cells [192] • Increase in IL-8 neutrophil attractant in human airway epithelial cells [193] • Down-regulates LPS-induced proinflammatory cytokine I*l-12* production in murine macrophages [187] • Significantly over-represented gene ontology of positive regulation of cytokine production in a transcriptome array of human airway epithelial cells treated with C12HSL [189]
Cox-2	• Increase in *Cox2* gene expression in murine fibroblasts [192] • Increase in *COX2* gene expression in human vascular endothelial cells [192] • Increased *COX2* in human lung fibroblasts [194]
Toll-Like Receptors (TLRs)	• Regulate TLR expression in monocytes [195]

Specific Feature	Effect
Nod-Like Receptors (NLRs)	• Significant over-representation of differentially expressed genes in the NLR signalling pathway in a transcriptome array of human airway epithelial cells treated with C12HSL [189]
Mitogen-activated protein kinases (MAPK)	• Stimulation of phagocytic activity through p38 MAPK pathway in human macrophages [196] • Significant over-representation of differentially expressed genes in the MAPK signalling pathway in a transcriptome array of human airway epithelial cells treated with C12HSL [189] • Significantly over-represented gene ontology of MAPK activity in a transcriptome array of human airway epithelial cells treated with C12HSL [189]
c-Jun N-terminal kinases (JNK)	• Significant over-representation of differentially expressed genes in the JNK cascade in a transcriptome array of human airway epithelial cells treated with C12HSL [189]
Apoptosis	
	• Murine macrophages[197, 198] and human macrophages [197] • Murine fibroblasts [192, 199] • Murine mast cells [191] • Human breast carcinoma cells [200] • Human epithelial colorectal adenocarcinoma cells [201] • Human Jurkat T lymphocytes [202] • Human vascular endothelial cells [192] • Human airway epithelia [203]
ER stress and unfolded protein response	
	• Activates PERK, an ER stress inducer, and inhibits protein synthesis in murine embryonic fibroblasts [204] • Increased UPR in human aortic endothelial cells [205] and mouse macrophages [206] • Depolarisation of mitochondrial membrane potential in human airway epithelial cells [203]
Epithelial integrity	
	• Impaired epithelial barrier function via delocalization of tight junction protein in human intestinal epithelia [207, 208] • Causes tight junction disassembly in airway epithelial cells [203]

Specific Feature	Effect
Calcium ion regulation	
	• Calcium release from ER into cytosol in murine fibroblasts [192] • Increased intracellular calcium release in murine and human mast cells [191] • Significantly over-represented gene ontology of calcium signalling in the $CD4^+$ T-cell receptor pathway in a transcriptome array of human airway epithelial cells treated with C12HSL [189] • Significantly over-represented gene ontology of response to calcium ions in a transcriptome array of human airway epithelial cells treated with C12HSL [189] • Significantly over-represented gene ontology of calcium sensitive transcription factors ATF-2, NFATC1 and NFATC2 in a transcriptome array of human airway epithelial cells treated with C12HSL [189] • Increased intracellular calcium release in human airway epithelial cell lines *wild-type* [189, 203] and ΔF508 [189]
Others	
	• Vasoconstriction in porcine coronary arteries [209] • Bradycardia in rats [210] • Induces damage to human spermatozoa [211]

protein response [188, 192, 197, 205, 212]. In fact, microarray analysis of a human alveolar epithelial cell line, A549, showed that treatment with 50 μM C12HSL caused significant changes in expression of approximately 11% of the cell's transcriptome (over 4000 genes) [213]. A similar experiment using C4HSL and 4,5-dihydroxy-2,3-pentanedione, a precursor to a family of signalling molecules widely used in the bacterial community, showed that expression of far fewer genes was affected, 105 and 116 genes respectively, indicating that the C4HSL molecule is far less effective at modulating host cell function. In addition, only 39 genes were common between those with altered expression caused by the three compounds studied [213]. This indicates that the structure of C12HSL may be vitally important for modulating the host immune responses to facilitate infection. In the same study, the authors also observed an increase in mRNA levels of mammalian genes involved in xenobiotic sensing and drug efflux. They followed up this finding with radiolabeled auto-inducer uptake assays and concluded that the host cells may be up-regulating mechanisms to expel C12HSL [213].The mechanisms by which C12HSL causes these changes are poorly understood, and only recently some progress has been made into understanding how the AHLs influence mammalian cellular activities.

In 2008, Jahoor and colleagues identified the mammalian nuclear hormone receptor and a major inflammatory regulator, peroxisome proliferator activated receptor γ (PPARγ) as a binding target for C12HSL [214]. PPARγ is a ligand-dependent transcription factor that binds to a specific peroxisome proliferator response element (PPRE) in the promoter region of a gene, in the form of a heterodimer with retinoid X receptor (RXR) [215, 216]. It then binds an agonist or antagonist that allows for a conformational change, enabling it to recruit co-activators or co-repressors and instigate or suppress transcription. Native PPARγ ligands are typically metabolic products of fatty acids, and are usually unsaturated fatty acids such as 15-hydroxy-eicosatetraenoic acid and prostaglandin J2. PPARs regulate inflammation by modulating NF-κB signalling and influencing the JAK/STAT (c-Jun activated kinase/Signal transducer and activator of transcription) and MAP kinase pathways [217]. C12HSL, through completive inhibition of binding of PPARγ ligands, prevents formation of PPARγ-PPRE transcriptional complex, thereby inhibiting PPARγ-dependent gene expression. In *in vitro* models, C12HSL behaves as a weak PPARγ agonist. In the *in vivo* environment however, where multiple PPARγ ligands are present, the net effect of C12HSL on PPARγ is hypothesized to be negative, because it interferes with stronger endogenous PPARγ agonists [218] through the mechanism summarized in Figure 1.10.

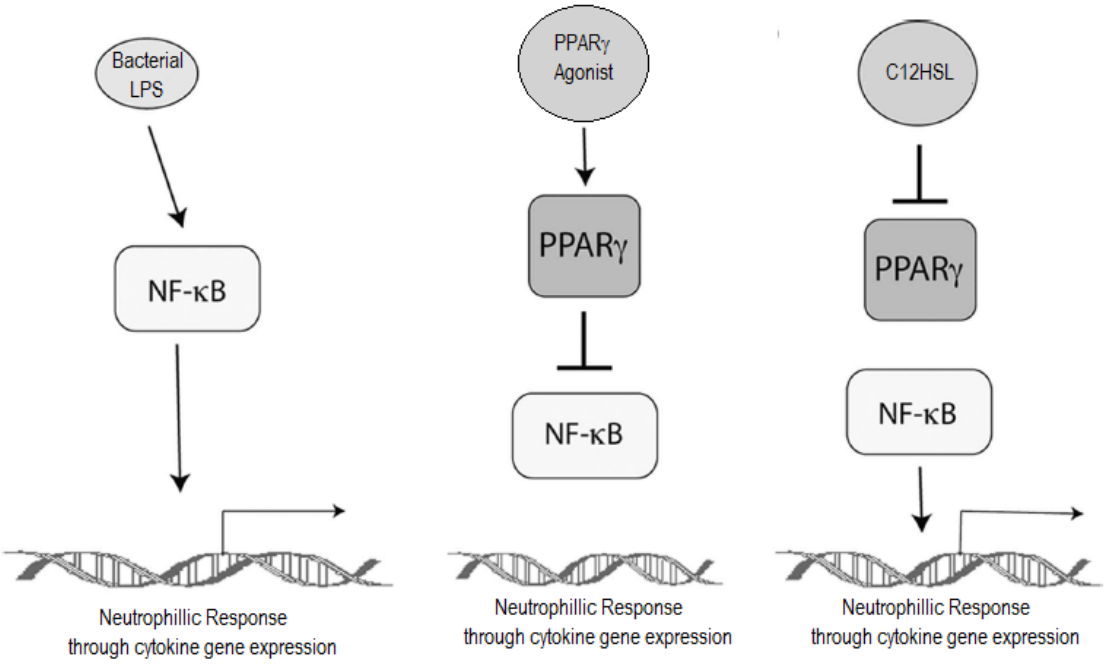

Figure 1.10 Hypothetical model for the disruption by C12HSL of PPARγ-mediated repression of NF-κB. LPS stimulates a neutrophilic response via NF-κB and ligand-bound PPARγ is responsible for the trans-repression of NF-κB regulated genes, exerting an anti-inflammatory effect [219]. C12HSL interferes with binding of normal PPARγ ligands and exerts a net negative effect on PPARγ. This allows it to prevent trans-repression of NF-κB and promotes prolonged inflammation [214]. Figure adapted from Jahoor *et al.*, 2008 [214].

In CF patients, PPARγ activity is also affected by mutations in CFTR. Studies involving *Cftr*-negative mice have shown decreased PPARγ nuclear localization, DNA binding and PPARγ co-activator recruitment [220, 221]. Treatment of the *Cftr*-deficient mice with a PPARγ agonist was able to reverse the effects of the mutation in the gut [220, 221]. Reduced PPARγ levels and/or function has also been demonstrated in CF airway epithelial cells [222], and reduced PPARγ expression was observed in bronchoalveolar lavage cells of children with CF infected with *P. aeruginosa* compared with those infected with other pathogens [223]. It is believed that CFTR defects result in increased oxidative stress that sustains tissue trans-glutaminase-2 activation and inhibits PPARγ SUMOylation (Small Ubiquitin-like Modifier). This favours crosslinking and proteasomal degradation of PPARγ, preventing PPARγ activity [224]. This combined effect of low constitutive PPARγ functionality and bacterial C12HSL competing with PPARγ ligands to bind to PPARγ may help to explain why *P. aeruginosa* is able to persist in the CF lung.

More recently, a second human C12HSL receptor molecule was identified, the GTPase-activating scaffolding protein IQGAP1 [225]. Membrane-bound IQGAP1 plays an essential

role in cell shape, vesicle trafficking, and directional migration [226]. C12HSL is thought to use IQGAP to trigger essential changes in the cytoskeletal network [225]. Reports into the consequences of C12HSL interacting with IQGAP are only beginning to emerge, but IQGAP contains a calmodulin (primary Ca^{2+} sensor)-binding motif, and has previously been described as providing a molecular integration of Ca^{2+}/calmodulin signalling and the cytoskeleton [227].

Increased understanding of the effects of C12HSL on the airways and the mechanisms through which these effects occur is vital in the development of strategies against C12HSL-induced inter-kingdom signalling effects on host cells. Such strategies could assist in reducing the morbidity and mortality associated with *P. aeruginosa* infection.

1.3 QUORUM SENSING INHIBITION

1.3.1 Targeting of QS as a novel therapeutic strategy

The reliance on inter-cellular communication to co-ordinate community wide activity represents an as yet underutilized mechanism through which pathogens can be targeted in the search for novel antibiotic therapies. QS is widely seen as a potential target for a new generation of antimicrobials, the quorum sensing inhibitors (QSI). By inhibiting QS, the control of major regulatory components of *P. aeruginosa* can be modulated, assisting targeted therapies against *P. aeruginosa*. Because many bacteria use QS systems to regulate multiple aspects of cellular function, increased understanding of the cell-to-cell communication in other CF pathogens may also allow for the use of QSI therapies against those pathogens.

The classical QS system seen in Gram-negative bacteria has three components: a) an inducer protein that assists in synthesis of b) the QS signal, and c) a cognate receptor that, when bound to the signal molecule, induces QS dependent gene expression. This model allows three potential mechanisms for QSI.

1.3.1.1 QSI of QS inducer protein

A number of conventional antibiotics used to treat CF patients, including ceftazadime, ciprofloxacin and azithromycin, display strong QSI activity [228, 229]. Though not yet fully understood, their anti-QS activity is thought to operate via their ability to inhibit bacterial protein synthesis, which results in the inhibition of the formation of QS signals by affecting expression of the inducers in the QS circuit. Azithromycin in particular also inhibits alginate formation, and clinical studies have shown its use to be linked with good outcomes in CF patients despite azithromycin having ineffective bactericidal activity at clinically relevant concentrations [229-231].

1.3.1.2 QS inhibition through the QS receptor protein

Competitive inhibition based on utilizing small molecules that mimic AHLs represents another promising QS inhibition strategy. One of the first naturally occurring class of compounds discovered to quench QS were the furanones [232]. Furanones compete with C12HSL to bind the LasR receptor [233], effectively interfering with C12HSL binding. Since the discovery of the furanones, chemically synthesized and structurally diverse furanones

have been shown to display QS inhibition to facilitate clearance of *P. aeruginosa* lung infection in a mouse model. However, there is concern about the toxicity of the furanones in mammals [234] and emerging evidence of *P. aeruginosa* resistance towards these molecules through up-regulation of efflux pumps [235, 236]. Another example of competitive inhibition through the QS receptor protein is the use of the synthetic AHL analogue, meta-bromo-thiolactone, which inhibits *P. aeruginosa* biofilm growth and pyocyanin production, and protects human lung epithelial cells from *P. aeruginosa* induced cell death *in vitro* [237].

1.3.1.3 QS inhibition via QS signal molecule

The most widely investigated QSI strategy is that of directly inactivating the signal molecule. One such strategy utilized antibodies against AHLs to encourage the host immune response to target AHLs and sequester the signalling molecule. Success with this strategy was initially limited because the relatively small size of the AHL molecules limits their immunogenicity. This issue was overcome by conjugating AHLs to larger proteins, and antibodies generated by this means have shown some promising results in protecting against *P. aeruginosa* in mice [238, 239]. However, research into the use of such immunopharmacotherapeutic strategies for QSI is still in its infancy and more research is required to establish its efficacy.

An alternate strategy to inactivate the signalling molecule involves enzymatic degradation. Three main types of enzymes capable of degrading AHLs have been reported in the literature: acylases, oxidoreductases and lactonases. The *P. aeruginosa* AHL acylase PvdQ cleaves the amide bond linking the acyl chain and the homoserine lactone ring, and has been shown to reduce the severity of *P. aeruginosa* infections in a nematode model of *P. aeruginosa* infection [240]. Oxidoreductases, including CYP102A1, a cytochrome from *Bacillus megaterium,* are able to oxidize C12HSL *in vitro*, although further investigation is required to establish how this oxidation affects C12HSL bioactivity and efficacy in *in vivo* [241].

The third type of enzymes capable of degrading QS signals, the lactonases, are perhaps the best studied and the most promising of the potential QS inhibitors. They function by hydrolysing the lactone ring of AHLs, a feature thought to be important in the binding of AHLs to their cognate receptors [242, 243]. Hydrolysis of the lactone ring effectively renders the AHLs incapable of participating in QS. Lactonases capable of degrading various AHLs have been found in a number of bacterial species including *Bacillus sp.* [242], *Agrobacterium tumefaciens* [244], *Ochrobactrum sp* [245] and *Microbacterium testaceum* [246]. More importantly however, a family of mammalian enzymes has been identified as

capable of specific lactonase activity towards AHLs, and particularly towards C12HSL. The paraoxonase (PON) family of enzymes have been shown to display lactonase activity *in vitro* [247, 248] and appear to attenuate *P. aeruginosa* virulence *in vivo* in drosophila and knockout mice models of infection [249, 250]. Because they are lactonase enzymes that are endogenous to mammals, the PONs warrant further scrutiny for their potential role as a component of the host immune response towards bacterial QS.

1.3.2 The paraoxonases

The PONs are a family of mammalian enzymes that consists of three proteins that play roles in inflammatory diseases and are known to hydrolyse bacterial AHLs. The first member of the PON family to be identified was PON1. In 1946, Mazur observed that extracts from a number of human and rabbit tissues were able to hydrolyse the organophosphate di-isopropyl fluorophosphates [251]. Aldridge extended the study by looking at the ability of sera from a number of animals to hydrolyse the organophosphate toxin paraoxon and found an esterase that could catalytically hydrolyse paraoxon, hence the name paraoxonase [252]. It wasn't until the 1996 that the other two PONs were identified by Primo-Parmo and colleagues by searching human cDNA libraries for *PON1* analogues [253]. They found that the PON sequences shared ~70% homology and were positioned adjacent to each other on chromosome 7. In addition, they identified *PON2* and *PON3* in other mammalian species including mouse, turkey and chicken. The PONs are glycosylated proteins with an apparent mass of 40–48 kDa. The protein structure of PON1 has been elucidated and is considered to be a 6-bladed β-propeller. The overall active site structure and catalytic machinery are thought to be conserved in PON2 and PON3 [254]. Much of the research on the PONs is focused on their ability to function as anti-artherogenic agents in both in *in vitro* and *in vivo* models. However, there are numerous reports of the ability of PON to hydrolyse AHLs and also provide protection against oxidative stress.

PON1 and PON3 are primarily expressed in the liver and PON1 is found in the serum, bound to high-density lipoproteins [255-257]. PON2 in contrast is ubiquitously expressed as a membrane-bound protein, mainly associated with the nuclear membrane, mitochondrial membrane and endoplasmic reticulum [258, 259].

1.3.2.1 Mammalian paraoxonases as QSI

From a bacterial infection perspective, the ability of the PONs to hydrolyse AHLs is significant, because it represents an endogenous mechanism through which the immune system counters bacterial QS. PONs are lactonase enzymes, capable of hydrolysing the lactone ring of AHLs. In the absence of the lactone ring, AHLs are incapable of mediating cognate receptor-bound regulation of QS-dependent gene expression [242, 243].

Chun and colleagues in 2004 were the first to observe the inactivation of C12HSL, but not C4HSL, in primary cultures of human airway epithelia and a cultured human bronchoalveolar cell line A549. Upon fractionating the A549 lysates and comparing the soluble cytosolic fraction with the membrane-containing particulate fraction, the authors found that the insoluble membrane fraction contained the majority of the C12HSL-hydrolysing activity. This indicated that the activity was more likely to be membrane associated, but they were unable to identify what was causing this activity [260]. Two subsequent studies showed that sera from humans, mice and a number of other mammals all hydrolysed C12HSL [247, 261]. Ozer and colleagues showed that treatment with PON inhibitors impaired the ability of human serum to hydrolyse C12HSL [247]. A later study showed that almost 90% of the C12HSL hydrolytic activity of human sera can be attributed to PON1 [262]. Ozer and colleagues also grew *P. aeruginosa* biofilms in the presence of sera from wild-type and PON1-KO mice and found that the biofilms grown with the wild-type sera were half the size of the biofilms grown with PON1-KO sera. PON1 has also been shown to have a protective effect against *P. aeruginosa* infection in a *Drosophila melanogaster* model of infection [263].

Draganov and colleagues tested the ability of recombinant PONs to hydrolyse a variety of AHLs, including C12HSL. They discovered that while all the PONs were able to hydrolyse AHLs to some extent, PON2 was far superior in hydrolysing all the AHLs tested [248]. A later study by Teiber and colleagues found that the specific activity of recombinant PON2 for C12HSL was ~25× more than that of PON1 and ~75× more than that of PON3 [262].

There is an increasing body of evidence, as detailed in Table 1.4, that PON2 has the ability to counter *P. aeruginosa* QS and confer *in vivo* protection against *P. aeruginosa* infection and virulence. Consequently, PON2 has potential as a novel therapy against *P. aeruginosa.* In contrast to PON1 and PON3 which are primarily expressed in the liver serum, [255-257], PON2 is ubiquitously expressed, and at particularly high levels in the lungs [264]. This strong expression further strengthens the hypothesis that PON2 may represent an

Table 1.4 Table of evidence for role of PON2 as a QSI and protector against *P. aeruginosa* infection

Evidence provided	Model tested	Reference
Lysates of murine tracheal epithelial cells from wild-type PON2 mice, but not PON2-KO mice, degrade C12HSL	Primary murine tracheal epithelial cells	[264]
PON2-KO derived macrophages show significant impairment of their ability to hydrolyse C12HSL	Primary murine macrophages	[249]
Decreased C12HSL hydrolysis in endothelial cell lines when PON2 expression is inhibited by siRNA	Hepatic and aortic endothelial cell lines	[262]
A human airway epithelial cell line uses PON2 to hydrolyse C12HSL	Human airway epithelial cell line A549	[265]
PON2 hydrolyses C12HSL and protects human keratinocytes from *P. aeruginosa* infection	Primary human keratinocytes	[266]
Rapid intracellular hydrolysis of C12HSL in cell lines from airway epithelia and accumulation of hydrolysed C12HSL within mitochondria	Primary human bronchial epithelial cells	[267]
Increased QS in PON2-KO mouse lungs using QS reporter strains	PON2-KO mice	[264]
PON2-KO mice cleared *P. aeruginosa* much more slowly than their wild-type counterparts	Acute systemic murine model of *P. aeruginosa* infection	[249]

endogenous mechanism through which the immune system counters bacterial QS. However, there are no reports that PON2 can exist as a secreted enzyme, and the intracellular localization of PON2 would indicate that any PON2-mediated hydrolysis of AHLs would be restricted to AHLs that have entered host cells. To target QS by *P. aeruginosa* in the airways, PON2 would need to be delivered to the airways as a purified, recombinant, extracellular protein. A combination of both exogenous rhPON2 and increased endogenous native PON2 would allow targeting of both the regulation of *P. aeruginosa* QS to susceptibility to antibiotics and host immune responses, and of C12HSL-mediated effects on host cells to allow host responses to deal effectively with infection. There are, however, no reports to date of the effects of recombinant human PON2 on *in vitro P.aeruginosa* cultures, and the use of rhPON2 in models of *P. aeruginosa* infection warrant further attention. In addition, the regulation of PON2 expression is poorly understood.

There are reports that PON2 expression is regulated via PPARγ in murine macrophages [268], and that PON2 expression increases as a result of increased oxidative stress through the PI3K pathway involved in cellular functions such as cell growth, proliferation, differentiation, motility, survival and intracellular trafficking [269-271]. Any attempt to pharmacologically increase endogenous PON2 expression will require further elucidation of the regulatory mechanisms of PON2 expression.

1.3.2.3 PON2 has anti-oxidant and anti-apoptotic activity

PON2 is thought to also protect against oxidative stress by reducing reactive oxygen species (ROS). Nuclear membrane- and endoplasmic reticulum-bound PON2 is thought to prevent the formation in and leakage of superoxides from the mitochondria, most likely by modulating Coenzyme Q on the inner mitochondrial membrane and consequently preventing superoxide production [259, 272, 273]. Neutrophils require ROS for the efficient clearance of microbes. During sustained infections, such as those seen in chronic *P. aeruginosa* infections, the accumulation of ROS from the protracted and overwhelming immune response towards persistent *P. aeruginosa* can damage host cells. It is important to note that while PON2 was able to prevent the generation of ROS in a human endothelial cell line, it was ineffective against existing free radicals, indicating that the anti-oxidative role of PON2 is not likely to function via enzymatic clearance of ROS. Therefore, increasing expression of PON2 may not be capable of reducing extracellular neutrophil derived ROS [273]. Further research is needed to better understand the ability of PON2 to protect against ROS, particularly in an infection setting, such as in macrophages or airway epithelia, before PON2 can be considered to protect against extracellular neutrophil derived ROS. However, detection of microbes in the airways by TLRs on host cells results in increased intracellular oxidative stress, and PON2 may play a valuable role in protecting host cells against this increased oxidative stress during infection [78].

One of the major effects of the *P. aeruginosa* QS molecule C12SHL on host cells is its ability to induce ER stress and subsequent cell death through the UPR. Horke and colleagues have shown in a human aortic endothelial cell line that PON2 expression is induced by the UPR and that PON2 can protect against UPR-stimulated apoptosis [259]. These observations were further corroborated by knocking down PON2 in human aortic endothelial cells [205]. Devarajan and colleagues investigated the ability of macrophages from PON2-KO mice to protect against ER stress, and found that PON2 is capable of regulating calcium homeostasis, another feature of the cell affected by C12HSL [189, 192], and facilitates cell survival under ER stress [274].

Furthermore, the anti-apoptotic and anti-oxidative capabilities of PON2 were shown by Altenhöfer and colleagues to be independent of its lactonase activity. These investigators found that abrogation of the lactonase activity of PON2 did not appear to affect the ability of PON2 to protect against ROS and apoptosis [273]. This adds to the complexity of the actions of PON2 and suggests that PON2 exerts dual, distinct, protective influences on host cells exposed to *P. aeruginosa* and its QS signals. When considering therapies that would involve increasing endogenous, native PON2, the additional anti-oxidative and anti-apoptotic roles of PON2 could provide an added layer of protection against C12HSL-mediated effects on host cells.

1.4 HYPOTHESIS AND AIMS

We hypothesized that PON2, the mammalian enzyme capable of hydrolysing the *P. aeruginosa* QS AHL signal molecules, can inhibit *P. aeruginosa* QS, and thereby protect host cells infected with *P. aeruginosa* from AHL-regulated bacterial virulence and AHL-mediated mammalian immunomodulatory activity and cytotoxicity. Consequently, PON2 could be a novel anti-Pseudomonal therapy.

The proposed use of PON2 as an anti-Pseudomonal therapy would involve pharmaceutically increased expression of endogenous native PON2, to provide protection to host cells against C12HSL-mediated effects, and/or application of extracellular rhPON2 to inhibit QS and thereby increase the susceptibility of *P. aeruginosa* to conventional antibiotics and the host immune response. Application of rhPON2 would also offer protection to mammalian cells against AHL-mediated modulation of gene expression by hydrolysing AHLs, thus preventing their accumulation in the extracellular environment and diffusion into host cells.

The work described in this thesis investigates multiple aspects of the use of PON2 as a novel anti-Pseudomonal therapy. Firstly, the effects of C12HSL, the AHL at the top of the *P. aeruginosa* QS hierarchy, on airway epithelial cells was further investigated to add to the already established literature on the topic. Next, we investigated the regulation of PON2 to determine the mechanisms through which endogenous, native PON2 could be up-regulated to provide protection to host cells against intracellular C12HSL-mediated effects. We then synthesized rhPON2 for extracellular application. Using this rhPON2, we investigated the ability of rhPON2 to inhibit *P. aeruginosa* QS and synergize with an antibiotic *in vitro*. Finally, we attempted to establish a murine model of chronic *P. aeruginosa* infection, one that closely mimics the CF phenotype, for *in vivo* investigations on the potential of PON2 as a novel anti-Pseudomonal therapy.

CHAPTER TWO – MATERIALS AND METHODS

2.1 MAMMALIAN CELL CULTURE

2.1.1 Cells used

Details of the mammalian cell lines used are listed in Table 2.1.

Table 2.1 Mammalian cell lines used in this study

Cell Line	Description	Source	Medium
BEAS-2B	Adherent non-cancerous human bronchial epithelial cell line from autopsy	American Type Culture Collection (ATCC)® CRL-9609	Complete Cell culture medium
NuLi-1	Adherent human bronchial epithelial cell line from healthy individual	ATCC® CRl-4011	Bronchial epithelial cell growth medium
CuFi-1	Adherent human bronchial epithelial cell line from individual with CF. Homozygous for ΔF508 *CFTR* mutation	ATCC® CRL4031	Bronchial epithelial cell growth medium

2.1.2. Cell culture methods

2.1.2.1 Media used

2.1.2.1.1 Complete cell culture medium

Cells were grown in complete cell culture medium (CCCM) which consisted of Dulbecco's Modified Eagle Medium (DMEM) (Life Technologies, Carlsbad, CA) supplemented with 10% (*v/v)* Australian origin foetal bovine serum(FBS; Bovogen, VIC, Australia), 500 U/mL penicillin (Life Technologies), 500 µg/mL streptomycin (Life Technologies) and 4 mM L-glutamine (Life Technologies).

2.1.2.1.2 Bronchial epithelial cell growth medium

Serum free bronchial epithelial cell growth medium (BEGM; Lonza, Walkersville, MD) was supplemented according to manufacturer's instructions with provided growth factors, cytokines and supplements. In addition, 500 U/mL penicillin (Life Technologies), 500 µg/mL streptomycin (Life Technologies) and 4 mM L-glutamine (Life Technologies) were added to the culture media.

2.1.2.2 Coating of cell culture surfaces

2.1.2.3.1 BEAS-2B cells

Flasks and plates for BEAS-2B culture were coated with cell culture coating medium prepared in CCCM (Section 2.1.2.1.1) consisting of 0.001 mg/mL bovine plasma fibronectin (Life Technologies), 0.03 mg/mL bovine collagen type-I (Life Technologies), 0.01 mg/mL bovine serum albumin (BSA) and Cohn Fraction V (Sigma, St. Louis, MO) made in Dulbecco's phosphate buffered saline (DPBS; Life Technologies).

Tissue culture surfaces were incubated in cell culture coating medium in a humidified 37°C incubator for 30 minutes before discarding the medium. Table 2.2 shows volumes required to completely coat the surfaces of regularly used culture flasks and dishes. Plates were air dried and stored in sealed bags at room temperature.

Table 2.2 Minimal volume of coating medium used for varying culture dish/flask sizes.

Flask/Dish	Approximate Surface Area	Minimum Volume to cover surface
T-75 flask	75 cm^2	3 mL
T-25 flask	25 cm^2	1 mL
6 well plate	9.5 cm^2	300 µL
12 well plate	3.8 cm^2	100 µL
96 well plate	0.15 cm^2	20 µL

2.1.2.3.2 NuLi and CuFi cells

Flasks and plates for NuLi-1 and CuFi-1 culture were also coated using the volumes specified in Table 2.2. Cell culture surfaces were incubated 18 hours at 37°C in 60 µg/mL human placental collagen Type IV (Sigma) made up in DPBS, before the collagen solution was removed. The surfaces were rinsing three times with ice-cold PBS before being air-dried in a sterile environment overnight. Plates were stored at 4°C.

2.1.2.3 Normal cell growth, counting and passaging

2.1.2.3.1 BEAS-2B

Cells were grown in a humidified incubator at 37°C with 5% CO_2. At each passage, cells were seeded at ~2×10^4 cells/cm^2. When the cells reached 90% confluency (density of ~1.5×10^5 cells/cm^2; 2–3 days after seeding), the cells were passaged. Care was taken to avoid

allowing cells to grow beyond confluency. Passaging involved removal of the medium from the flask before washing the cells in pre warmed (37°C) DPBS (Life Technologies). The cells were then trypsinized with 0.25% Trypsin-EDTA (Life Technologies; 1 mL for T-25, 3 mL for T-75) for five minutes at 37°C or until the adherent cells had detached. An equal volume of CCCM was then added to deactivate the trypsin. The cells were subsequently counted by trypan blue exclusion using a haemocytometer. Next, the cells were centrifuged at 500 × *g* for five minutes. Finally, the supernatant was discarded, and the cells resuspended in fresh medium to appropriate cell density.

2.1.2.3.2 NuLi and CuFi

Cells were grown in a humidified incubator at 37°C with 5% CO_2. At each passage, cells were seeded at ~1×10^4 cells/cm^2. When the cells reached 90% confluency (density of ~5×10^4 cells/cm^2; 2–3 days after seeding), the cells were passaged. This involved removal of the medium from the flask before washing the cells in pre warmed (37°C) DPBS (Life Technologies). The cells were then trypsinized with 0.25% Trypsin-EDTA (Life Technologies (1 mL for T-25, 3 mL for T-75) for five minutes at 37°C or until the adherent cells had detached. An equal volume of BGEM, supplemented with 1% FBS, was then added to deactivate the trypsin. The cells were subsequently counted by trypan blue exclusion using a haemocytometer. Next, the cells were centrifuged at 500 × *g* for five minutes. Finally, the supernatant was discarded, and the cells resuspended in fresh medium to appropriate cell density.

2.2 REAL TIME QUANTITATIVE PCR (qPCR)

2.2.1 Primers

2.2.1.1 Primer design for qPCR

Primers were designed using Primer-Blast (http://www.ncbi.nlm.nih.gov/tools/primer-blast/index.cgi?LINK_L°C=BlastHome) from the National Centre for Biotechnology Information (NCBI) website. Amplicon lengths were kept below 200 bp and primer melting temperatures in a 3°C range around 60°C. Primers were designed to avoid amplification of contaminating genomic DNA by selecting the 'primers must span an exon-exon junction' option. Primers were then picked against cDNA sequences of the genes in question. Primers selected typically had a C or G nucleotide at the 3′ end, an even mix of GC and AT residues and a low self-complementary score.

2.2.1.2 Primers used

Table 2.3 DNA primers used in study

Primer	Forward Sequence	Reverse Sequence	Source
Human PON2 F655, R783	5'-TGCCACAAATGACCACTACTTCT-3'	5'-GGTGAAATATTGATCCCATTTGCTG-3'	This study
pUC/M13	5'-CCCAGTCACGACGTTGTAAAACG-3'	5'-AGCGGATAACAATTTCACACAGG-3'	[275]

Table 2.4 *P. aeruginosa* qPCR primers used in study

Gene	Forward Sequence	Reverse Sequence	Source
psd7	5′-CAAAACTACTGAGCTAGAGTACG-3′	5′-TAAGATCTCAAGGATCCCAACGGCT-3′	[276]
lasI	5′-CAAGTGTTCAAGGAGCGC-3′	5′-GCCAGCAACCGAAAACC-3′	This study
rhlI	5′-GCTGGAAGGGCTTTCCG-3′	5′-GGATGGTCGAACTGGTCG-3′	This study
pqsA	5′-CCCGATACCGCCGTTTATCA-3′	5′-CTGGCCTGGGAGAGAATGTAG-3′	This study
lasR	5′-CCCTGTGGATGCTCAAGGACTAC-3′	5′-GCTTCCGAGCAGTTGCAGATAAC-3′	This study
lasB	5′-GCCGCAAGACCGAGAATG-3′	5′-TCAGGTAGGAGACGTTGTAGAC-3′	This study
algD	5′-GCGACCTGGACCTGGGCT-3′	5′-TCCTCGATCAGCGGGATC-3′	[277]
hcnB	5′-CGGTCGGCTATGGCTTCATC-3′	5′-GCTGCCAGACGTTGCATTC-3′	This study
phz1	5′-ATTCCCAATGCACGCAGTTTC-3′	5′-GAATTCCTGTTCCGCCAGGG-3′	This study
vfr	5′-GCGAAACGCTGTTCTTCATC-3′	5′-AATCACCGCTGTTGAGGTAG-3′	This study

Table 2.5 Human qPCR primers used in study

Gene	Forward Sequence	Reverse Sequence	Source
PON2	5′-GCCAACAATGGGTCTGTTCTCC-3′	5′-CAGCTTCCCATCATACACTGAGGC-3′	[223]
PPARG	5′-AGCTGAACCACCCTGAGTCC-3′	5′-TCATGTCTGTCTCCGTCTTCTTG-3′	[223]
ACTB	5′-GGCTGGCCGGGACCTGACTGA-3′	5′-CTTCTCCTTAATGTCACGCACG-3′	[223]
IL6	5′-TTCTCCACAAGCGCCTTCGGTCCA-3′	5′-AGGGCTGAGATGCCGTCGAGGATGTA-3′	[278]
IL8	5′-TGCTAGCCAGGATCCACAAG-3′	5′-GCTTCCACATGTCCTCACAAC-3′	This study
MAP3K2	5′-GCCAGGGGGTTCAATTAAGG-3′	5′-CTGGCCCCAAAATCTCCTA-3′	This study
TANK	5′-GCAAAAGACTGAGAACTATGAGCAG-3′	5′-CAAGCAGAGGAACACAGCCA-3′	This study
ABCF1	5′-GCCGGAAGCGGAAATAGCAC-3′	5′-ACTTTGTCTGATGGGCTCGTG-3′	This study
MST1	5′-CACTCCTGCTGCTTCTGACT-3′	5′-GAAGGCCCGGCAGTCCATTA-3′	This study
MUC2	5′-CTACTGGTGTGAGTCCAAGG-3′	5′-GGCACTTGGAGGAATAAACTG-3′	[279]
USP40	5′-ACTGGCAGTTTCAAGAGGAAAA-3′	5′-GATTGCTTTTAGAATCATCAGTGGA-3′	This study
XBP1	5′-CCATGGATTCTGGCGGTATTGACT-3′	5′-CCACATTAGCTTGGCTCTCTGTCT-3′	[278]
ATF3	5′-TTGCAGAGCTAAGCAGTCGTGGTA-3′	5′-ATGGTTCTCTGCTGCTGGGATTCT-3′	[278]
CASP3	5′-CATCCAGCCGGAGGCCAGAGC-3′	5′-GCAGTGACGGCTCCGCACCTG-3′	This study
CASP7	5′-TTCAAAGCTGAGGGAGCGTC-3′	5′-ATCATCTGCCATCCCACAAGG-3′	This study
CASP8	5′-ACACTTGGATGCAGGGTTTGA-3′	5′-TAGCTGGATTCTGCAGGCTT-3′	This study
NGFR	5′- GAGGCACCTCCAGAACAAGAC-3′	5′-GCTGTTCCACCTCTTGAAGGC-3′	This study

2.2.1.3 Primer validation

Primers were validated by measuring the PCR efficiency of serial dilutions of cDNA prepared from RNA that contained gene of interest transcripts. The cDNA was diluted 1/4, 1/16, 1/64 and 1/256 and the qPCR carried out using the primers. The cycle crossing threshold (C_T) of the product for each reaction was then noted. The natural logarithm of the cDNA dilution factor was plotted against the C_T. (See method in Table 2.6). The efficiency of the PCR was calculated from the gradient of the line plotted between the natural logarithm of cDNA dilution and the CT. An efficiency of 2 suggested that there was a doubling of DNA at each PCR cycle and that the primers were highly efficient at amplifying the target cDNA. Primers with efficiencies between 1.7 and 2.1 were acceptable, provided the melt curves of the PCR products did not show primer dimerization and were consistent with one PCR product being amplified. Finally, amplicon size was checked by separating PCR products by agarose gel electrophoresis followed by staining with SYBR-II DNA gel stain (Life Technologies).

Table 2.6 Method of qPCR primer efficiency determination		
cDNA dilution	**Plot these two**	
	ln (cDNA dilution)	**C_T**
1	0	from PCR
$\frac{1}{4}$	–1.3863	from PCR
$\frac{1}{16}$	–2.7726	from PCR
$\frac{1}{64}$	–4.1589	from PCR
$\frac{1}{256}$	–5.5451	from PCR
Gradient	Linear regression of the line to find gradient	
PCR Efficiency	$= \mathbf{10}^{(\frac{-1}{gradient})}$	

2.2.2 RNA isolation by phenol–chloroform

RNA isolation by phenol–chloroform was carried out using TRIzol® (Life Technologies), following the manufacturer's instructions with minor modifications as detailed below.

2.2.2.1 Cell lysis for RNA isolation

For cells grown in a six well plate, 1 mL of TRIzol® was sufficient per well. Medium was first removed from the cells and the cells rinsed with DPBS. TRIzol® was added directly to the culture dish and the surface of the well scraped with pipette tip immediately after TRIzol® application. The cells were then lysed in the wells by pipetting up and down several times until homogenous. The lysate was then collected and transferred to a microcentrifuge tube for RNA extraction. Lysates could also be stored at –80°C at this stage for later RNA isolation

2.2.2.2 RNA isolation

The cell lysates were incubated at room temperature for five minutes before 200 μL of chloroform (Merck) was added per mL of cell lysate. The mixture was shaken vigorously by hand for 15 seconds and then incubated at room temperature for three minutes before centrifuging at 12,000 × *g* for 15 minutes at 4°C. This separated the mixture into three distinct phases, with the upper aqueous phase exclusively containing the RNA. The aqueous

phase was carefully aspirated without disturbing the other phases and transferred to a fresh microcentrifuge tube.

When isolating RNA from cells with an expected low yield, 5 μg glycogen was used as an RNA carrier and added at this stage. For every mL of cells homogenized in TRIzol®, 500 μL of 100% isopropanol (Merck) was added to precipitate the RNA. The mixture was shaken and incubated for 10 minutes at room temperature before being centrifuged at 12,000 × *g* for 10 minutes at 4°C.

The supernatant was removed from the tube, leaving only the RNA precipitate. The RNA pellet was rinsed with ice-cold 75% ethanol prepared in nuclease-free water, 1 mL per mL of cell homogenate. Once the 75% ethanol was added, the tubes were briefly vortexed before centrifuging at 7,500 × *g* for five minutes at 4°C. The supernatant was then carefully removed without disturbing the pellet before repeating the rinse step. Once the supernatant was removed, the tube was air dried in a sterile cabinet, though care was taken to not completely dry out the RNA pellet. The pellet was then resuspended in an appropriate volume of nuclease-free water and heated at 65°C for 10 minutes. RNA solution was stored at –80°C for further use.

2.2.2.3 DNase treatment of isolated RNA

DNase treatment of recovered RNA was performed using TURBO DNA-*free*™ Kit (Life Technologies) according to the manufacturer's instructions. A typical reaction consisted of 50 μL of RNA solution with <10 μg total RNA. Briefly, the 10× DNase I buffer was added, followed by 1 μL of TURBO™ DNase (2 units). The reaction was incubated at 37°C for 30 minutes. A 1/10 volume of DNase inactivation reagent was then added to stop the DNase reaction. After a five minute incubation at room temperature with periodic mixing, the tube was centrifuged at 10,000 × *g* for 90 seconds at room temperature. The supernatant containing the RNA was transferred to a fresh tube for quantification, storage and subsequent cDNA synthesis.

2.2.3 R NA extraction by spin column

RNA was also extracted from cells stored in RNALater (Life Technologies) using the ReliaPrep™ RNA Cell Miniprep System (Promega, Madison, WI). Cells in RNALater (Life Technologies) were pelleted by centrifugation at 500 × *g* for five minutes. The supernatant was discarded and the pellet carefully rinsed with ice-cold sterile 1× DPBS (Life Technologies). The cells were then pelleted by centrifugation at 500 × *g* for five minutes and the supernatant discarded. Five hundred microlitres of fresh BL+TG buffer (32.5 μL 1-Thioglycerol (TG) to 3.25 mL BL buffer) was added to the pellet. The pellet was pipetted 7–10 times and then incubated at 4°C for five minutes before pipetting a further 7–10 times to ensure complete lysis of the cells. Then, 170 μL of isopropanol was added to the lysate and mixed by vortexing. The lysate was transferred to a ReliaPrep™ minicolumn assembled according to the manufacturer's specifications and centrifuged at 14,000 × *g* for 30 seconds at room temperature. The liquid in the collection tube was discarded and then 500 μL RNA wash solution was added. The columns were then centrifuged at 14,000 × *g* for 30 seconds at room temperature.

Next, the RNA was DNase-treated by adding 30 μL of DNase I incubation mix (24 μL Yellow Core buffer, 3 μL 0.09 M $MnCl_2$ and 3 μL of DNase I enzyme) to the membrane inside the minicolumn. The membrane was allowed to incubate at room temperature for 15 minutes before 200 μL of column wash buffer solution was added to the minicolumn. The minicolumn was then centrifuged at 14,000 × *g* for 30 seconds. Next, 500 μL of RNA wash solution was added to the minicolumn and centrifuged at 14,000 × *g* for 30 seconds. The collection tube was discarded and the minicolumn moved to a fresh collection tube. A further 300 μL of RNA wash solution was added to the minicolumn and centrifuged at 14,000 × *g* for two minutes. The minicolumn was then transferred to an elution tube and allowed to dry for two minutes.

Finally, to elute the RNA, 20 μL of nuclease free water was added to the minicolumn membrane and the minicolumn centrifuged at 14,000 × *g* for one minute at room temperature. The collected RNA was quantified and then stored at –80°C.

2.2.4 Nucleic acid quantification and quality determination

All purified nucleic acids were quantified using a NanoDrop 1000 spectrophotometer (Thermo Scientific, Waltman, MA, USA). The instrument was blanked with the appropriate diluent before 1.5 μL of nucleic acid sample was loaded for measurement using the 'nucleic acid' setting to determine concentration by measuring absorbance at 260 nm. By comparing the ratios of absorbance at 260/280 nm, the quality of the nucleic acid was determined. For subsequent cDNA synthesis and qPCR, only RNA with absorbance 260/280 nm ratios of 1.8–2.2 were used.

2.2.5 cDNA synthesis

cDNA was synthesized using Transcriptor First Strand cDNA Synthesis Kit (Roche, Mannheim, Germany) according to the manufacturer's instructions. cDNA was synthesized in 20 μL reactions. A maximum of 1 μg of RNA was included, up to a maximum volume of 8 μL in PCR-grade water.

For mammalian RNA, anchored-oligo$(dT)_{18}$ primers, 50 pmol/μL were added to a final concentration of 2.5 μM. The template-primer mixture was then heated at 65°C for 10 minutes to denature secondary RNA structures before immediately cooling on ice. Next, 4 μL of 5× Transcriptor reverse transcriptase reaction buffer, 0.5 μL of Protector RNase inhibitor, 2 μL of 10 mM deoxynucleotide mix and 0.5 μL of Transcriptor reverse transcriptase were added to the reaction tube. The tube was centrifuged briefly and then incubated 30 minutes at 55°C, then 85°C for 10 minutes before finally chilling on ice. The cDNA was stored at –80°C, or used for qPCR.

For bacterial RNA, random hexamer primers, 600 pmol/μL were added to a final concentration of 60 μM. The template-primer mixture was then heated at 65°C for 10 minutes to denature secondary RNA structures before immediately cooling on ice. Next, 4 μL of 5× Transcriptor reverse transcriptase reaction buffer, 0.5 μL of Protector RNase inhibitor, 2 μL of 10 mM deoxynucleotide mix and 0.5 μL of Transcriptor reverse transcriptase were added to the reaction tube. The tube was centrifuged briefly and then

incubated 10 minutes at 25°C, then 50°C for 60 minutes before finally chilling on ice. The cDNA was also stored at –80°C, or used for qPCR.

2.2.6 Quantitative PCR

Real time quantitative PCR (qPCR) was carried out on the LightCycler® 480 II instrument (Roche) using LightCycler® 480 SYBR Green 1 Master Mix (Roche). Reaction volumes were typically 10 μL and prepared in 96 or 384 well plates using a CAS-1200N liquid handling robot (Corbett Robotics, Sydney, NSW, Australia). A typical 10 μL reaction consisted of 5 μL of 2× master mix, 2 μL of primer mix to a final concentration of 0.5 μM, 1 μL of PCR grade water and 2 μL of cDNA template. The plates were sealed with LightCycler® 480 multi-well sealing foil (Roche) before being centrifuged briefly to collect the reactions at the bottom of the wells, at 1500 × *g* at room temperature for two minutes. A typical run used the run conditions outlined in Table 2.7.

Table 2.7 Typical qPCR run conditions

Temperature (°C)	Acquisition Mode	Hold Time (seconds)	Ramp rate (°C/second)	Acquisitions (per °C)
Pre-incubation (1 cycle)				
95	None	600	4.8	-
Amplification (45 cycles)				
95	None	10	4.8	-
60	None	10	2.5	-
72	Single	30	4.8	-
Melting Curves (1 cycle)				
95	None	5	4.8	-
65	None	60	2.5	-
97	Continuous	-	-	10
Cooling (1 cycle)				
40	None	10	2.0	-

2.2.6.1 qPCR Data analysis

The fluorescence data from the qPCR was interpreted by the LightCycler® Software (Roche). The cycle threshold (C_T) was determined using the absolute/second derivative maximum method. The raw C_T values were exported into Excel (Microsoft) spreadsheets for analysis. Melt curves were generated using the melting temperature (T_m) calling analysis.

To calculate fold change of gene expression, the following formula, developed by Livak and Schmittgen, was used [280].

Fold Change in target gene expression relative to untreated sample, relative to reference

$$= \frac{\boldsymbol{PCR\ Efficiency\ of\ target\ gene}^{(\boldsymbol{CT\ Control\ Sample} - \boldsymbol{CT Experimental\ Sample})}}{\boldsymbol{PCR\ Efficiency\ of\ reference\ gene}^{(\boldsymbol{CT\ Control\ Sample} - \boldsymbol{CT Experimental\ Sample})}}$$

2.3 PROTEIN IMMUNOBLOTTING AND DETECTION

2.3.1 Buffers and solutions

2.3.1.1 Cell lysis buffer

Cell lysis buffer consisted of 50 mM Tris-HCl at pH 7.5, 138 mM NaCl, 5 mM EDTA and 1% Triton™ X-100 (Sigma). Prior to use, one tablet of complete, mini, EDTA-free protease inhibitor cocktail (Roche) was added to 10 mL of cell lysis buffer and the complete buffer was stored for up to 3 months at –20°C until use.

2.3.1.2 10% resolving gel solution

The resolving, lower gel for sodium dodecyl sulphate polyacrylamide gel electrophoresis (SDS-PAGE) was a 10% gel capable of resolving proteins with a size of 15–100 kDa. It consisted of 10% (*v/v*) acrylamide/bis solution 37.5:1 (Bio-Rad) in degassed distilled water with 375 mM Tris-HCl (pH 8.8) and 0.1% (*w/v*) SDS. To initialize the polymerization of the gel, 0.1% (*w/v*) ammonium persulphate (Sigma) and 1×10^{-4} % (*v/v*) TEMED (Sigma) were added.

2.3.1.3 5% stacking gel solution

The stacking upper gel for SDS-PAGE consisted of 5% (*v/v*) acrylamide/bis solution 37.5:1 (Bio-Rad) in degassed distilled water with 125 mM Tris-HCl (pH 6.8) and 0.1% (*w/v*) SDS. To initialize the polymerization of the gel, 0.1% (*w/v*) ammonium persulphate (Sigma) and 0.01% (*v/v*) TEMED (Sigma) were added.

2.3.1.4 10× tris-glycine running buffer

The 10× tris-glycine running buffer consisted of 250 mM Tris base (Sigma), 14.4 % (*w/v*) glycine (Sigma), and 1% (*w/v*) SDS in Milli-Q water.

2.3.1.5 Coomassie stain solution

Coomassie stain solution contained 10% acetic acid, 50% methanol with 0.25% (*w/v*) Coomassie Brilliant Blue R-250 (Bio-Rad) in Milli-Q water.

2.3.1.6 Coomassie de-stain solution

Coomassie de-stain solution was 10% acetic acid, 30% methanol in Milli-Q water.

2.3.1.7 10× transfer buffer

The 10× transfer buffer consisted of 250 mM (*w/v*) Tris base (Sigma), 14.4 % (*w/v*) glycine (Sigma) in Milli-Q water.

2.3.1.8 1× protein transfer buffer

The 1× protein transfer buffer was made by diluting 10× transfer buffer ten-fold in Milli-Q water with 20% methanol.

2.3.1.9 Phosphate-buffered saline

Phosphate-buffered saline (PBS) was prepared by dissolving 1 PBS tablet (Thermo Scientific) in 100 mL of Milli-Q water.

2.3.1.10 Blocking buffer

Blocking buffer was a 2% (*w/v*) solution of skim milk powder (Devondale, WA, Australia) in PBS. The buffer was filtered prior to use to prevent spotting downstream.

2.3.1.11 Antibody incubation buffer

Antibody incubation buffer was a 2% (*w/v*) solution of skim milk powder (Devondale) in PBS with the addition of 0.1% (*v/v*) Tween 20 (Sigma). The buffer was filtered prior to the addition of detergent to prevent spotting downstream.

2.3.1.12 Membrane wash buffer

Membrane wash buffer was PBS with the addition of 0.1% (*v/v*) Tween 20 (Sigma).

2.3.1.13 Membrane stripping buffer

Membrane stripping buffer was made up in Milli-Q water and contained 1.5% (*w/v*) glycine, 0.1% (*w/v*) SDS and 1% (*v/v*) Tween-20 (Sigma). The pH was adjusted to 2.2 with HCl.

2.3.2 Preparation of cell lysates for protein analysis

Medium was removed from cells before washing the cells with ice-cold DPBS (Life Technologies). Cell lysis buffer (section 2.3.1.1) was then added to the cells. For six-well plates, 300 μL of ice-cold cell lysis buffer was added per well while for a T-25 flask, 1 mL was used. The cells were incubated at 4°C for 20 minutes, while rocking. Any remaining adherent cells were then scraped off and the cell homogenates transferred to a microcentrifuge tube. The lysates were subjected to ultra-sonication with Microson™ Misonix XL sonicator (Misonix, NY, USA) at the 'high' setting, 20 cycles of five seconds on,

five seconds off, on ice. The homogenized cells were then centrifuged at 2,000 × *g* for 30 seconds at 4°C to pellet cellular debris. The supernatant was collected and stored at –80°C or used for analysis.

2.3.3 Protein quantification

Protein quantification by a modified Lowry assay was carried out using *DC*™ Protein Assay (Bio-Rad), providing a detergent-compatible solution for protein quantification. The microplate assay protocol was used according to the manufacturer's instructions. Protein standards were prepared using BSA in cell lysis buffer, with five concentrations in a range of 200 to 1500 μg/mL. After incubating at room temperature for15 minutes, the absorbance of the samples was determined at 750 nm on a SpectraMax M2 plate-reader (Molecular Devices, Sunnyvale, California). Concentrations of protein were determined against the BSA standards. Second-order polynomial correlation coefficients were typically 0.99 or higher.

2.3.4 Sodium dodecyl sulphate polyacrylamide gel electrophoresis (SDS-PAGE)

2.3.4.1 SDS-PAGE gels

Where possible, 4%–12% Bis-Tris polyacrylamide gels (Bolt® Mini; Life Technologies) were used. When not convenient, Tris-glycine gels were prepared as follows. Gels were prepared in 1.0 mm empty gel cassettes (Life Technologies). Six millilitres of 10% resolving gel solution (Section 2.3.1.2) was added into the gel cassettes. A layer of 0.1% SDS was then carefully layered on top of the resolving gel and the gel allowed to set (~15 minutes). Once it was set, the SDS layer was poured off and a volume of stacking gel (2.3.1.3) applied such that it filled the cassette (~2 mL). An appropriate comb was then slotted into the top and the gel allowed to set. Once set, the cassettes were moved to an XCell *SureLock™* Mini-Cell (Life Technologies) electrophoresis apparatus filled with 1× Tris-glycine running buffer for SDS-PAGE (10× SDS PAGE Tris-glycine running buffer dissolved ten-fold in distilled water).

2.3.4.2 Preparation of samples and electrophoresis conditions

Typically, the sample volume loaded into an SDS-polyacrylamide gel was 20 μL, consisting of between 20–40 μg of total protein. Deionized water and protein together made up 13 μL of the sample volume. Five microlitres of Novex LDS sample buffer (Life Technologies) and 2 μL of Novex reducing agent (Life Technologies) were added to make up the volume to 20 μL.

Samples were then heated at 70°C for 10 minutes before being loaded into the wells of prepared Tris-glycine gel or precast Bolt® Mini gels (Life Technologies). Five microlitres of SeeBlue® Plus2 pre-stained protein standard (Life Technologies) were loaded as molecular weight markers. Electrophoresis was carried out in 1× Tris-glycine running buffer for prepared Tris-glycine gels and MES buffer (Life Technologies) or MOPS buffer (Life Technologies) for the precast Bolt® minigels. The electrophoresis gels were run at the voltages shown in Table 2.8 for the desired times or until the leading dye front reached the bottom.

Table 2.8 Run conditions for SDS-PAGE gels

Type of Gel	Running Buffer	Voltage	Running Time
Poured Tris-glycine	1× Tris-glycine running buffer	100 V	80 minutes
Precast Bis-Tris	1× MES (Life Technologies)	165 V	35 minutes
	1× MOPS (Life Technologies)	165 V	45 minutes

2.3.5 Transfer of protein to nitrocellulose

Wet transfers were carried out when immunoblotting was necessary for precise identification of the protein of interest. Once the SDS-PAGE was complete, the gel was removed from the tank, rinsed in Milli-Q and transferred to a fresh container with pre chilled 1× protein transfer buffer (Section 2.3.1.8). Wet transfers were performed using the Mini Trans-Blot® cell (Bio-Rad) apparatus. The wet transfer assembly was set up as shown in Figure 2.1, submerged in ice-cold 1× protein transfer buffer using nitrocellulose membrane (Hybond-C Extra; Amersham, Arlington Heights IL). Transfer was carried out with 1× protein transfer buffer for 80 minutes at 100 V at room temperature, or overnight at 4°C at 20 V.

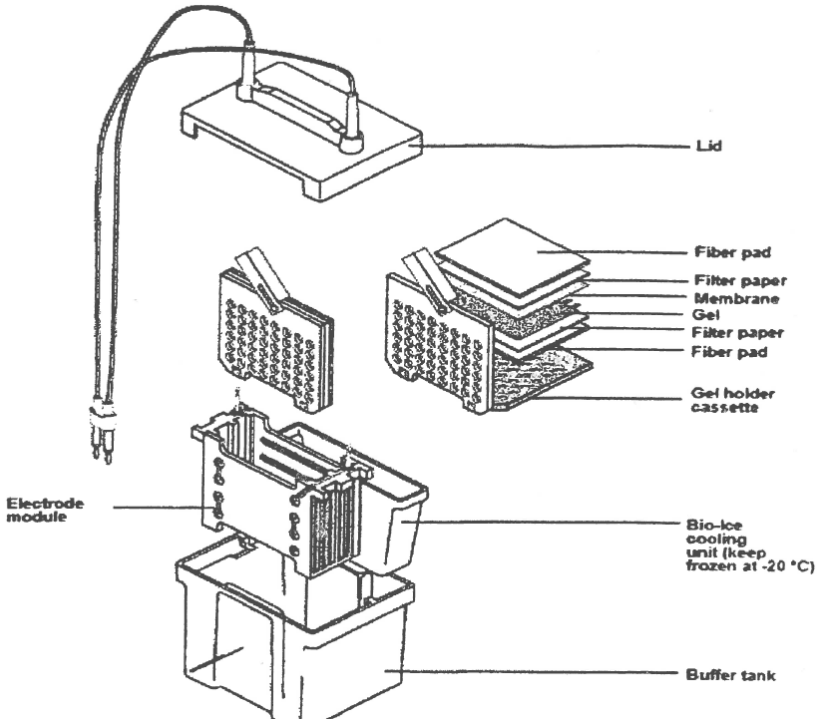

Figure 2.1 Mini Trans-Blot® cell apparatus wet transfer assembly

2.3.6 Visualization of separated proteins on polyacrylamide gels

2.3.6.1 Coomassie staining

Once the SDS-PAGE was completed, the gels were rinsed for one minute in Milli-Q water before the addition of Coomassie stain solution (Section 2.3.1.6). The gels were incubated for 4 hours (or overnight) at room temperature on a shaker, rotating at 40 revolutions per minute (RPM) in an enclosed container. The gels were then transferred to Coomassie de-stain solution and placed on a shaker at 40 RPM. The de-stain solution was replaced regularly until all excess dye had been removed and the protein bands of interest were clearly visible. De-stained gels were visualized on a light box and photographed using a flatbed scanner (Epson 880F; Epson, Suwa, Japan).

2.3.6.2 Silver staining

The more sensitive method for protein detection, silver staining, was carried out using the Silver Stain Plus kit (Bio-Rad). Briefly, each gel was fixed for 20 minutes using 50 mL of fixative enhancer solution containing 50% (*v/v*) methanol, 10% (*v/v*) acetic acid, and 10% supplied fixative enhancer concentrate in Milli-Q water. The gel was rinsed in water twice, 10 minutes each time, using fresh Milli-Q water. Next, the gels were stained in 25 mL of staining solution prepared according to the manufacturer's instructions. Silver stains typically took 20 minutes to develop to the desired intensity. Before excessive background

could develop, the development of the stain was stopped by discarding the stain solution and adding 30 mL of 5% acetic acid solution in Milli-Q water. After incubating for 15 minutes in the stop solution, the gels were transferred to Milli-Q water and visualized on a light box or photographed using a flatbed scanner (Epson 880F; Epson).

2.3.6.3 Immunoblotting of membrane

2.3.6.3.1 Immunoblotting procedure

Once the proteins had been transferred, the membrane was rinsed in Milli-Q water. In order to prevent nonspecific background, the membranes were first incubated for one hour at room temperature (or at 4°C overnight) in blocking buffer. Once blocking was complete, the membranes were transferred to a fresh container containing primary antibody (See Table 2.9 for full list of antibodies used) at the required dilution in antibody incubation buffer. The membrane was incubated for 2 hours at room temperature (or overnight at 4°C). Once again, the membrane was washed in membrane wash buffer, four times, 5 minutes each, using fresh buffer each time. The membrane was then incubated in the appropriate secondary biotinylated antibody in antibody incubation buffer for 1 hour at room temperature. The membrane was then washed again, in membrane wash buffer, four times for 5 minutes each. The membrane was next incubated with the Streptavidin–horse radish peroxidase (HRP; 1:5000 dilution; AbD Serotech, Oxford, UK) conjugate in antibody incubation buffer for 1 hour at room temperature. Finally, the membrane was washed again, in membrane wash buffer, four times, 5 minutes each, using fresh buffer each time.

Table 2.9 Antibodies and dilutions used in study

Antibody Name	Source	Use	Dilution for use	Company
PON2 (C-5)	Mouse Monoclonal	Primary Antibody	1:2500 – 1:5000	Santa Cruz, (Santa Cruz, CA)
β-actin	Mouse Monoclonal	Primary Antibody (loading control)	1:5000	Santa Cruz
Goat Anti-Mouse IgG/A/M (H/L): Biotin	Goat Polyclonal	Secondary Anti-Mouse Antibody	1:5000	AbD Serotech
Streptavidin: HRP	-	Binding to biotin-labelled antibody, HRP based detection	1:5000	AbD Serotech

The washed membrane was allowed to dry before chemiluminescent detection of the protein. Chemiluminescent detection was carried out using Immobilon Western Chemiluminescent HRP substrate (Millipore, ThermoFisher). Working HRP substrate was prepared by mixing in equal quantities the luminol reagent and peroxide solution. Approximately, 100 μL of the working HRP substrate was required per cm^2 of membrane. The working substrate was allowed to warm up to room temperature before being applied to the membrane, ensuring complete and equal coverage. The membrane was incubated for 5 minutes at room temperature before chemiluminescent detection using Carestream Image Station 2000 (Carestream Molecular Imaging; Rochester, NY).

2.3.6.3.2 Stripping membranes

When investigating more than one protein on the same blot, membranes were stripped prior to re-staining for the second protein. The membranes were incubated at room temperature for 15 minutes with the membrane stripping buffer before the buffer was discarded. The process was then repeated. Next the membrane was rinsed twice with antibody incubation buffer, 10 minutes each time. The membrane could then be blocked and immunoblotted again as per section 2.3.6.3.1.

2.3.6.3.3 Dot blot

Dot blots were used for rapid detection of protein without the use of SDS-PAGE. Protein samples were directly applied to nitrocellulose membranes (Hybond-C Extra; Amersham) in pre-marked 2 cm^2 boxes, a maximum of 5 μL per box. Whole cells could also be applied to the membrane but were boiled first. The membrane was then allowed to air dry for 30 minutes. Once dry, the membrane was rinsed with Milli-Q water before the immunoblotting method described in section 2.3.6.3.1 was used to detect the protein.

2.4 TRANSFECTIONS AND LUCIFERASE ASSAYS

2.4.1 Preparation of mammalian cells for transfection

BEAS-2B cells were seeded at 1.5×10^5 cells per well in a 12 well plate or 1.5×10^4 cells per well in a 96 well plate in CCCM without antibiotics. The cells were allowed to recover overnight in a humidified incubator at 37°C with 5% CO_2 prior to transfection.

2.4.2 Mini/midi preps

To obtain large quantities of plasmid DNA, mini/midi preps were required. The preps were carried out using PureYield™ Plasmid Mini-prep/Midi-prep System (Promega) following the manufacturer's instructions for standard DNA purification by centrifugation. The eluted DNA was quantified using the nucleic acid quantification method described in section 2.2.4 and stored at 4°C.

2.4.3 Transfection of mammalian cells

Transfection-quality DNA from mini/midi preps was used for the transfections and the $A_{260/280}$ ratios were confirmed to be between 1.7–1.9. The medium used for transfections was Opti-MEM® (Life Technologies). Transfection complexes were prepared in 60 μL reactions. Opti-MEM® was added to a fresh microcentrifuge tube so that upon the addition of transfection reagent and DNA, the final volume would be 60 μL. A total of 1 μg of DNA was added to the Opti-MEM® and vortexed to mix. For co-transfections, the total DNA comprised a predefined ratio of the plasmid DNAs being transfected. The transfection reagent FuGENE® HD (Promega) was then added drop wise, directly into the medium. The reagent was not allowed to make contact with the side of the tube. Three microlitres of the transfection reagent were used per μg of DNA. The complexes were mixed immediately and allowed to incubate at room temperature for 15 minutes. Sixty microlitres of the complex

was then added to each well of a 12 well plate. For 96 well plates, 6 μL were used per well. The cells were then returned to the humidified 37°C incubators.

All transfected plasmids were co-transfected with a plasmid constitutively expressing Renilla luciferase (pGL4.75 (hRLUC/CMV) to normalize for transfection efficiency (For list of plasmids used, refer to Table 3.2.1).

2.4.4 Luciferase assay

Luciferase expression in the transfected cells was measured using the Dual-Luciferase® Reporter assay system (Promega). At the time of measurement, the medium was removed from the cells and the cells rinsed with DPBS. All liquid was removed from the well and the supplied passive lysis buffer added to the cells, 100 μL per well, in 12 well plates. The plate was incubated for 2 minutes at room temperature before the cells were scraped with a pipette tip and then aspirated into a fresh microcentrifuge tube. Care was taken to minimize the generation of bubbles. The cells were frozen at –20°C immediately and then allowed to thaw. The thawed lysates were then frozen overnight at –80°C prior to assay.

Once two freeze-thaw cycles had been achieved, 10 μL of the samples were added to each well of a white flat-bottomed 96-well microplate. LARII reagent was prepared according to the manufacturer's instructions and 50 μL added to each well. The firefly luciferase activity was measured using the GlowMax® (Promega) instrument. The Stop & Glow® reagent was then prepared according to the manufacturer's instructions and 50 μL added to each well. This time, the Renilla luciferase activity was measured using the GlowMax® (Promega) instrument.

2.5 BACTERIAL CULTURE

2.5.1 Buffers and Media

2.5.1.1 Lysogeny broth (LB) (Lennox)

LB was prepared using the Lennox formulation, with 1% (*w/v*) tryptone (Thermo Fisher), 0.5% (*w/v*) yeast extract (Thermo Fisher) and 0.5% (*w/v*) NaCl (Thermo Fisher) in distilled water. The broth was then sterilized by autoclaving at 121°C.

2.5.1.2 LB agar with/without antibiotics

LB agar was prepared using the same formulation as LB, with the addition of 1% (*w/v*) bacto-agar (Thermo Fisher). The solution was autoclaved at 121°C to sterilize before cooling to 50°C. At this point any relevant antibiotics (ampicillin at 100 μg/mL and kanamycin at 50 μg/mL; Sigma) were added to the medium. The medium was then poured into sterile 90 mm petri dishes, ~15 mL per dish, and allowed to cool before storing at 4°C.

2.5.1.3 0.85% saline

The 0.85% saline solution was prepared by dissolving NaCl (Thermo Fisher) 0.85% (*w/v*) in distilled water and autoclaving at 121°C to sterilize.

2.5.1.4 2× glycerol freezing medium

Glycerol freezing medium for storage of bacterial cultures was prepared by mixing glycerol (manufacturer) 50% (*v/v*) in LB medium. The medium was then autoclaved at 121°C to sterilize.

2.5.1.5 Crystal violet biofilm stain

Crystal violet stain was a 0.1% (*w/v*) solution of crystal violet (Sigma) in Milli-Q water.

2.5.2 Culture methods

2.5.2.1 Streaking plates

Using a sterile inoculation loop, a single colony from a petri dish, or revived from a glycerol stock, was transferred to a fresh agar medium plate. The plates were then inverted and allowed to incubate in the appropriate growth conditions. Typically, for *Escherichia coli* and *P. aeruginosa*, this was 37°C.

2.5.2.2 Spread plating

A known volume (typically 100 μL) of bacterial culture was transferred to a fresh agar medium plate. Using a sterile spreader, the inoculum was spread over the plate to ensure complete coverage. The plates were then inverted and allowed to incubate under the appropriate growth conditions. Typically, for *E. coli* and *P. aeruginosa*, this was 37°C.

2.5.2.3 Overnight culture

To grow bacteria to stationary phase overnight, an overnight broth was used. A 2 mL volume of sterile culture medium in a 15 mL loosely capped polypropylene (BD Falcon, Bedford, MA) centrifuge tube was inoculated with a single colony of bacteria and grown overnight (~18 hours). The culture was then incubated in the appropriate growth conditions. Typically, for *E. coli* and *P. aeruginosa*, this was 37°C, with shaking at 220 RPM.

2.5.2.4 Planktonic growth

For the planktonic growth of cultures, a sterile flask with the desired volume of media was inoculated with the desired number of bacteria. The volume of media was less than 40% of the volume of the flask to provide adequate aeration of the medium during growth. The culture was then incubated in the appropriate growth conditions. Typically, for *E. coli* and *P. aeruginosa*, this was 37°C, with shaking at 220 RPM.

2.5.2.5 Glycerol stocks

Glycerol stocks were prepared in LB broth using 2× glycerol freezing media. Cultures were grown to stationary phase in LB and then mixed 1:1 in 2× glycerol freezing media. This gave a final glycerol concentration of 25%. Stocks were then stored at –80°C.

2.5.3 Enumeration

2.5.3.1 Optical density

To determine the optical density at 600 nm (OD_{600nm}) of a culture, 100 μL was transferred in triplicate to a three wells of a 96 well microplate and the absorbance at 600 nm was read using a SpectraMax M2 plate-reader (Molecular Devices).

2.5.3.2 Determination of colony forming units (CFU)

In order to enumerate the CFU in a culture, 100 μL aliquots were removed from culture and serially diluted ten-fold in sterile 0.85% saline. Each dilution was then spread-plated onto agar medium plates, 100 μL per plate, in triplicate. The plates were inverted and incubated at 37°C overnight. The spread plates where the number of colonies were between 30 and 300 were counted, averaged and the final CFU established by accounting for the dilution factor. When the cell density of cultures could be estimated, only those dilutions expected to have between 30 and 300 colonies were spread-plated.

2.5.3.2 qPCR

The bacterial strains were grown to stationary phase in a 10 mL overnight culture. The OD_{600nm} was measured and then the cultures ten-fold serially diluted to 10^{-4} in triplicate, in 1.1 mL volumes. A 100 μL aliquot was taken from each dilution for CFU determination by spread plating. RNA was extracted from the remaining volume by centrifuging at 500 × *g* for 5 minutes to remove the culture medium and resuspending in TRIzol®. The RNA was extracted using TRIzol®, DNase treated, cDNA synthesized and then qPCR carried out on the cDNA using primers specific for the bacteria using the LightCyler platform (Roche) as described in section 2.2. For *P. aeruginosa,* the primer target was the 16S ribosomal RNA, using *psd7* primers designed by Matsuda and colleagues[276] (sequence in Table 2.3). The cell counts were used to generate a standard with their corresponding C_T values and OD_{600nm}, the slope of which allowed enumeration of bacteria from a given C_T value or OD_{600nm}.

2.6 INSECT CELL CULTURE

2.6.1 Cell lines

Details of the insect cell lines used are listed in Table 2.10.

Table 2.10 Insect cell lines used

Cell Line	Details	Source	Source (Lot Number)	Medium
Sf9 in Sf900III medium [281]	Clonal isolate of IPLBSF21-AE cell line	Pupal ovarian tissue of fall army worm *Spodoptera frugiperda*	Life Technologies (906942)	Sf900 III(Life technologies)
High Five™[282]	BTI-TN-5B1-4 cell line	Ovarian cells of cabbage looper *Trichoplusia ni*	Life Technologies (1031955)	Complete High Five culture medium

2.6.2 Culture media and methods

2.6.2.1 - Complete High Five culture medium

Complete High Five culture medium consisted of Express Five™ medium containing 10 μg/mL gentamycin (Sigma) and 20 mM L-glutamine (Life Technologies).

2.6.2.2 Microscopic visualisation of cells

Insect cells were regularly monitored for growth, confluency and signs of infection using microscopic visualisation. In addition, during baculovirus infection, progress of infections was monitored by microscopic imaging of cultures at intervals. Microscopic visualisation and photography was carried out using a Leica DM IL inverted microscope (Leica Microsystems, Wetzlar, Germany) with a Leica DFC320 camera (Leica Microsystems).

2.6.3 Culturing insect cells

2.6.3.1 Resuscitating cells from cryostorage

2.6.3.1.1 Sf9 cells in Sf900III

Sf9 cells were resuscitated from storage in liquid nitrogen as follows. Vials containing cells were thawed rapidly before the contents were transferred to a 250 mL flat-bottom polycarbonate Erlenmeyer shaker flask with vented polypropylene cap (Corning, Corning, NY)) containing 28.5 mL Sf-900-III medium (Life Technologies) pre-warmed to 28°C. The shaker flask was then moved to an orbital shaker at 28°C under atmospheric conditions and shaken at 130 RPM in the dark.

2.6.3.1.2 High Five™ cells

High Five™ cells were resuscitated from storage in liquid nitrogen as follows. Vials containing cells were thawed rapidly before the contents were transferred to 15 mL polypropylene centrifuge tubes (BD Flacon) containing 4 mL of pre warmed complete High Five™ culture medium. The tube was centrifuged at room temperature for 5 minutes at 500 × *g*. The supernatant was discarded and the cells resuspended in 5 mL complete High Five™ culture medium.

A frozen vial of High Five™ cells was rapidly thawed by rolling between the palms of the hand. One millilitre of cells at 3×10^6 cells/mL was transferred to a 15 mL centrifuge tube containing 4 mL of pre-warmed complete High Five™ culture medium. The tube was centrifuged at room temperature for 5 minutes at 500 × *g*. The supernatant was discarded and the cells resuspended in 5 mL complete High Five™ culture medium. This was done to remove the cytotoxic DMSO in the freezing medium. The mixture was used to seed a T-25 tissue culture flask (vented lid) at cell density of 2.5×10^4 cells/cm^2 and the flask incubated in a humidified incubator at 28°C under atmospheric conditions.

2.6.3.2 Adherent cell culture and passage

Once the adherent High Five™ cells had reached a density of 1.5×10^5 cells/cm^2, the cultures were passaged. High Five™ cells have an approximate doubling time of 18–24 hours and this, along with observing the cultures under a microscope for signs of confluency, allowed establishment of the best time to passage the cells. The cells were also monitored daily for signs of distress and microbial contamination.

The cells were detached by sloughing the adherent monolayer. All but 1 mL of medium was removed from the flask (5 mL when growing cells in T-75s). The flask was tilted on its side so that the medium collected in one corner. Some media was drawn up with a sterile Pasteur (or plastic dropper) pipette and starting from the bottom corner of the flask, media was gently streamed across the cells in a side to side motion, moving upwards each time. This process was repeated as gently as possible until all the cells were dislodged. The cells were then counted by trypan blue exclusion, and the viability determined. The cells were diluted to 5×10^5 cells/mL and 5 mL transferred to a fresh T-25 flask. When expanding the culture to a T-75 flask, 15 mL of 5×10^5 cells/mL were used. A seeding density of 2.5×10^4 cells/cm^2 was maintained. The flasks were then incubated in a humidified incubator at 28°C under atmospheric conditions.

2.6.3.3 Adapting cells to suspension culture

High Five™ cells needed to be adapted to suspension growth before they could be infected with PON2-expressing baculovirus. Before they could be moved to suspension culture, the High Five cells needed to be growing healthily in a monolayer. Once consistent passages of >90% viability were obtained from the adherent cultures, the cells could be transferred to a suspension culture. A minimum total volume of 40 mL of 7×10^5 cells/mL were required to initiate the culture. Once enough cells were available in adherent culture, the cells were detached, quantified and concentration adjusted to 7×10^5 cells/mL.

Forty millilitres of cells were then transferred to a 250 mL flat-bottom polycarbonate Erlenmeyer shaker flask with a vented polypropylene cap (Corning). The medium was supplemented with 10 units/mL of porcine heparin (Sigma) to prevent cell aggregation. The shaker flask was then moved to an orbital shaker at 28°C and shaken at 130 RPM in the dark. The cells were monitored for viability and doubling time at each passage. The cells were considered to be adapted to suspension culture once the viability was >98% and the cells were doubling every 18–24 hours. Once adapted, the cells were weaned off the heparin by adding medium with decreasing heparin concentrations when passaging cells. High Five™ cells were typically weaned off heparin in 2–3 passages.

2.6.3.4 Passaging suspension cultures

During normal growth, and during infections, both Sf9 and High Five ™ cells were grown in suspension cultures, in the dark, in an orbital shaker. The cells were grown at 28°C under atmospheric conditions in 250 mL flat-bottomed polycarbonate Erlenmeyer shaker flasks with vented polypropylene caps (Corning). Confluency of the shaker cultures was

approximately 2×10^6 cells/mL. The Sf9 cells doubled every 72 hours and High Five cells doubled every 18–24 hours. Once the cultures were estimated to be confluent, they were passaged. Firstly, the cells were enumerated by trypan blue exclusion and the viability of the cells determined. The cells were then diluted to 5×10^5cells/mL in the appropriate medium in fresh culture flasks and returned to the orbital shaker.

2.6.3.5 Cryostorage of insect cells

Cells were stored in liquid nitrogen at the densities indicated in Table 2.9 below. The cells were centrifuged at $500 \times g$ at room temperature for 10 minutes. The supernatant was removed and used as conditioned medium for preparing the freezing medium. The cells were then resuspended at the appropriate concentration in the freezing medium as per Table 2.11 and the appropriate volume dispensed into sterile, pre chilled cryovials. The cryovials were placed in a cryo-cooler overnight at –80°C before moving to liquid nitrogen stores.

Table 2.11 Cryostorage conditions for cultured insect cells

Cell Line	Freezing Medium	Density (cells/mL)	Total volume / cryovial
Sf9	46.25% conditioned Sf900 III medium 46.25 fresh Sf900 III medium 7.5% DMSO	1×10^7	1.5 mL
High Five	42.5% conditioned High Five medium 42.5% fresh High Five medium 10% DMSO 5% FBS	3×10^6	1.0 mL

2.6.4 Baculovirus titre determination

Viral titres were determined using the end-point dilution method [281], based on estimation of the dilution of virus that would infect 50% of cultures. Briefly, ten-fold serial dilutions of virus stock were prepared and dilutions of 10^{-5}–10^{-9} were appropriate for most. Ten microliter aliquots of each dilution was mixed with 100 μL aliquots of Sf9 cell suspensions (in SF900 III medium; 1×10^5 cells/mL) and used to seed wells in 96-well cell culture plates (Corning). Each viral dilution along with Sf9 cells was seeded with 12

technical replicates (one row on 96 well plates). Sf9 cells without virus were used as a control. Plates were incubated in the dark at 28°C in a humidified environment to prevent dehydration. Cells were examined by light microscopy for virus replication and resultant Sf9 cell death after three days. All wells that showed signs of infection were scored as positive, and the results tabulated. The plaque forming units were determined as described by O'Reilly and colleagues [281]. An example of the calculation of the viral titre based on the endpoint dilution method can be found in Appendix 8.1

2.7 DATA HANDLING AND STATISTICS

Digital images were processed with the GIMP2 software (v 2.8; http://www.gimp.org). Immunoblot intensities were analysed by densitometry using ImageJ (v.146; NIH, Bethesda, MD). All statistical analysis was performed with GraphPad Prism (v 6.0; GraphPad, San Diego CA).

CHAPTER THREE – *P. AERUGINOSA* QS SIGNAL C12HSL EXERTS CONCENTRATION-DEPENDENT EFFECTS ON HUMAN AIRWAY EPITHELIA

3.1 INTRODUCTION

Many Gram-negative bacteria produce acylated homoserine lactone (AHL) molecules, to sense and co-ordinate their population growth via the quorum sensing (QS) mechanism. In *P. aeruginosa, N*-3-oxo-dodecanoyl-*L*-homoserine lactone (C12HSL) is the principal signalling molecule in this organisms hierarchical QS systems.

C12HSL consists of a homoserine lactone ring with a fatty *N*-acyl group, and its intracellular and extracellular concentrations have been shown to vary in response to the growth phase of bacterial cells. Thus for example, during its planktonic growth phase, *P. aeruginosa* has been shown to secrete sub-micromolar (μM) amounts of C12HSL, while concentrations as high as 600 μM have been detected in mature biofilms produced by this organism [283]. Importantly, for the purposes of this study, the C12HSL produced by *P. aeruginosa* during infection has been shown to readily traverse mammalian cell membranes and to influence the normal functions of multiple cellular processes. C12HSL has been shown to inhibit T-lymphocyte proliferation and function [184, 186, 187, 284], as well as modulate antibody production by B-lymphocytes [186, 187, 284]. In addition, C12HSL has been demonstrated to affect host protein synthesis by inducing endoplasmic reticulum stress, modulating calcium transport [192] and modifying ER structures [212]. C12HSL also appears to be a potent inducer of genes whose protein products are involved in the unfolded protein response (UPR) and apoptosis [192, 197, 202, 203]. The precise intracellular concentrations of C12HSL required to elicit these multiple cellular responses in the host is not known. Moreover, intracellular concentrations of C12HSL are also likely to be influenced by host proteins and varying pH levels, which all together often make it difficult for investigators to determine the precise biologically relevant dose of C12HSL to use in *in vitro* studies. In line with this, it is also generally realised that the *in vitro* effects of C12HSL on inflammation are dependent upon the concentration of C12HSL. Concentrations as low as one pico molar C12HSL have been shown to have immunomodulatory activity, at least in *in vitro* experiments [285], whereas 10-100 μM, or else higher concentrations of C12HSL, have been widely used by investigators interested in provoking more pronounced immunomodulatory responses [187, 188, 192, 197, 205, 212]. In this context, it is important to point out that concentrations of C12HSL below 10 μM, appear to induce anti-inflammatory responses, while concentrations above 20 μM seem to activate pro-inflammatory and pro-apoptotic mechanisms [217].

To gain further insight into the cellular pathways induced by C12HSL, Bryan and colleagues (2010) performed a whole transcriptome analysis in human alveolar epithelial (A549) cells exposed to 50 μM C12HSL. These authors observed significant changes in the expression levels of over 4000 genes, representing ~ 11% of the transcriptome of the alveolar epithelial cells. [213]. In addition, the results of their study seemed to suggest that 50 μM C12HSL induced proinflammatory responses in treated cells [15], which is consistent with a previous report showing that high concentrations (above 20μM) of C12HSL are pro-inflammatory and pro-apoptotic [14]. On this line, research in our laboratory recently performed a whole transcriptome study in human bronchial epithelial cells being exposed to a concentration of C12HSL (10 μM), largely assumed only to trigger anti-inflammatory responses. [Unpublished Honours Thesis [286]](Table, 3.1; Appendix 8.2 for complete data set).

Table 3.1 Selected details of an array probed with RNA extracted from airway epithelia treated with 10 μM C12HSL [Unpublished honours thesis [286]]. See Appendix 8.2 for complete data set

Array Details		
Array platform	GeneChip Human Transcriptome array 2.0 (Affymetrix)	
Array details	High-resolution array consisting over six million probes encompassing coding regions and non-coding transcripts/exon-exon splice junctions.	
Experimental Details		
Cell type	Human Airway Epithelial Cell line – BEAS-2B	
Treatment	Treatment – Six hour exposure to 10 μM C12HSL dissolved in 1% DMSO (*v/v*) in cell culture medium Control – Six hour exposure to 1% DMSO (*v/v*) in cell culture medium 1% DMSO (*v/v)* in cell culture media for six hours	
Analysis software	Ingenuity Pathway analysis (IPA, Ingenuity Systems)	
Selected Results		
Genes differentially Expressed	2941 (cut-off - greater than two fold with $p < 0.05$)	
Selected altered pathways (as determined by Ingenuity Pathway Analysis)	**Ingenuity Canonical Pathways**	**–Log (P-value) (>1.3 = significant)**
	Protein kinase Signalling	3.47
	3-phosphoinositide biosynthesis	2.56
	Calcium signalling	2.44
	PPAR signalling	2.38
	NF-κB signalling	1.68

Surprisingly, that study produced similar results to those reported by Bryan and colleagues, in so far as genes involved in calcium signalling, cell cycling, apoptosis, and the UPR pathway were all found to be differentially expressed in 10μM C12HSL- treated bronchial epithelial cells compared to control (Table 3.1). Up until this point, however, the results of the whole transcriptome study [Unpublished Honours Thesis 286]] have not been validated.

In this section of the thesis, an attempt was made to validate some of the results obtained in the whole transcriptome study involving human bronchial epithelial cells (with and without functional CFTR) being exposed to 10 μM C12HSL[Unpublished Honours Thesis [286]]. The ability of C12HSL to induce apoptosis in respiratory epithelial cells, as well as its effects on cell viability and metabolism, were also investigated.

3.2 MATERIALS AND METHODS

A description of the materials and methods for this chapter is provided in chapter two. Additional materials and methods specific to this chapter are described below.

3.2.1 Cell lines

The respiratory epithelial cell lines BEAS-2B (wild-type *CFTR*), Nuli-1 (wild-type *CFTR*) [287], and CuFi-1 (ΔF508/ΔF508 *CFTR*) [287] were cultured as described previously (chapter two).

3.2.2 Microarray validation by RT-qPCR

To validate the gene expression changes observed in our transcriptome study in human bronchial epithelial cells exposed to 10 μM C12HSL, RT-qPCR was performed as described in chapter two to measure the expression levels of various genes (Table 3.2). The primers used are shown in Table 2.5. Complimentary DNA synthesis was carried out on the total RNA samples used in our initial transcriptome study, as described in chapter two. Gene expression measured by RT-qPCR was normalized to the commonly used reference gene *ACTB* which codes for the human β-actin protein. This reference gene is widely used in the literature to study changes in gene expression of epithelial cells and results in our lab show that the gene is stably expressed in the studied cell lines.

3.2.3 Flow cytometry detection of apoptosis

Apoptosis was detected using FITC-Annexin V (BD Biosciences, Mountainview, CA) antibody and propidium iodide (PI) dye. Annexin V detects the apoptosis-specific cell surface marker phosphatidylserine (PS). BEAS-2B cells were seeded in six well plates at 2×10^5 cells/well 24 hours prior to treatment. The growth medium was then changed, and fresh medium was

added containing either 1% DMSO as a vehicle control, or else varying concentrations of C12HSL (10, or 50 μM) also prepared in 1% DMSO. Solubility of C12HSL was checked by dissolving C12HSL to both concentrations and then measuring against pre-prepared standard using UPLC-MS. After six hours of treatment, the growth medium was removed, and cultured cells trypsinized and pelleted at 500 × *g* for five minutes before the pellet was washed twice in ice cold PBS. Cells were then resuspended in ice cold 1× binding buffer (0.01 M HEPES (pH 7.4), 0.14 M NaCl, and 2.5 mM $CaCl_2$) at a concentration of 1×10^6 cells/mL. Next, a 100 μL aliquot of cells was removed and mixed with 5 μL of FITC Annexin V and 10 μL of PI (50 μg/mL stock). The FITC-conjugated Annexin V binds PS to the surface of apoptotic cells, while PI dye enters cells that have lost their membrane integrity; in turn, this assay can successfully differentiate between early apoptotic (Annexin V positive, PI negative cells) and necrotic/late apoptotic cells (Annexin V and PI positive) cells. The tubes were gently vortexed and incubated at 25 °C in the dark for 15 minutes. A further 400 μL of 1 × binding buffer was then added; the cells passed through a nylon filter; and analysis carried out using a BD FACS Canto II flow cytometer (BD Biosciences). Ten thousand cells were counted for each sample. FITC and PE compensation controls were used for software compensation of spectra overlap for FITC and PE fluorescence. Software compensation and analysis of the results was carried out using FlowJo (TreeStar, San Carlos, CA) and GraphPad prism (La Jolla, CA). Apoptotic cells were considered to be those that stained FITC Annexin V positive and PI negative.

3.2.4 Effects of C12HSL on cytotoxicity and cell metabolism

To determine the cytotoxic effects of C12HSL on airway epithelia, the CellTox Green Cytotoxicity assay (Promega) was used. The assay employs a proprietary asymmetric cyanine dye that is usually excluded from viable cells and preferentially stains the DNA from dead cells. This assay was multiplexed with RealTime-Glo™ MT Cell Viability assay (Promega), which is a bioluminescent assay that measures the reducing potential of cells, thereby allowing the effects of C12HSL on the metabolic activity of the cell lines also to be determined. Cells were seeded at 1×10^4 cells/well in a 96 well plate for 24 hours prior to treatment. The growth medium was then changed and fresh medium supplemented with varying concentrations of C12HSL, along with the manufacturer-specified amount of dye, and luciferase and substrate added. The fluorescence (485 nm excitation and 525 nm

emission) and luminescence were measured over 20 hour period using a SpectraMax M2 plate-reader (Molecular Devices, Sunnyvale, California). To measure cell toxicity, the blank corrected fluorescence was normalized against the fluorescence of the non-treated cells for each time point, while in the case of assessing the metabolic activity of the cells; the blank corrected luminescence was normalized against the luminescence of each treatment group at time zero.

3.2.6 Effects of C12HSL on gene expression of NuLi (wt *CFTR*) and CuFi (*CFTR*-deficient) cells

NuLi and CuFi cells were seeded in six well plates at 2×10^5 cells/well 24 hours prior to treatment. The growth medium was then changed and fresh medium was added containing either 10 μM C12HSL in 1% DMSO or 1% DMSO as a vehicle control. Solubility of C12HSL was checked by dissolving C12HSL to both concentrations and then measuring against pre-prepared standard using UPLC-MS. After six hours of treatment, the cells were harvested, the RNA extracted and cDNA synthesized as previously described in chapter two (Section 2.2) Quantitative PCR was carried out as previously described in chapter two . For analysis of the qPCR results, expression of the genes was normalized to the reference gene *ACTB*.

3.3 RESULTS

3.3.1 Validation of whole transcriptome microarray data

Previously, a whole transcriptome study in airway epithelial cells (BEAS-2B) treated with 10 μM C12HSL, found that ~ 3000 genes were differentially expressed, including those involved in immune signalling and apoptosis [Unpublished Honours Thesis 286]]. In the present study, RT-qPCR was used to validate certain results. The changes in gene expression obtained by RT-qPCR were then compared to those changes captured by the whole transcriptome array (Table 3.2).

Changes in gene expression levels of five (*TANK, MUC2, USP40, XBP1* and *ATF3*) out of 15 selected genes from the microarray panel (Table 3.2) were validated (*t*-test, $p < 0.05$) successfully using RT-qPCR. (Table 3.2). Although the expression levels of four additional genes (*ABCF1, MST1, CASP8* and *IL6*) measured by RT-qPCR were similar to those obtained in the microarray study, the results were not statistically significant. Of the five genes whose expression failed to reach statistical significance, *ABCF1* showed a trend toward significance (-4.97 fold change in microarray *vs.* -5.12 fold change in RT-qPCR, p=0.0570). In all, the expression levels of only two of the 15 genes, as measured by RT-qPCR, were different to those obtained on the microarray platform. On the basis of these results, it seems that the microarray data [Unpublished Honours Thesis [286]] provides a significant and robust insight into the likely effects of 10 μM C12HSL on the BEAS-2B transcriptome.

The results of the transcriptome study showed that the expression of two important UPR genes, namely, *XBP1* and *ATF3* were significantly diminished, in response to treatment with 10 μM C12HSL, which was validated by RT-qPCR ($p < 0.05$) (Table 3.2). Although dysregulation of the UPR could be suspected to lead to apoptosis, up-regulation of two genes (*CASP3* and *CASP*7) involved in apoptosis as captured by the microarray could not be validated by RT-qPCR (Table 3.2). Instead, the results of the RT-PCR analysis would seem to suggest that 10 μM C12HSL did not induce the expression of apoptotic pathways in BEAS-2B cells.

Since the whole genome expression study also indicated that 10 μM C12HSL modulated immune signalling it was decide to verify changes in gene expression of some of these immune-responsive genes by RT-qPCR. RT-qPCR confirmed the down regulation of TANK and MAP3K2, which are involved in NF-κB signalling. In addition, while no change in the

Table 3.2 Panel of genes from microarray chosen for validation by RT-qPCR

Gene	Description	Description of Gene	Relative Expression (Treated: Vehicle Control)		
			Microarray ($p < 0.05$)	RT-qPCR Relative to *ACTB*	
				Fold Change	*p*-value
ABCF1	ATP-binding cassette, sub-family F (GCN20), member 1	Immune Inflammation	-4.97	-5.12	0.0570
PPARG	Peroxisome proliferator-activated receptor gamma	Immune Inflammation	+3.43	-1.23	0.6742
TANK	**TRAF family member-associated NFKB activator**	**Immune NF-κB Signalling**	**-4.33**	**-7.36***	**0.0094**
MAP3K2	Mitogen-activated protein kinase kinase kinase 2	Immune NF-κB Signalling	+2.02	-3.49*	0.0170
MST1	Macrophage stimulating 1 (hepatocyte growth factor-like)	Cilliary Motility in lung epithelia	+3.19	+19.54	0.3957
MUC2	**Mucin 2, oligomeric mucus/gel-forming**	**Mucin Production**	**-3.11**	**-7.39***	**0.0045**
USP40	**Ubiquitin specific peptidase 40**	**Deubiquinating enzyme**	**-5.16**	**11.31*****	**0.0002**
XBP1	**Xbox binding protein**	**UPR**	**-1.47**	**-2.73***	**0.0051**
ATF3	**Activating transcription factor 3**	**UPR**	**-1.86**	**-3.55***	**0.0046**
CASP3	Caspase 3, apoptosis related cysteine peptidase	Apoptosis	+4.55	-3.71*	0.0045
CASP7	Caspase 7, apoptosis related cysteine peptidase	Apoptosis	+2.17	-1.10	0.7599
CASP8	Caspase 8, apoptosis related cysteine peptidase	Apoptosis	-2.81	-2.97	0.3080
IL6	Interleukin 6	Inflammatory cytokine	-1.07	-1.18	0.1840
IL8	Interleukin 8	Inflammatory cytokine	No change	-1.49*	0.0297
TNF	Tumor necrosis factor	Immune Cell Signalling	No change	+2.46	0.3100

Genes whose change in expression as indicated by microarray was validated by RT-qPCR are highlighted in **bold**. Mean of three independent experiments. * = $p < 0.05$, *** = $p < 0.001$ based on unpaired *t*-test.

expression level of the inflammatory cytokine *IL8* gene was observed in the transcriptome study, RT-qPCR showed a small decrease in *IL8* expression (-1.49 fold). Taken together, the RT-qPCR analysis of the whole transcriptome study seems to suggest that 10μM C12HSL treatment has an anti-inflammatory effect on BEAS-2B cells.

3.3.2 C12HSL induces apoptosis in BEAS-2B cells in a concentration-dependent manner

Although C12HSL has been reported to be able to induce apoptosis in a number of different cell types, including lymphocytes, macrophages, and aortic endothelial cells [192, 197, 202], there appears to be some debate in the literature on whether human epithelial cells are similarly affected by treatment with C12HSL. Tateda and colleagues showed that apoptosis was not induced in human epithelial cell lines exposed to up to 24 μM C12HSL [197]. In contrast, Schwarzer and colleagues reported activation of caspase 3/7 (the executing caspases in apoptosis), in human airway epithelia upon treatment with C12HSL concentrations greater than 10 μM [288]. To test whether C12HSL induces apoptosis in airway epithelial cells, the BEAS-2B airway epithelial cell line was exposed to 10 μM and 50 μM C12HSL and subjected to a flow cytometry-based apoptosis assay (Section 3.2.3).

The results of the flow cytometry analysis of BEAS-2B cells treated with varying concentrations of C12HSL for six hours show an induction of apoptosis in these cells. Importantly, apoptosis was induced in a C12HSL dose-dependent manner (Figure 3.1). It is clear from the results that after a six hours exposure to 10 μM C12HSL, no difference in the overall numbers of apoptotic cells able to be detected between C12HSL-treated and vehicle control-treated BEAS-2B cells. In contrast, treating BEAS-2B cells with 50 μM C12HSL for six hours induced a greater than two-fold increase in the percentage of early apoptotic cells (from 4.4% to 10.4%, $p < 0.0001$) compared to control.

A

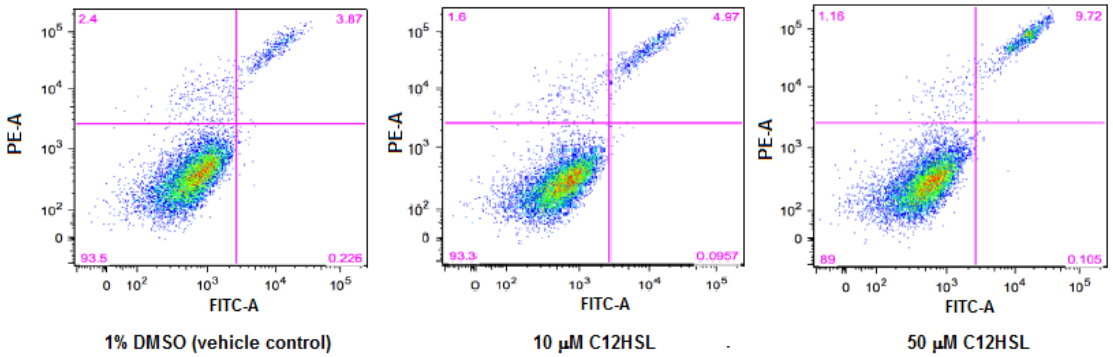

B

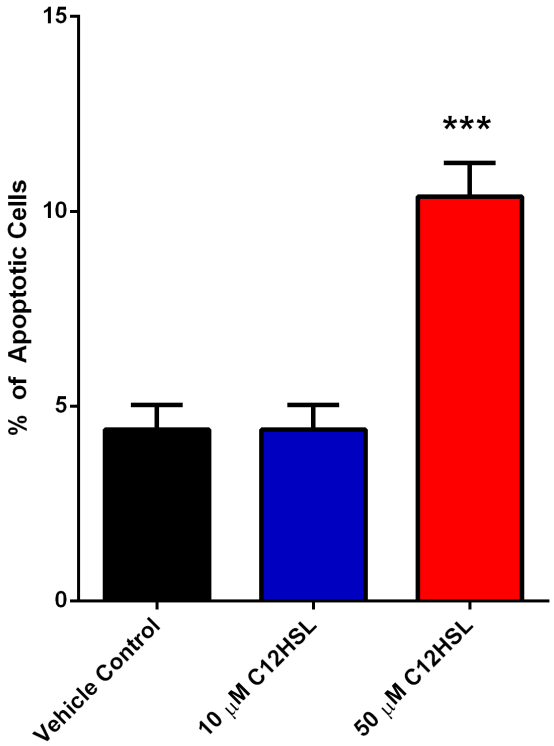

Figure 3.1 Induction of apoptosis in respiratory epithelial cells by C12HSL is concentration dependent.

BEAS-2B cells were treated with 10 µM and 50 µM C12HSL for six hours before being collected and stained with FITC-Annexin V and PI. The induction of apoptosis was measured by flow cytometry. Three biological replicates were run and representative flow cytometry plots are shown in (A). Apoptotic cells stain positive for Annexin V and can be seen in the quadrants on the right. The mean % of apoptotic cells from three experiments are shown in (B). Error bars represent S.D; *** $p < 0.001$ (One way ANOVA).

3.3.3 The cytotoxic and metabolic effects of C12HSL on airway epithelial cells

Given that apoptosis was observed in BEASE-2B cells treated with 50 μM C12HSL, the cytotoxic effects of 10 μM and 50 μM C12HSL (over a period of 20 hours) on BEAS-2B cells was investigated using the CellTox Green Cytotoxicity assay (Promega). In addition, changes in cellular metabolism across the same time period was also determined concurrently using a separate assay. Three airway epithelial cell lines were used: BEAS-2B (wild-type CFTR); CuFi, an airway epithelial cell line with homozygous ΔF508 *CFTR* mutation and NuLi, an identically transformed (to CuFi) cell line which possesses wild-type *CFTR* [287]. By both NuLi and CuFi cells the effect(s), if any, of the CFTR mutation on the response of these cells to C12HSL treatment could be determined.

A C12HSL-dose-dependent cytotoxic effect was observed in our airway epithelial cells (Figure 3.2). Of the three airway epithelial cells tested, C12HSL induced the greater cytotoxic effects on BEAS-2B cells, while the NuLi and CuFi cells appeared less susceptible to the cytotoxic effects of C12HSL. The *CFTR*-deficient CuFi cells appeared to be the most protected from C12HSL-mediated cytotoxicity. Treatment with 10 μM C12HSL did not increase cell toxicity when compared to the (vehicle treated) control in any of the three airway epithelial cell lines. Treatment with 50 μM C12HSL, however, caused immediate (within two hours of treatment) significant ($p < 0.05$) increases in cell cytotoxicity in three airway epithelial cells tested. *CFTR*-deficient CuFi cells appeared to be less susceptible to C12HSL mediated toxicity when compared to the wild-type *CFTR* NuLi cells. In CuFi cells, there was no discernable increase in cytotoxicity over the 20 hours with 10 μM C12HSL. With the higher concentration of 50 μM C12HSL, the cytotoxicity effects were similar but less pronounced in CuFi cells when compared to the wild-type CFTR cells.

Ten micromolar C12HSL did not have any effect on cell metabolism in any of the cell lines (Figure 3.3). Typically, as cell toxicity increases, cell metabolic activity is expected to decrease [289-292]. However, the BEAS-2B cells, in which C12HSL caused the greatest increase in cytotoxicity (50 μM C12HSL) did not display a corresponding decrease in cell metabolic activity. In fact, within 30 minutes of treatment of BEAS2-B with 50 μM C12 HSL, there was an increase in cell metabolism compared with the vehicle-treated cells ($p<0.05$). After two hours of treatment, metabolic activity still remained elevated. After four hours of 50 μM 12HSL treatment, cell metabolic activity began to fall. By 10 hours, there was no

difference in metabolic activity (p>0.05) and by 24 hours there was a trend to decreased metabolic activity when compared with the (vehicle treated) control.

The increase in cytotoxicity in the NuLi cells in response to 50 μM C12HSL treatment coincided with a decrease in cell metabolic activity. There was an immediate but modest decrease in metabolic activity with 50 μM C12HSL treatment (p<0.05 after 30 minutes), further supporting that the NuLi cells are less affected by C12HSL-mediated cytotoxicity than the BEAS-2B cells. The metabolic activity remained consistently lower than the (vehicle treated) control throughout the 20 hour treatment of 50 μM C12HSL.

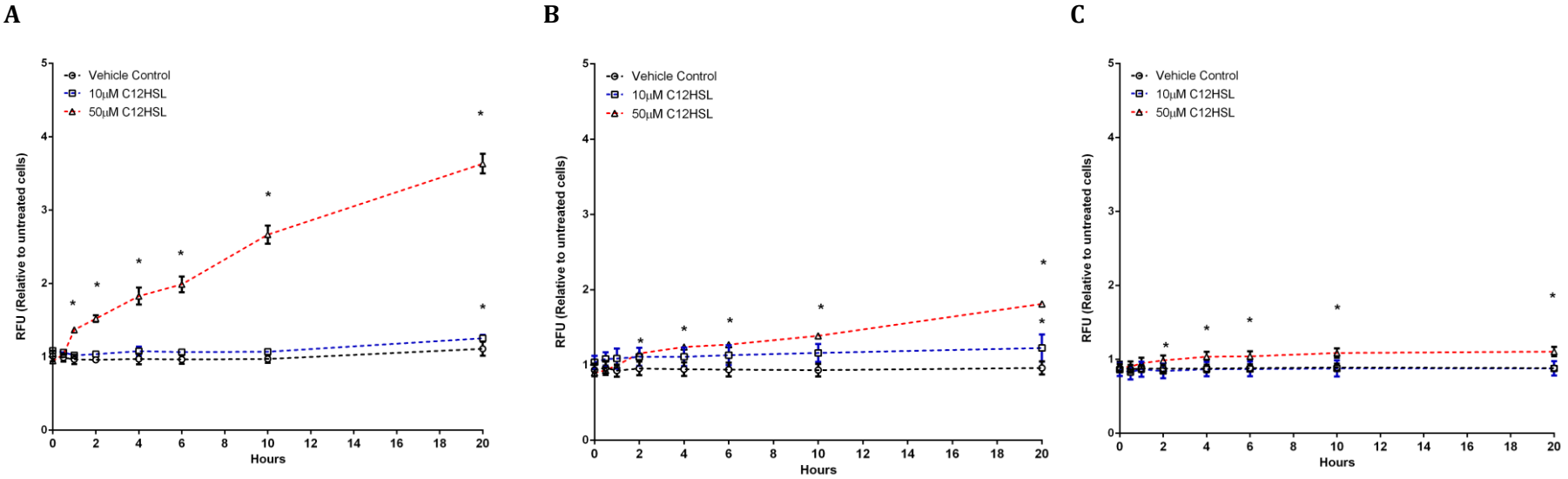

Figure 3.2 C12HSL-induced cell toxicity in BEAS-2B, NuLi and CuFi cells. BEAS-2B (A), NuLi (B) and CuFi (C) cells were treated with 10 µM and 50 µM C12HSL and then assayed for cell toxicity for 20 hours using the Cell-Tox Green assay (Promega). Cell toxicity is shown as relative fluorescence units (RFU), the blank corrected fluorescence relative to the blank corrected fluorescence of an untreated control. The mean of four independent experiments is shown. Error bars show SD. * $p<0.05$ based on Holm multiple t-tests.

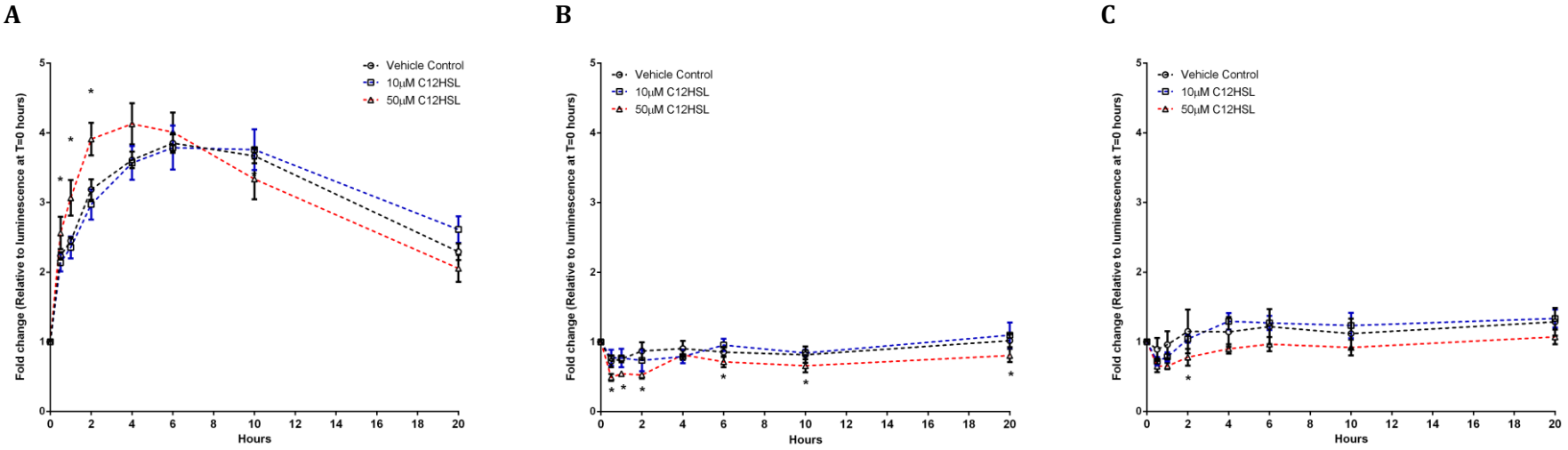

Figure 3.3 Effect of C12HSL on BEAS-2B, NuLi and CuFi cell metabolism. BEAS-2B (A), NuLi (B) and CuFi (C) cells were treated with 10 μM and 50 μM C12HSL and then assayed for cell metabolism for 20 hours using the RealTime-Glo MT Cell Viability assay (Promega). Cell metabolism is shown as fold change of luminescence units relative to luminescence at time = zero. The mean of four independent experiments is shown. Error bars show SD. * $p<0.05$ based on Holm multiple t-tests.

The CuFi cells once again appeared to be the most resistant to the effects of C12HSL, with a very small decrease in metabolic activity after two hours ($p < 0.05$) but this effect was not persistent, since by four hours, there was little to no difference between the treated cells and vehicle control.

3.3.4 CFTR-dependent effects of C12HSL on airway epithelia gene expression

Even 10 μM C12HSL, was able to dramatically impact gene expression in the BEAS-2B bronchial epithelial cells. In order to investigate how mutations in *CFTR* influences C12HSL-mediated gene expression in airway epithelial cells, RT-qPCR was used to investigate changes in the same panel of genes used to validate the microarray results, as well as several other genes of interest.

Table 3.3 Change in gene expression (by RT-qPCR) in NuLi and CuFi treated with 10 μM C12HSL for six hours

Gene	Description of Gene	Relative Expression (Treated: Vehicle Control)			
		NuLi		CuFi	
		Fold Change	*p*-value	Fold Change	*p*-value
MAP3K2	Immune, NF-κB Signalling	+1.71	0.174	+1.38	0.602
TANK	Immune, NF-κB Signalling	+1.39	0.241	+1.11	0.745
ABCF1	Immune, Inflammation	+1.12	0.713	-2.20	0.317
MST1	Cilliary Motility in lung epithelia	+1.08	0.870	-1.69	0.402
MUC2	Mucin Production	-1.14	0.662	-2.22	0.245
USP40	Deubiquinating enzyme	**+1.71***	**0.035**	+1.52	0.252
XBP1	UPR	+1.72	0.442	-1.86	0.468
ATF3	UPR	+1.34	0.082	-2.38	0.232
CASP3	Apoptosis	+1.08	0.704	-1.31	0.517
CASP7	Apoptosis	+1.04	0.909	-2.90	0.474
CASP8	Apoptosis	-2.77	0.138	-2.27	0.317
NGFR	Apoptosis	+2.88	0.181	-1.33	0.662
IL6	Inflammatory cytokine	+1.07	0.753	-1.70	0.095
IL8	Inflammatory cytokine	+1.22	0.301	+1.15	0.600
TNF	Immune, Cell Signalling	-1.938	0.278	-2.51	0.059

Mean of three independent experiments; * = $p < 0.05$, based on unpaired *t*-test.

From the panel of genes listed in Table 3.3, only *USP40* was significantly up-regulated in the NuLi cells (+1.71 fold, $p<0.05$). Two genes showed a trend to significance, *ATF3* in NuLi cells (+1.34 fold up-regulation, $p=0.0820$) and *TNF* in CuFi cells (-2.51 fold up-regulation, $p=0.059$).

When the relative expression of the treated cells to untreated cells is compared between the two cell lines, the results showed that all of the NF-κB signalling genes examined showed the same directional regulation, however the expression of inflammation, UPR and apoptosis genes were up-regulated in NuLi cell and down-regulated in CuFi cells, suggesting that modulation of these pathways by 10 μM C12HSL might well be CFTR-dependent.

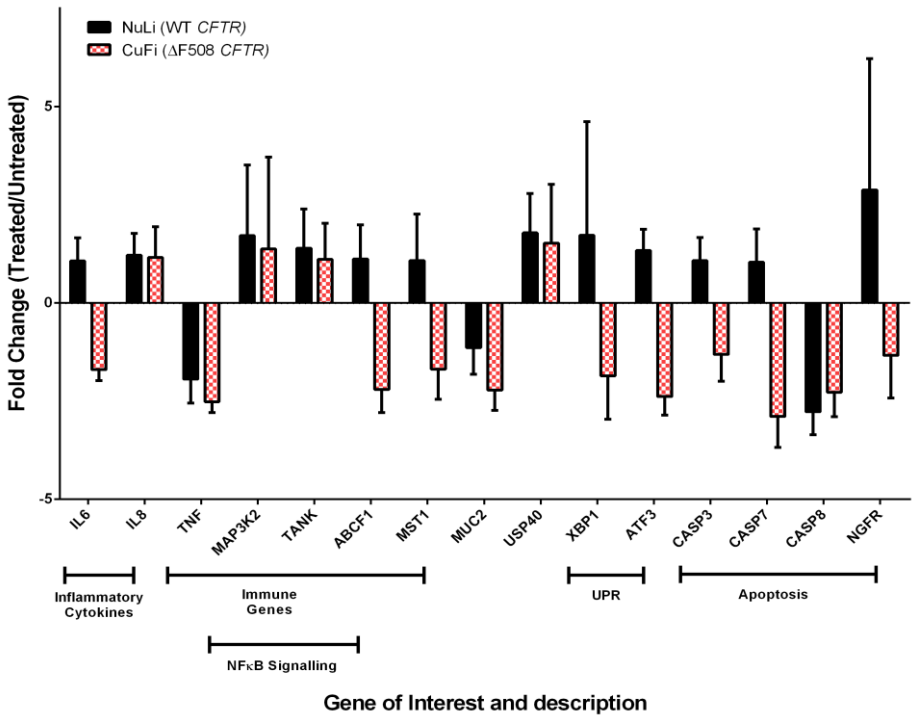

Figure 3.4 CFTR dependent effects of C12HSL on NuLi and CuFi gene expression. NuLi (wild-type CFTR, solid bars) and CuFi (ΔF508, spotted bars) cells were treated with 10 μM C12HSL for six hours and the RNA extracted to measure change in gene expression in response to treatment. The expression of each gene was normalized to reference gene ACTB and then the fold change of C12HSL treated/vehicle control treated cells calculated. The bars show fold change of each gene relative to vehicle control with associated standard error bars.

3.4 DISCUSSION

In this section of the thesis, 15 differentially expressed genes reported in an earlier transcriptome study [286] were chosen for validation, based on their biological significance and on their expression levels. Transcriptome-wide analyses provide a valuable insight into change in global gene expression levels of numerous genes change between varying tissues and cell types, and across different disease states, as well as in response to varying environmental stimuli. DNA microarrays are widely accepted as powerful tools to capture genome wide changes in transcription patterns; in turn, and with the advent of bioinformatics tools such as pathway analysis, network analysis and systems biology, DNA microarrays now allow investigators to generate testable hypotheses. However, the quality of the data obtained in microarray-based studies can be highly variable, owing in part at least to variations in the types of microarray platforms used; the quality of the starting RNA material [293]; and the bioinformatics programs used to perform the microarray analysis [294]. In order to translate microarray data into biologically significant findings, other gene expression technologies are often used to validate data obtained in microarray studies. In this context, there is no universally agreed upon method to validate microarray data, however, RT-qPCR has long been considered the gold-standard method to investigate differential gene expression in biological studies [295, 296].

Investigators typically approach validation in one of two ways: validating (i) a set of top hits based on biological and statistical significance, or else (ii) large random subset of results [297]. Given that the results of the RT-PCR experiments performed in this study were mostly consistent with those obtained in our microarray analysis, it seemed reasonable to conclude that the microarray results broadly represented the likely cellular changes being triggered in BEAS-2B cells by 10 μM C12HSL exposure. The data from both the transcriptome array and RT-qPCR analysis show that C12HSL, even at the relatively low concentration of 10 μM, was capable of influencing the expression levels of a number of genes involved in the host immune response. In this context, numerous *in vitro* studies have described the immunomodulatory effects of C12HSL on the human airway [184, 186, 197, reviewed in 217, 284]. The results described here show the strong down-regulation of *TANK* by 10 μM C12HSL. *TANK* encodes a protein that stimulates NF-κB activation [298] and thereby, the immune response. The suppression of inflammation found in this study is consistent with reports showing C12HSL having anti-inflammatory effects at concentrations below 10 μM [187, 217].

The change in expression of the pro-inflammatory cytokine genes *IL6* and *IL8* was also investigated, given that both genes have been reported to be up-regulated in airway epithelia in response to >25μM C12HSL [189, 299]. While there was no change in expression of *IL6*, 10 μM C12HSL down-regulated *IL8* expression, suggesting that this concentration of C12HSL may have a suppressive effect on inflammation, possibly through the suppression of neutrophil chemotaxis [193]. These results lend further support to the hypothesis that concentrations of C12HSL below 10 μM provoke anti-inflammatory responses [217].

Jahoor and colleagues identified the transcription factors PPARβ/δ and PPARγ as putative mammalian C12HSL receptors through which C12HSL could modulate mammalian host responses [214]. The microarray data indicated that in response to C12HSL PPAR signalling, and that *PPARγ* expression was up-regulated. However, RT-PCR analysis failed to validate this change in *PPARγ* expression. While there is some indication that PPARγ may regulate its own expression [300], antagonism by relatively low levels of C12HSL may only affect PPARγ protein activity and not its expression thus a transcript-based method like RT-qPCR may not be the ideal technique with which to validate the C12HSL dependent effects on PPAR signalling. The results from chapter four, using a functional promoter assay, shows that 10 μM C12HSL was able to competitively bind to PPARγ and increase PPARγ activity. This is a small increase in activity, however, and under normal cellular conditions could be expected to be balanced by inhibition of binding of C12HSL by stronger endogenous agonists. Given the proposed role of PPARγ as a mammalian C12HSL receptor, PPARγ-dependent immune signalling in response to C12HSL will require further investigation.

The microarray data also indicated that C12HSL might be inducing cellular stress by altering the expression levels of genes involved in the UPR and ubiquination. The expression of three genes involved in the UPR and ubiquination was validated by RT-qPCR. The expression of *XBP1* and *ATF3*, two key UPR genes, was down-regulated in response to C12HSL treatment. Increased *XBP1* usually indicates a shift towards a protective response to misfolded proteins, while decreased *ATF3* usually indicates a shift to a deleterious, apoptotic response to misfolded proteins. The reduced expression of both genes indicates a shift towards *ATF3* dependent induction of apoptosis. Although no increase in cytotoxicity was observed in BEAS-2B cells six hours after treating with 10 μM C12HSL (compared to control treated cells), this decreased *ATF3* offers a potential mechanistic explanation for how C12HSL might be able to induce cytotoxicity. The expression of *USP40*, a peptidase specific to ubiquitin, is also down-regulated. Deubiquinating enzymes are not merely ubiquitin recyclers, as there

are emerging reports of their involvement in DNA replication, cell division and cell death [301, 302]. The accumulation of misfolded proteins, as caused by the disruption of the UPR by C12HSL, results in cytotoxicity. By also affecting deubiquinating enzymes, it is tempting to speculate that C12HSL could possibly further hamper the ability of a cell to respond to misfolded proteins, thereby exacerbating the cytotoxic effects of C12HSL on the cells.

Given the down-regulation of the UPR by C12HSL in BEAS-2B, increased cytotoxicity was expected. It is widely reported that C12HSL is able to induce apoptosis in a number of cell types including airway epithelia [192, 200, 202, 203]. As a result, the apoptotic effect of C12HSL in the BEAS-2B cells was further investigated. The transcriptome study indicated that the expression of some of the caspase genes were affected by 10 μM C12HSL. However, none of the changes in expression of the caspase genes could be validated by RT-qPCR. In fact, the results of the RT-qPCR analysis indicated that the expression of *CASP3* was down-regulated by 10 μM C12HSL after six hours. Another independent method of investigating the apoptotic effect of C12HSL on the BEAS-2B cells was therefore used. The results of the flow cytometry analysis of induction of apoptosis showed that 10 μM C12HSL did not induce apoptosis in the cells following six hours of treatment. Increasing the C12HSL concentration to 50 μM induced apoptosis in the cells, implying C12HSL has a concentration-dependent ability to induce apoptosis in BEAS-2B cells. Schwarzer and colleagues also investigated the induction of apoptosis by C12HSL in airway epithelial cells and found a concentration-dependent effect of C12HSL on induction of caspase 3/7 activity in airway epithelial cells. However, their methodology showed that concentrations of 10 μM C12HSL increased caspase 3/7 activity.[288]

Investigations of the effects of C12HSL was extended to the effect of C12HSL on the viability and metabolic activity of airway epithelial cells. At the lower concentration, the two wild-type *CFTR* cell lines showed a small decrease in viability after 20 hours but at higher concentrations, an immediate (within two hours) decrease in cell viability was observed. This further confirmed the C12HSL-dose dependent induction of apoptosis. The two wild-type *CFTR* bronchial epithelial cell lines (BEAS-2B and NuLi) behaved similarly in regards to viability, although the NuLi cells were less affected by C12HSL.

The processes of cell metabolism and apoptosis are intertwined but the mechanisms through which cell metabolism and apoptosis are linked remain to be fully elucidated. The triggering of apoptosis is thought to result in an overall decrease in cellular metabolic activity [289-292]. In the wild-type *CFTR* NuLi cell line, as expected, there was a marked

decrease in cell viability in the cells that displayed increased cell cytotoxicity in response to C12HSL treatment. However, BEAS-2B cells treated with 50 μM C12HSL demonstrated an increase in cell metabolic activity. The initiation of apoptosis is a metabolically taxing activity with ATP being required for the activation of caspases, enzymatic activity, bleb formation and chromatin condensation [291]. The observed increase in BEAS-2B cell metabolism could be a result of the cells initiating the apoptotic processes. Such an increase may not have been observed in the NuLi cells because they appear to be more resistant to the effects of C12HSL, and perhaps a greater concentration of C12HSL is needed to induce the apoptotic processes being observed in the BEAS-2B cells. However, in order to completely reconcile the differences between the BEAS-2B and NuLi cells the possibility that these observations may be due to the cells being in different growth phases and at different cell densities needed to be eliminated. Even though the cell lines were seeded at the same density, any differences in growth rates of the cell lines may need to be determined to ensure that these factors do not contribute to the effects seen with the BEAS-2B and NuLi cells.

What is clear, is that C12HSL is able to influence the airway epithelia in a number of different ways, and that these effects vary in magnitude and direction depending on the concentration of C12HSL. Ten micromolar C12HSL, a concentration lower than that generally studied in the literature, still dramatically affected airway epithelial cells. While this concentration did not elicit apoptosis or affect cell metabolic activity, it was still able to induce significant changes in expression of a number of important genes. Thus, these findings provide further support for the notion thatC12HSL plays important roles in *P. aeruginosa* pathogenesis.

The whole transcriptome study identified altered calcium signalling as another major change effected by 10 μM C12HSL-treated BEAS-2B cells. Interestingly, the microarray reported the down-regulation of the GTPase-activating protein IQGAP1. Briefly, and with the exception of PPAR's, IQGAP1 is the only other identified mammalian C12HSL receptor [225]. C12HSL is thought to use IQGAP to trigger essential changes in the cytoskeletal network [225]. IQGAP1is a scaffolding protein that plays an essential role in cell shape, vesicle trafficking, and directional migration [226]. It contains a calmodulin-binding motif, and calmodulin is a major Ca^{2+} sensor. Although it is unknown whether C12HSL directly interacts with calmodulin-binding motif, C12HSL may use IQGAP1 to affect intracellular Ca^{2+} levels. Furthermore, the presence of *CFTR* mutations modulates the influence C12HSL has on intracellular calcium [303, 304]. Schwarzer and colleagues investigated the effects of

C12HSL on intracellular and endoplasmic reticulum (ER) Ca^{2+} concentrations in the wild-type *CFTR* Calu-3 airway epithelial cell line. They found increasing intracellular and decreasing ER Ca^{2+} with C12HSL concentrations as low as 10 μM [305], while cells with defective CFTR demonstrated a considerably increased release of Ca^{2+} when treated with 100 μM C12HSL [189]. This movement of Ca^{2+} has been linked to apoptosis in murine fibroblasts [192] and is thought to affect host defence mechanisms against *P. aeruginosa* [265]. Thus it is difficult to tease apart whether the C12HSL-mediated effects on BEAS-2B result from C12HSL acting through PPARγ or IQGAP1 or even through another as yet unidentified C12HSL receptor. Clearly, further investigations are required to determine how exposure to C12HSL treatment induces changes in intracellular Ca^{2+} levels.

We investigated further which of the effects of C12HSL are influenced by the *CFTR* mutation. RT-qPCR was used to measure changes in gene expression in NuLi and CuFi cells treated with 10 μM C12HSL for 6 hours to isolate *CFTR*-dependent effects of 10 μM C12HSL. Only one gene showed a significant change in expression: *USP40* in the wild-type *CFTR* NuLi cell line, which showed an increase (<2 fold) in expression. It is difficult to draw any conclusions from such a small change in expression of only one gene, particularly since *USP-40* expression was strongly down-regulated in another wild-type *CFTR* cell line (BEAS-2B). Instead changes in gene expression between the wild-type *CFTR* and *CFTR*-deficient cell lines were compared to elucidate any *CFTR*-dependent effects.NF-κB signalling is considered to be PPARγ dependent [214], and PPARγ protein activity is believed to impaired by *CFTR* mutation [224]. As a result, we would expect the gene expression profiles of genes involved in NFκB signalling in wild-type *CFTR* to be different to that of *CFTR*-deficient cells. However, RT-qPCR results showed similar trends in change in expression of NF-κB signalling genes in both wild-type *CFTR* and *CFTR*-deficient cells. As expected, genes involved in the UPR, a process that can be activated by both PPARγ[306] and modulated by calcium signalling induced ER stress [307], showed opposing trends in change in expression. Without statistically significant results it is difficult to draw conclusions from these findings, however it is possible that C12HSL-dependent effects on inflammation and apoptosis may occur through independent mechanisms. Research into novel receptors of C12HSL is required.

The experiments were therefore extended to analyse changes in cell toxicity and metabolic activity in the CuFi cells in response to C12HSL treatments. The *CFTR* deficient CuFi cells appeared to be protected against C12HSL mediated changes in cell toxicity and metabolic activity, even more so than the NuLi cells. This is consistent with another study [189] where

concentrations of 100 μM C12HSL were required to elicit a hyperinflammatory response in *CFTR*-deficient cell cultures. Further understanding of the protective mechanisms of increased intracellular Ca^{2+} is required before any protective effect(s) of C12HSL can be attributed to disrupted calcium signalling. One possible explanation of the protective effect of the ΔF508 mutation is to consider the effect of the mutation on the inflammatory regulator PPARγ. PPARγ has a net suppressive effect on inflammation and *CFTR* mutations are thought to decrease its expression and activity [221, 222, 224]. Since PPARγ has been reported to be a mammalian C12HSL receptor, decreased PPARγ expression/function in *CFTR* deficient cell lines may render them less sensitive to the effects of C12HSL. Given the already hyper-inflammatory nature of the CF cell line, any pro-inflammatory and apoptotic effects of C12HSL would be muted. However, the differences between the wild-type *CFTR* and *CFTR*-deficient cell lines in our experiments were small, possibly due to decreased CFTR in the wild-type as a consequence of C12HSL treatment (transcriptome array indicates decreased *CFTR* expression in response to C12HSL treatment) although there is some evidence that C12HSL-induced apoptosis may be independent of *CFTR* mutations [288, 308].

One factor to consider is that the CuFi cells may have an underlying proinflammatory bias. Voisin et al 2014 [309] demonstrated (using microarrays) a general up-regulation of inflammatory genes in the CuFi cells even in the absence of a pathogen compared to NuLi cells. Therefore there may be an underlying immune bias associated with a dysfunctional CFTR protein. They also demonstrated that under conditions of oxidative stress CuFi cells are more resistant to apoptosis than NuLi cells which fits with the results in this thesis. In the data analysis NuLi data was compared to NuLi control and the same for CuFi, and thereby negates this bias. Both the NuLi and CuFi cells appear to be more protected against C12HSL mediated effects when compared to the BEAS-2B cells and it is difficult to establish which cells, the NuLi or the BEAS-2B most closely reflect C12HSL mediated effects in the airway. The use of primary cell cultures, which more accurately reflect the *in vivo* characteristics of airway epithelia, may enable the determination of which cell line more closely represents the airway and proves most valuable in future studies involving C12HSL.

Another consideration for future studies would be to accurately determine the LD50 of C12HSL when studying cytotoxicity, for each individual cell line. Such determination would lead to improved understanding of the varying effects of C12HSL at different concentrations when compared to studying the effects of C12HSL at established anti/pro inflammatory concentrations.

The results in this chapter show that even at low concentrations (10μM) C12HSL significantly affects airway epithelial cells, the first point of contact in the establishment of *P. aeruginosa* infection. These effects of C12HSL appear to be concentration dependent. The results described here suggest that at low concentrations of C12HSL appear to be anti-inflammatory and deregulates the UPR but does not induce apoptosis. In addition, the *CFTR* mutation seems to offer some protection to C12HSL-mediated effects, but better understanding of the mechanisms through which *CFTR* mutations may facilitate chronic *P. aeruginosa* infections on a cellular level. With increased understanding of how C12HSL facilitates infections in the CF lung, therapies can be developed to target this aspect of *P. aeruginosa* pathogenesis.

CHAPTER FOUR – REGULATION OF PON2 EXPRESSION

4.1 INTRODUCTION

The three members of the human paraoxonase enzyme family, *PON1, PON2 and PON3*, are found adjacent to each other on chromosome 7 and possess significant homology [310]. PON1 and PON3 are primarily found bound to high-density lipoproteins in circulation [257, 311], while PON2 is absent from plasma, but is expressed by most human tissue and functions as an intracellular enzyme [258]. All the PONs display anti-artherogenic properties in murine models [312-314] and an ability to hydrolyse varying types of lactones *in vitro* [248]. PON2 also displays anti-oxidative and anti-apoptotic properties but it is thought that these processes are mechanistically independent of its lactonase activity. [259, 315]. PON2 lactonase activity is generally much lower than that of other PONs with the exception of its activity against acyl homoserine lactone (AHL) substrates, where PON2 activity is orders of magnitude higher in comparison with PON1 and PON3 [248].

AHLs are widely recognized as important quorum sensing (QS) signals in many Gram-deficient bacteria. Of particular interest to this project is the *P. aeruginosa* QS signalling molecule C12HSL. C12HSL is the signal molecule at the top of the *P. aeruginosa* QS hierarchy and is integral to the bacterium's virulence, in particular to the formation of biofilms, which afford *P. aeruginosa* significant protection against host immune responses and conventional antibiotics [125, 157, 316, 317]. *P. aeruginosa* is particularly problematic in people with cystic fibrosis (CF) where it is the major lung pathogen in adults, and causes chronic infections leading to much of the CF-related morbidity and mortality. Of the paraoxonases, PON2 has the highest lactonase activity against C12HSL. As a result, C12HSL is widely considered to be the natural substrate of PON2 [248, 262]. PON2 deficiency hinders *P. aeruginosa* clearance and enhances its quorum sensing in murine models [249, 264] suggesting that PON2 must play a protective role against co-ordinated bacterial virulence and infection.

Apart from its bacterial signalling function, C12HSL is also able to modulate mammalian cellular function, because its lipophilic tail structure facilitates entry into mammalian cells. C12HSL interferes with inflammatory pathways involving NF-κB [188] by acting as a weak agonist of the anti-inflammatory nuclear transcription factor PPARγ (peroxisome proliferator activated receptor γ) [214]. PPARγ is a ligand-dependent transcription factor that binds to a specific peroxisome proliferator response element (PPRE) as a heterodimer with a retinoid X receptor (RXR) [215, 216]. It can then bind an agonist that allows for a

conformational change enabling it to recruit co-activators and/or co-repressers and modulate transcription. PPARγ influences inflammation by the modulation of signalling through toll-like receptors (3,4 & 9), NF-κB signalling and by inducing phosphorylation of p38 MAPK [217, 318, 319], producing a net suppressive effect on inflammation. C12HSL competes with unknown endogenous PPARγ agonists and exerts a net antagonistic effect on PPARγ activity, possibly allowing for sustained inflammation when the host is infected with *P. aeruginosa* [214, 217].

In people with CF, PPARγ function is affected by mutations in the cystic fibrosis transmembrane conductance regulator (*CFTR*) gene and *Cftr*-deficient mice display decreased PPARγ nuclear localization, PPARγ DNA binding, PPARγ co-activator recruitment and overall gene expression [221]. Reduced PPARγ levels and/or function have also been demonstrated in CF human airway epithelial cell lines [222]. It is believed that CFTR defects generate oxidative stress that sustains tissue trans-glutaminase 2 activation. This inhibits PPARγ SUMOylation, favouring PPARγ crosslinking and proteasomal degradation [224]. Consequently, there is decreased PPARγ functionality, which may explain, in part, the hyperinflammatory nature of the CF lung.

The regulation of PON2 expression is as yet poorly understood. Investigations into PON2 regulation have been mostly limited to macrophages, where PON2 expression is influenced greatly by a number of factors induced by oxidative stress [268-271, 321, 322]. In endothelial cells, PON2 transcript and protein expression was induced via the unfolded protein response to endoplasmic reticulum stress [259], while in cultured airway epithelial cells, C12HSL has been shown to down-regulate expression of PON2 [265]. Several studies have shown that PON1 is activated by PPARγ agonism [323-326] and PPARγ agonism by rosiglitazone leads to up-regulation of PON2 transcript and protein in mouse macrophages

Table 4.1 Identified (*in silico*) putative PPARγ binding sites in hPON2 promoter.

Putative PPARγ Binding site	Relative to hPON2 transcription start		Strand	Matrix Similarity Score	Association with RXR Binding site
	Start	Stop			
1.	–66	–88	Forward	0.916	Yes
2.	–719	–813	Reverse	0.839	No

Putative PPARγ binding sites were identified within the 1100 bp up-stream of human PON2 transcription start with 'good' matrix similarity score. Matrix similarity scores of 0.8 or more are considered to be a 'good' score. Analysis done using the *in silico* transcription factor binding site analysis in Genomatix MatInspector [320].

in a dose-dependent manner [268]. The mechanisms behind PPARγ regulation of PON2 are less clear. PPARγ functions as a transcription factor and unpublished results in our lab indicate the presence of putative PPREs in the PON2 promoter (Table 4.1) [320]. Results from our lab have also indicated that PPARγ and PON2 expression is correlated in the lungs of CF patients (Figure 4.1). These findings strongly suggest that PPARγ transcriptionally regulates PON2.

The transcriptional regulation of PON2 by PPARγ has important implications for individuals with CF. The combined suppression of PPARγ function by defective CFTR and *P. aeruginosa* QS signal may hamper the protective functions of PON2. The cells in the airway would then be unable to degrade intracellular *P. aeruginosa* QS signal, allowing *P. aeruginosa* to establish the chronic infections characteristic of CF patients. In addition, with decreased PON2, the airways also are less protected from cellular stresses induced by defective CFTR and the oxidative damage associated with infection and the hyperinflammatory conditions.

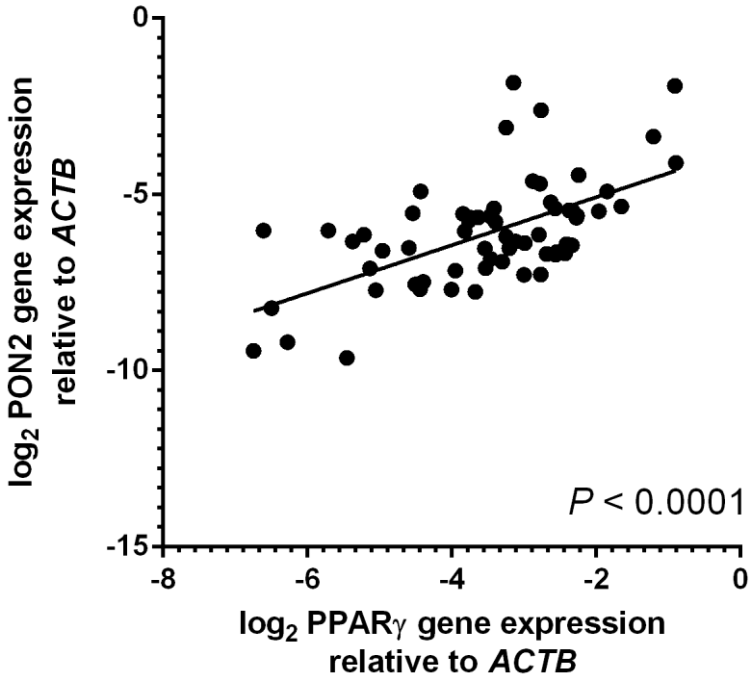

Figure 4.1 Correlation between PON2 and PPARγ expression in children with CF. Figure shows $\log_2$ expression of PON2 and PPARγ in RNA extracted from bronchoalveolar lavage from 80 CF patients showing a correlation ($p<0.0001$) (Spearman $r = 0.5152$) between expression of the two genes. [Unpublished]

Pharmaceutical regulation of PON2 expression by PPARγ agonism might allow for the correction of decreased PON2 by treatment with known PPARγ agonists. Such a therapy would protect host cells against the intracellular effects of C12HSL. In this study, we investigate the ability of PPARγ to regulate PON2 expression

.

4.2 MATERIALS AND METHODS

The materials and methods for this chapter are described in chapter two. Additional materials and methods specific for this chapter are described below.

4.2.1 Plasmids used

To measure PPARγ transactivation of PON2, the plasmid pXP1-hPON2p1000 with 1098 bp of the human PON2 promoter cloned into the promoter-less luciferase reporter vector pXP1 was used [Honours Thesis, Naseem Ali 320]. The pcDNA3-PPARγ1 plasmid was used to overexpress PPARγ because of the reported low expression of PPARγ in BEAS-2B, the cell line used in these experiments [327, 328], while the PPAR-responsive PPRE3x-TK-LUC plasmid was used to detect the presence of activated PPARγ. The pGL4.75 (hRLUC/CMV) plasmid expressing renilla luciferase was used to normalize transfections and the empty vector pcDNA3.1 and firefly luciferase expressing pGL3 were used as controls. These plasmids are summarized in table 4.2.

Table 4.2 Plasmids used in transfection experiments

Name	Source	Description	Promoter	Size	Marker
pcDNA3.1	Life Technologies	Empty vector	CMV	5.3 kb	Ampicillin
pXP1	[329]	Promoter-less luciferase reporter	None	6.1 kb	Ampicillin
pXP1-hPON2p1000	[320]	Human PON2 promoter with luciferase reporter	Human PON2 promoter (1098 bp up-stream from start)	7.2 kb	Ampicillin
pGL3	Promega	Firefly luciferase expression	SV40	5.3 kb	Ampicillin
PPRE3x-TK-LUC	[330]	3× PPAR response element driving luciferase expression	3× PPRE	6.8 kb	Ampicillin
pcDNA3-PPARγ1	[331]	Full-length human PPARγ1 expression vector	CMV	8 kb	Ampicillin
pGL4.75 (hRLUC/CMV)	Promega	Renilla luciferase expression	CMV	4.3 kb	Ampicillin

Schematic representations of pxXP1, pXP1-hPON2p1000 and PPRE3x-TK-LUC plasmids, are shown in Figure 7a.

4.2.2 Transient transfections

BEAS-2B cells were transfected with the plasmids listed in table 4.2 using FugeneHD (Promega) as described in chapter 2 (Section 2.4) . For co-transfections using two genes, a 7:3 ratio of luciferase-expressing plasmid:secondary plasmid was used. This has previously been shown to be optimal for our experiments [320]. For co-transfections, a range of ratios were tested for optimum expression and a ratio of 7:2:1 of firefly luciferase-expressing plasmid: renilla luciferase-expressing plasmid: tertiary plasmid was then used in experiments. Transfected cells were incubated for six hours and media changed prior to treatments.

4.2.3 Treatment of BEAS-2B cells

The compounds listed in table 4.3 were used to treat BEAS-2B cells. Powdered stocks were dissolved in ethanol and aliquoted into working stocks. The ethanol was then evaporated in a hood before storage at –20 °C. Prior to experiments, the compounds were dissolved in cell culture buffer and added to the cells at the desired concentrations. For treatments with more than one compound, the cells were pre-treated with one compound for 30 minutes prior to addition of the second compound. Transfected cells were typically treated for 16 hours prior to lysis and analysis of luciferase activity.

Table 4.3 PPARγ agonists and antagonists used in study

Name	Source	Effect on PPARγ activity
Rosiglitazone (RG)	Cayman Chemicals, MI, USA	Agonist
Pioglitazone (PIO)	Cayman Chemicals, MI, USA	Agonist
C12HSL	Cayman Chemicals, MI, USA	Weak Agonist
GW9662	Cayman Chemicals, MI, USA	Antagonist

4.3 RESULTS

4.3.1 Determination of optimum ratio for three-plasmid co-transfections

When co-transfecting cells, it is important to account for varying transfection efficiencies. This is particularly important when transfecting different experimental groups with different plasmids with the intention of making comparisons between the groups. In our experiments, we used the renilla luciferase-expressing plasmid pGL4 to normalize luciferase expression to transfection efficiency. Because we were transfecting with two different luciferase reporters, we needed to optimize the ratios of the plasmids being transfected in order to get optimum levels of expression of both luciferase reporters.

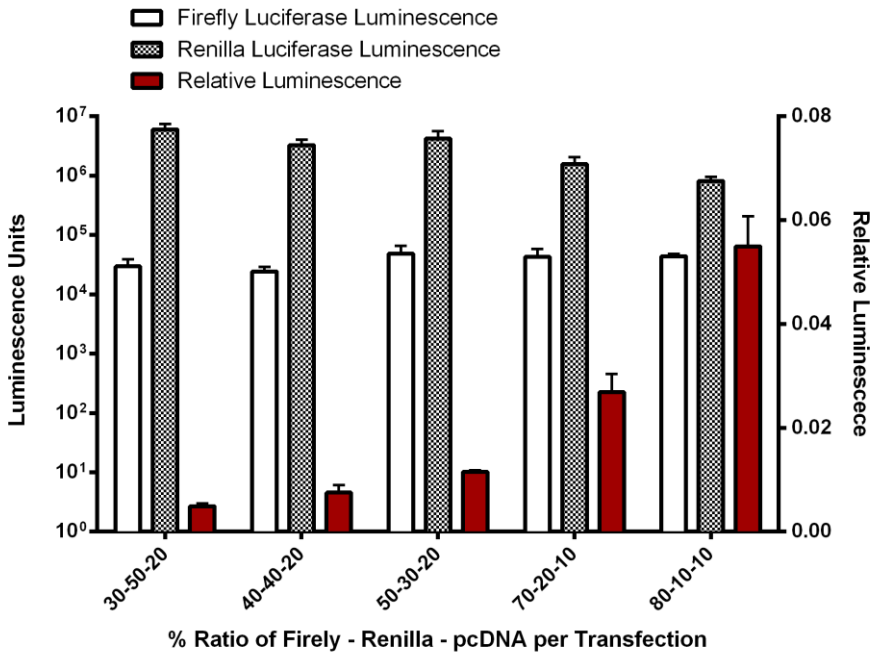

Figure 4.2 Expression of firefly and renilla luciferase and relative luminescence in co-transfections with three plasmids at a range of ratios. BEAS-2B cells were transiently co-transfected for 72 hours with varying ratios of pGL3 firefly luciferase expression vector, pGL4.75 renilla luciferase expression vector and pcDNA3.1 empty vector. Luminescence units of firefly and renilla luciferase were assayed from cell lysates. Results expressed as firefly luciferase expression (right axis) and firefly luciferase expression relative to renilla luciferase expression (left axis). Error bars represent S.D.; n = 3.

The BEAS-2B cells were transfected with five different ratios of firefly luciferase: renilla luciferase: reporter-less pcDNA3.1 (Figure 4.2) for 72 hours to allow for luciferase to accumulate. The lysates of the cells were assayed for both firefly and renilla luciferase expression and the firefly-to-renilla luciferase ratio calculated for each group. The mean of three biological replicates is shown (Figure 4.2) and demonstrates that a continuous, but modest, decrease in renilla luciferase expression was observed as the percent of renilla plasmid decreased from 50% to 10%. As the percent firefly luciferase increased from 30% to 70%, the firefly luciferase expression increased modestly. The levels remained fairly constant between 70% and 80% firefly luciferase plasmid. A ratio of 70%:20%:10% firefly luciferase: renilla luciferase: pcDNA3.1 was considered to be the optimum, because no major increase in firefly luciferase expression could be obtained by increasing further the percent firefly luciferase. This ratio was used in all further experiments.

4.3.2 BEAS-2B cells require PPARγ overexpression

PPARγ is widely recognized to be expressed in the airway, but studies have reported different expression levels in BEAS-2B [327, 328]. It was important to firstly establish that the known PPARγ agonist rosiglitazone could activate PPARγ-dependent signalling in our BEAS-2B. BEAS-2B cells were transfected with the PPARγ-sensitive A-Ox3-TKSL-PPRE plasmid [330], a reporter plasmid with three PPREs that can bind activated PPARγ. The cells were co-transfected with either a reporter-less plasmid pcDNA3 or the PPARγ expression plasmid pcDNA3-PPARγ1 [331]. The cells were then treated with 50 nM, 100 nM or 280 nM rosiglitazone for 16 hours before cell lysates were assayed for luciferase expression. The mean results of three biological replicates are shown in figure 4.3. In cells without PPARγ overexpression, 50 nM rosiglitazone did not activate luciferase expression, while treatment with 100 nM and 280 nM rosiglitazone elicited modest increases in luciferase expression. When PPARγ was overexpressed in cells, we observed significant increases in luciferase expression with all three concentrations of rosiglitazone treatment compared with the cells without PPARγ overexpression and the vehicle control ($p < 0.05$).

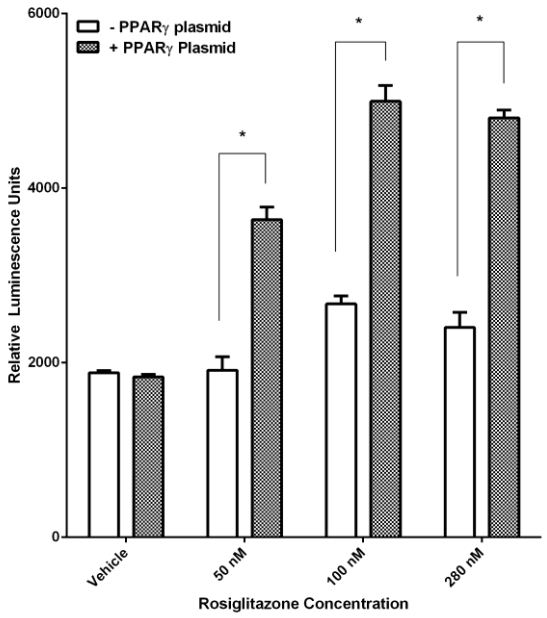

Figure 4 3 Dose response of PPARγ activation in cells transfected with PPRE-containing reporter. BEAS-2B cells were transiently co-transfected with A-Ox3-TKSL-PPRE, a PPAR-responsive luciferase expression vector, pGL4 to normalize for transfection efficiency and one of either pcDNA3.1 empty vector or pcDNA3-PPARγ1, a PPARγ expression vector. The cells were then treated for 16 hours with varying concentrations of rosiglitazone (RG) and the lysates assayed for luminescence. Results expressed as firefly luciferase expression relative to renilla luciferase expression. Error bars represent S.D.; n = 3. *$p < 0.05$, *t*-tests comparing two groups.

4.3.3 Characterising PPARγ activation in BEAS-2B cells overexpressing PPARγ

As we were over-expressing PPARγ in the cells and using the increasing luciferase expression of the A-Ox3-TKSL-PPRE plasmid in response to PPARγ activation as a measure of PPARγ activation, we needed to demonstrate modulation of PPARγ activation using known PPARγ agonists and antagonists. The BEAS-2B cells were co-transfected with the PPARγ-sensitive A-Ox3-TKSL-PPRE and PPARγ-expressing pcDNA3-PPARγ1 plasmids. The cells were then treated for 16 hours with a range of concentrations and combinations of known modulators of PPARγ activity. The lysates of the cells were then assayed for luciferase expression. The mean results (n = 3–7) are shown in Figure 4.4. Rosiglitazone, the most potent of the PPARγ agonists used in this study, at 50 nM and 100 nM produced significant dose-dependent increases in luciferase expression compared with vehicle-

treated transfected cells, suggesting increased PPARγ activation ($p < 0.001$). PPARγ activation could be irreversibly prevented by pre-incubating the cells with 1 μM GW9662, a known PPARγ antagonist [332] for 30 minutes prior to treating with 100 nM rosiglitazone. Treating with 500 nM pioglitazone, another PPARγ agonist, did not increase luciferase expression. However, a small but significant ($p < 0.05$) increase in PPARγ activation was observed when the cells were treated with 1 μM pioglitazone. The *P. aeruginosa* signalling molecule C12HSL is also reported to agonize PPARγ and treatment of cells with 10 μM C12HSL produced a small but significant increase in PPARγ activation. We also investigated the ability of C12HSL to prevent rosiglitazone from activating PPARγ by pre-incubating the cells with 10 μM C12HSL for 30 min prior to treating with 100 nM rosiglitazone. C12HSL was unable to completely prevent rosiglitazone-mediated PPARγ activation, but a 20% decrease in PPARγ activation was observed with C12HSL pre-treatment.

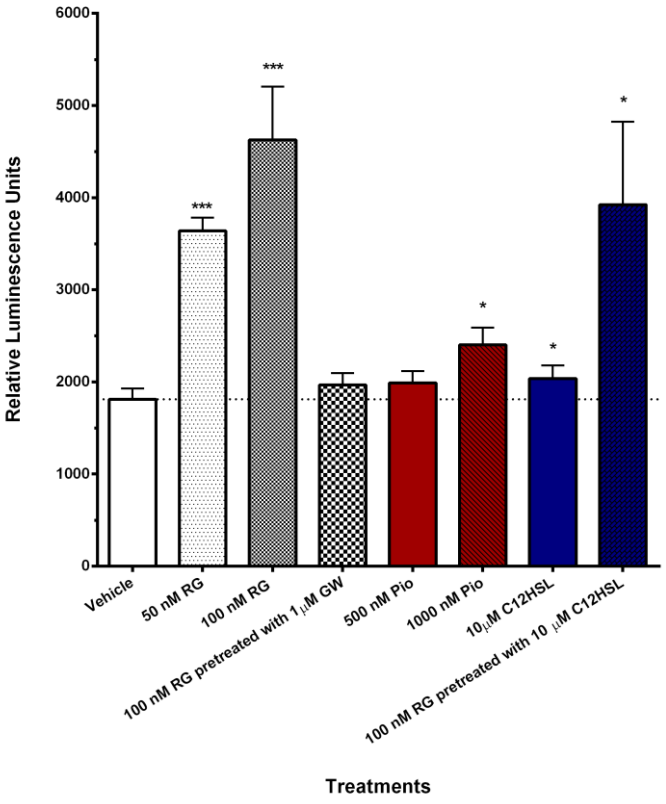

Figure 4.4 PPARγ activation by a number of PPARγ agonists and antagonists. BEAS-2B cells were transiently co-transfected with A-Ox3-TKSL-PPRE, a PPAR-responsive luciferase expression vector and pcDNA3-PPARγ1, a PPARγ expression vector. The cells were then treated for 16 hours with varying doses of the agonists rosiglitazone (RG), pioglitazone (Pio) and C12HSL. Cells were also pre-treated with GW9662 (GW) and C12HSL for 30 minutes prior to rosiglitazone treatment. The lysates were assayed for luminescence. Results expressed as firefly luciferase expression relative to renilla luciferase expression. Error bars represent S.D.; n = 3–7. *$p < 0.05$; ***$p < 0.001$ relative to vehicle control (*t*-test).

4.3.4 PON2 gene and protein expression induced by PPARγ activation

The correlation of PPARγ and PON2 gene expression in CF lungs (Figure 4.1) prompted the investigation of whether PON2 expression is directly induced by PPARγ activation. The known PPARγ agonist rosiglitazone was used to activate PPARγ in the BEAS-2B human airway epithelial cell line. After treatment with 100 nM rosiglitazone, changes in PON2 gene and protein expression were measured by quantitative PCR (n = 4) and western blot analysis, respectively, over a period of 16 hours.

The changes in PON2 gene expression in BEAS-2B cells over 16 hours treatment with rosiglitazone are shown in figure 4.5. There is an immediate trend towards an increase in *PON2* transcription after one hour of PPARγ activation. By four hours, *PON2* expression in rosiglitazone-treated BEAS-2B cells is significantly higher than that in the vehicle control ($p<0.05$). A similar increase in PON2 protein expression was observed in response to rosiglitazone treatment (Figure 4.6). By 16 hours, PON2 gene expression was significantly down-regulated ($p < 0.05$) and the increase in PON2 protein had also diminished by 16 hours (Figure 4.6).

PPARγ expression remained more stable than *PON2* following rosiglitazone treatment. A significant increase in *PPARγ* expression was observed at four hours post treatment ($p < 0.05$) (Figure 5), similar to the rosiglitazone effect on *PON2* gene expression, but this was not apparent by 16 hours, when there was a trend towards down-regulation of *PPARγ* expression ($p < 0.057$).

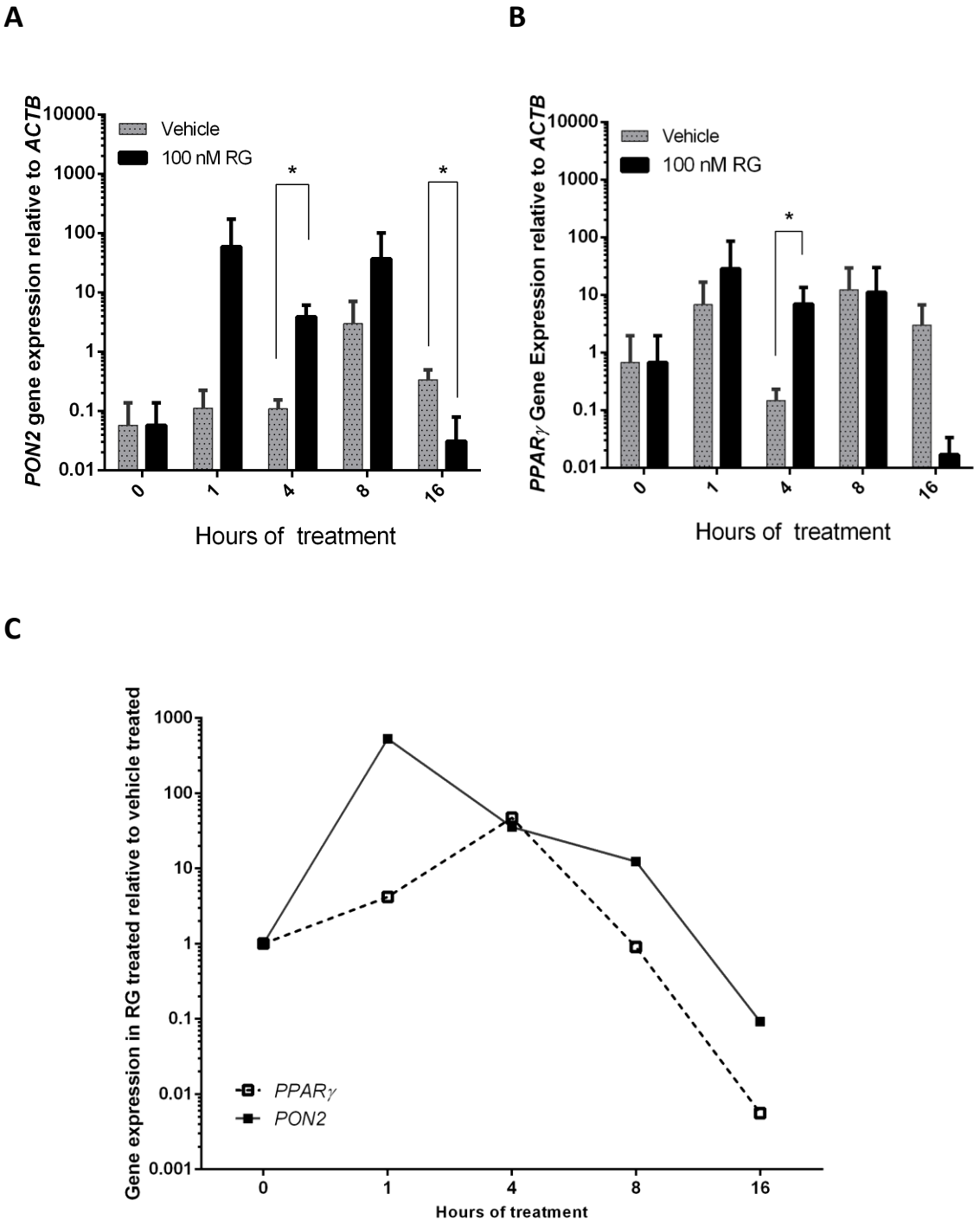

Figure 4.5 Change in relative gene expression of PON2 and PPARG in BEAS-2B cells treated with rosiglitazone. BEAS-2B cells treated for 16 hour with 100 nM rosiglitazone (RG) (black) or vehicle (grey). Total RNA extracted from cells and *PON2* (**A**) and *PPARG* (**B**) gene expression relative to β-actin expression measured using real time quantitative PCR. Results expressed as $\log_{10}$ expression relative to β-actin. The $\log_{10}$ expression of *PON2* (solid line) and *PPARG* (dashed line) in RG-treated cells relative to vehicle-treated cells is shown in (**C**). Error bars represent S.D; n = 4. * $p < 0.05$, *t*-test comparing rosiglitazone-treated to vehicle-treated at each time point.

A

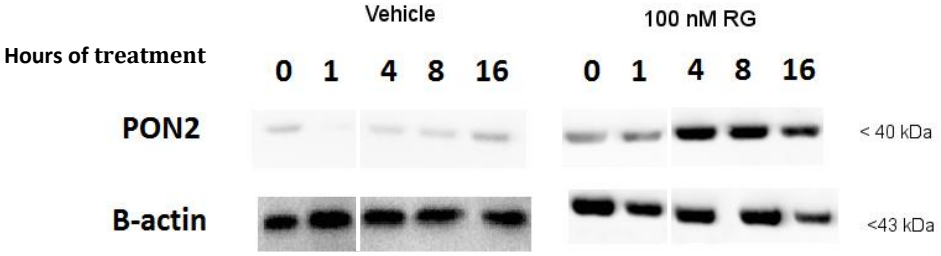

B

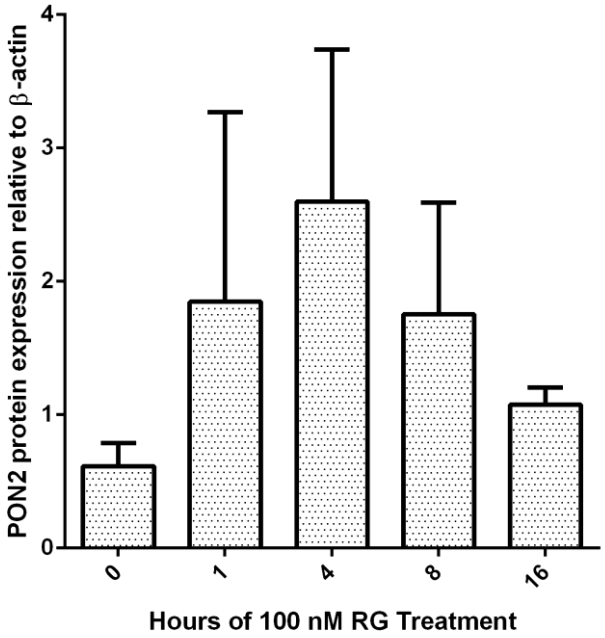

Figure 4.6 Change in PON2 protein expression in BEAS-2B cells treated with rosiglitazone (RG).
Change in PON2 protein expression over time period observed by a) western blot analysis of cell lysates and b) densitometry of western blots. Error bars represent S.E.M; n = 2.

4.3.5 PPARγ does not transactivate PON2 via the first 1100 bp of its promoter

To investigate the ability of PPARγ to transactivate PON2 expression, the pXP1-hPON2p1000 reporter vector was used [320]. The pXP1-hPON2p1000 reporter vector contains the first 1100 bp immediately up-stream of the human PON2 transcription start, the section containing the putative PPREs (Table 4.1). The activation of PPARγ by treatment of the cells with 100 nM rosiglitazone for 16 hours was detected using the PPARγ-responsive A-Ox3-TKSL-PPRE plasmid. When PPARγ is activated it binds to the PPREs and initiates the transcription of luciferase, which can then be assayed (Figure 4.7A). PPARγ activation can be prevented by pre-incubating the cells with 1 μM GW9662 for 30 minutes

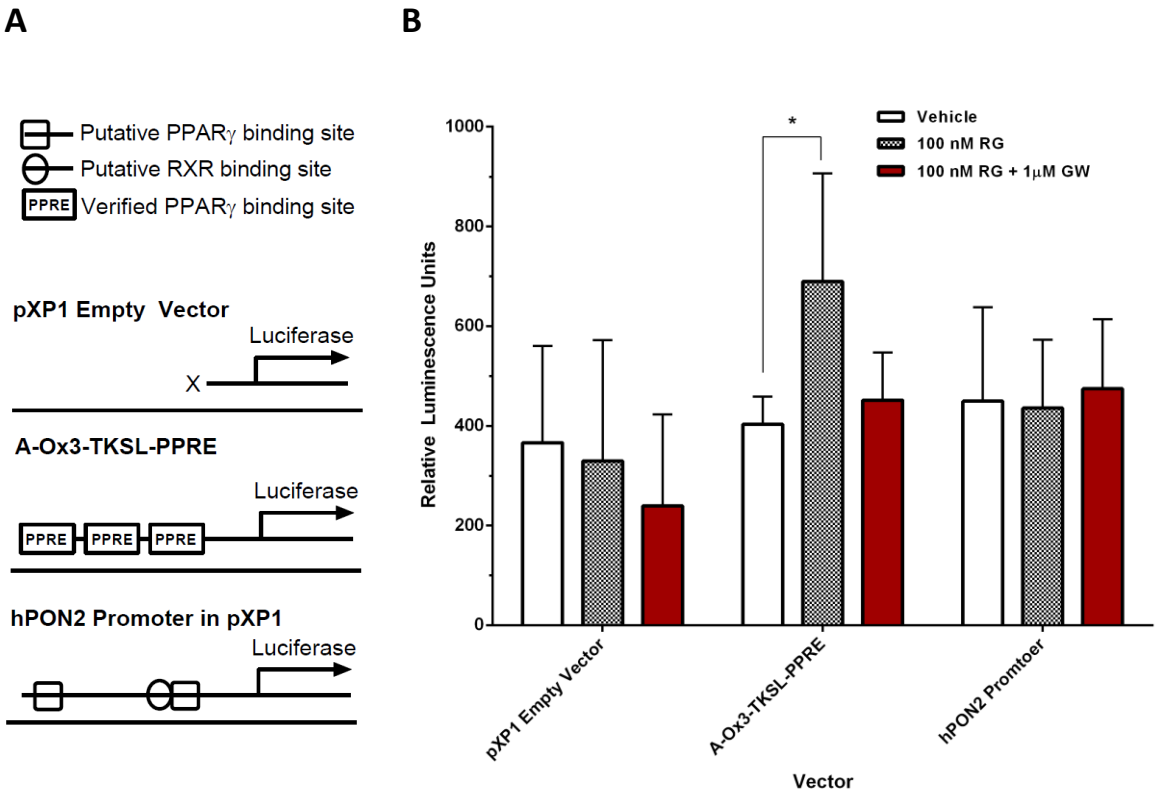

Figure 4.7 Activated PPARγ does not transactivate the human PON2 promoter within the first 1100bp. BEAS-2B cells were transiently transfected with pXP1 (promoter-less vector into which hPON2 promoter was cloned), A-Ox3-TKSL-PPRE (PPARγ responsive vector), human PON2 promoter vector and PGL4 (renilla luciferase expressing vector). A. Schematic representation of the three plasmid constructs used to assay PON2 promoter transactivation. B. Transfected cells were treated with vehicle or 100 nM rosiglitazone (RG) for 16 hours or 1μM GW9662 (GW) for 30 minutes prior to 16 hours with 100 nM rosiglitazone. Cell lysates were collected and luciferase expression assayed. Results expressed as firefly luciferase relative to renilla luciferase. Error bars represent S.D.; n = 5. * = $p < 0.05$, *t*-test comparing two groups.

prior to rosiglitazone treatment. Cells were also transfected with the promoter-less pXP1 vector to control for leaky luciferase expression from the plasmid. All the cells were co-transfected with the PPARγ expression plasmid pcDNA3-PPARγ1[331] to ensure adequate PPARγ was present and with pGL4 to normalize luciferase expression to assess transfection efficiency.

When cells were transiently transfected with the promoter-less pXP1 vector, pcDNA3-PPARγ1 and pGL4, no change in relative luciferase expression was observed after treatment with PPARγ agonist or antagonist (Figure 4.7B). In the positive control, where cells were transiently transfected with the PPARγ-responsive A-Ox3-TKSL-PPRE, pcDNA3-PPARγ1 and pGL4, a significant increase in luciferase expression relative to the vehicle-treated cells was observed when PPARγ was activated by treatment with 100 nM rosiglitazone for 16 hours ($p < 0.05$). When cells were treated with GW9662, this effect was abolished and no difference was observed between the vehicle-treated and GW9662-treated cells. When the cells were transiently transfected with hPON2 promoter reporter vector containing putative PPREs, activating PPARγ in the cells with 100 nM rosiglitazone did not lead to transactivation of the PON2 promoter. Similarly, no effect was observed in response to treatment with PPARγ antagonist GW9662.

4.4 DISCUSSION

This is the first study that describes PPARγ-mediated modulation of PON2 gene and protein expression in human airway epithelial cells. Much of the research into PON2 regulation has primarily focused on the ability of PON2 in macrophages to protect against oxidative stress. The first point of contact for the establishment of *P. aeruginosa* infection in the lungs is the airways, where bacteria establish and begin producing QS molecules. As acyl homoserine lactones, including *P. aeruginosa* QS molecules, are widely considered to be the natural substrate of PON2, it is appropriate to improve our understanding of the regulation of PON2 in the airways in response to infection, as a component of the innate defence mechanisms.

We observed an increase in PON2 mRNA and protein expression within 4 hours post treatment with100 nm rosiglitazone, a concentration previously shown to activate PPARγ [218]. This effect had essentially disappeared by 16 hours of treatment. Shiner and colleagues found that PPARγ activation by rosiglitazone induced PON2 mRNA and protein in the J774A.1 mouse macrophage cell line [268]. The authors observed a significant increase in *PON2* mRNA, but not PON2 protein, after 18 hours treatment with 10 μM rosiglitazone, although both PON2 mRNA and protein were increased after 18 hours treatment with at least 25 μM rosiglitazone. This group did not study earlier time points, so we cannot directly compare our results with theirs, but it is possible that higher concentrations of rosiglitazone are required to sustain increased PON2 levels for a prolonged time. What is striking about our findings is the early (within 2 hours) increase in PON2 mRNA and protein expression in response to PPARγ activation. This suggests the regulatory relationship between the two is direct or very close. Our *in silico* identification of 'good' putative PPREs in the PON2 promoter [320] further strengthens the hypothesis that PPARγ transcriptionally regulates PON2. *In silico* based methods of transcription factor binding site analysis such as MatInspector are useful in identifying the potential of a site to bind the protein in question. However, it is the context of the site that separates a functional regulatory region from a physical sequence. The presence of binding sites for dimers is one such factor. The context of the PPREs we identified by MatInspector is deserving of consideration. Their close proximity to the PON2 start codon coupled with the presence of an adjacent RXR binding site makes them ideal candidates to explore experimentally.

We also observed an increase in *PPARG* expression when PPARγ was activated. This was unexpected, as rosiglitazone is a PPARγ ligand which, upon binding to PPARγ, instigates the

conformational changes required for the complex to recruit co-activators or co-repressors and alter transcription. It should not necessarily increase PPARγ mRNA, however, increased PPARγ mRNA and protein have been reported in BEAS-2B cells and other airway epithelial cells in response to rosiglitazone treatment [300], suggesting that a positive feedback loop exists. A marked increase in *PPARG* expression 16 hours post rosiglitazone treatment was observed but not found statistically significant. While this observation may call into question, the validity of the assay, in reality, this anomaly was caused by an outlier in the biological replicates that could not be excluded and only applies to this time point and only for the *PPARG* gene.

When using transfection based reporter assays, it is important to have a well-characterized assay system. The use of a second constitutively expressed reporter to normalize transfections is important to control for the potential differences in transfection efficiency. We optimized our assay system to achieve optimum expression of luciferases from both reporters and we established that BEAS-2B cells express endogenous PPARγ that could be activated by rosiglitazone and detected by our PPAR-responsive reporter. However, this activation of PPARγ was modest, and only seen after treatment with higher concentration of rosiglitazone (100 nM and 280 nM). Pawliczak and colleagues carried out western blot analysis of PPAR isoforms in four human airway epithelial cell lines (NHBE, BEAS-2B, A549, and H292 cells), and found that BEAS-2B cells expressed the least amount of PPARγ protein. Because our studies are based on PPARγ-mediated signalling, we needed to ensure that enough PPARγ was present to observe any PPARγ-mediated effects on PON2 expression. When we overexpressed PPARγ in our cells, we observed strong activation of PPARγ after rosiglitazone treatment at all the tested concentrations, underlining the importance for our experiments of overexpressing PPARγ. The highly selective PPARγ agonists rosiglitazone and pioglitazone [333] were both able to induce PPARγ activation as predicted. When our cells were pre-treated with the PPARγ antagonist GW9662 prior to rosiglitazone treatment, we observed an irreversible inhibition of PPARγ activation, as reported previously in the literature [332]. We also demonstrated the weak agonist activity of 10 μM C12HSL on PPARγ and its ability to interfere with rosiglitazone-mediated activation of PPARγ, as reported by Cooley and colleagues [218]. GW9962 is thought to modify cysteine residues is the ligand binding domain of PPARγ when bound to PPARγ [332] and thereby preventing further ligand binding. C12HSL interference with PPARγ ligand binding does not appear to be irreversible, so the mechanisms of antagonistic activity of GW9662 and C12HSL are likely to be distinct.

Our transcription factor reporter assays indicate that PPARγ does not transactivate the expression of PON2 by binding within the first 1000 bp of the human PON2 promoter. However, direct transactivation of PON2 by PPARγ is still the most likely explanation for the speed with which activation of PPARγ leads to PON2 expression. It may be that the functional PPARγ binding site in the PON2 promoter is further up-stream or down-stream than investigated in our transcription factor reporter assays. Functional PPREs have been located as far as 3300 bp up-stream from the transcription start [334]. Co-regulatory elements can be involved in transcription irrespective of their location in regards to the promoter [Reviewed in 335] and can be as much as 1 Mb from the promoter, as is the case with the limb bud enhancer for the mouse sonic hedgehog (*Shh)* gene [336]. Perhaps a PPARγ-mediated regulation of PON2 could then be observed if a larger section of the PON2 promoter was studied that could be identified based on a better understanding of the regulatory elements involved in PON2 transcription.

It is also possible that PPARγ activation of PON2 gene expression is indirect rather than directly linked. The effects of PPARγ activation on the immune system are numerous and far reaching, and a number of down-stream factors may be involved in subsequent regulation of PON2, especially given the roles that PON2 plays as an anti-oxidant, anti-artherogenic and anti-apoptotic agent.

Interestingly, rosiglitazone has also been shown using microarrays in murine PPARγ$^{-/-}$ macrophages to have PPARγ-independent effects, and it is impossible to disregard the possibility of a rosiglitazone-mediated, PPARγ-independent effect on PON2 expression [337-340]. Rosiglitazone is a class of medications that contain a thiazolidine functional group which serves as a dione known as thiazolidinediones (TZD's). Perez-Ortiz and colleagues have demonstrated PPARγ-independent effects of another member of the family of TZDs, ciglitazone, also a known PPARγ agonist. Ciglitazone was able to induce PPARγ-independent cellular toxicity by producing reactive oxygen species and rapidly depolarizing the mitochondrial membrane in primary murine astrocytes [341]. As PON2 protects against oxidative stress, the TZDs may induce PON2 expression by a PPARγ-independent pathway. Further research is needed into these PPARγ-independent effects to identify a possible mechanism by which rosiglitazone-mediated PPARγ-independent up regulation of PON2 would be possible. This could be done by using GW9662, a well-characterized selective and irreversible PPARγ antagonist, to observe PPARγ-independent effects of rosiglitazone.

As the modulation of PPARγ expression/activity in the CF lung, both as a consequence of defective CFTR and of possible antagonism by C12HSL becomes clearer, our need to understand the influence of PON2 in lung and airways becomes more pressing. Decreased PPARγ expression has been observed in human CF cell lines and *Cftr*-deficient mice [220, 222, 342], while we have previously observed that *P. aeruginosa* infection is correlated with low PPARγ expression in the bronchoalveolar lavage fluid of people with CF [223]. Given the suggested protective role of PON2 against C12HSL-mediated signalling in bacteria and its effects on respiratory epithelium, and our observation that PPARγ activation increases expression of PON2, the modulation of PPARγ in CF may have important consequences in terms of innate defence mechanisms and disease progression.

Increased levels of PON2 expression in airway cells in response to rosiglitazone treatment would be beneficial from the perspective of preventing/ameliorating infection. PON2-deficient mice have been shown to be less adept than wild-type mice at clearing *Pseudomonas* infections [249], and the ability of PON2 to degrade *P. aeruginosa* QS signals is well established [248, 260, 262, 264]. PON2 may also protect the airways themselves from the oxidative stress and proapoptotic effects of the *P. aeruginosa* QS C12HSL. In a CF setting, an increase in PPARγ activity with rosiglitazone treatment may go some way into correcting the detrimental effects the CFTR mutations have on PPARγ activity, including modulation of the immune response. Treating *Cftr*-deficient mice with a synthetic PPARγ agonist reversed some of the effects of the CFTR deficiency and reduced disease severity in the gut [220]. In *Cftr*-deficient mice acutely infected with *P. aeruginosa,* administration of a synthetic PPARγ agonist protected against the exaggerated inflammatory response in the airways that is usually seen in *P. aeruginosa* infected *Cftr*-deficient mice [222, 343].

Rosiglitazone is a member of the TZD group of chemicals. A number of TZDs have been approved for clinical use, mostly to treat insulin resistance, but numerous severe side effects have since been discovered. Troglitazone has been withdrawn from the market because of liver toxicity in some patients [344], while the use of both rosiglitazone and pioglitazone have been associated with an increased risk of heart failure and increased fluid retention, meaning that their use is now limited [345, 346]. In late 2013, the FDA released a statement removing the prescribing and dispensing restrictions for rosiglitazone and it can once again be used to improve control of blood sugar in patients with type 2 diabetes mellitus [347]. The use of TZDs to increase endogenous PON2 expression is a therapeutic strategy that needs to be balanced with the risks it poses. Instead of using TZDs, we could

also focus our attention on increasing PON2 in the lungs by alternate methods such as extracellular application of recombinant protein, a proposal that will be explored further in subsequent chapters of this thesis.

CHAPTER FIVE – RECOMBINANT HUMAN PON2 AS A NOVEL ANTI-PSEUDOMONAL THERAPY

5.1 INTRODUCTION

P. aeruginosa utilises a cell-density dependent and intercellular communication system, called quorum sensing (QS), to co-ordinate and regulate virulence factor production, as well as biofilm formation. *P. aeruginosa* has multiple, hierarchically arranged QS systems, as described in Section 1.2.4.1. At the top of the *P. aeruginosa* QS hierarchy is the Las system, which utilizes C12HSL, an acyl homoserine lactone (AHL) signalling molecule. In addition, the Las system also regulates the activity of the Rhl system. The Rhl system also utilizes an AHL, C4-HSL as its signalling molecule [Reviewed in 119, 140, 348]. Together, the Las and Rhl systems regulate the third *P. aeruginosa* QS system, PQS. These three QS systems play an important role in the regulation of a number of virulence determinants including the biosynthesis of elastase, alginate, hydrogen cyanide, rhamnolipid and pyoverdine. There are also overarching regulators of QS, including the virulence factor regulator Vfr and the GacS/GacA two component regulatory system, which transcriptionally and post-transcriptionally regulate the QS systems [119, 140, 348].

As QS is important for *P. aeruginosa* virulence and biofilm formation, and responsible for regulating virulence of many other Gram-negative bacteria, it is seen by many investigators to represent a target for novel antimicrobial therapies. One potential mechanism for QS inhibition is degradation of the QS signal molecules themselves. Enzymatic degradation of the QS signal, particularly through the hydrolysis of lactone rings of AHLs is perhaps one of

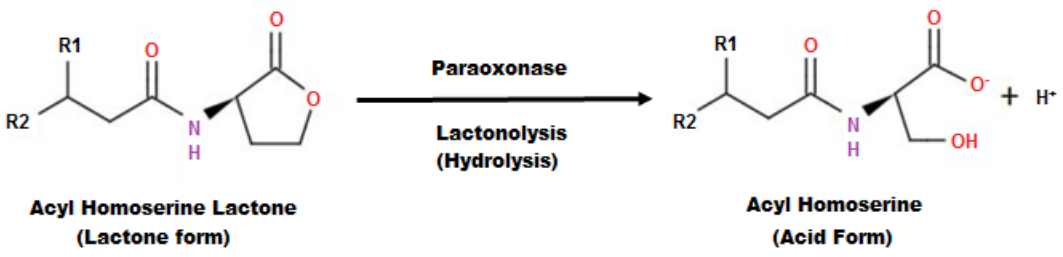

Figure 5.1 Lactonolysis of AHL's. Acyl homoserine lactones (AHL's) comprise of a five-membered homoserine lactone ring amide-linked to a variable acyl chain. In nature, the AHL's have *N*-acyl moieties that range from 4 to 14 carbons atoms in length (R2). The acyl chains may be saturated or unsaturated and also may contain a hydroxy or oxo substituent (R1). The lactone ring of the AHL's can be spontaneously hydrolysed (and condensed once hydrolysed) in a pH and temperature dependent manner to the hydrolysed acid form [243].The lactonolysis of AHL's by paraoxonases also involves hydrolysis of the lactone ring. The resultant molecule is the acid form of the AHL.

the more promising forms of QS inhibition (Figure 5.1). Hydrolysis of the lactone ring effectively inactivates AHLs, thereby rendering them unable to signal through their cognate receptors [242, 243]. A number of lactonases have been identified in several bacterial species [242, 244-246]. Interestingly, mammals also produce enzymes with intrinsic lactonase activity, the so-called paraoxonases, which have been reported to exhibit highly specific *in situ* hydrolytic activity against certain bacterial AHLs [247, 248, 262, 264]. Some of these mammalian paraoxonases have been demonstrated to attenuate *P. aeruginosa* virulence in KO-mice and Drosophila models of *P. aeruginosa* infection [249, 250], underscoring their potential as QS inhibitors.

The paraoxonase family consists of three distinct proteins, PON1, PON2 and PON3, which display considerable sequence homology [253]. While PON1 and PON3 are primarily expressed in the liver and sera, PON2 is ubiquitously expressed, especially in respiratory epithelia, as an intracellular membrane-bound protein, mainly associated with nuclear and mitochondrial membranes and the endoplasmic reticulum [253, 255-259]. Of the three PONs, PON2 has the highest recorded AHL lactonase activity of all the paraoxonases tested, and has been demonstrated to have maximal activity against C12HSL [248, 262].

To date, PON2 studies have largely been confined to over expression and knockout models. However, simply augmenting native PON2 expression might prove less useful therapeutically against *Pseudomonas* because PON2 is an intracellular protein, whereas the bacterial QS signals accumulate mostly in the extracellular environment. A more effective therapeutic approach might instead involve the application of a recombinant human form of PON2 (rhPON2) into the *P. aeruginosa* infected airways, where PON2 would be expected to disrupt QS through lactonolysis of bacterially produced C12HSL. In turn, inactivation of the C12HSL would prevent bacterial QS and associated biofilm formation and virulence and as a result could be expected to increase the susceptibility of *P. aeruginosa* to conventional antimicrobial therapies already in use in CF clinics such as tobramycin. Importantly, known C12HSL-mediated effects on host cells could also be prevented.

Tobramycin, while not considered to not have anti-QS activity, is an important component of the CF antibiotic regime. Study of anti-QS therapies, in combination with tobramycin, allow for the isolation of the specific effects of the anti-QS therapy and as such, tobramycin was selected for use in this study.

Whilst there are a number of studies involving rhPON2 [248, 258, 262, 272, 273, 349, 350], there are few, if any, studies in the literature documenting the effects of recombinant PON2

on growth, QS and virulence of *P. aeruginosa*. Instead, there are some studies describing the effects of recombinant bacterial acylases on *P. aeruginosa* QS and virulence. Bacterial acylases are another class of enzymes that degrade C12HSL via hydrolysis of the amide bond between the acyl chain and the homoserine lactone ring. Recombinant acylases have been shown to be effective in decreasing the accumulation of C12HSL produced by *P. aeruginosa* and have been reported to decrease QS and QS-dependent virulence of this organism *in vitro* [351-355]and *in vivo* [352, 353]. There are, however, several advantages to using a mammalian therapeutic protein instead of a bacteria-derived C12HSL hydrolysing enzyme, the most important of which concerns safety. Given that human PON2 is normally expressed in the mammalian host, a recombinant hPON2 protein is far less likely to be immunogenic, reducing the likelihood of both inactivation and adverse effects of the hPON2 protein, and thereby increasing the likelihood of regulatory approval.

Active rhPON2 has usually been cloned and purified using three independent methods: i) directed evolution in *Escherichia coli* followed by purification using a GST tag [258], ii) baculovirus infection of *Trichoplusia ni* insect cells and subsequent purification using liquid chromatography techniques [248, 262], and iii) expression in mammalian cells followed by the use of either clarified cell lysates [349] or else further purification using affinity chromatography [273].

Certain considerations must be kept in mind when attempting to produce rhPON2. First, a polymorphism has been reported in PON2 that alters its lactonase activity. Substitution of cysteine for serine at codon 311 diminished but did not eliminate rhPON2 lactonase activity [349]. Second, the paraoxonases are glycoproteins, and carbohydrates account for around a sixth of their molecular mass [356]. rhPON2 being produced in insect or mammalian cells, unlike that produced in bacteria such as *E. coli,* is usually glycosylated, even though insect cells do not glycosylate the protein to the same extent as human cells [262]. Glycosylation has been reported by some investigators to be critical to the lactonase activity of rhPON2 [273, 349], while others have described glycosylation as being important for the stability but not the hydrolytic activity of paraoxonases [357, 358].

In the studies described in this chapter, rhPON2 was synthesized by infecting *Trichoplusia ni* insect cells with a baculovirus made to express human PON2 (Ser^{311} variant). The lactonase activity of the purified rhPON2 was then tested against C12HSL. We hypothesized that rhPON2 would inhibit *P. aeruginosa* QS by inactivating C12HSL and as a consequence, increase the susceptibility of *P. aeruginosa* to conventional antibiotic therapy.

The results of this chapter demonstrate that (i) rhPON2 was effective at preventing *P. aeruginosa* QS, and (ii) exposing cells of *P. aeruginosa* to rhPON2 increased the susceptibility of *P. aeruginosa* to the antibiotic tobramycin. Taken together, the data presented in this chapter lend strong support to the idea of using rhPON2 as a novel QS inhibitor.

5.2 MATERIALS AND METHODS

The materials and methods for this chapter are described in Chapter 2. Additional materials and methods specific to this chapter are described below.

5.2.1 Generation of a recombinant human PON2-expressing baculovirus

5.2.1.1 Generation of recombinant human PON2 vector.

The human PON2 transcript (isoform 1, NCBI accession NM_000305.2, Ser^{311} variant) was codon optimized for expression in insect cells and synthesized by DNA2.0 (Menlo Park, California, US) (Figure 5.2). The transcript included a *Bam*HI restriction enzyme site seven bp upstream from the PON2 translation start codon, and a *Not*I restriction site immediately following the translation stop codon. Following restriction digestion, the PON2 transcript was ligated into the multiple cloning site of the pFastBac1 vector (Life Technologies, Carlsbad, California) using the *Bam*HI and *Not*I restriction sites to generate the recombinant human PON2 vector pFastBac1.hPON2 (Figure 5.3).

```
G GAT CCT ATA AAT ATG GGT AGG TTG GTC GCT GTT GGT CTG CTC GGT ATT GCG TTG GCA CTG CTG GGC GAA CGC CTT TTG GCT CTG CGT AAT AGA CTG AAG  < 100
              M   G   R   L   V   A   V   G   L   L   G   I   A   L   A   L   L   G   E   R   L   L   A   L   R   N   R   L   K
          10          20          30          40          50          60          70          80          90

GCC TCA AGA GAA GTC GAA TCA GTT GAT CTC CCT CAC TGC CAC CTC ATC AAA GGT ATC GAG GCT GGC TCG GAG GAC ATT GAT ATT CTG CCA AAT GGA CTT G  < 200
 A   S   R   E   V   E   S   V   D   L   P   H   C   H   L   I   K   G   I   E   A   G   S   E   D   I   D   I   L   P   N   G   L   A
          110         120         130         140         150         160         170         180         190

CA TTC TTT TCG GTG GGC CTC AAG TTC CCC GGA CTC CAT AGC TTC GCT CCA GAC AAG CCA GGA GGA ATC TTG ATG ATG GAT TTG AAG GAA GAG AAA CCT CG  < 300
   F   F   S   V   G   L   K   F   P   G   L   H   S   F   A   P   D   K   P   G   G   I   L   M   M   D   L   K   E   E   K   P   R
          210         220         230         240         250         260         270         280         290

C GCT AGG GAG CTC CGC ATA TCC CGT GGC TTC GAC CTG GCG TCC TTC AAT CCT CAC GGT ATT AGT ACC TTC ATC GAT AAC GAC GAC ACT GTT TAC CTT TTC  < 400
  A   R   E   L   R   I   S   R   G   F   D   L   A   S   F   N   P   H   G   I   S   T   F   I   D   N   D   D   T   V   Y   L   F
          310         320         330         340         350         360         370         380         390

GTG GTC AAC CAC CCC GAG TTC AAG AAT ACA GTT GAG ATT TTC AAG TTT GAG GAG GCC GAG AAC TCC TTG CTG CAC CTC AAG ACC GTG AAG CAC GAA CTC C  < 500
 V   V   N   H   P   E   F   K   N   T   V   E   I   F   K   F   E   E   A   E   N   S   L   L   H   L   K   T   V   K   H   E   L   L
          410         420         430         440         450         460         470         480         490

TT CCG AGC GTC AAC GAC ATC ACA GCA GTG GGC CCT GCT CAC TTT TAC GCC ACG AAC GAC CAC TAC TTT TCC GAT CCG TTC TTG AAG TAC TTG GAA ACC TA  < 600
   P   S   V   N   D   I   T   A   V   G   P   A   H   F   Y   A   T   N   D   H   Y   F   S   D   P   F   L   K   Y   L   E   T   Y
          510         520         530         540         550         560         570         580         590

T CTG AAT CTC CAC TGG GCC AAC GTC GTG TAC TAC TCC CCC AAC GAG GTG AAA GTT GTC GCG GAG GGT TTC GAC AGC GCG AAC GGC ATC AAC ATC AGT CCC  < 700
  L   N   L   H   W   A   N   V   V   Y   Y   S   P   N   E   V   K   V   V   A   E   G   F   D   S   A   N   G   I   N   I   S   P
          610         620         630         640         650         660         670         680         690

  GAT GAC AAA TAC ATC TAC GTA GCC GAC ATC CTT GCT CAT GAG ATC CAT GTA CTG GAA AAG CAT ACC AAT ATG AAC CTG ACG CAA CTG AAA GTG TTG GAG C  < 800
   D   D   K   Y   I   Y   V   A   D   I   L   A   H   E   I   H   V   L   E   K   H   T   N   M   N   L   T   Q   L   K   V   L   E   L
          710         720         730         740         750         760         770         780         790

TC GAC ACT TTG GTC GAC AAC CTG TCA ATT GAT CCG TCA TCT GGT GAT ATA TGG GTC GGA TGT CAT CCT AAC GGA CAA AAG CTG TTC GTC TAT GAC CCC AA  < 900
   D   T   L   V   D   N   L   S   I   D   P   S   S   G   D   I   W   V   G   C   H   P   N   G   Q   K   L   F   V   Y   D   P   N
          810         820         830         840         850         860         870         880         890

T AAC CCT CCA TCT TCT GAA GTG TTG CGT ATA CAG AAC ATC CTT AGT GAA AAG CCA ACC GTG ACT ACT GTT TAT GCA AAC AAC GGC AGC GTA CTG CAG GGT  < 1000
  N   P   P   S   S   E   V   L   R   I   Q   N   I   L   S   E   K   P   T   V   T   T   V   Y   A   N   N   G   S   V   L   Q   G
          910         920         930         940         950         960         970         980         990

TCA TCT GTA GCA TCC GTG TAC GAT GGA AAA CTC CTG ATC GGC ACA CTT TAT CAC AGG GCC TTG TAC TGC GAA CTT TAA GCG GCC GC  < 1086
S   S   V   A   S   V   Y   D   G   K   L   L   I   G   T   L   Y   H   R   A   L   Y   C   E   L   *
          1010        1020        1030        1040        1050        1060        1070        1080
```

Figure 5.2 Nucleotide and protein sequence of synthesised human PON2 transcript. Figure shows human PON2 transcript (isoform 1, NCBI accession NM_000305.2, with Ser311) (top line) and translated AA sequence (middle line), with codon optimization for insect cell protein synthesis by DNA2.0. The transcript includes a *Bam*HI restriction site seven bp upstream from the PON2 translation start codon, and a *Not*I restriction site immediately downstream from the translation stop codon.

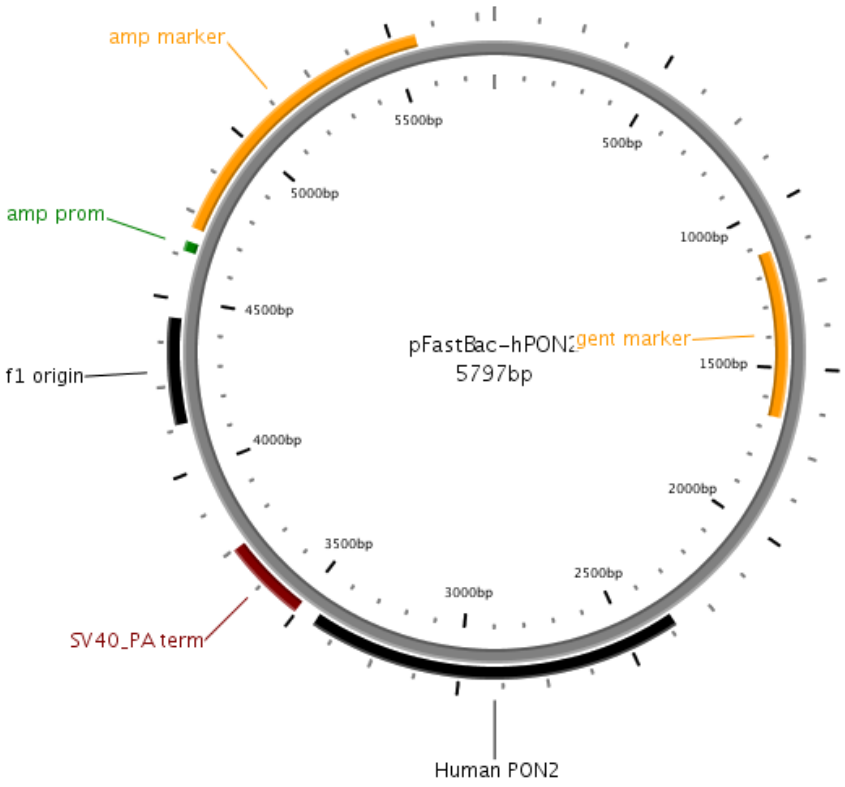

Figure 5.3 Vector map of pFastBac.hPON2, a hPON2-containing plasmid vector. The synthesized hPON2 sequence was inserted into the MCS of pFastBac to give pFastBac-hPON2, a 5797 bp plasmid with SV40 promoter and ampicillin and gentamycin resistance cassettes.

The pFastBac1.hPON2 construct was transformed into One Shot® TOP10 Competent Cells (Life Technologies) following to the manufacturer's recommended chemical transformation protocol. Briefly, 5 µL of construct DNA was added to one vial of OneShot® TOP10 Competent Cells. The mixture was incubated on ice for 30 minutes, heat-shocked for 45 seconds at 42°C without agitation, and immediately chilled on ice for a further two minutes. A 250 µL aliquot of S.O.C. medium was added and the mixture shaken at 150 RPM at 37°C for one hour.

Transformed cells (20 µL, 50 µL and 120 µL aliquots) were then spread-plated on LB agar plates supplemented with 100 µg/mL ampicillin. The plates were incubated at 37°C overnight. The following day, single colonies were isolated from the plates and used to inoculate fresh LB-ampicillin plates. Selected colonies were used to inoculate 2 mL LB medium and grown overnight at 37°C, with shaking at 220 RPM. DNA from overnight cultures was isolated using a plasmid mini-prep kit (Promega, Madison, WI) (Chapter 2.4.2) and subjected to PCR using hPON2 primers (sequences in table 2.3) and gel electrophoresis

used to verify correct insertion. DNA and glycerol stocks of pFastBac1.hPON2 were stored at −80°C for future use.

5.2.1.2 Generation of recombinant hPON2 bacmid and isolation of recombinant hPON2 bacmid DNA

The hPON2 bacmid was generated using the Bac-to-Bac® Baculovirus expression system (Life Technologies) according to the manufacturer's protocols. The pFastBac1 vector's expression cassette recombines with the parent bacmid in the MAX Efficiency® DH10Bac cells to form an expression bacmid. Briefly, 5 µL of pFastBac1.hPON2 DNA (200 pg/µL in TE, pH 8.0) was added to 100 µL of MAX Efficiency® DH10Bac™ in a pre-chilled 15-mL polypropylene tube. The cell-DNA mixture was incubated on ice for 30 mins, heat shocked for 45 seconds at 42°C, then immediately chilled on ice for a further two minutes. Finally 10-fold serial dilutions were prepared in S.O.C medium before being plated onto LB plates supplemented with 50 µg/mL kanamycin, 7 µg/mL gentamicin, 10 µg/mL tetracycline, 40 µg/mL X-gal, and 40 µg/mL IPTG. The plates were incubated for 48 hours at 37°C after which time several white colonies were picked and struck onto fresh selective medium to obtain single colonies. A single colony was used to inoculate LB containing 50 µg/mL kanamycin, 7 µg/mL gentamicin and 10 µg/mL tetracycline and grown overnight at 37°C with shaking at 220 RPM. Bacmid DNA was then isolated using plasmid mini-preps (Promega) (Section 2.4.2.3) and PCR and gel electrophoresis was used to verify the presence of recombinant hPON2 constructs using primers: pUC/M13 primers (Table 2.3) The DNA and glycerol stocks of pFastBac1.hPON2 bacmid were stored at −80°C for future use.

5.2.1.3 Generation of recombinant hPON2 baculovirus stocks

Baculovirus stocks were generated in *Spodoptera frugiperda* Sf9 cells (Life Technologies), which were transfected with recombinant bacmid DNA using the Cellfectin® reagent supplied with the Bac-to-Bac® Baculovirus expression system (Life Technologies) and following the manufacturer's instructions. Briefly, recombinant hPON2 bacmid DNA was diluted to 500 ng/µL in TE Buffer, pH 8.0. Stationary phase Sf9 cells (~1×10^7 cells/mL) were diluted to 2×10^6 cells/mL. In six-well plates, 2 mL of unsupplemented Grace's Insect Medium was added to each well followed by the addition 8×10^5 Sf9 cells in SF900III medium. The cells were allowed to rest and attach to plates at room temperature for 15 minutes. The DNA–transfection reagent complexes were prepared at various ratios of DNA to transfection reagent in unsupplemented Grace's Insect Medium to determine the optimum DNA to transfection reagent ratio. The DNA–transfection reagent complexes were

added drop-wise to the cells. The cells were then incubated in a humidified incubator at 27°C for 6 hours before growth medium was replaced with SF900-III serum-free medium and further incubated in a humidified incubator at 27°C. Cells were monitored daily for signs of viral infection (Table 5.1). Once cells showed signs of late infection (Table 5.1), the growth medium from the wells was removed and centrifuged at 500 × *g* for five minutes to remove any cells and debris. The supernatant containing virus particle was collected and FBS was added to a final concentration of 2% (v/v). This yielded the P1 baculoviral stock. P1 baculoviral stock was stored short-term at 4°C, protected from light, or at −80°C for long-term storage. Immunoblot analysis of cell lysates was carried out with PON2 antibody to establish the presence of rhPON2 protein and viral titre determined by the endpoint titre method as described in Chapter 2 (Section 2.6.4). For long-term storage, the P1 baculoviral stock was stored at −80°C.

The baculoviral stock was further amplified by infecting more Sf9 cells. Stationary phase Sf9 cells were diluted to 2×10^6 cells/mL in 50mL in a vented, flat-bottom polycarbonate Erlenmeyer flask. P1 baculovirus was added to the cells at a multiplicity of infection (MOI) of 0.1. The inoculum required was calculated using the following formula:

$$\text{Inoculum required (mL)} = \frac{\text{MOI } \left(\frac{\text{pfu}}{\text{cell}}\right) \times \text{number of cells}}{\text{baculovirus stock titer } \left(\frac{\text{pfu}}{\text{mL}}\right)}$$

The inoculated Sf9 cells were incubated at 27°C, with shaking at 120 RPM in the dark. After 48 hours, the cell suspension was collected and centrifuged at 500 × *g* for five minutes to remove any cells and debris. The supernatant was collected and FBS added to a final concentration of 2% (v/v), which constituted the P2 baculoviral stock. P2 baculoviral stock

Table 5.1 Characteristics of viral infection in Sf9 and High Five™ insect cells.
Adapted from Bac-to-Bac baculovirus expression system user guide, 2013. [275]

Signs of Infection	Phenotype	Description
Early (First 24 hours)	Increased cell diameter	A 25%–50% increase in cell diameter may be seen.
	Increase in cell nuclei size	Nuclei may appear to "fill" the cells.
Late (24–72 hours)	Cessation of cell growth	Cells appear to stop growing when compared to a cell-only control.
	Granular appearance	Signs of viral budding; vesicular appearance of cells.
	Detachment	Cells release from the plate or flask.
Very late (>72 hours)	Cell lysis	Cells appear lysed, and show signs of clearing in the monolayer.

was stored as described for P1 stocks and viral titre was determined by the endpoint titre method.

5.2.2 Expression of recombinant hPON2

The *Trichoplusia ni* cell line High Five™ (Life Technologies) has been reported to allow up to five-fold higher expression of recombinant paraoxonases than Sf9 cells [248, 356], and hence was used exclusively to express rhPON2 for purification. Stationary phase High Five™ cells were diluted to 1×10^6 cells/mL in Express Five medium and inoculated with P2 baculovirus at MOIs ranging from 0.5 pfu/cell to 5.0 pfu/cell to determine the optimum MOI for rhPON2 expression. The cells were monitored daily for signs of viral infection and harvested at the earliest signs of late infection (~48–72 hours). To harvest cells, the cell suspension was centrifuged at $1{,}000 \times g$ for 5 minutes at 4°C. The cell pellet was collected and stored at −80°C and later used for immunoblotting, activity determination and further protein purification.

5.2.3 Purification of recombinant hPON2

Recombinant hPON2 was purified via a three-step purification protocol as described by Draganov and colleagues [248]. Differential centrifugation was used to isolate the crude membrane fraction of infected High Five™ cells, followed by diethylaminoethyl (DEAE) anion exchange chromatography and Concanavalin A affinity chromatography. Purification was initially optimised and performed in our lab, but because of technical difficulties (equipment failure), cell pellets from hPON2 baculovirus infected High Five™ cells were sent to Monash Protein Production Unit (Monash University, Victoria, Australia) for large-scale rhPON2 purification.

5.2.3.1 Buffers

All buffers were filter sterilized and degassed with a 0.22 μm filter under vacuum prior to use.

5.2.3.1.1 Homogenization buffer

Homogenization buffer was 5 mM Tris/HCl at pH 7.4, 1 mM $CaCl_2$, 2 μg/mL leupeptin (Sigma Aldrich, St Louis, MO, US) and two tablets of EDTA-free protease inhibitors/100 mL buffer (Roche, Mannheim, Germany).

5.2.3.1.2 Extraction buffer

Extraction buffer was 25 mM Tris/HCl at pH 7.4, 1 mM $CaCl_2$, 10% glycerol, 1% *n*-dodecyl-β-D-maltoside (DDM) (Anatrace, Maumee, OH, US), 2 μg/mL leupeptin (Sigma) and one tablet of mini-EDTA-free protease inhibitors/10 mL buffer (Roche).

5.2.3.1.3 DEAE column buffer and DEAE elution buffer

DEAE column buffer was 25 mM Tris/HCL at pH 7.4, 1mM $CaCl_2$, 10% glycerol and 0.05% DDM (Anatrace). DEAE elution buffer was DEAE column buffer supplemented with 1 M NaCl.

5.2.3.1.4 Concanavalin A column equilibration buffer

Concanavalin A column equilibration buffer was 25 mM Tris/HCl at pH 7.4, 2 mM $CaCl_2$, 1 mM $MgCl_2$, 0.5 M NaCl and 0.05% DDM (Anatrace).

5.2.3.1.5 Concanavalin A column wash buffer and Concanavalin A column elution buffer

Concanavalin A column washing buffer was 25 mM Tris/HCl, pH 7.4, 1 mM CaCl2, 10% glycerol and 0.05% DDM (Anatrace). Concanavalin A column elution buffer was Concanavalin A column wash buffer supplemented with 200 mM methyl-α -D-mannopyranoside (Sigma).

5.2.3.2 Isolation of crude membrane fractions from rhPON2 baculovirus-infected High Five cells.

Cell pellets from 150 mL rhPON2 baculovirus-infected High Five were thawed in 30 mL ice-cold homogenization buffer, lysed with 20 × five-second passes with a Teflon homogenizer and centrifuged at 2,000 × *g* at 4°C for 10 minutes. The supernatant was discarded and the cell pellet resuspended in a further 30 mL ice-cold homogenization buffer and the homogenization process repeated twice more. The final resuspended cell pellet was centrifuged at 20,000 × *g* for 30 minutes at 4°C and the supernatant was discarded. The pellet containing the membrane-bound rhPON2 was resuspended in 20 mL ice-cold extraction buffer and solubilized overnight at 4°C on a rolling platform, and centrifuged at 2,000 × *g* at 4°C for five minutes to remove debris. The supernatant containing rhPON2 was centrifuged at 100,000 × *g* for one hour and filtered using a 0.22 μm syringe filtration unit.

5.2.3.3 DEAE anion exchange chromatography

The isolated rhPON2 containing membrane fraction was loaded onto a 5 mL DEAE-Sepharose HiTrap FF Column (GE Healthcare Life Science, Chalfont UK) at 0.5 mL/min in

DEAE column buffer on an AKTA pure FPLC system (GE). The column was washed in DEAE column buffer with 10%–50% DEAE elution buffer over 30 column volumes. Fractions were collected and the presence of rhPON2 determined by immunoblot analysis with PON2 antibody and SDS-PAGE. The SDS-PAGE gels were imaged with a Criterion Stain Free™ Gel Imaging system (BioRad, Hercules, CA, US). The PON2-containing fractions were pooled.

5.2.3.4 Concanavalin A affinity chromatography

The pooled rhPON2-containing fractions from the DEAE chromatography were mixed by rotating overnight with 1 mL of loose Concanavalin A Sepharose (GE) equilibrated with Concanavalin A column equilibration buffer by rotation at 4°C. After overnight incubation, the resin was poured into a column and washed with five column volumes of Concanavalin A column wash buffer. The bound protein was eluted with 15 column volumes of Concanavalin A column elution buffer and 2 mL fractions were collected. Following the collection of the first, second and third fractions, flow was stopped for 30, 20 and 10 minutes, respectively, to maximise recovery of rhPON2. The eluted fractions were analysed for the presence of rhPON2 by immunoblotting with anti-PON2 antibody and SDS-PAGE. SDS-PAGE gels were imaged with silver staining as described in Chapter 2 (Section 2.3). The protein concentration of individual fractions was determined according to a BSA standard curve using the BioRad protein assay. Second-order polynomial correlation coefficients were typically 0.998 or above. Because the DDM detergent was predicted to interact with the protein assay dye, all diluents contained the appropriate buffer detergent concentration and individual standard curves were prepared for each of the buffers used.

The purified protein was stored at 4°C in the Concanavalin A column elution buffer. These storage conditions resulted in minimal loss of activity over a four month period.

5.2.4 Characterizing rhPON2 lactonase activity

Recombinant human PON2 lactonase activity was measured at defined intervals *in vitro* using a PON2 C12HSL hydrolysis reaction buffer as described by Teiber and Draganov [359]. The reactions were then stopped, and the proportions of C12HSL lactone and acid were measured by UPLC-MS at the UTAS Central Science Laboratory as described below.

5.2.4.1 Buffers

5.2.4.1.1 PON2 C12HSL hydrolysis reaction buffer

The reaction buffer was 2.5 mM Tris/HCl (pH 7.4) and 1 mM $CaCl_2$. The buffer was sterilised by passing through a 0.22 μm filter prior to use.

5.2.4.1.2 PON2 C12HSL hydrolysis inhibitory reaction buffer

The reaction buffer was 2.5 mM Tris/HCl (pH 7.4) and 0.5 mM EDTA. The buffer was sterilised by passing the mixture through a 0.22 μm filter.

5.2.4.2 C12HSL hydrolysis by rhPON2

Recombinant human PON2 was resuspended in hydrolysis reaction buffer, (5 μL rhPON2 in 94 μL hydrolysis reaction buffer). To start the reaction, 1 μL of 10 mM C12HSL (Cayman Chemicals, Ann Arbor MI) in HPLC grade acetonitrile (Sigma) was added to the reaction mixture to give a starting C12HSL concentration of 100 μM. The reactions were incubated for 5, 30, 45 and 60 minutes. To stop the reaction, 100 μL of ice-cold HPLC grade acetonitrile was added and the mixture stored on ice for further analysis. rhPON2 has Ca^{2+}-dependent lactonase activity. To verify that C12HSL hydrolysis was dependent on rhPON2, a separate reaction involving inhibitory buffer (5.2.4.1.2), containing the metal ion-chelating EDTA and lacking Ca^{2+}, was prepared.

5.2.4.3 Analysis of rhPON2-mediated C12HSL hydrolysis

5.2.4.3.1 Standard mixture for instrument calibration

rhPON2 hydrolysis reactions were diluted and analysed by UPLC-MS. The instrument was calibrated using an external standard curve consisting of mixtures, in equal proportions, of C12HSL (closed lactone ring) and C12HSL-acid (open ring).

The C12HSL-acid form was synthesized from the lactone form as follows. Ten millimolar C12HSL (Cayman Chemicals) in HPLC grade acetonitrile (Sigma) was diluted to a final concentration of 100 μM in an aqueous 1 mM NaOH solution by adding 1 μL of the C12HSL to 99 μL of the 1 mM NaOH. The reaction was mixed by vortexing and incubated at room temperature for 30 minutes. Finally, the reaction was stopped by adding and mixing 100 μL of HPLC grade acetonitrile (Sigma) containing 1 mM HCl. This mixture now contained 50 μM C12HSL-acid.

Next, 1 μL of 10 mM C12HSL (Cayman Chemicals) in HPLC grade acetonitrile (Sigma) was added to 99 μL of degassed, distilled H_2O. One hundred millilitres of HPLC grade acetonitrile

with 1 mM NaOH and 1 mM HCl was immediately added to the reaction mixture to give a 50 μM C12HSL mixture.

The 50μM solutions of C12HSL and C12HSL-acid were mixed in equal proportion and the resulting solution diluted to the following concentrations: 5.0 μM, 2.5 μM, 1.25 μM, 625 nm, 312.5 nM, 104 nM and 52 nM. A 50:50 solution of degassed, distilled H_2O and HPLC-grade acetonitrile was used as the diluent when preparing these mixtures.

5.2.4.3.2 UPLC-MS of C12HSL solutions

Samples were analysed by UPLC-MS using a Waters Acquity H-series UPLC coupled to a Waters Xevo triple quadrupole mass spectrometer (Waters Inc., Manchester UK). A Waters Acquity UPLC BEH C18 column (2.1 x 100mm x 1.7 micron particles) was used. The solvents were 1% acetic acid (Solvent A) and acetonitrile (Solvent B).

The UPLC program was 50% A: 50% B to 10% A: 90% B at 4 minutes, followed by immediate re-equilibration to starting conditions for 3 minutes. The flow rate was 0.35 mL/min, the column was held at 35°C and the injection volume was 10 μL.

The mass spectrometer was operated in positive-ion electrospray mode with a needle voltage of three kV, and multiple reaction monitoring (MRM) mode was used to detect and quantify the analytes. The ion source temperature was 130°C, the desolvation gas was nitrogen at 950 L/hour, the cone gas flow was 100/hour and the desolvation temperature was 450°C. All data was analysed using MassLynx software (Waters Inc.).

The MRM channels were:

C12HSL-acid — m/z 316.2 to 95.0, m/z 316.2 to 144.05 and m/z 316.2 to 197.1.

C12HSL-lactone — m/z 298.2 to 95.0, m/z 298.2 to 102.0, m/z 298.2 to 197.1.

Cone voltage was 30 V and collision energy 20 V for all channels. Dwell time was 50 ms per channel.

Calibration was against an external standard calibration mixture of the two analytes at seven different concentrations ranging from 53 nM to 5000 nM as outlined in Section 5.2.4.3.1. Second-order polynomial correlation coefficients were typically 0.9998 or higher in all cases. Samples were bracketed by full standard curves run after every ten samples, and a single quality control calibration point (625 nM) was also acquired in the middle of

each set of ten samples. Quantification was carried out using the sum of the three MRM channels for each compound.

5.2.4.3 Activity calculation

From the UPLC-MS determined concentrations of C12HSL, the total amount of C12HSL hydrolysed was calculated in nMol. One activity unit (U) was defined as 1 nMol of C12HSL hydrolysed per minute. Total activity was defined as activity units from the total protein sample while the specific activity was defined as U per mg of protein.

$$\text{Activity Unit (U)} = \frac{\text{amount of C12HSL hydrolysed (nMol)}}{\text{Time taken (minutes)}}$$

$$\text{Activity of sample of fraction } \left(\frac{\text{U}}{\text{mL}}\right) = \frac{\text{Activity Units (U)}}{\text{Volume of sample used to determine activity units (mL)}}$$

$$\text{Total Activity (U)} = \text{Activity of sample of fraction(U/mL)} \times \text{Total Volume collected of fraction(mL)}$$

$$\text{Specific Activity } \left(\frac{\text{U}}{\text{mg}}\right) = \left(\frac{\text{Total Activity (U)}}{\text{Total Protein in sample (mg)}}\right)$$

$$\text{or } \left(\frac{\text{amount of C12HSL hydrolysed (nMol)}}{\text{Time taken (minutes)} \times \text{Protein in reaction (mg)}}\right.$$

5.2.5 Determination of the effects of rhPON2 on PAO1 growth, C12HSL accumulation and QS-dependent gene expression

Overnight stationary-phase cultures of *P. aeruginosa* strain PAO1 strain ATCC 15692 were diluted to approximately 5×10^5 cells in LB media. Cultures were treated at time of dilution (pre-exponential) or after six hours incubation (mid-exponential) at 37°C with shaking at 220 RPM. The Concanavalin A elution buffer (buffer in which rhPON2 is dissolved and contains 0.05% DDM) was used as a control. Treatments were (i) 5 U/mL rhPON2, (ii) 25 U/mL rhPON2, (iii)10 μg/mL tobramycin, (iv) 5 U/mL rhPON2 + 10 μg/mL tobramycin and (v) 25 U/mL rhPON2 + 10 μg/mL tobramycin. All cultures included a final concentration of 0.0005% (w/v) DDM. Cells were incubated at 37°C with shaking at 220 RPM. At intervals, aliquots were removed for bacterial enumeration, pH determination, determination of C12HSL lactonolysis and concentration, and RNA extraction for subsequent gene expression analysis by RT-qPCR.

5.2.5.1.1 Bacterial enumeration and pH determination

At intervals, 100 μL aliquots of cultures were ten-fold serially diluted and colony forming units (CFU) per mL determined by plating as described in Chapter 2. (Section 3.5.3.2) The pH of 1 mL aliquots of PAO1 cultures was determined.

5.2.5.2 Analysis of C12HSL accumulation and lactonolysis

One-millilitre aliquots of bacterial cultures were taken at intervals and centrifuged at 500 × *g* for five minutes to clarify the supernatant. The cell pellets were preserved in RNA*Later* (Life Technologies) at −20°C for subsequent RNA extraction (5.2.5.3). The culture supernatants collected were used to analyse the concentration of C12HSL (lactone and acid forms). Stored supernatants were thawed and diluted 1:4 into acetonitrile: water (2:1, both solvents HPLC grade) to give a final ratio of solvents of 1:1 organic: aqueous. The samples were then analysed by UPLC as described in Section 5.2.4.3.2.

5.2.5.3 RT-qPCR Analysis of QS and QS-dependent gene expression

RNA was extracted from stored pellets using the ReliaPrep RNA Cell Miniprep kit (Promega) and complimentary DNA was synthesised for quantitative-PCR; all methods and primer sequences are described in Chapter 2 (Section 2.2). The genes analysed (*psd7, lasI, rhlI, pqsA, lasR, lasB, algD, hcnB, phz1,* and *vfr*) are described in Table 5.2. Gene expression was normalized to the reference gene *psd7*, which encodes *P. aeruginosa* 16S ribosomal RNA.

Table 5.2 *P. aeruginosa* QS genes analysed by RT-qPCR and their role in QS

Gene	Description	Involvement in QS
lasI	Catalyses production of C12HSL	Catalyses production of C12HSL, the main *P. aeruginosa* QS signal. Regulates the other two major *P. aeruginosa* QS systems.
rhlI	Catalyses production of C4HSL	Catalyses production of C4HSL, the signal molecule of the second *P. aeruginosa* QS system. The Rhl system is induced by the Las system.
pqsA	Catalyses production of 2 heptyl-3-hydroxy-4-quinolone.	Catalyses production of 2 heptyl-3-hydroxy-4-quinolone the signal molecule of the third *P. aeruginosa* QS system. Regulated by both the Las (positive) and Rhl (negative) systems
lasR	Cognate receptor of C12HSL	Transcriptional regulator which drives LasI expression when bound to C12HSL.
lasB	In the production of the virulence factor production	Expression regulated by both the Las and Rhl systems
algD	Alginate biosynthesis. Responsible for the mucoid phenotype and biofilm formation	Expression regulated partly by LasI
hcnB	Produces the virulence factor hydrogen cyanide.	Expression regulated partly by RhlI
phz1	Involved in biosynthesis of the phenazines, including the virulence factor pyocyanin	Expression regulated by RhlI and Pqs.
vfr	Virulence factor regulator	Regulates *P. aeruginosa* virulence factor production, partly through the Las system.

5.2.5.4 Determination of the minimal inhibitory concentration (MIC) of tobramycin for PAO1

Overnight cultures of PAO1 were diluted to approximately 5×10^5 cells in LB medium supplemented with increasing concentrations (1, 2.5, 4, 5, 7, 8.5, 10, 12, 15 μg/mL) tobramycin (Sigma-Aldrich). The cultures were incubated for 24 hours at 37°C with shaking at 220 RPM. The optical density of the cultures at 600 nm was then measured to determine MIC, which was defined as the lowest concentration of tobramycin that inhibited detectable growth of PAO1.

5.3 RESULTS

5.3.1 Successful cloning of human PON2 into bacmid expression vector.

To express hPON2 in insect cells, hPON2 transcript was cloned into a bacmid vector to produce a baculovirus stock capable of infecting insect cells and producing rhPON2. Figure 5.4 depicts agarose gel electrophoresis of the PCR products derived from amplification of the rhPON2 bacmid DNA using pUC/M13 primers.

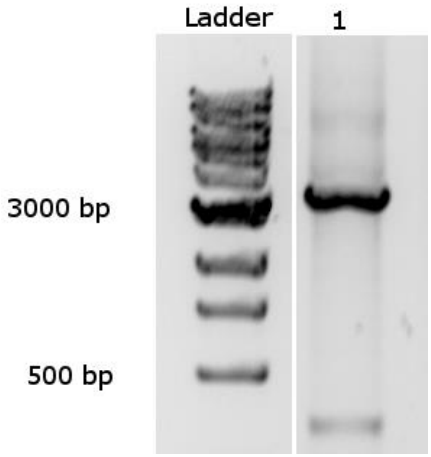

Figure 5.4 PCR verification of cloning of hPON2 transcript into baculoviral expression vector. PCR was carried out on baculovirus DNA to verify recombination of hPON2 transcript into the baculovirus expression vector. Successful recombination produced a 3,400 bp PCR product. Baculovirus that did not undergo recombination would produce a 300 bp product.

5.3.2 Production of high-titre, rhPON2-expressing baculovirus stock.

Baculovirus stocks were created by transfection and subsequent infection of the SF9 insect cell line. To obtain high titres of hPON2-expressing baculovirus stock, the optimum DNA: transfection reagent ratio was determined. A range of ratios of DNA: transfection reagent was used for transfecting SF9 cells with the DNA of the hPON2 vector. Using immunoblot analysis (Figure 5.5) and microscopic visualization of baculovirus infected SF9 cells (result not shown), the optimum DNA: transfection reagent ratio was determined to be 4.0 µg DNA

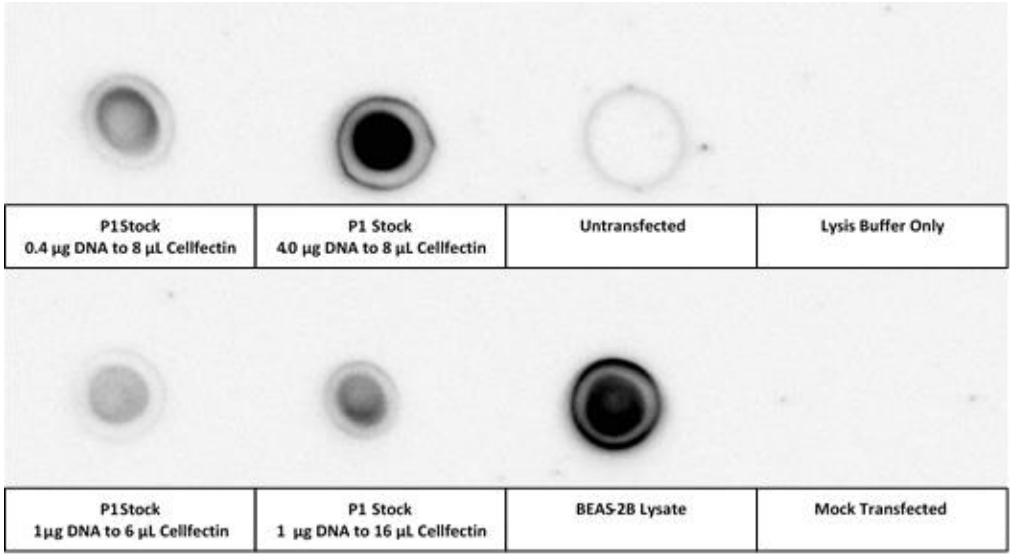

Figure 5.5 Optimizing transfection of Sf9 cells with hPON2-expressing baculovirus DNA using immunoblot analysis. Sf9 cells were transfected with DNA from the hPON2-expressing baculovirus vector with varying ratios of DNA:transfection reagent (Cellfectin). Immunoblot analysis of lysed cells, using a hPON2 antibody, determined the optimum ratio of DNA: transfection reagent to be 4 µg DNA:8 µl Cellfectin.

per 8 µL transfection reagent. Using this optimum ratio of DNA:transfection reagent, SF9 cells were transfected with hPON2-expressing baculovirus to produce passage one (P1) stock with a titre of 2.19×10^6 pfu/mL. P1 stock was used to infect fresh SF9 cells to produce passage two (P2) baculovirus stock with a titre of 1.89×10^7 pfu/mL (Table 5.3). The titres were determined using the end-point dilution method and were similar to those titres indicated in the Bac-to-Bac manufacturer's instructions [275].

Table 5.3 Titres of baculovirus stock calculated by end-point dilution

End-Point Dilution Counts							
Passage one (P1)stock				Passage two (P2)stock			
Virus Dilution	Infected	Non-infected	% Infected	Virus Dilution	Infected	Non-infected	% Infected
10–4	20	1	95.20	10–4	23	0	100
10–5	7	7	50.00	10–5	11	3	75.57
10–6	1	18	5.26	10–6	2	13	13.33
10–7	0	30	0.00	10–7	0	25	0

Calculated Viral Titres		
Virus passage	Titre (plaque forming units/mL)	Used to infect
P1	2.19 × 106	Sf9 Cells – generate P2 stock
P2	1.89 × 107	Sf9 cells – Test hPON2 expression Hi-Five – Express hPON2

5.3.3 Determination of High Five insect cell infection conditions for maximal rhPON2 expression.

To ensure maximal production of rhPON2 in the High Five insect cell line, the optimal multiplicity of infection (MOI) and duration of infection were determined. The amount of rhPON2 in the infected insect cells varies over time as the infection progresses, and baculovirus infection eventually causes cell death. Too little baculovirus usually results in lower rhPON2 production, while too much virus usually causes immediate cell lysis and hence reduced protein yield. The optimum MOI was determined by immunoblot analysis of lysates of cells infected with rhPON2 baculovirus expression vector (Figure 5.6 and by microscopic visualization of infected cells. (Figures 5.7 and 5.8) of the lysates of the infected High Five cells. These analyses determined that the optimum MOI and duration of infection required for maximal production of rhPON2 was 3–4 days of infection with a MOI of 2.5. Using lower MOIs did not yield as much PON2, while MOI of 5 resulted in quick cell death hence yielding reduced rhPON2.

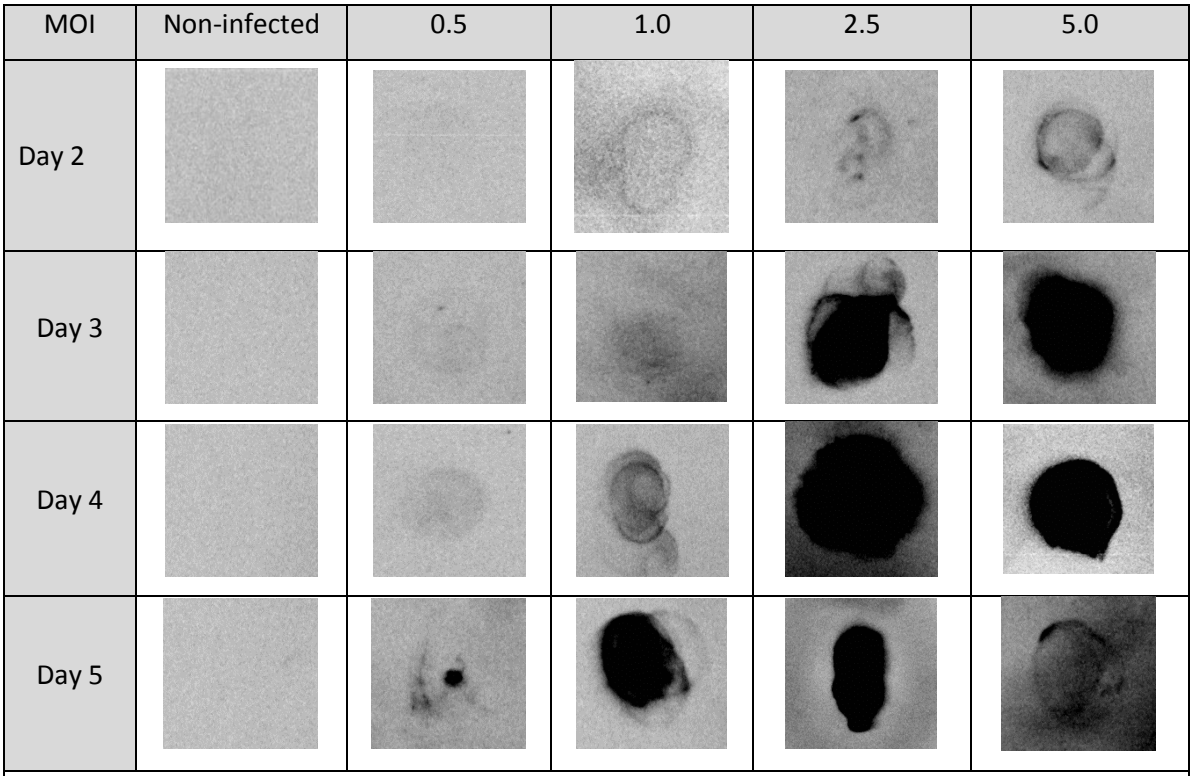

Figure 5.6 Optimizing infection of High Five cells with hPON2-expressing baculovirus using immunoblot analysis. Figure shows immunoblot analysis, using hPON2 antibody, of High Five cell lysates infected with varying MOI of hPON2-expressing baculovirus and the progress of infection over five days, with increasing MOIs.

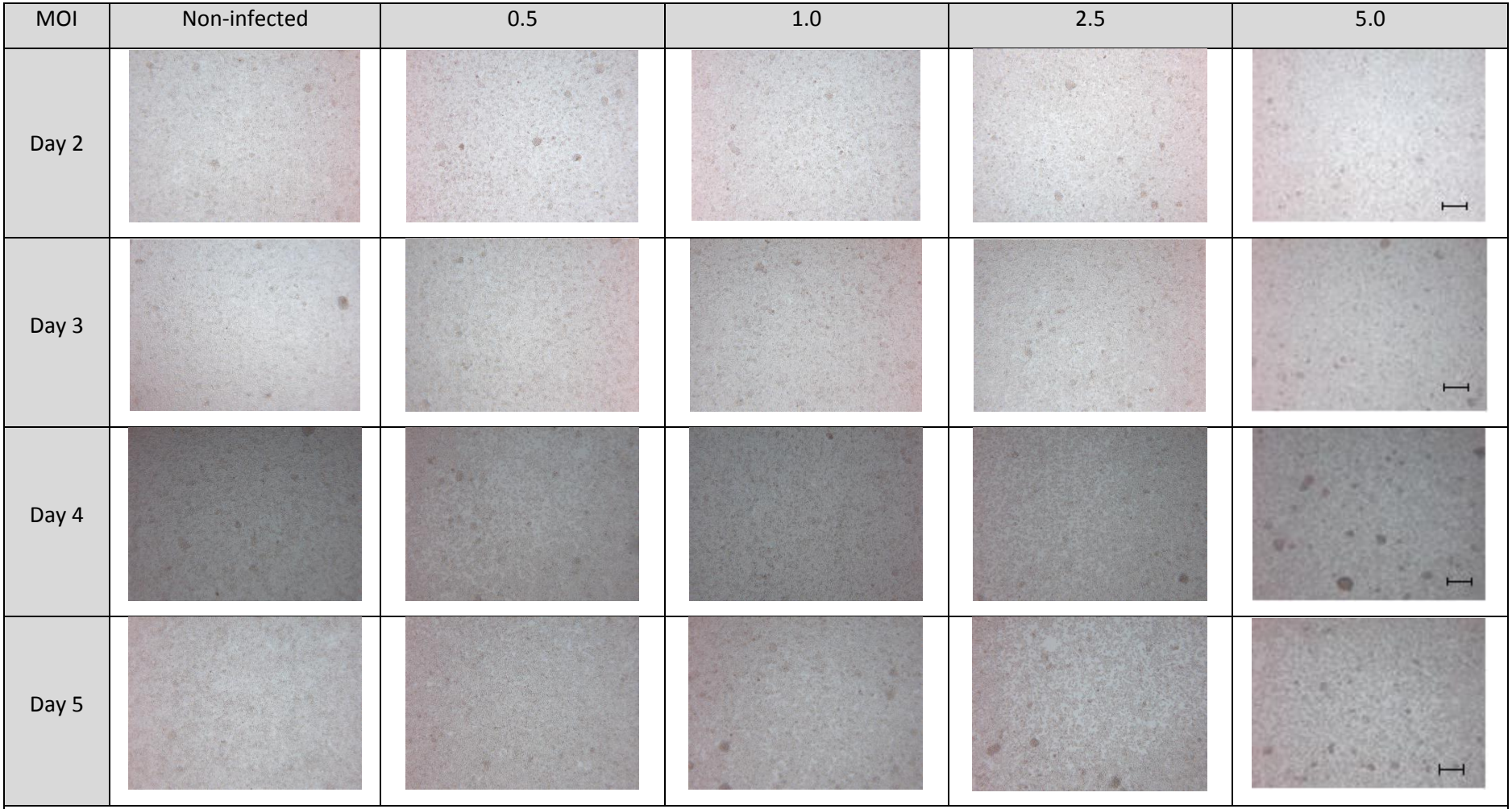

Figure 5.7 Progression of infection of HIgh Five cellswith hPON2-expressing baculovirus observed at 40× magnification. Figure shows High Five cells infected with varying MOIs of hPON2-expressing baculovirus and the progress of infection was monitored using light microscopy at 40× magnification starting at day two post infection. At this magnification, the cessation of growth and the clearing of the adherent cell monolayer can be observed starting at day two in High Five cells treated with MOI ≥ 2.5. With the progression of infection the cessation of growth and the clearing of the adherent cell monolayer can also be observed with MOI ≤ 1. Scale bar represents 500 µm.

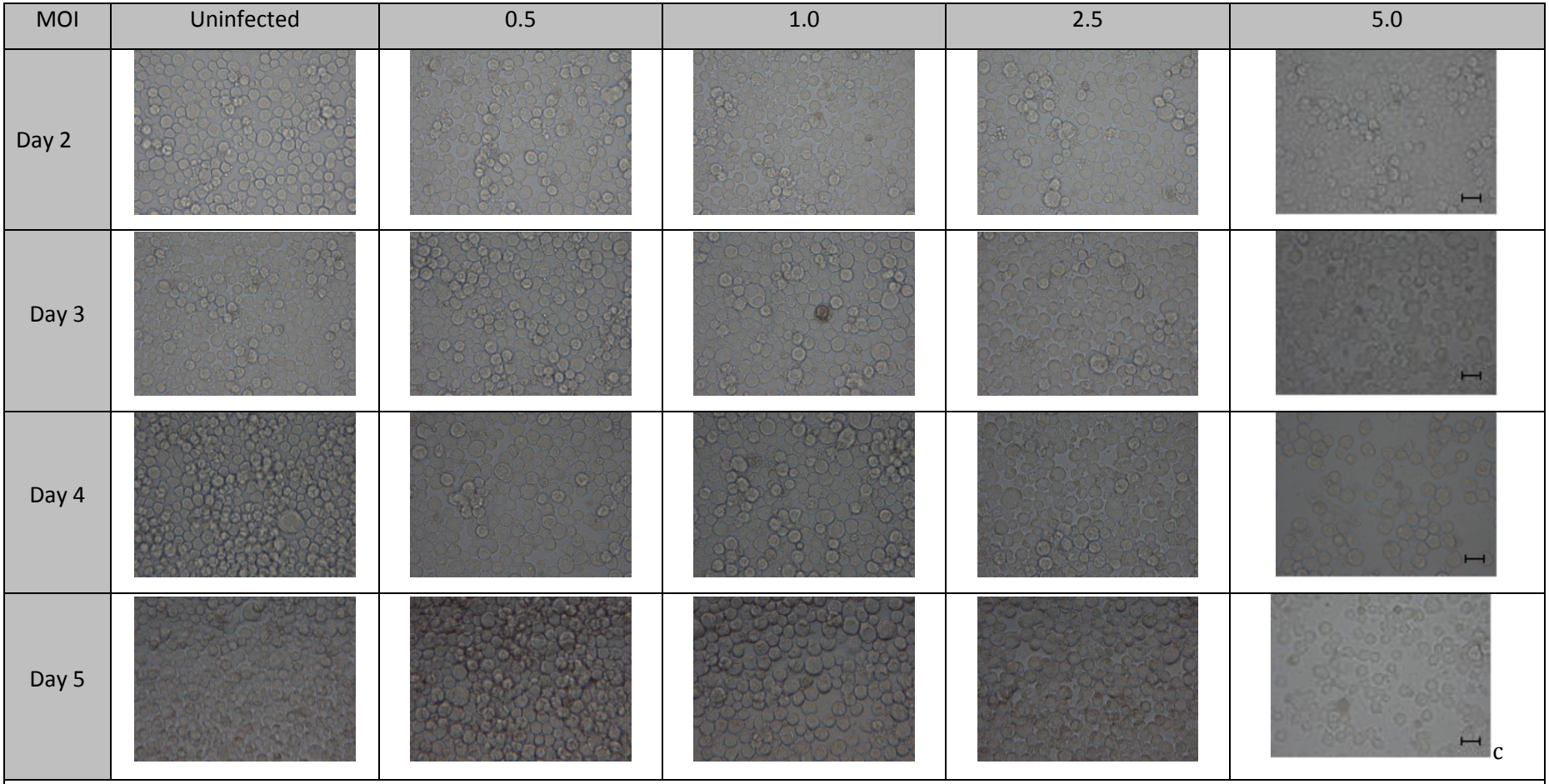

Figure 5.8 Progression of infection of High Five cells with hPON2-expressing baculovirus observed at 400× magnification. Figure shows High Five cells infected with varying MOI of hPON2 expressing baculovirus and the progress of infection was monitored using light microscopy at 400× magnification, starting at day two post infection At this magnification, the increase in cell size, nuclear diameter, granular appearance and lysis of the cell can be observed starting at day two in High Five cells treated with MOI ≥ 2.5. With the progression of infection the increase in cell size, nuclear diameter, granular appearance can also be observed with MOI ≤ 1. Scale bar represents 50 µm.

5.3.4 Purification and characterization of rhPON2

Recombinant human PON2 was purified by differential centrifugation and using a two-step liquid chromatography protocol as previously described by Draganov and colleagues. Firstly, the membrane fractions from High Five cells infected with the rhPON2 baculovirus were purified by differential centrifugation. This step increased the purity of rhPON2 12-fold and resulted in a membrane fraction with a specific lactonase activity (64.656 units/mg protein) towards C12HSL (Table 5.4, Figure 5.9).

The membrane fractions were then further purified using DEAE anion chromatography. The eluted fractions were analysed by Coomassie-stained SDS-PAGE to detect the presence/absence of rhPON2 (Figure 5.10). The rhPON2 eluted as a broad peak at a NaCl concentration between 100 mM and 300 mM NaCl. This purification step resulted in a 27-fold increase in purification from crude lysates and the pooled fractions had a specific activity of 148.213 U/mg (Table 5.4, Figure 5.9).

The final purification step involved concanavalin A affinity chromatography. The concanavalin A binds glycosylated rhPON2 and the protein was eluted by a mannopyranoside sugar containing buffer that disrupted the concanavalin A lectin binding. The eluted fractions were analysed by SDS-PAGE and immunoblot analysis to detect the presence/absence of rhPON2 (Figure 5.11). Pooled rhPON2 fractions had a specific activity towards C12HSL of 323 U/mg (nMols min^{-1} mg^{-1}) (Table 5.4, Figure 5.9), representing a 59-fold purification of specific activity compared with whole cell lysates.

Table 5.4 Summary of purification of rhPON2 from High Five insect cells (C12HSL hydrolysis)

Fraction	Volume (mL)	Protein (mg)	Total Activity (Units)	Specific Activity (Units/mg)	Yield %	Fold Purification *n*
Whole-cell lysate	300	897.00	4920	5.485	100	1
Membrane fraction	20	61.00	3944	64.656	80.2	12
DEAE anion exchange (pooled)	12	24.88	3682	148.213	74.8	27
Concanavalin A affinity purification (pooled)	6	6.96	2251	323.448	45.7	59

Results are given for representative purifications. Activity was calculated against 100 µM C12HSL, as described in Section 5.2.4. Units are defined as nMols of C12HSL hydrolysed per minute. Yield = (Total activity of fractions at step)/ (Total activity of whole cell lysate). Fold purification is the change in specific activity at each step relative to the specific activity of the whole-cell lysate.

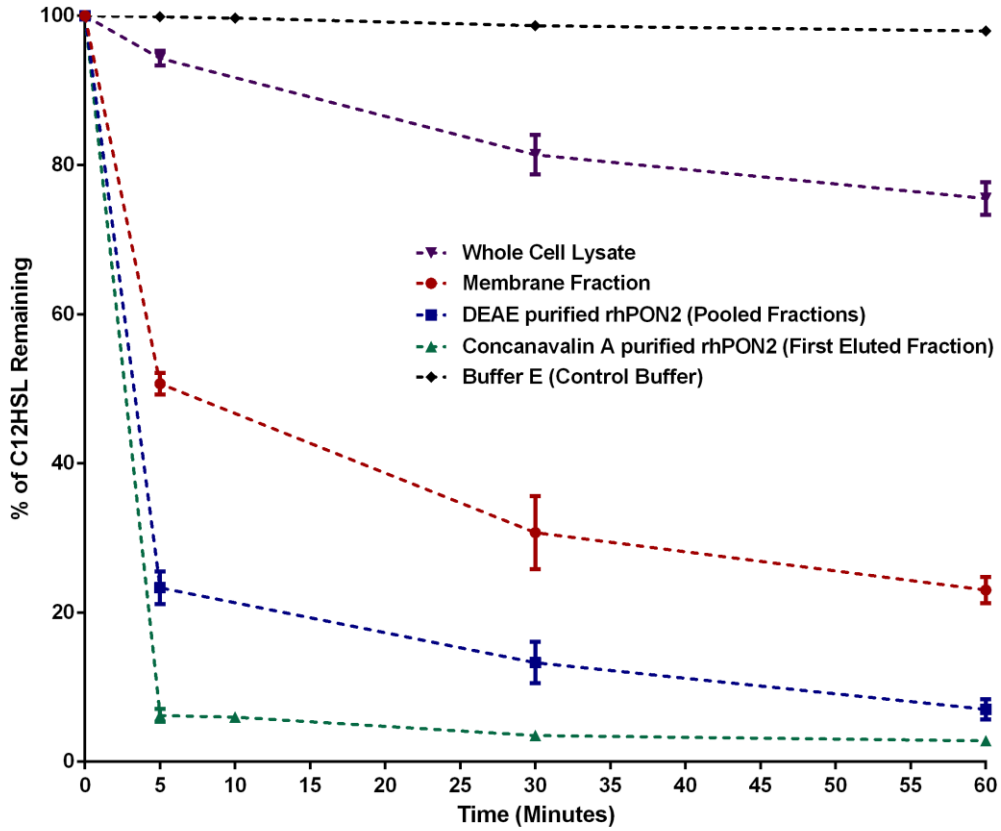

Figure 5.9 Recombinant human PON2 lactonolysis of C12HSL. 100 µM C12HSL was incubated for 60 min with rhPON2 from each purification step and the percentage of remaining C12HSL determined using UPLC-MS. Figure shows the mean percentage of un-hydrolysed C12HSL remaining from three independent reactions. A buffer-only control (Concanavalin A column elution buffer, black line) or a 5 µl aliquot of each rhPON2 sample was used; whole cell lysates (purple line), membrane fraction (red line), pooled DEAE anion exchange purified rhPON2 (blue line), first eluted fraction of Concanavalin A purified rhPON2 (green line). Error bars indicate S.D.

The purified rhPON2 mix contained three major protein bands, as revealed by SDS-PAGE analysis (Figure 5.10). Two of these proteins differed in size by ~5 KDa but both were identified as rhPON2, as demonstrated by immunoblot analysis (Figure 5.12). These two forms of rhPON2 most likely differed in their extent of post-translational glycosylation [described previously in 248]. A third protein was a contaminating protein of ~25 KDa.

No C12HSL hydrolysis was observed when reactions were carried out in the presence of the metal ion chelating agent EDTA and absence of Ca^{2+}, indicating that purified rhPON2 had Ca^{2+}dependent lactonase activity, consistent with previous reports [262]. Furthermore, lysates or purified fractions derived from not-infected insect cells showed no lactonase activity towards C12HSL (Figure 5.13), demonstrating that the lactonase activity was indeed associated with rhPON2.

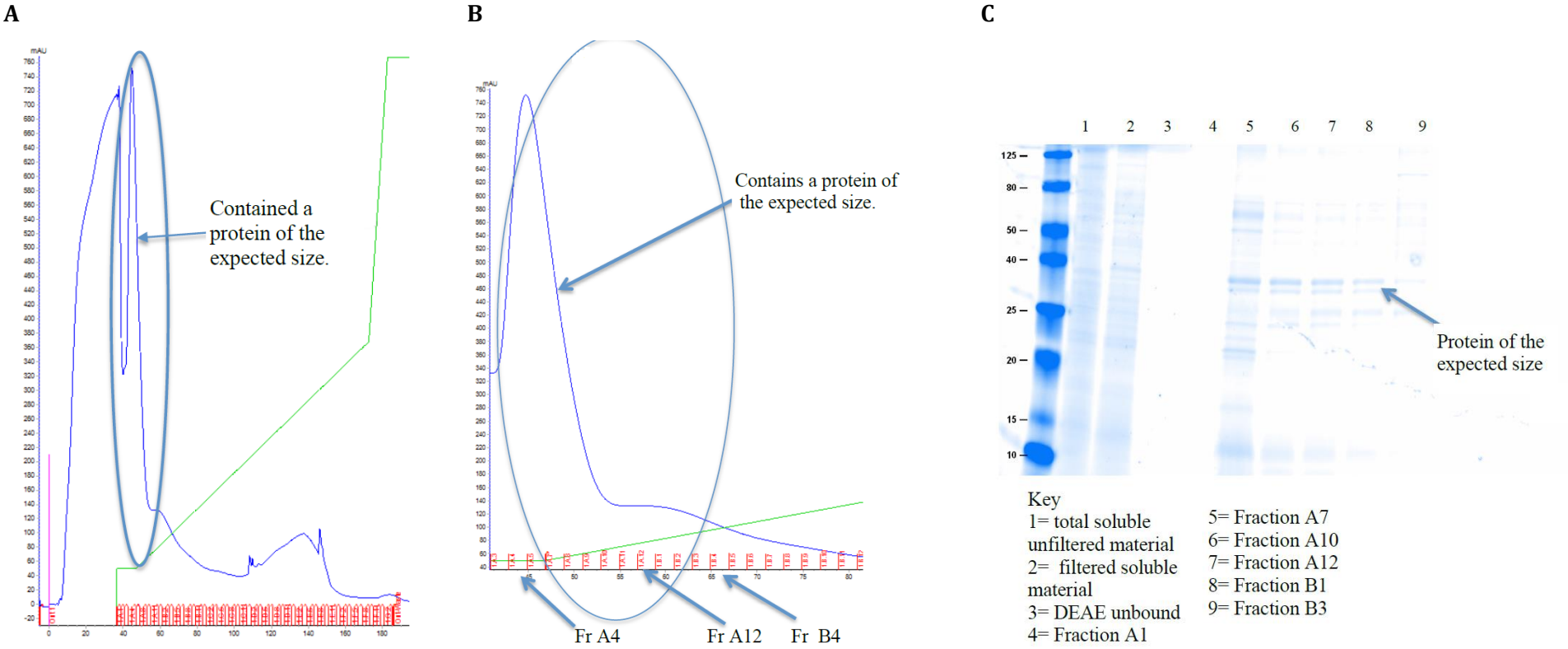

Figure 5.10 Purification of membrane fractions of lysates from infected High Five cells by anion exchange chromatography. The membrane fractions of lysates from hPON2-expressing baculovirus-infected High Five cells were purified using DEAE anion exchange liquid chromatography. A) Traces of UV absorbance from FPLC system (purple) overlaid with elution buffer NaCl concentration (green) and the fractions in which the eluted samples were collected (red). Figure indicates which peak contained proteins with a size similar to that of PON2 as determined by SDS-PAGE. B) Magnified peak of UV absorbance indicating where proteins with a size similar to PON2, as determined by SDS-PAGE, were eluted. C) Stained SDS-PAGE of fractions obtained from DEAE purification of hPON2 baculovirus-infected High Five cell membrane fractions.

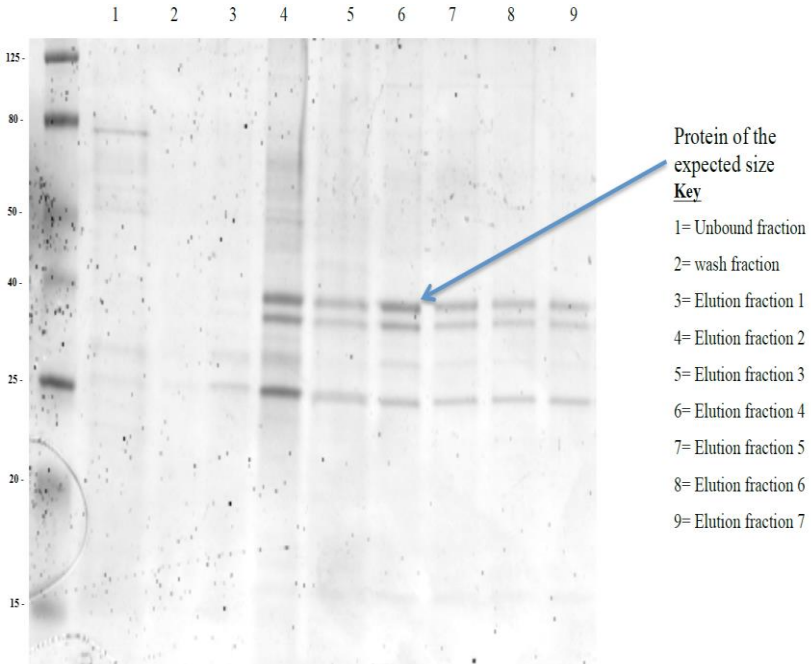

Figure 5.11 Affinity purification of rhPON2. The pooled rhPON2-containing fractions from DEAE anion exchange chromatography were purified further using Concanavalin A affinity chromatography and the eluted fractions analysed by SDS-PAGE (lanes 1–9).

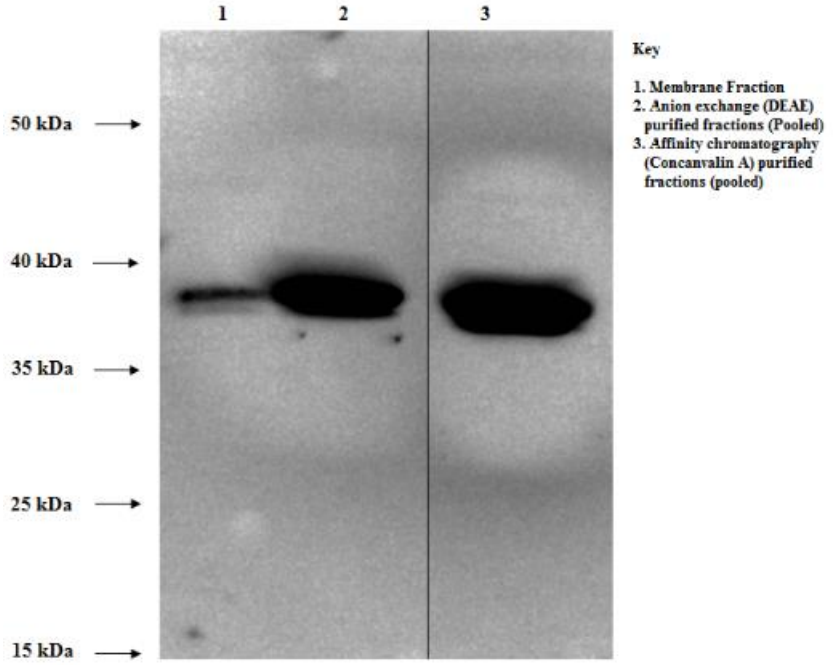

Figure 5.12 Immunoblot of purified hPON2 fractions. SDS-PAGE was carried out on the membrane fractions isolated from crude lysates of hPON2-expressing baculovirus-infected High Five cells, along with the pooled fractions from the DEAE anion exchange chromatography and the Concanavalin A affinity chromatography. Figure shows immunoblot analysis with a hPON2 antibody. rhPON2 can be observed as a doublet of bands at ~39 kDa (lanes 1–3).

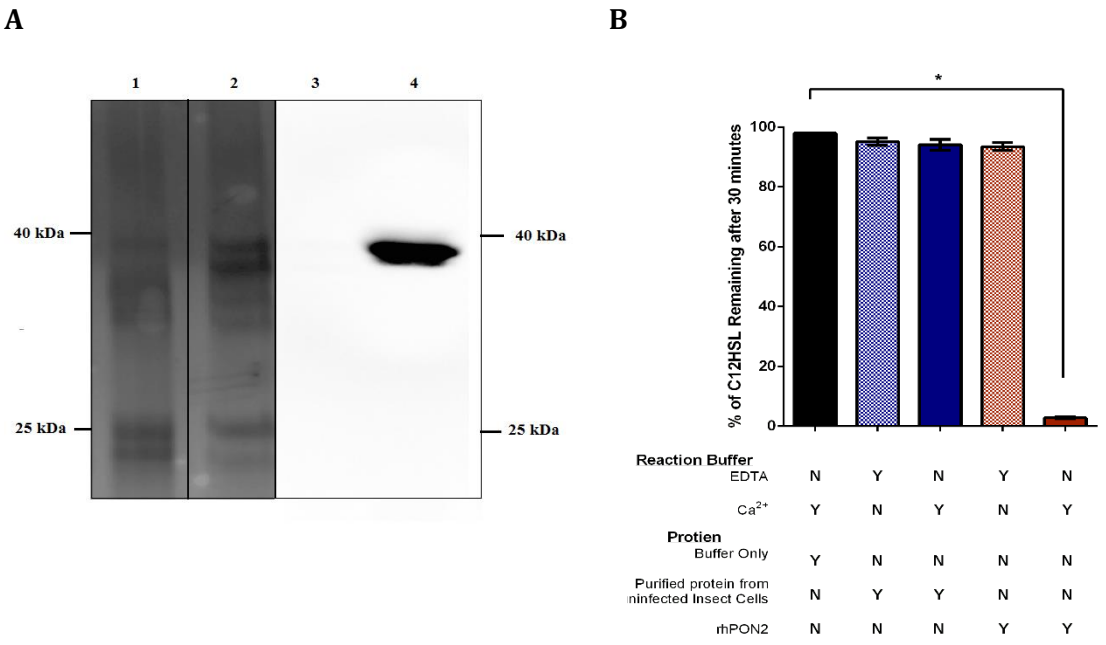

Figure 5.13 SDS-PAGE gels, immunoblot analysis and lactonase activity of High Five cells not infected with rhPON2. Lysates of uninfected High Five cells underwent the same protein purification protocol as infected High Five cells. A) Figure shows SDS-PAGE (lanes 1, 2) and immunoblotting (lanes 3, 4) of purified lysates from uninfected High Five cells (lanes 1, 3) and infected cells (lanes 2, 4). B) Mean lactonase activity of purified lysates from uninfected and infected cells, in the presence and absence of EDTA and Ca^{2+} from three independent experiments. Errors bars indicate S.D., * $p < 0.05$.

5.3.5 Effect of rhPON2 on *P. aeruginosa* strain PAO1 growth, QS and virulence

5.3.5.1 Determination of rate of PA01 growth and C12HSL accumulation and hydrolysis.

Cultures of bacteria undergo four distinct growth phases, each with different characteristics. We hypothesized that the effect of rhPON2 on *P. aeruginosa* QS and virulence would differ depending upon which growth phase the bacteria were in at the time of exposure to the paraoxonase. A previous report demonstrated the accumulation and disappearance of C12HSL during exponential phase and stationary phase, respectively [243]. To determine the rate of growth and the cell density associated with each growth phase of PA01, bacterial growth was monitored by determining CFU/mL at specific time points (2, 6, 10, 14, 24 hours). As depicted in Figure 5.14A, following a short lag phase, strain PAO1 rapidly entered exponential growth with growth peaking at approximately 12 hours ($\sim 1 \times 10^9$ CFU/mL), followed by stationary-phase growth as nutrients became limited.

The stability and associated activity of C12HSL are influenced by the pH of the media [243]. At high pH, ring opening occurs by hydroxide ion-mediated hydrolysis, while at low pH, ring closure is predominant. Therefore, the pH of the growth medium inoculated with PAO1 was monitored during the different stages of growth. As depicted in Figure 5.14A, the pH of the growth medium decreased during growth from 7.6 to 7.0 over 24 hours, conditions that should favour ring closure.

Accumulation and hydrolysis of C12HSL was also measured during the growth of PAO1. Figure 5.14B shows that initial levels of C12HSL were below detectable limits. This was followed by rapid accumulation of C12HSL-acid (open-ring form) during exponential growth, with a peak concentration of 800 nm. There was little detectable C12HSL open-ring form until mid-exponential growth (around six hours). The C12HSL disappearance during stationary-phase is associated with ring opening, as demonstrated by the parallel increase in the open-ring form (peak concentration of 300 nM).

A

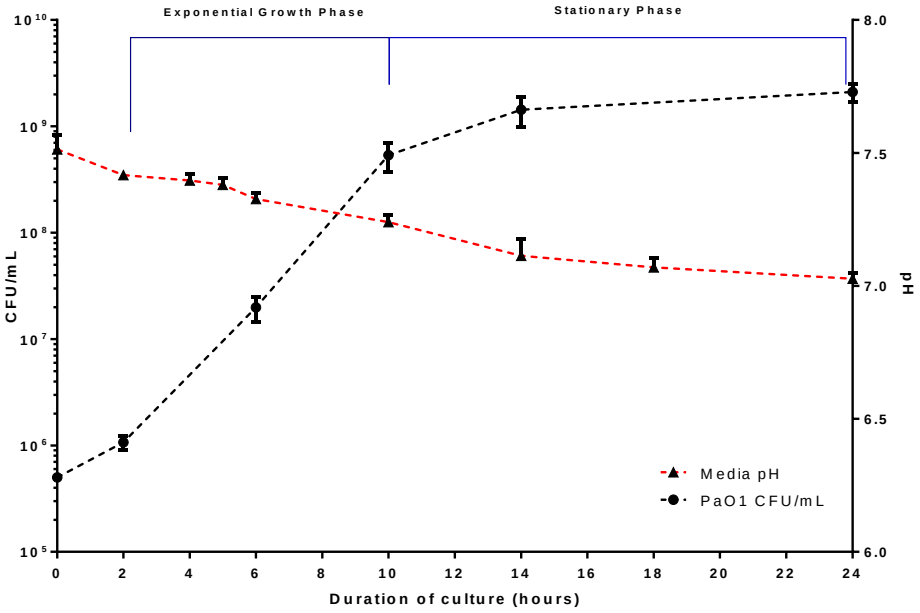

B

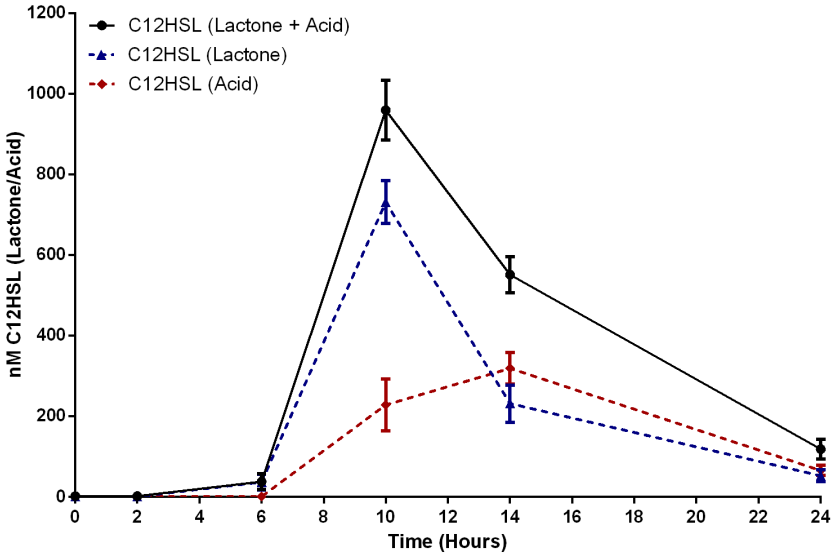

Figure 5.14 Growth curve of PAO1 at 37°C in LB media LB media was inoculated with 5×10^5 colony forming units per mL (CFU/mL) of PAO1 and samples collected at various intervals to count cell numbers, measure media pH and determine C12HSL (lactone and acid) concentrations over a 24 hour period. A) Figure shows the mean CFU/mL of PAO1 (black line) and pH of media (dotted red line) from three independent experiments. The exponential and stationary growth phases are bracketed (dotted blue). B) Figure shows C12HSL lactone (blue-dashed line), C12HSL acid (red-dashed line) and C12HSL lactone + acid (black solid line) concentrations in the culture supernatants as determined at 0, 2, 6, 10, 14 and 24 hours. Error bars show S.D. from three independent cultures.

5.3.5.2 Determination of PAO1 tobramycin minimal inhibitory concentration

To study the effects of tobramycin on the growth of PAO1, the MIC of tobramycin was determined. A stationary phase PAO1 culture was diluted to 5×10^5 colony forming units per mL (CFU/mL) in LB medium supplemented with 0,1, 2.5, 4, 5, 7, 8.5, 10, 12, 15 µg/mL of tobramycin.. The cultures were grown for 24 hours and the absorbance at 600 nm measured for three independent cultures. The concentration of tobramycin required to completely inhibit growth was determined to be ~5 µg/mL (Figure 5.15).

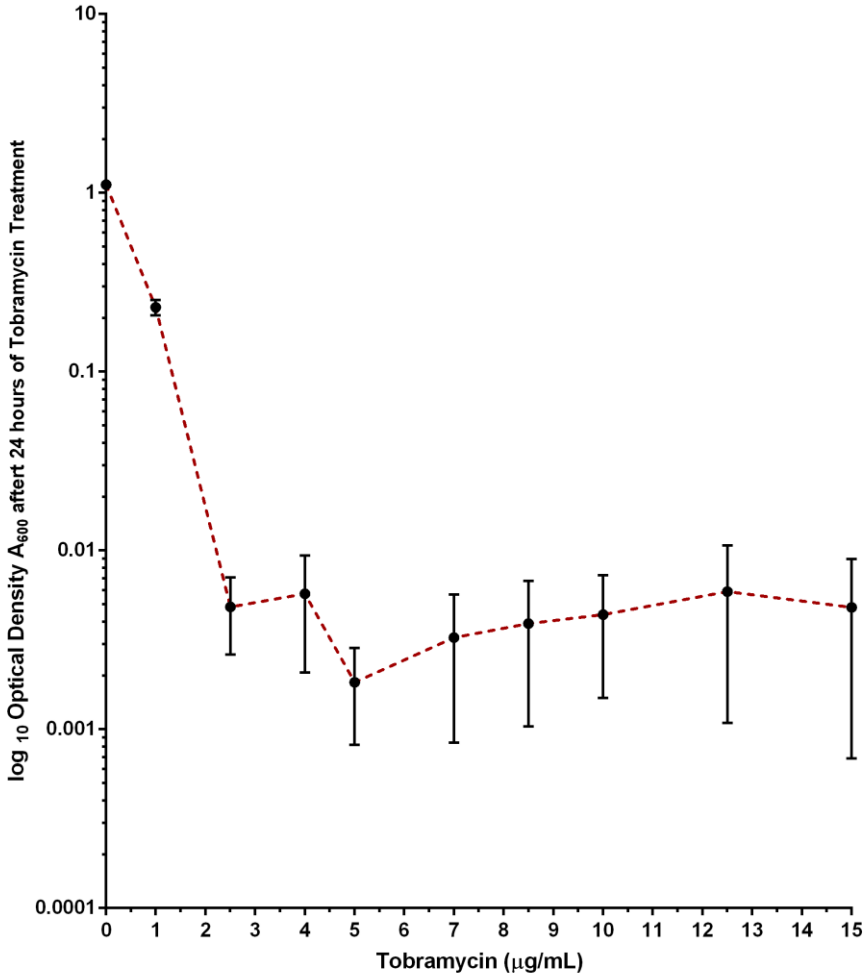

Figure 5.15 Dose-dependent killing of PA01 by tobramycin. LB media was inoculated with 5×10^5 colony forming units per mL (CFU/mL) of PAO1 and tobramycin (0–15 µg/mL). The cultures were grown at 37°C for 24 hours with shaking and absorbance at 600 nm measured. Figure shows mean optical density of cultures from three independent experiments after 24 hours. Error bars show S.D.

5.3.5.3 Recombinant human PON2-mediated lactonolysis of C12HSL during PAO1 growth increases PAO1 antibiotic susceptibility

To quantitatively investigate the effects of rhPON2 on PAO1 growth, QS, virulence and tobramycin susceptibility, PAO1 cultures were co-treated with rhPON2 and tobramycin. PAO1 cultures either in pre-exponential growth-phase (Figure 5.16) or mid-exponential growth (Figure 5.17) were treated with 0, 5 or 25 U/mL rhPON2 and either with 0 or 10 μg/mL (2× MIC) tobramycin. We hypothesised that treatment of pre-exponential cultures would prevent bacterial QS and that treatment of mid-exponential phase cultures would dampen QS-mediated virulence. Samples were collected from three independent experiments at 0, 2, 6, 12, 14 and 24 hours and analysed to determine the CFU/ml and C12HSL concentration (both open and closed ring forms).

Treatment of pre-exponential phase cultures of PAO1 with 5 U/mL rhPON2-alone did not affect bacterial growth (as seen in Figure 5.16A) but prevented accumulation of C12HSL (closed-ring form) presumably by promoting C12 HSL lactonolysis (open-ring form, Figure 5.16B). The maximum amount of C12HSL (closed-ring form) occurred during exponential growth and was significantly reduced in the presence of rhPON2. There was a corresponding increase in concentration of the C12HSL-acid (open-ring form) that reflected the extensive activity of rhPON2 over the entire 24 hour period. The increased C12HSL-acid detected in rhPON2-treated culture supernatants compared to those collected from not-infected controls suggested that the bacteria might be compensating for the lack of C12HSL in their growth environment by increasing their overall production of C12HSL, which in would have been hydrolysed to the acid form being detected (Fig. 5.16B)

When pre-exponential growth phase cultures were treated with 2× MIC tobramycin, no viable bacterial cells were able to be recovered 24 hours post treatment. There also appeared to be little, if any, effect on the rate of antibiotic-mediated killing when cultures were co-treated with 5 U/mL rhPON2 and 2× MIC tobramycin and no detectable C12HSL (open- or closed-ring form, data not shown), most likely as a consequence of the rapid bacterial cell death. In summary, treatment of pre-exponential phase cultures had no detectable effect on bacterial growth, prevented accumulation of C12HSL (by rapid hydrolysis to form C12HSL-acid) and did not alter bacterial susceptibility to tobramycin (2× MIC) most likely because of rapid killing of the cells by tobramycin.

A

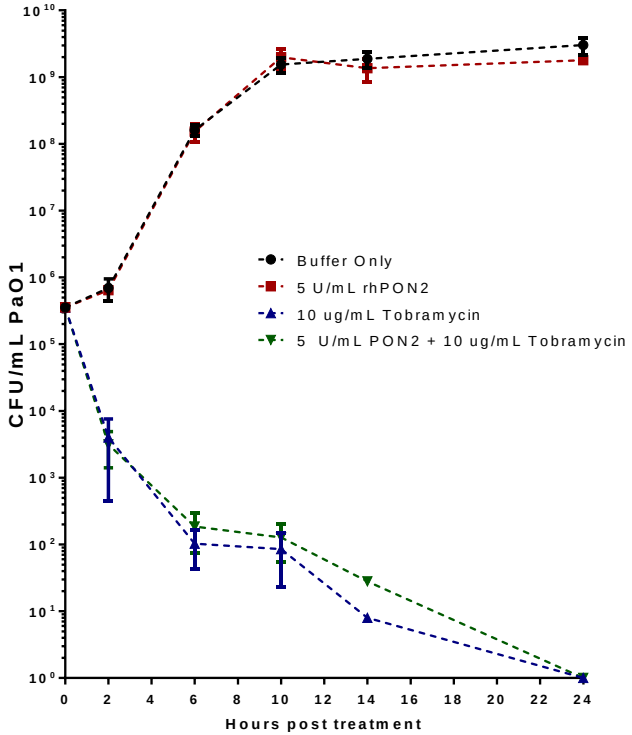

B

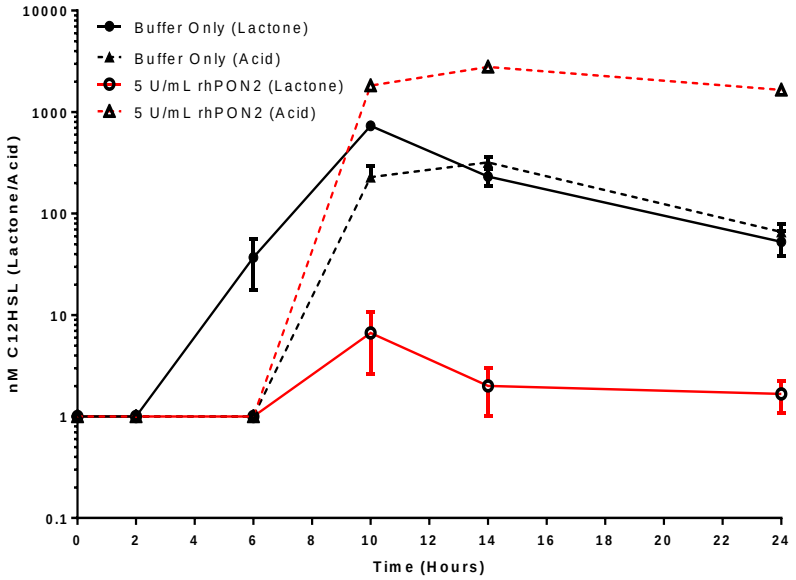

Figure 5.16 Time-dependent effect of rhPON2 in combination with tobramycin on pre-exponential phase PAO1. LB media was inoculated with 5×10^5 colony forming units per mL (CFU/mL) of PAO1. Recombinant hPON2 (5 U/ml) with or without tobramycin (2× MIC) was added at the time of inoculation and the cultures were grown at 37°C for 24 hours. Bacteria were enumerated and the C12HSL (lactone and acid) concentrations in the culture supernatants were determined at 0, 2, 6, 10, 14 and 24 hours. Figure shows A) Bacterial growth rate and B) C12HSL-lactone (solid line) and C12HSL-acid (dotted line) concentration. Error bars represent S.D. from three independent experiments.

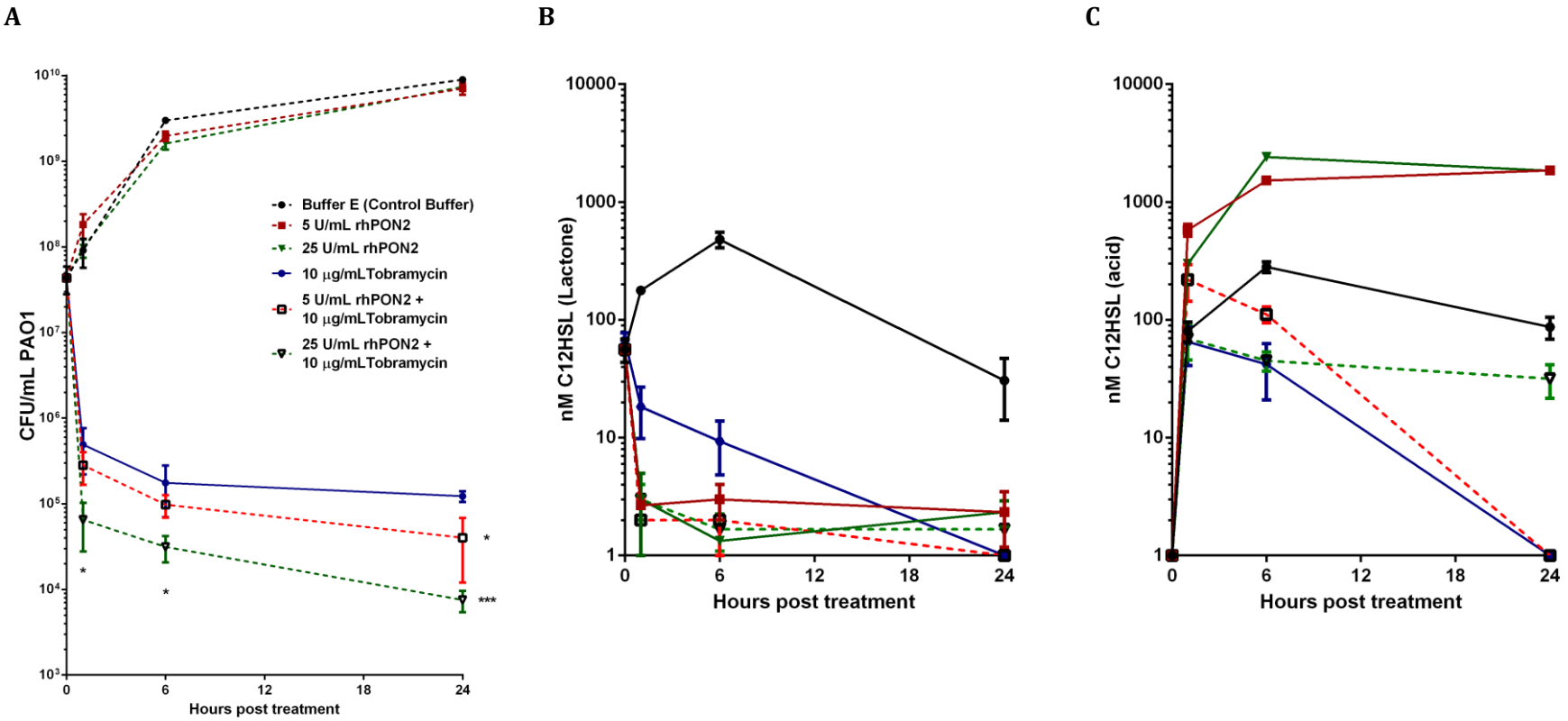

Figure 5.17 Time-dependent effect of rhPON2 in combination with tobramycin on mid-exponential phase PAO1. LB media was inoculated with 5 × 105 colony forming units per mL (CFU/mL) of PAO1. Recombinant hPON2 (5 U/ml) with or without tobramycin (2× MIC) was added six hours post-inoculation (mid-exponential growth) and the cultures were grown at 37°C for 24 hours. Bacteria were enumerated and the C12HSL (lactone and acid) concentrations in the culture supernatants were determined at 0, 1, 6 and 24 hours. Figure shows A) Bacterial growth rate, B) C12HSL-lactone concentration and C) C12HSL-acid concentration. Error bars represent S.D. from three independent experiments.

When mid-exponential phase cultures of PAO1 that had already accumulated significant levels of C12HSL (~800 nm) were treated with either 5 U/mL or 25 U/mL rhPON2, bacterial growth was unaffected (Figure 5.17A). There was, however, rapid (over 10-fold decrease within the first hour of treatment) and almost complete hydrolysis of the accumulated C12HSL (less than 5 nM C12HSL remaining, Figure 5.17B) to the open-ring C12HSL acid form (Figure 5.17C).

These mid-exponential cultures were also resistant to complete killing by 2× MIC tobramycin (Figure 5.17A). Tobramycin treatment alone decreases C12HSL concentration because of the decrease in cell numbers, as seen in Figure 5.17B, without substantial increases in the open-ring C12HSL acid form (Figure 5.17C). This is most likely the result of rapid bacterial killing causing a decrease in C12HSL production. However, when these cultures were co-treated with rhPON2 and 2× MIC tobramycin there was a significant (*t*-test, $p < 0.05$) dose-dependent increase in bacterial killing in the presence of rhPON2, which coincided with hydrolysis of C12HSL (Figure 5.17C).

5.3.5.4 Effect of rhPON2 with or without antibiotics on strain PAO1 QS and virulence gene expression

Treatment of mid-exponential phase PAO1 cultures with either 5 or 25 U/mL rhPON2 did not affect bacterial growth but rapidly converted accumulated C12HSL to the open-ring form, with a concomitant increase in the susceptibility of the bacterial cells to tobramycin. To investigate the effects of rhPON2 treatment on QS signalling, the expression levels of nine QS regulatory and QS-dependent genes were measured (Table 5.5 lists the genes) in bacteria treated with rhPON2 with and without 2× MIC tobramycin.

In the cultures treated with rhPON2 (5 or 25 U/mL) alone, there were no significant changes in gene expression (Figure 5.18). One hour post-treatment there was, however, a general trend towards decreased expression of QS-regulatory and QS-dependent gene expression in cultures treated with 5 U/mL rhPON2 but not in those treated with 25 U/mL rhPON2. After six hours of exposure to rhPON2, both 5 and 25 U of rhPON2 caused a general decrease in expression of all of the QS-related genes tested.

Treatment of cultures with 2× MIC tobramycin resulted in rapid but incomplete bacterial killing. Surviving bacteria had significantly (*t*-test, $p < 0.05$) increased expression of all the QS-related genes compared with no antibiotic treatment controls (Figure 5.19). Up-regulation of the expression of *algD, hcnB* and *phz* was observed at both time-points, while an increase in *vfr* expression was only observed one hour post treatment, and *lasB*

expression was up-regulated six hours post treatment. Although it was not significant, there was a trend towards increased expression of *lasI* and *rhlI*, the two genes catalysing the production of the two QS signal molecules at the top of the *P. aeruginosa* QS hierarchy, compared with the control treated cells, while significant up-regulation of *pqsA* compared with the control treated cells was observed six hours post treatment with tobramycin.

When mid-exponential phase cultures were co-treated with 5 or 25 U/mL rhPON2 and 2×MIC tobramycin there was an increased susceptibility to tobramycin, however, bacterial killing was still incomplete. One hour post treatment surviving cells showed little to no change in gene expression compared with untreated controls, regardless of the dose of rhPON2 used (Figure 5.19). This is in contrast to the general up-regulation of these genes that occurs following one hour of tobramycin treatment alone, suggesting that rhPON2 treatment prevents the early tobramycin-associated up-regulation of QS-associated genes. In contrast, at six hours post-treatment there was a general trend towards up-regulation of all genes tested. However, only the higher concentration of rhPON2 (25 U/mL), in conjunction with tobramycin, elicited significant increases (Figure 5.19). A greater than 10-fold up-regulation of the C12HSL synthase *lasI* was observed with a similar increase in expression of *lasR.* There was also strong and significant, up-regulation of the QS-dependent virulence factor-encoding genes *lasB* and *algD* and the QS regulator *vfr.* The strong up-regulation of *lasI* in response to treatment with 25 U/ml rhPON2 and tobramycin seem to indicate that when the bacterial cells were placed under stress (by the addition of tobramycin) they responded by attempting to up-regulate *lasI.* However, almost all the C12HSL released into the intercellular environment would be expected to be hydrolysed by the extracellular added rhPON2. In spite of the relative absence of C12HSL, expression of the associated QS-dependent genes were nonetheless up-regulated.

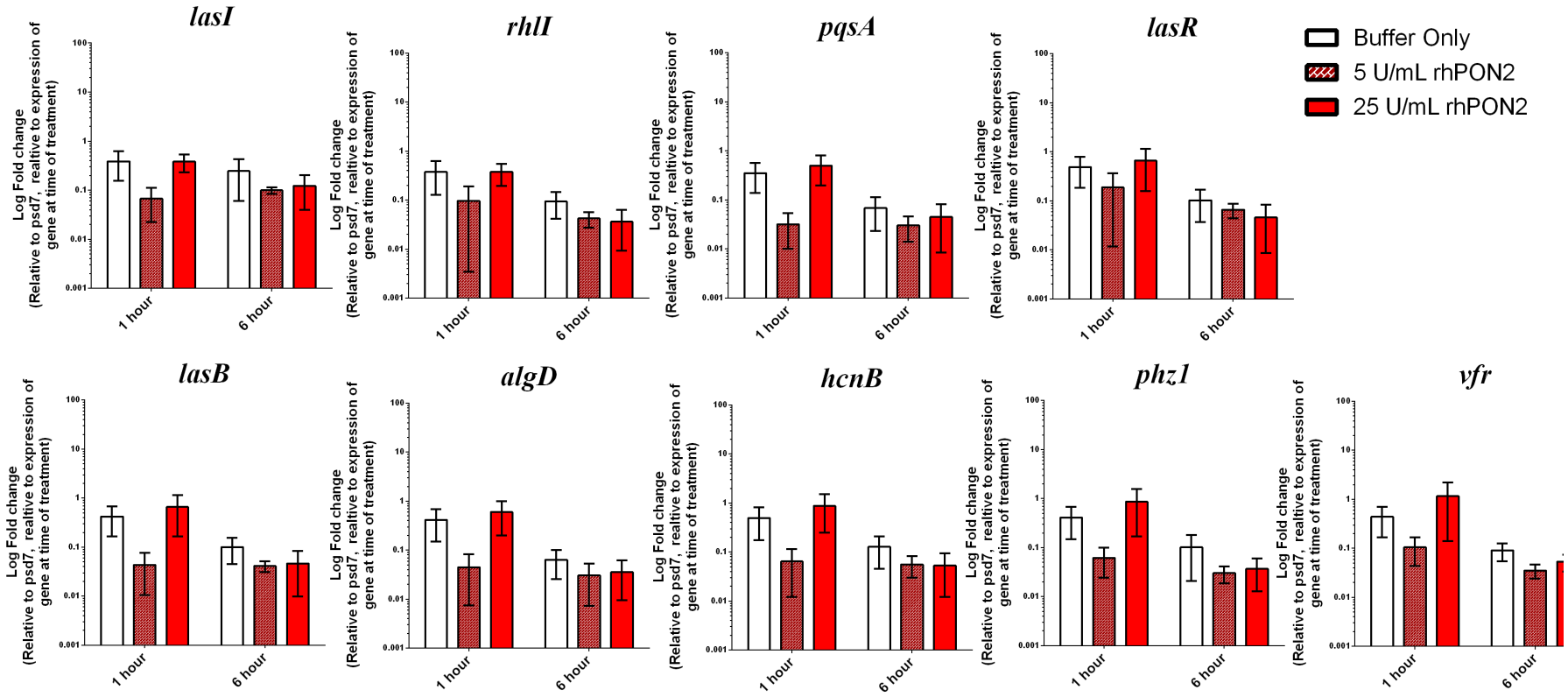

Figure 5.18 Effect of rhPON2 on PAO1 QS-associated gene expression. LB media was inoculated with 5×10^5 CFU/mL PAO1. Six hours post-inoculation (mid exponential phase), the cultures were treated with recombinant hPON2 at either 5 U/mL (dark-red) or 25 U/mL (solid-red) and grown at 37°C with shaking. RNA was extracted from cultures at one hour and six hours post-treatment to measure expression of nine QS-associated genes by RT-qPCR. Figure shows the average change in gene expression relative to expression of 16S rRNA (*psd7*) and relative to expression of the same gene at the start of treatment (time 0). Error bars represent S.D. from three independent experiments.

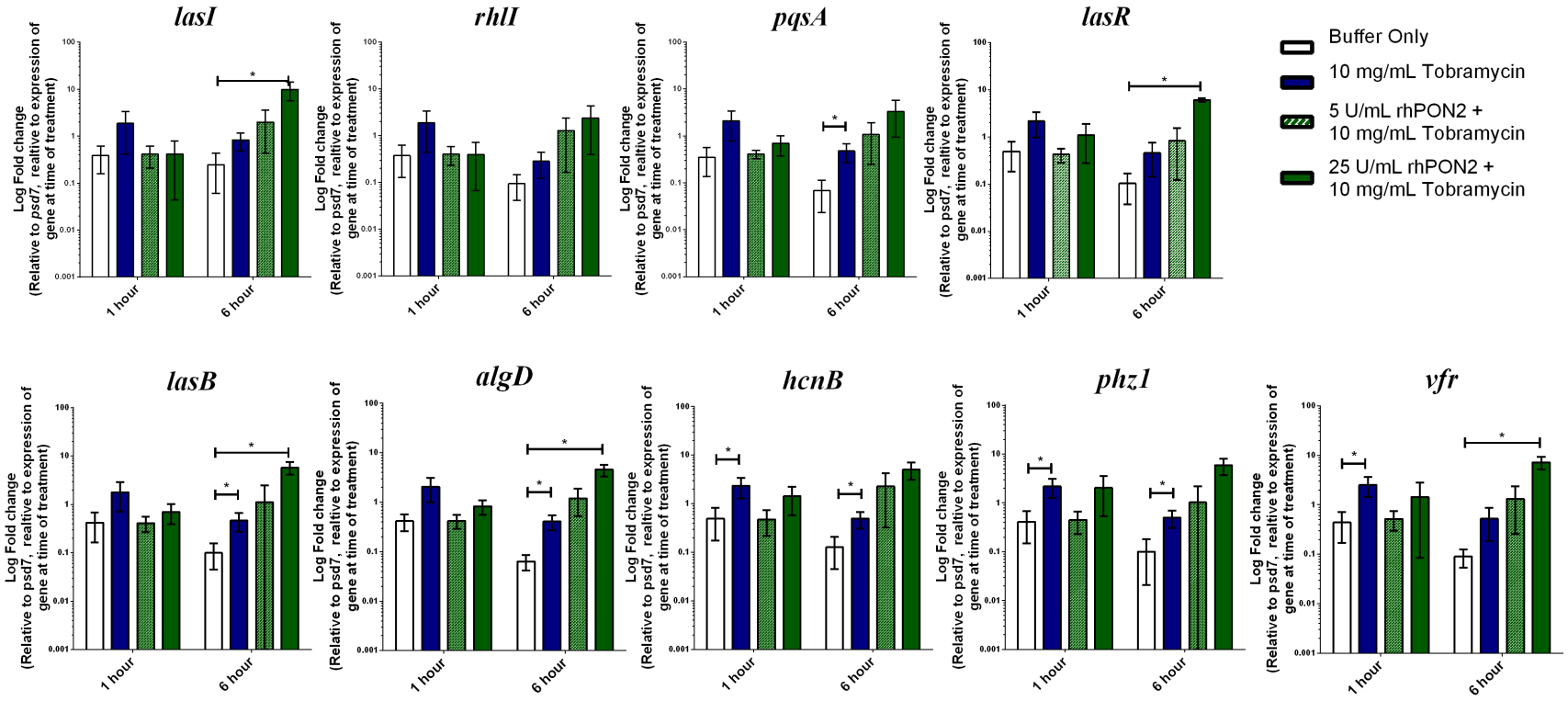

Figure 5.19 Effect of combined rhPON2 and tobramycin treatment on PAO1 QS-associated gene expression. LB media was inoculated with 5 × 105 CFU/mL PAO1. Six hours post-inoculation (mid exponential phase), the cultures were treated with tobramycin (2× MIC; solid blue) alone or in combination with recombinant hPON2 at either 5 U/mL (shaded green) or 25 U/mL (solid green) and grown at 37°C with shaking. RNA was extracted from cultures at one hour and six hours post-treatment to measure gene expression of nine QS-associated genes by RT-qPCR. Figure shows the average change in gene expression relative to expression of 16S rRNA (*psd7*) and relative to expression of the same gene at the start of treatment (time 0). Error bars represent S.D. from three independent experiments.
* $p < 0.05$ by Students *t*-test.

5.4 DISCUSSION

Recombinant human PON2 was successfully expressed via a baculovirus infection system and purified using the method described by Draganov and colleagues [248]. The purity of the final protein preparation was ~70%. A contaminating ~25kDa protein found in the protein preparation was also similarly reported by Draganov and colleagues [248]. Importantly, the 25kDa protein did not have detectable PON2-associated lactonase activity. When the cell lysates from non-infected insect cells underwent the same purification protocol, the ~25 kDa protein was once again detected, suggesting that this protein was endogenous to the *Trichoplusia ni* insect cells. Removal of this contaminating protein might be possible with inclusion of an additional purification step, perhaps one involving gel filtration chromatography to separate the proteins based on their molecular mass. However, each additional purification step comes at the cost of decreased protein yield, and because there was no detectable PON2 activity associated with lysates prepared from non-infected insect cells (since insects do not possess PON2) the benefits of any additional purification is expected to be minimal.

The specific activity of the rhPON2 preparation towards C12HSL was Ca^{2+}-dependent and was determined to be 323 U/mg total protein. This was comparable to the rhPON2 specific activity reported by Draganov and colleagues (459 U/mg total protein) [248]. Teiber and colleagues also produced rhPON2 using a similar method to that described by Draganov and colleagues but reported a much higher specific activity, 7647 U/mg [262]. The reason(s) for these discrepancies are not understood.

Next the hypothesis that rhPON2 treatment of *P. aeruginosa* would decrease bacterial QS and QS-associated virulence and increase bacterial susceptibility to tobramycin was tested. While synthetic rhPON2 was produced in this study laboratory and its lactonase activity verified, this hypothesis was tested using rhPON2 that had been produced by a large scale preparation at the Monash Protein Production Unit.

The results presented in Figure 5.16 are the first demonstration that an extracellularly applied mammalian lactonase is capable of hydrolysing C12HSL produced during the growth of *P .aeruginosa.* In control PAO1 cultures, C12HSL-lactone accumulated in culture supernatants during the early exponential phase, peaking at the end of the exponential phase before decreasing to a stable level during the stationary phase. Treatment of pre-exponential PAO1 with rhPON2 largely prevented C12HSL-lactone from being detected in

culture supernatants, as indicated by the sustained accumulation of the acid form of C12HSL in rhPON2 treated cultures. Treatment of mid-exponential cultures with rhPON2 led to rapid and almost complete hydrolysis of C12HSL-lactone. This observation indicated that, in addition to preventing the accumulation of C12HSL in early cultures, rhPON2 was also able to hydrolyse C12HSL being produced by older cultures. Sustained (24 hours) prevention of C12HSL accumulation by rhPON2 also indicated that the rhPON2 was reasonably stable in treated bacterial cultures. Taken together, these findings demonstrate the ability of rhPON2 to hydrolyse and prevent accumulation of C12HSL-lactone in *P. aeruginosa* cultures. It seems reasonable to suspect that a significant proportion of C4HSL, the signalling molecule of the second *P. aeruginosa* QS system, also undergoes lactonolysis. While this phenomenon was not directly measured in this study, rhPON2 reportedly displays similar lactonase activity towards C4HSL [248].

Interestingly, C12HSL-acid was also detected in control cultures, indicating that C12HSL hydrolysis occurred in *P. aeruginosa* cultures even in the absence of rhPON2 treatment. Yates and colleagues also observed the accumulation of C12HSL-acid in *P. aeruginosa* cultures during their experimentation [243].These authors found that hydrolysis of C12HSL in cultures was not enzyme-dependent but instead pH dependent. Unlike the observations of Yates and colleagues, the present study found that the pH decreased only slightly during growth of the bacterial cells but most importantly remained neutral. There are no reports describing native *P. aeruginosa* enzymes able to hydrolyse C12HSL. Thus the reason for spontaneous hydrolysis of C12HSL in *P. aeruginosa* cultures is not known. As the acid form accumulates during PAO1 exponential growth, preceding the accumulation of the lactone form, one explanation could be that C12HSL was being hydrolysed after binding to its cognate receptor as part of a hitherto unknown self-regulating mechanism of QS. One such proposed self-regulating mechanism of QS is thought to be through PvdQ QS [360]. PvdQ is an acylase that inactivates AHLs by cleaving the acyl chain from the homoserine lactone, rendering the molecule inactive [361]. Whether this sort of system is responsible for the "spontaneous" hydrolysis C12HSL observed in the absence of rhPON2 treatment remains to be determined. While the treatment with rhPON2 did not affect the growth of *P. aeruginosa,* the expression of most QS-associated genes, however, showed a trend towards decreased expression six hours post-treatment with rhPON2. Higher doses of rhPON2 may have initially (after one hour) increased QS and QS-dependent virulence, most likely through stress, but these effects were no longer evident six hours post treatment. Decreased QS and QS-dependent virulence as a result of hydrolysis of C12HSL is consistent with the findings of

other studies where C12HSL-dependent signalling was prohibited either through QS knockout studies [135, 316, 362, 363] or treatment with C12HSL degrading enzymes [351-353, 355].

P. aeruginosa cultures were treated with the CF-relevant aminoglycoside antibiotic tobramycin. Treatment with 2× MIC tobramycin completely killed pre-exponential but not mid-exponential cultures within 24 hours. This was not unexpected as growth rates are known to influence susceptibility to antibiotics. Mid-exponential cultures treated with tobramycin alone yielded lower C12HSL concentrations compared with controls, most likely as a consequence of antibiotic-mediated cell death. Treatment with tobramycin alone also seemed to induce QS and QS-dependent virulence gene expression. For example, the expression of QS-dependent virulence genes involved in elastase biosynthesis (*lasB*), alginate synthesis (*algD*), hydrogen cyanide production (*hcnB*) and phenzine production (*phz*) were all significantly up-regulated at certain time points in response to tobramycin treatment alone. Intriguingly, tobramycin treatment had a lesser effect on the expression of genes coding for the QS signals. While there appeared to be a trend towards increased expression of *lasI* and *rhlI* in response to tobramycin treatment at both one and six hours post treatment, the expression of *pqsA* only seemed to increase six hours post treatment. The general increase in virulence gene expression in PAO1 in response to tobramycin treatment, was most likely the result of the stress induced by tobramycin. Tobramycin binds to the 30S and 50S bacterial ribosomes, preventing formation of the 70S complex, which eventually causes inhibition of mRNA translation inducing ribosomal stress [364]. Ribosomal stress is known to induce the *P. aeruginosa* stress response via the MexXY-OprM multidrug efflux system [365, 366]. The MexXY-OprM efflux system is thought to influence the expression of a number of virulence genes also normally regulated by QS [367]. A number of studies have reported that in *P. aeruginosa,* QS forms part of the cellular response to various stresses including antibiotics [368-372]. In addition, bacteria seem to increase their biofilm formation, a QS-determinant, in response to antibiotic stress [373].

To investigate whether rhPON2-mediated C12HSL hydrolysis might increase the susceptibility of *P. aeruginosa* to the inhibitory effects of antibiotics, *P. aeruginosa* cultures were treated with varying concentrations of rhPON2 together with tobramycin at 2× MIC. Treatment of mid-exponential cultures, but not pre-exponential cultures, showed that rhPON2 treatment increased the susceptibility of the bacterial cells to tobramycin. At 2× MIC, tobramycin effectively killed most of the bacterial cells in pre-exponential cultures, making it difficult to observe whether co-treatment with rhPON2 increased their

susceptibility to the antibiotic treatment. In contrast, mid-exponential cultures treated with both rhPON2 and tobramycin showed a rhPON2-dose-dependent increase in the susceptibility of PAO1 to tobramycin. These results are consistent with those studies showing QS deficient *P. aeruginosa* strains [171] and those treated with QS inhibitors are more susceptible to tobramycin than control [171, 374]. However, complete killing was not achieved, even with combined rhPON2+tobramycin treatment. Remarkably, some populations of bacterial cells seemed to up-regulate the expression of QS and QS-dependent virulence gene expression. In particular, there was a strong up-regulation of *lasI*, indicating that some bacterial cells at least were attempting to compensate for the decreased extracellular C12HSL concentration by up-regulating LasI, most likely to co-ordinate a response to the antibiotic stress. The attempt was futile however, as rhPON2 degrades the QS signal. This up-regulation of QS-dependent virulence genes must be independent of C12HSL. However, the expression levels of QS-dependent virulence genes can be regulated independently of QS. Thus for example, *las* and *rhl* mutants are still capable of producing low levels of elastase [135, 362, 363] and pyocyanin [362] despite being unable to use these two systems to co-ordinate expression. In addition, the major transcriptional repressor of the Las system, RsaL, can regulate pyocyanin and hydrogen cyanide synthesis independently of Las system, [375]. In fact, emerging evidence indicates that there is added complexity in the QS systems of *P. aeruginosa.* It is proposed that the expression of the QS virulence determinants may be regulated independently of QS under sub-optimal conditions. One such example is the recent discovery of a new QS signal, IQS, which, during growth in nutrient rich media, was regulated by the Las system [376]. However, under phosphate depletion stress, IQS can be produced independent of the Las system, and still signal the Rhl and PQS QS systems and stimulate gene expression of virulence determinants usually regulated by QS. As a result, it is plausible that up-regulation of *lasI* and the QS-dependent virulence genes in the absence of C12HSL could take place via a C12HSL/Las independent mechanism. Further investigations will be required to establish the mechanism through which this occurs. Global gene expression analysis using microarrays may be an ideal method to further explore the mechanisms by which *P. aeruginosa* responds to antibiotic stress in the absence of C12HSL.

Treatment of mid-exponential cultures with both rhPON2 and tobramycin resulted in rapid hydrolysis of C12HSL, faster than that observed with tobramycin-treatment alone. This difference in rates of hydrolysis further supports the hypothesis that the tobramycin treatment-associated decrease in C12HSL was predominantly due to increased cell death.

In summary, rhPON2 was capable of hydrolysing C12HSL able to be produced in *P. aeruginosa* cultures, and although it did not affect bacterial growth, it did appear to decrease QS and QS-dependent virulence gene expression in this organism. More importantly, when used in combination with tobramycin, rhPON2 increased the bactericidal effects of the tobramycin. Overall, the results described in this chapter suggest that rhPON2 might well be an effective quorum sensing inhibitor and novel anti-Pseudomonal therapy.

CHAPTER SIX – NEONATAL MOUSE MODEL OF *P. AERUGINOSA* INFECTION

6.1 INTRODUCTION

The ubiquitous bacteria *P. aeruginosa* is a common pathogen in nosocomial infections, burns, people with immune deficiencies and people with cystic fibrosis (CF). CF is the most common life-limiting single gene disorder in Caucasians and is characterized by chronic respiratory infections. These respiratory infections severely compromise lung function in patients and are a major contributor to morbidity and mortality in CF [5, 19, 377]. CF is the result of mutations to the CF transmembrane conductance regulator (*CFTR*) gene. These mutations facilitate the establishment of chronic infections in young people with CF by pathogens thought to be acquired from the environment. A number of theories attempt to explain why CF patients have a high incidence of chronic lung infections and these include impaired mucociliary clearance [43, 378, 379] and compromised immune function[380]. Once *P. aeruginosa* is in the airway, bacterial cellular components such as lipopolysaccharides (LPS), flagella and pili facilitate attachment to host cells. This then stimulates the pathogen to produce virulence factors such as toxins and proteases and to trigger a host immune response. Healthy hosts clear the infection through a combination of an effective immune response and mechanical forms of protection such as mucociliary clearance, preventing the pathogen from establishing an infection. The impaired mucociliary clearance and compromised immune function in people with CF allows the pathogen to persist in the airway. Over time, *P. aeruginosa* begins to produce more virulence factors and uses quorum sensing to establish biofilms. The increased bacterial virulence has a detrimental effect on the airways while the biofilms aid the pathogen to shield itself from the host immune response. The immune response of the host, and conventional antibiotics, find it almost impossible to penetrate these biofilms, facilitating the establishment of a persistent bacterial infection [170, 171].

While the holy grail of CF research is ultimately correction of the defective CFTR channel, research has traditionally been focused on improving the quality of life of patients by countering the pulmonary, pancreatic and gastrointestinal manifestations of the disease. Developing drugs and novel therapies relies on the use of cell- and animal-based models of CF to test efficacy and provide a more comprehensive understanding of the mechanisms involved in the disease. These models provide us with an insight into how pathogens such as *P. aeruginosa* colonize and persist in the CF lung. There exist a number of *in vitro* CF models including primary, wild-type and *CFTR*-deficient cell lines. However, the

invasiveness of obtaining tissues from CF patients limits the use of primary cell lines [381] and cultured cell

Table 6.1 Non-murine animal models of CF and chronic *P. aeruginosa* infection

Animal	Type of Infection
Rhesus Monkey	Chronic endobronchitis by intrabronchial instillation of *P. aeruginosa* agar beads [382]
Cat	Pneumonia by repeated intrapulmonary inoculation of viable *P. aeruginosa* [383]
Guinea pig	Pneumonia by tracheobronchial instillation of *P. aeruginosa* agar beads [384]
Ferrets	*CFTR*-deficient with multiple characteristics of human CF including gastrointestinal abnormalities and predisposition to lung infection (but not chronic infections and not *P. aeruginosa*) [385]
Pigs	*CFTR* -deficient [386]that develop CF like lung disease with spontaneous lung infection (but not with *P. aeruginosa*) and exhibit difficulty in clearing bacterial infection from birth [387]

lines rarely maintain epithelial cell properties and cellular differentiation for prolonged periods. Cell lines are also hardly representative of the complex relationships seen in intact organs or whole animals, a feature that is important when studying a multi-organ disease like CF. Thus animal models remain a valuable tool in understanding the pathophysiology of the CF phenotype. No natural animal models that mimic human CF have yet been described [388] and instead a number of models have been developed to represent different aspects of the disease, particularly respiratory complications associated with infections by *P. aeruginosa,* and are summarized in Table 6.1. With recent advances in techniques, more appropriate transgenic animals have also been developed, including *CFTR*-deficient ferrets [385] and the promising *CFTR*-deficient pigs [386]. However, murine models have featured prominently due to their ease of use, availability and the increasing number of available transgenic variants.

With the mapping of the human *CFTR* gene as the defect present in CF [27] and subsequent identification of its murine equivalent [389], Snouwaert and colleagues were able to develop the first transgenic mouse by incorporating a null mutation of *Cftr.* This resulted in *Cftr*$^{-/-}$ mice with numerous pathological changes similar to those in humans with CF [390]. However, gastrointestinal complications shortened the lifespan of these mice and this was consistent across all the early null mutation based *Cftr*-deficient mice [391-393]. When mice were created with the clinically relevant mutations ΔF508 [394], G551D [395] and G480C

[396] the mortality rate due to the gastrointestinal complications decreased but was still a major hindrance towards using these models. In order to overcome this complication, a *Cftr*-deficient mouse with the transgenic expression of human *CFTR* in the gut epithelium was created, *Cftr*^{tm1Unc}-Tg*(FABPCFTR)*1Jaw/J, which displayed a significantly improved survival rate [397]. Another promising transgenic mouse strain for studying CF is the *Scnn1* mutant in which specific airway epithelial Na^+ channels are over expressed. This increases Na^+ absorption and produces a CF like lung disease in the mice [42]. While a number of authors have claimed that under challenge with bacterial pathogens, CF mice find it more difficult to clear infection [377, 398, 399], the establishment of the most challenging phenotype of CF, chronic *P. aeruginosa* infection, has been difficult under standard laboratory conditions and even when infections do develop, they do not completely resemble those of human CF [400]. A number of reasons for this have been put forward, all suggesting that the physiology of mice allows them to be intrinsically more capable of clearing bacterial infections by mechanisms including compensation for the CFTR defect by other ion channels. A further factor limiting the experimental use of transgenic mice is the expense associated with maintaining the animals. Breeding pairs are normally heterozygous and thus offspring have to be typed and only a limited number of animals per litter can be used in the experiments. While transgenic *Cftr*-deficient mice are the best available analogues of CF lung disease amongst murine models, the strains currently available need to be better characterized and adjusted to give us models more typical of human CF.

P. aeruginosa infections were first successfully established in inbred mice in 1968 to facilitate the study of lung infection [401], with the establishment of acute infections achieved by aerosolization of bacteria into the lung. While aerosolized challenges remain popular, acute infections can now also be established intranasally, [402] and intratracheally [403]. *P. aeruginosa,* upon establishing infection in a human CF host, initiate biofilm formation. Biofilm growth affords *P. aeruginosa* significant protection against host defence mechanisms and conventional antibiotics, facilitating the establishment of chronic infections. Chronic infections are difficult to establish in mice as the mice mechanically clear the infection[404] and aerosol challenges have had limited success in aiding their establishment, even under controlled conditions and using immunocompromised mice [405, 406]. Instead investigators generally embed *P. aeruginosa* into a bead-shaped artificial matrix such as agar or alginate and then infuse it intratracheally into mice [407-409]. Two studies using intratracheal challenges [410, 411] have largely succeeded in mimicking the persistent *P. aeruginosa* infections seen in the CF lung. Both studies demonstrate the

persistence and proliferation of *P. aeruginosa* in the lungs with a bacterial load of 1×10^5 CFU/lung 7–21 days post infection. Hoffman and colleagues demonstrated foci of *P. aeruginosa* biofilms in the alveoli of CF mice infected intratracheally with *P. aeruginosa* [410] and histological analysis of the samples from the lungs showed damage to the airway similar to that seen in CF patients. However, both authors conceded that the use of intratracheal challenges does not reflect the natural history of *Pseudomonas* infection in CF and the use of beads may cause blockages and mechanical damage to the airway of the mice resulting in added inflammation.

Intranasal infection strategies represent an easy and more natural way of establishing infections. Tang and colleagues adapted a neonatal model of acute pulmonary infection by *Bordetella pertussis* [412] to establish acute *P. aeruginosa* pneumonia in neonatal BALB/c mice [402]. They placed bacterial suspensions onto the nares of seven-day-old mice and allowed the pups to inhale the bacteria. They demonstrated evidence of pulmonary infection within 4 h post inoculation. All mortalities occurred in the first 24 hours and, of the animals that survived, most had cleared the infection by 48 hours and by 96 hours, *P. aeruginosa* was undetectable. The authors also showed that adult mice tolerated several orders of magnitude of bacterial load higher than infant mice without obvious signs of pneumonia or bacteraemia. This increased susceptibility to bacterial infection in infant mice was attributed to the naive immune system in the neonates. Further research on the susceptibility of neonatal mice to infection by Diavatopoulos and colleagues enabled the establishment of a chronic bacterial infection in a neonatal murine model by intranasal application by initially priming the mice with influenza A virus [413]. The authors infected 5 day old C57BL/6 mice with 2×10^3 colony forming units (CFU) of *Streptococcus pneumoniae* and the infants retained the bacteria with the nasopharangeal carriage at 9 days post infection increasing to 1×10^5 CFU in the nasopharynx. An intranasal neonatal model of chronic *P. aeruginosa* would have a number of advantages. Firstly, it would not necessitate the sedation of the animal as required for intratracheal inoculation. Secondly, it can be done quite quickly. Tang and colleagues were able to inoculate each pup in less than 1 minute [402]. More importantly though, CF patients acquire pathogens from the environment by inhaling them and then develop chronic infections, partially due to the limitations placed on them by their immune deficiencies. The under-developed immune systems of the neonates offer a similar setting to establish and study chronic bacterial infections. Finally, there are significant cost savings in using more conventional non-transgenic models, and using well-characterized strains of mice allows us to better understand the implications of any

infection. In this study, we attempt to establish intranasal chronic *P. aeruginosa* infection in inbred BALB/c neonates. Establishment of such a model will enable the investigation the potential of rhPON2 as an anti-Pseudomonal in an *in vivo* infection model.

6.2 MATERIALS AND METHODS

Most of the materials and methods for this chapter are described in Chapter 2. Any additional materials and methods specific for this chapter are described below.

6.2.1 Ethics statement

Animal experiments were approved by the University of Tasmania (A0012571) and complied with the Prevention of Cruelty to Animals Act (1986) and the National Health and Medical Research Council (NHMRC) Australian Code of Practice for the Care and Use of Animals for Scientific Purposes 2004.

6.2.2 Bacterial strain and culture conditions

PAO1 (ATCC 15692) was grown in LB media, shaking at 37 °C overnight until stationary phase as measured by optical density at 600 nm (OD_{600} = 1–2). They were diluted in LB media to OD_{600} of 0.05 and grown at 37 °C for eight hours with shaking at 200 RPM. Aliquots were taken at regular intervals to determine CFU/mL at particular OD_{600} levels and standard curve generated. A mid-log phase aliquot (OD_{600} = 0.2–0.4) was then serially diluted and aliquots of each dilution were frozen in LB supplemented with 8% glycerol at –20 °C for infecting mice. Additional aliquots of each dilution were either stored in RNAlater (Life Technologies, Carlsbad CA) for quantitative PCR, or plated for CFU determination.

Bacterial suspensions for mouse infection were prepared by thawing glycerol stocks and diluting in PBS to the desired CFU/mL with reference to a standard curve. Bacteria were then washed once with PBS and diluted 2:1 in 6 mg/mL Evans Blue dye (Life Technologies, Carlsbad CA) in PBS. In addition, the bacterial load was determined as described in chapter two (Section 2.5.3).

6.2.3 Neonatal mouse model of infection

Visibly pregnant BALB/c mice (UTAS breeding colony) were housed in individual cages containing Pure-o'Cel bedding (Able Scientific, Canning Vale WA, Australia). Following birth, the cages were issued to the experimental room where they were housed in an Optimice microisolated ventilated rack system. Five-day-old mice (5–9 mice per group depending on litter size) were inoculated with 3 μL of PAO1 suspensions at different bacterial concentrations (10^3 to 10^8 CFU), one treatment concentration per litter. The pups were inoculated by applying the 3 μL of suspension directly to the nares of pups while they were being restrained gently in the hand. The pups reflexively inhaled the bacteria and care was taken to ensure that pups completely inhaled the suspensions. Pups were then returned to the mother and monitored for signs of infection and/or distress. At 12 hours, two days, five days and 12 days post-inoculation; mice were euthanized by CO_2 asphyxiation. In a sterile environment, the chest was opened and the lungs carefully harvested and transferred to 1 mL of RNAlater (Life Technologies, Carlsbad CA). The lungs were cut into smaller pieces to ensure complete permeation of RNAlater, then weighed and stored at –20 °C for subsequent RNA extraction.

6.2.4 Tissue homogenization, RNA extraction and quantitative PCR

RNAlater was drained from lung tissue and the lung tissue transferred to 750 mL Trizol (Life Technologies, Carlsbad CA) in a 2 mL tube containing 1 mL of 0.1 mm zirconia/silica beads (Daintree Scientific, St Helens, TAS, Australia). Another 650 mL of Trizol was then added to fill the tube and the tissue homogenized by bead-beating for 1 minute using a bead beater (Daintree Scientific). Bead-beating was repeated until the lung tissue was completely homogenised. Beads and cellular debris were pelleted by centrifugation at 10,000 × *g* for 10 min at 4 °C and the clarified supernatant transferred to a fresh tube for RNA extraction using Trizol and for subsequent cDNA synthesis as described in chapter 2 (Section 2.2).

PCR was carried out on the LightCycler480 instrument using LightCYcler480™ SYBR Green I Mastermix (Roche) as described in Chapter 2 (Section 2.2.6), with one exception. PCR conditions were as follows, 95 °C (5 minutes) then 55 cycles instead of 45 cycles (as described in chapter two) of 95 °C (10 seconds), 60 °C (10 seconds) and 72 °C (30 seconds) followed by melt curve analysis. Bacterial concentration was determined using primers

specific for *P. aeruginosa* 16s rRNA [276]. Expression of bacterial genes was determined using primers described in chapter 2 (Table 2.4).

6.3 RESULTS

6.3.1 Observational assessment of animal behaviour in response to intranasal infection with bacteria.

Observations made of the behaviour animals in response to the intranasal applications are summarized in Table 6.2. Briefly, it was difficult to apply a consistent dose to each animal as not all pups reflexively inhaled the inoculum. Some pups initially exhaled the inoculum before re-inhaling, presumably resulting in them receiving a lower dose than the pups that completely inhaled the inoculum without exhaling. No other signs of distress from the experimental procedure were observed. No mortality associated with infection was observed.

Table 6.2 Observational assessment of animal behaviour in response to intranasal application of bacteria

Assessment Criteria	Observations
Viscosity of inoculum	Inoculum containing higher doses of bacteria were more viscous
Efficacy of intranasal application of bacteria	Some pups reflexively inhale the complete inoculum while others initially exhaled before re-inhaling.
Signs of distress	No major indicators of distress upon application of inoculum. Some pups rested for a few minutes before freely moving around
Mortality	None associated with infection

6.3.2 Neonatal mice developed low-level chronic infections via intranasal inoculation

When infecting mice with bacteria, the dosage needs to carefully considered, especially if attempting to establish a chronic infection. Too few bacteria, and a sufficiently robust infection will not develop. Too many bacteria, and the mice may succumb to bacterial pneumonia. We first attempted to establish an optimum dose of infection by infecting five day old BALB/c mice with doses of PAO1 ranging from 1×10^3 to 1×10^7 CFU. The mice were euthanized two days post inoculation, the lungs harvested and the CFU remaining in

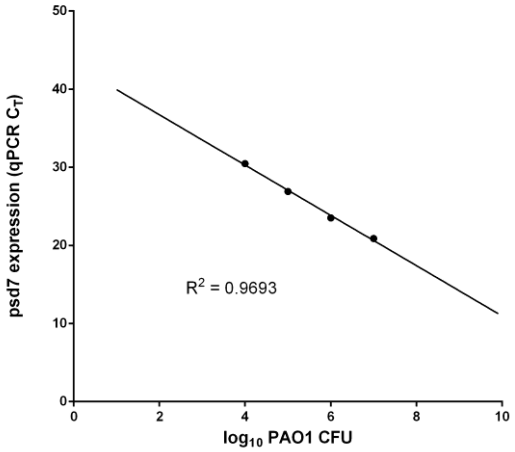

Figure 6.1 Relationship between qPCR cycle threshold (CT) of psd7 expression and log_{10} PAO1 CFU. Cycle threshold of *psd7* expression of RNA extracted from PAO1 cultures compared to the number of CFU in those cultures. *n* = 2

the lungs was enumerated by qPCR of the bacterial 16srRNA gene (*psd7*). The CFU was calculated by comparing the cycle threshold (C_T) of *psd7* expression in lung tissue with a standard curve relating C_T to PAO1 CFU (Figure 6.1). A linear relationship was observed (R^2 = 0.9693) allowing us to relate C_T of *psd7* expression to number of CFU. The CFU enumerated in each mouse are displayed in Figure 6.2, along with the mean CFU (*n* = 5–8) of each treatment dose.

No dose dependent effects were observed relating to bacterial load of infected mice. In addition, none of the mice had enough CFU in the lungs to be considered to have an infection as decided by our arbitrary cut-off of $>10^3$ CFU/ml. In fact, for between 2-4 mice in each group of 5-8 mice we found no detectible *P. aeruginosa* in their lungs. The mice that received the highest dose of *P. aeruginosa*, 1×10^7 CFU, were the most capable of clearing the infection with 4/5 mice having no detectible *P. aeruginosa* in their lungs two days post infection.

In order to determine if establishment of chronic infection is possible using this model, five day old mice were infected with 1×10^8 CFU of PAO1. This dose was used because the lower doses were unable to cause infection with $>10^5$ CFU/mL that persisted two days post infection, and did not have any obvious detrimental effects on the animals. PAO1 CFU in the lungs was enumerated by qPCR from lungs harvested from the mice 12 hours, five days and 12 days post infection. The number of CFU in the lungs of each mouse and the mean CFU (*n* = 6–9) in the lungs of mice for each time point are displayed in Figure 6.3. At the earliest

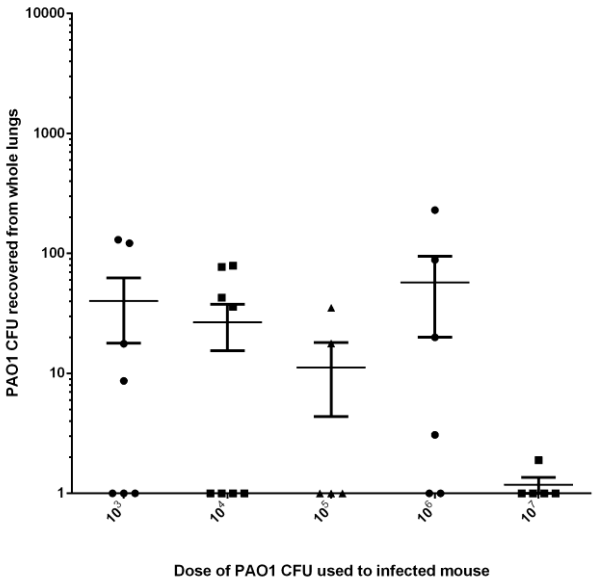

Figure 6.2 Bacterial load of *P. aeruginosa* infected mice lungs two days post infection. Five day old neonatal mice infected with a range of CFU's of PAO1 and bacterial load two days post infection of individual calculated by qPCR. Results expressed as $\log_{10}$ CFU recovered from whole lung. Mean CFU recovered indicated by horizontal line, while error bars represent S.E.M. Significant differences assessed using Kruskal–Wallis non-parametric test with Dunn's post-test. *n* = 5–8. Mice with no detectible *P. aeruginosa* shown on logarithmic scale as 1.

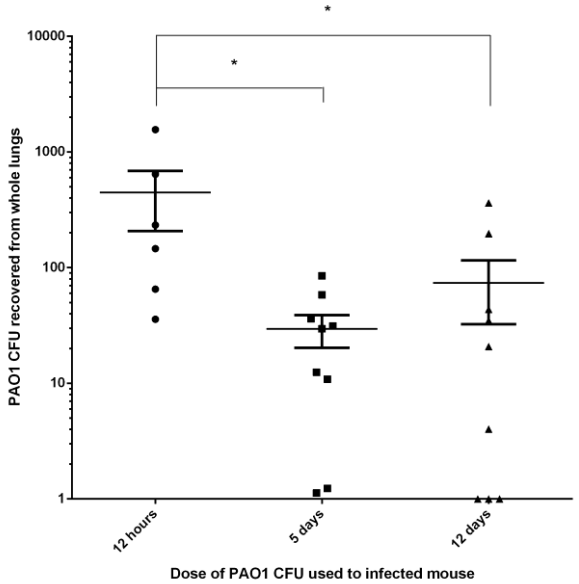

Figure 6.3 Bacterial load of *P. aeruginosa* infected mice lungs over 12 days. Five day old neonatal mice infected with 1×10^8 CFU of PAO1 and bacterial load 12 hours, five days and 12 days post infection determined by qPCR. Results expressed as $\log_{10}$ CFU recovered from whole lung. Mean CFU recovered indicated by horizontal line, while error bars represent S.E.M. Significant differences assessed using Kruskal–Wallis non-parametric test with Dunn's post-test.* $p < 0.05$. n = 6–9. Mice with no detectible *P. aeruginosa* shown on logarithmic scale as 1.

time point, 12 hours post infection, the *P. aeruginosa* load was highest, with 1/6 mice having $>10^3$ CFU in the lung. However, the mice cleared most of the bacteria within this short time period suggesting that an immediate acute infection was not established. The numbers of CFU detected in the lungs decreased significantly ($p < 0.05$) by day five to less than $<10^2$ CFU. The number of CFU detected in the lungs by day 12 post infection remained similar, demonstrating that small numbers of bacteria were persisting in the lungs.

However, 3/ 9 mice had completely cleared the infection. Though the number of *P. aeruginosa* detected at the later time points were inconsistent, and orders of magnitude lower than the infection dose, the persistence of low levels of bacteria is consistent with establishment of a low-level chronic infection in 30% of the mice.

To investigate whether a virulent infection had been established, we measured the expression of a number of bacterial QS and virulence genes summarized in Table 6.3. We used qPCR to quantify gene expression in the mouse lung tissue from two mice from each group with the highest reported bacteria loads. However, there was no detectable expression of the virulence genes by qPCR.

Table 6.3 Expression of bacterial virulence and QS genes in two mice from each group with highest bacterial carriage by qPCR

Genes	Role	Expression
lasI	QS signal (C12HSL-HSL inducer) synthesis	No detectable expression
lasB	Elastase B synthesis	No detectable expression
rhlI	QS signal (C4-HSL inducer) synthesis	No detectable expression
algD	Alginate biosynthesis	No detectable expression
pqsA	*Pseudomonas* quinolone signal synthesis	No detectable expression

6.4 DISCUSSION

Establishment of an intranasal chronic *P. aeruginosa* infection model will enable the *in vivo* investigation of rhPON2 as a novel anti-Pseudomonal therapy. The intranasal method of *P. aeruginosa* bacterial delivery to the neonatal mouse lung investigated in this chapter enabled the development of a low-level chronic infection. Chronic infections are characterized by surviving animals having a stable bacterial load, often with intrapulmonary replication, in the airway, typically for at least two weeks. In our study we saw persistence of a relatively small numbers of bacteria (10^2–10^3 CFU) 12 days post infection. This rate of PAO1 carriage in the mouse lungs is on the lower end of the scale of carriage rates reported by other authors who have established chronic *P. aeruginosa* infections in BALB/c mice. Hoffmann and colleagues intratracheally challenged 12–14 week old BALB/c with 5×10^7 CFU of a mucoid *P. aeruginosa* strain and recovered between 10^3 and 10^9 CFU/mouse seven days post infection and between 10^5 and 10^7 CFU/mouse 13 days post infection [410]. Lazenby and colleagues intratracheally challenged 8–12 week old BALB/c with 1×10^6 CFU PAO1 and the investigators recovered between 10^3–10^4 CFU/g lung tissue 24 hours post challenge and $\sim 10^4$ CFU/g lung tissue 10 days post challenge (average weight of 8–12 week mouse lung 200 mg–400 mg) in their study. [362]. We were however unable to establish whether this level of infection is physiologically relevant, as there was no detectable expression of *Pseudomonas* virulence and QS genes. This inability to detect expression of *Pseudomonas* virulence and QS genes may be a result of the low bacterial numbers. Without histopathological analysis of the lungs, it is difficult to determine whether this level of bacteria can be considered to be pathological.

It must also be noted that the mice were monitored for signs of distress and none was evident. In comparable studies, intratracheal challenges with the higher doses of PAO1, such as those used in our study (10^8), have normally resulted in neutrophilic pneumonia, bacteraemia and death within the first 24–48 hours in neonates [402, 404, 410]. The fact that all the mice survived suggests the bacteria were unable to produce sufficient virulence to harm the mice. Our mice were challenged with 10^8 CFU of PAO1 but 12 hours post infection only $\sim 10^3$ CFU were detected. It is plausible that the majority of the bacteria were cleared mechanically by the mice before any infection was initiated. Intranasal infections have generally displayed a lower effectiveness at delivering bacteria to the lungs than more invasive methods such intratracheal infection or a tracheotomy [414]. This raises the prospect that our delivery method for bacteria may need to be further developed to reduce

the mechanical clearance of the bacteria perhaps through application of smaller volume of, but multiple doses of bacterial suspensions.

The low bacterial loads in the mice poses some intriguing questions. Tang and colleagues were successfully able to establish an acute *Pseudomonas* infection in BALB/c neonates. Upon application of 1×10^5 CFU, 12/15 mice had increased CFU 24 hours post infection. By 96 hours, no bacteria remained in the lungs [402]. Morissette and colleagues infected a number of inbred mouse strains with low doses (10^4 CFU) of *P. aeruginosa* and found BALB/c to be resistant to infection based on both their mortality and bacterial load post infection [409]. This suggests that the BALB/c strain has high resistance to *P. aeruginosa* infection. The authors considered the C57BL/6 mouse strain to be of an intermediate phenotype while the DBA/2 strain was the most susceptible to infection. Tam and colleagues investigated the susceptibility of BALB/c and C57BL/6 mice to chronic *P. aeruginosa* and observed two thirds of their BALB/c mice cleared the infection by 28 days post inoculation [415]. However, almost 80% of the C57BL/6 mice had persistent infections. These differences have been attributed to the differing intrinsic inflammatory and immune response in the two strains, particularly the lower tumour necrosis factor-α gene expression and protein secretion [416, 417], increased nitric oxide production [417], and reduced proliferative responses from lung T cells [408]. Sapru and colleagues reported a considerably stronger immune response in C57BL/6 mice when compared to the BALB/c mice, with a higher count of polymorphonuclear cells in the bronchoalveolar lavage fluid and this correlated with increased susceptibility to infection [417]. An exaggerated inflammatory response may thus predispose the C57BL/6 mouse to infection and also more accurately mimic the CF disease pathophysiology. It is therefore possible that the strain of mouse selected for this study may have contributed to the inability to establish chronic high-level colonization of the lungs by *P. aeruginosa* and that this could be overcome by using an alternate mouse strain. It may also be still possible to use the current mouse strain but prime the immune system using microbial ligands such as LPS, flagellin [418, 419] or protein from pili [402] to stimulate the immune response. We could also adopt a strategy whereby we initially challenge the mice with an intermediate dose (10^6 CFU/mL) before re-challenging the mice with a higher dose (10^8) 24 hours later.

Given the low levels of bacteria persisting in the lungs in this study, the use of a PCR based method to quantify bacteria is validated. Numerous studies have investigated the suitability of real-time quantitative PCR to quantify bacterial load. Provided sensitive methods are used to detect the bacteria, such as quantifying high expression genes like 16S ribosomal

RNA, as in this study, bacteria can be reliably enumerated down to a single colony forming unit [276]. While there are studies that indicate that PCR may be less sensitive than conventional culture methods [420], most studies generally agree that PCR is as good as if not more sensitive than culture based methods for enumerating bacteria [276, 421-423]. The inability to detect the expression of QS and virulence genes explored in this study can most likely be attributed to the low levels of bacteria present in the mouse lungs.

A promising development in imaging technology has been the advent of *in vivo* imaging of mice infected with a GFP- or luciferase-tagged *P. aeruginosa.* This enables the real-time, sensitive monitoring of infection in mice without the need to use multiple groups to study multiple treatment conditions, thereby reducing inter-animal variations [424, 425]. There is the added advantage of the ability to monitor the progression of bacteria from the nares into the lower lung, and give a good indication of where the mice establish the infection.

Further studies will be required to develop a suitable intranasal murine model of *P. aeruginosa* infection. This study has provided some important insight into how this could be achievable. Such a model would have numerous advantages, particularly the ability to rapidly check the effectiveness of novel therapies such as rhPON2 and better understand the pathophysiology of chronic infection.

CHAPTER SEVEN – GENERAL DISCUSSION

7.1 INTRODUCTION

This thesis investigates human PON2 as a quorum sensing inhibitor of *P. aeruginosa*. The inhibition of QS is of particular interest because conventional antibiotic therapy is ineffective against chronic *P. aeruginosa* infections. The efficacy of these antibiotics might be rescued using a therapeutic approach that combines conventional antibiotic therapy with anti-virulence therapy. Anti-virulence therapies have the advantage of targeting the pathogenicity of bacteria in an infection setting without necessarily affecting viability. With attenuated virulence, the bacteria are unable to cause pathological infections, allowing the host immune response to respond effectively. In addition, because anti-virulence therapies do not affect microbial growth, the general consensus amongst researchers is that such therapies are less likely to exert selective pressures towards resistance development [426].

The C12HSL QS molecule is a potent signalling molecule produced by *P. aeruginosa* during infection. C12HSL induces the production of many bacterial host-damaging virulence factors and is involved in biofilm formation by this organism. C12HSL also has important roles in conditioning host cells for infection and even at low concentrations induces host-cell immune pathways, the unfolded-protein stress-responses, as well as intra-cellular calcium signalling. Consequently, C12HSL represents a potential target for novel anti-virulence therapies. The results described in thesis demonstrate the potential usefulness of human PON2 as an anti-Pseudomonal therapy, with the added advantage of abrogating the negative effects of QS signalling molecules on host-cells.

7.2 THE IMPORTANCE OF C12HSL-BASED QUORUM SENSING IN *P. AERUGINOSA* INFECTION IS NOT YET FULLY UNDERSTOOD

The combination of the high prevalence of *P. aeruginosa* lung infections in individuals with CF, together with the extensive associated lung damage have made *P. aeruginosa* the most widely studied CF-related pathogen. Yet, once *P. aeruginosa* infections become established in the CF lung it is virtually impossible to clear, and currently available eradication therapies have thus far proven to be ultimately unsuccessful [5, 140, 348]. These sustained *P. aeruginosa* infections are widely thought to stem from the ability of this pathogen to form biofilms. Cell-to-cell communication by QS is considered to be important in the formation of biofilms in addition to its role in the regulation of virulence factor production.

The most important QS molecule of *P. aeruginosa* is C12HSL whose synthesis is catalysed by the LasI protein, and whose signalling-effects are relayed through its cognate receptor LasR. There is however some debate about the importance of the role of the Las system in *P. aeruginosa* infections. Involvement of the QS circuitry in the regulation of biofilm formation, important for *P. aeruginosa* persistence, was originally reported by Davies and colleagues [152]. Mutations to *lasI* result in flat, undifferentiated biofilms compared to the complex structures formed by the wild-type. Importantly, the *lasI* mutant biofilms were more susceptible to a biocide than those of the wild type [152]. Subsequently, the Las system was implicated in an important role in the later stages of biofilm development and *lasI* mutants showed reduced *in vivo* virulence in mouse burn wound models of *P. aeruginosa* infection [427, 428]. In contrast, other studies observed no difference in biofilm formation and structure in *lasI* mutants [135, 429, 430]. These differences were attributed by some authors to variations in experimental conditions [431] but more detailed consideration is required. Despite using a strain in which both the inducer and receptors of both the top *P. aeruginosa* QS systems (i.e. *lasIRrhlIR* quadruple mutant) were knocked out, Lazenby and colleagues observed no difference between the mutant and wild type *P.* aeruginosa in immunogenicity, infectiveness or persistence of infection, in an acute mouse model of *P. aeruginosa* infection [362]. This, however, does not suggest that QS has no role in chronic infection, where a loss of QS can only confer an advantage to a minority sub-population of bacteria. In lung cell assays, O'Loughlin and colleagues observed that the *lasR, rhlR* double mutant was more virulent than wild type, possibly because of misregulation of virulence factors [237]. It is possible that QS alone is not a definitive determinant of *P. aeruginosa* pathogenesis and biofilm formation. Further investigation is required to define the role of

QS in both *in vitro* and *in vivo* biofilm development. However, it is unquestionable that QS is essential to the regulation of many virulence determinants of *P. aeruginosa* [136, 137]. Studies involving the inhibition rather than the knockout of the Las system have proved quite successful in attenuating *P. aeruginosa* virulence, pathogenicity and biofilm formation (Table 7.1).

Table 7.1 Table of evidence that QSI attenuates *P. aeruginosa* virulence, pathogenicity and biofilm formation

QS inhibitor	Description of QSI	Effect on *P. aeruginosa*	Reference
mBTL	LasR, RhlR inhibitor	Inhibits production of pyocyanin virulence factor in *in vitro biofilm formation* Protects human epithelial cells lines and nematodes from *P. aeruginosa*	[237]
Halogenated furanones	LasR inhibitor	Inhibit biofilm formation, protect mice against chronic infections	[232, 432]
5-imino-4,6-dihydro-3H-1,2,3-triazolo [5,4-d]pyrimidin-7-one (G1)	LasR inhibitor	Inhibits QS gene expression Inhibits biofilm formation by reducing extracellular DNA release (controlled by PQS system) Inhibits elastase production	[433]
P. aeruginosa acylase	Hydrolyse QS signal	Reduced virulence factor production, Reduced severity of infection in nematode model of *P. aeruginosa* infection	[353, 355] [240]
Bacterial lactonases	Hydrolyse QS signal	Reduced virulence factor production and biofilm production of UTI *P. aeruginosa* isolates, increased antibiotic sensitivity	[434, 435]
Anti-AHL antibodies	Sequester and instigate immune reaction to QS signal	Protect mice against chronic infections	[238, 239]

Importantly, QS AHL signals have been detected in CF sputum (in the pico- to nano-molar range) [157, 436] and lung tissue [437]. Thus, QS is relevant in clinical *P. aeruginosa* infections. However, the level of dependence on QS that *P. aeruginosa* has during chronic human lung infections, is still unclear. It is understood that QS plays an important role in the early stages of development of chronic infection [438]. However, QS mutants accumulate during chronic infection. In particular *lasR* mutations (able to produce C12HSL but unable to respond to it), accumulate in the colonizing bacteria, most likely as an adaptation to the specific nutrient conditions of the lung [439-441]. The occurrence of QS mutants can be explained by the concept of 'QS cheaters', the idea that some individuals in a bacterial population derive an advantage from bacterial cooperation in cell-to-cell communication without themselves participating in the metabolically expensive production of public goods [442]. The implication is that QS-inactive members of the biofilm communities avoid the cost of participating in cooperative behaviour and can therefore spread [443]. Over time, as chronic infections develop, the requirement for virulence production is reduced, allowing cheaters to become more prominent. The accumulation of QS mutants means that therapeutic QS inhibition (QSI) is likely to be more effective when administered prior to, or in the early stages of, establishment of chronic infections. More research into bacterial interactions during infection and the role of QS would be beneficial when developing clinical therapies that target QS.

7.3 BACTERIALLY PRODUCED C12HSL MODULATES GENE EXPRESSION IN HOST RESPIRATORY EPITHELIAL CELLS IN A CONCENTRATION-DEPENDENT MANNER

The effects of QS are not restricted to the bacteria alone. The primary *P. aeruginosa* QS signal molecule, C12HSL, is able to enter mammalian host cells during infection and modulate the host immune system and induce host cytotoxicity (covered in detail in Chapter 1, Section 1.2.6). As it is difficult to determine the precise concentrations of C12HSL that are present *in situ* during *P. aeruginosa* infection, studies into the effects of C12HSL have used a range of concentrations. Typically, the effects of C12HSL *in vitro* on host cells appear to be concentration-dependent. Concentrations of C12HSL above 20 μM are generally proinflammatory, while concentrations below 10 μM are considered to be anti-inflammatory. It has been suggested that AHL concentrations localized around biofilm cells are higher than those detected in clinical samples. On the other hand, away from the *P. aeruginosa* cells, the C12HSL concentration would be expected to be lower. The existence of an AHL concentration gradient is an important consideration when the effects of C12HSL on host cells are examined. Immediately adjacent to *P. aeruginosa* cell clusters, C12HSL could be proinflammatory and cause damage or death of the closely associated epithelia and immune cells. Away from the pockets of infection, the anti-inflammatory effect may hamper the recruitment of immune cells to the site of infection. Therefore, it is important to further develop our understanding of C12HSL-mediated effects on host cells.

The results described in this thesis support and augment the previous reports of concentration-dependent effects of C12HSL on host cells by demonstrating that low-concentration (10 μM) C12HSL affects airway epithelial cell gene expression differently to the gene modulation at higher concentrations (50 μM) of C12HSL. In particular, the effects on expression of genes involved in immune signalling, the unfolded protein response (UPR) and intra-cellular calcium signalling was significantly altered.

The results described in this thesis confirmed the ability of C12HSL to competitively interfere with the binding of ligands to PPARγ, a major regulator of inflammation. Therefore, the decreased immune signalling seen in response to 10 μM C12HSL is most likely to be PPARγ-dependent. PPARγ agonism/antagonism is known to modulate the expression of numerous genes in mammalian cells [444].

Gene expression analysis of two key UPR genes, *XBP1* and *ATF3*, indicated that endoplasmic reticulum stress was induced by the deregulation of the UPR with 10 μM C12HSL. This would cause accumulation of misfolded proteins in the host cell and subsequently result in cytotoxicity. However, when the apoptosis and the cytotoxic effects of C12HSL were investigated, the results indicated a concentration-dependent effect, with high concentrations (50 μM) but not low (10 μM) concentrations inducing apoptosis. On the basis of these results, and in the context of local C12HSL concentrations in the airway, cells close to the site of infection would undergo apoptosis whereas, cells more distal to the site of infection and therefore exposed to lower C12HSL concentrations, would show induction of the UPR but not undergo apoptosis. As a result there would be an accumulation of cells (including immune cells) distal from the infection site, whose function is compromised because of the build-up of misfolded proteins, thereby further compromising the recruitment of immune cells to the site of infection.

Finally the CFTR-dependent effects of C12HSL were investigated by comparing the cytotoxic and metabolic effects of C12HSL in a wild-type and CFTR-negative cell line, the later of which is thought to be defective in calcium signalling [351] but also to have impaired PPARγ function [224]. In addition, the effects of C12HSL on expression of immune, apoptosis and UPR genes in CFTR-negative cells was also investigated. Surprisingly, we found that CFTR-negative cell lines were more resistant to the harmful effects of C12HSL than wild-type cells. In the CF lung, it is thought that the UPR may be triggered by the ΔF508 mutation [445]. C12HSL produced by *P. aeruginosa* during infection can also trigger the UPR. The combined result of these factors in cells in the airway should be an exaggerated induction of the UPR and subsequent cytotoxicity. However, the results described in this thesis indicate that CFTR-negative cells appear to be protected from the cytotoxic effects of C12HSL. This can be explained by an observation of Bartoszewski and colleagues, who showed that UPR activation in airway epithelial cells overexpressing ΔF508 CFTR preceded reduced expression of endogenous wild-type CFTR [445]. This finding would suggest that the triggering of UPR by C12HSL in CFTR-negative cells reduces subsequent CFTR expression and thereby dampens any further CFTR-dependent C12HSL-mediated effects on the cell. The ΔF508 mutation is also thought to contribute to impaired function of PPARγ [224], which is also a mammalian receptor for C12HSL. Impaired PPARγ function in the CFTR-negative cells would also explain why the CFTR-negative cells are generally protected from C12HSL-mediated effects.

Intriguingly, changes in gene expression revealed that C12HSL influenced the wild-type and CFTR-negative cell line differently in regards to UPR and apoptosis genes but less so with the immune genes. We postulated that modulation of immune signalling and apoptosis may be distinct consequences of C12HSL, possibly through the C12HSL interacting with different cellular receptors. There are two identified mammalian C12HSL receptors, PPARγ (immune signalling) [214] and IQGAP (may influence calcium signalling) [354], However, more detailed understanding of the effects of C12HSL on mammalian cells is required before we can fully appreciate how C12HSL causes the reported and observed detrimental effects on mammalian cells.

7.4 THERAPUETIC USE OF PARAOXONASE 2 (PON2)

PON2 demonstrates lactonase activity towards multiple lactones, but it displays the highest activity towards AHL's, the family of lactones that includes the two most important *P. aeruginosa* QS signalling molecules C12HSL and C4HSL [248]. This specific ability of PON2 to hydrolyse AHL's *in vitro*, along with the fact that its expression is widely conserved amongst mammals [352], have lead many researchers to speculate that PON2 may be a component of the mammalian innate immune response towards *P. aeruginosa* and other Gram-negative AHL-producing pathogens. A recent study shows that PON2, an intracellular, membrane-bound protein, rapidly causes C12HSL hydrolysis in airway epithelial cells and the researchers proposed a central regulatory role for PON2 against host cell C12HSL-mediated effects [267]. Previous studies have shown that PON2 plays a role in protecting against *P. aeruginosa* infections. Horke and colleagues observed that PON2 attenuates ROS production induced by the *P. aeruginosa* virulence factor pyocyanin [265], while importantly, Devarajan and colleagues observed significantly impaired clearance of *P. aeruginosa* from the lungs of PON2-deficient mice [249]. These findings are suggestive that PON2 has potential as anti-Pseudomonal therapy.

7.4.1 Up-regulation of endogenous PON2 could protect host cells from C12HSL-mediated effects

Increasing endogenous PON2 expression could protect host cells from C12HSL-mediated effects by hydrolysing intracellular (host cell) C12HSL. The work presented in this thesis demonstrates, for the first time, that endogenous PON2 expression can be up-regulated in respiratory epithelial cells by agonism of PPARγ. Fortunately, the PPARγ agonist used in the study is already approved for pharmaceutical use as an anti-inflammatory drug and could relatively easily be used in a CF clinical setting.

Furthermore, preliminary data from our laboratory demonstrates that lactonolysis of C12HSL can abolish the C12HSL-dependent cytotoxic and immune modulatory effects in human cells (unpublished data). This therapy however, would not protect host cells against the accumulation of C12HSL acid in cell organelles which was recently demonstrated to exert pH-dependent effects [267]. The authors of the study noted a PON2-dependent

hydrolysis of C12HSL in airway epithelial cell organelles. However, the resultant accumulation of C12HSL acid in the organelles caused acidification of the cytosol, an associated release of Ca^{2+} into the cytosol and an increase in a marker of cellular stress. Therefore, it remains to be elucidated for host cells how effective the hydrolysis of C12HSL will be in reducing C12HSL-mediated cytotoxic and immune modulatory effects.

Importantly, the protective roles of PON2 are not solely restricted to lactonolysis of C12HSL. PON2 has anti-oxidative activity independent of its lactonase activity [273]. Such anti-oxidant activity is likely to dampen the oxidative stress associated with hyperinflammatory environments, providing to the host cells an added layer of protection from *P. aeruginosa* infection. CFTR mutations in CF contributes to increased intracellular oxidative stress [446]. The anti-oxidant activity of PON2 could thus also help to reduce the oxidative-stress burden in the CF lung. Protection of host cell from the effects of *P. aeruginosa* infection would mean that, the host immune response is better able to respond to the infection.

Pharmaceutically increasing endogenous PON2 would benefit all host cells exposed to C12HSL during *P. aeruginosa* infection, because of the ubiquitous nature of PON2 expression in humans. There have been reports of increased PON2 mRNA and protein in murine macrophages in response to agonism of the C12HSL receptor PPARγ [268]. We used a potent synthetic PPARγ agonist in an airway epithelial cell line and PPARγ agonism, resulted in an almost immediate increased PON2 mRNA and protein. The swiftness of the increase in PON2 in response to PPARγ agonism, together with the fact that PPARγ is a well-described transcription factor regulating the immune system, lead us to hypothesize that PPARγ may be transcriptionally regulating PON2 expression. Our hypothesis was further strengthened by the identification of putative PPAR response elements in the human PON2 promoter through *in silico* analysis. We therefore investigated, using functional promoter assays, whether PPARγ transcriptionally regulates *PON2* expression. However, the results indicate that the region of the human PON2 promoter studied does not appear to be involved in PPARγ-dependent PON2 gene expression. Therefore either PPARγ agonist-mediated up-regulation of PON2 operates via a PPARγ-independent mechanism or our reporter construct did not fully encapsulate all the regulatory elements required for PPARγ-mediated *PON2* transcription. It is not uncommon for regulatory elements such as enhancers to be widely dispersed and thus making it difficult to capture in a single reporter construct [359]. Further study is required into other factors that may be involved in PON2 regulation including the regulatory elements involved in its PPARγ-dependent expression. Most importantly though, we were able to identify a mechanism through which PON2

expression could be regulated, i.e. through PPARγ agonism. An added advantage of PPARγ agonists may be alleviation of the hyperinflammatory state of the CF lungs because decreased PPARγ activity in the CF lung is thought to contribute to the chronic hyperinflammatory state.

7.4.2 Treatment with extracellular rhPON2 could protect host cells from C12HSL-mediated effects and prevent bacterial QS and virulence

There are no reports of PON2 being secreted from mammalian cells. Through the use of PON2 siRNA inhibition and overexpression, investigators have determined that lysates of human epithelial cells and murine macrophages can hydrolyse C12HSL [249, 262, 264]. However, intact cells were not able to do so, suggesting that the PON2-mediated hydrolysis of C12HSL is restricted to the intra-cellular environment [264]. Therefore, the efficacy of pharmaceutically boosting endogenous intracellular PON2 would be limited by the amount of C12HSL that enters cells, and is unlikely to significantly affect the extracellular concentration of C12HSL that is critical to QS. As a result, such a therapy would offer no protection against *P. aeruginosa* QS and virulence. In addition, intracellular PON2-mediated hydrolysis of C12HSL would result in accumulation of C12HSL acid in the organelles, causing pH-mediated effects in the cells. Application of extracellular rhPON2 as a therapeutic approach would instead have the benefit of hydrolysing C12HSL in the bacterial environment, working as a QSI and preventing autoinduction of bacterial C12HSL synthesis. With reduced C12HSL in the bacterial environment, less C12HSL would enter host cells, reducing C12HSL-mediated effects on host cells and the excess accumulation of hydrolysed C12HSL inside the host cell. By combining the effects of extracellular rhPON2 and increased endogenous native PON2 (Figure 7.1), we could address both prevention of bacterial QS and virulence and protect against host cell modulation. Such a therapy could be prescribed as a prophylactic to CF patients to target *P. aeruginosa* before the pathogen has a chance to establish chronic infections.

This study demonstrated for the first time that rhPON2-mediated prevention of C12HSL accumulation during *P. aeruginosa* growth in culture was combined with a trend towards reduced expression of QS-associated virulence genes without affecting bacterial growth. Because rhPON2 is reported to also have high specific activity towards C4HSL [248], then presumably C4HSL is also prevented from accumulating during P. aeruginosa growth, and

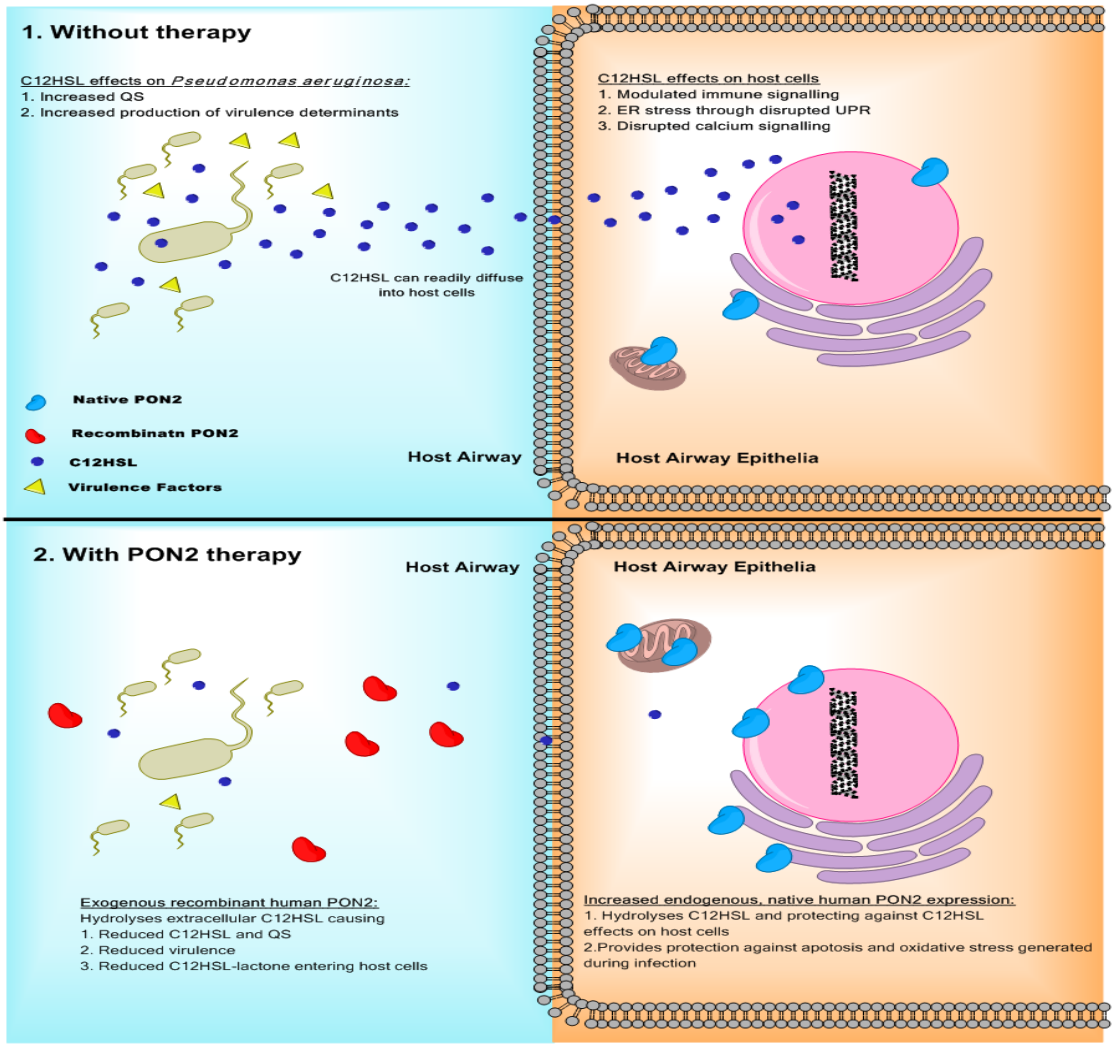

Figure 7.1 The potential of PON2 as a novel anti-Pseudomonal therapy. 1) *P. aeruginosa*, in the airways of infected hosts, utilizes QS to co-ordinate cell-density-dependent virulence factor production. Diffusible signalling molecules, the most important of which is C12HSL, mediate QS.. These virulence factors help to sustain bacterial infection and in the process, harm host cells, particularly the host epithelia but also macrophages, neutrophils, fibroblasts and the endothelial cells of capillaries closely associated with lung tissue. In addition, the QS molecule C12HSL is able to enter these cells through passive diffusion. Once inside, C12HSL has multiple negative effects on the cell, particularly modulated immune signalling and cytotoxicity. 2) The proposed PON2 therapy would address both the extracellular and intracellular consequences of C12HSL. In the extracellular environment through the use of recombinant human PON2 (rhPON2) and intracellularly through the increased expression of native PON2. In the extracellular environment, i.e. the host airway, recombinant human PON2 can hydrolyse C12HSL, preventing accumulation of the signal. Consequently, there would be reduced QS and subsequent attenuation of QS-mediated virulence determinants. The hydrolysis of C12HSL would also decrease the accumulation of C12HSL in the extracellular environment, substantially reducing the amount of C12HSL passively diffusing into host cells. In the intracellular environment, including host airway epithelia, increased native PON2 expression would offer protection against the detrimental effects of C12HSL. The hydrolysis of endogenous QS signal by PON2 and abrogation of the effects of C12HSL through its lactonase activity-independent anti-apoptotic and anti-oxidative properties contribute to the effectiveness of increased endogenous, native PON2.

although we did not specifically measure C4HSL levels, expression of C4HSL-mediated genes also tended to decrease with rhPON2 treatment. Importantly, in addition to quenching QS, rhPON2 therapy significantly increased the susceptibility to tobramycin of actively proliferating *P. aeruginosa* in a dose-dependent manner. Cells surviving tobramycin treatment alone and combined tobramycin and rhPON2 treatment had significantly increased expression of QS-associated genes, presumably as a stress response. The expression of QS-dependent virulence genes, in the absence of C12HSL was unexpected, because the expression of C12HSL's cognate receptor, the LasR transcription factor, was virtually undetectable in cultures, therefore the stress response is presumably co-ordinated independently of LasR. This would also explain the observation by O'Loughlin and colleagues that in lung cell assays the *lasR, rhlR* double mutant was more virulent than wild type [237]. Of note, is that bacterial intracellular levels of C12HSL were not measured in our study and as rhPON2 cannot enter the bacterial cells, intracellular C12HSL would be unaffected by rhPON2. Intracellular C12HSL could potentially bind to its cognate receptor LasR causing regulation of the operon in a mechanism that does not involve community-wide coordination. It is therefore important in future studies to determine the intracellular (bacterial) levels of C12HSL and to elucidate LasIR-independent virulence mechanisms.

The level of tobramycin used in these experiments was well above the levels that are clinically achievable, so artificial over-activation of stress response pathways may have occurred. If rhPON2 and tobramycin are to be used as an anti-Pseudomonal therapy, another avenue for further investigation is the use of a more clinically-relevant tobramycin concentration. In this study, tobramycin was used at a concentration of 10 μg/mL. The MIC50 (minimum inhibitory concentration that inhibits 50% of *P. aeruginosa*) of tobramycin for *P. aeruginosa* in CF sputum was determined to be 2 μg/mL although this value may vary between different strains of *P. aeruginosa* [447] while the clinically achievable dose of tobramycin in the epithelial lining fluid of the CF lung is estimated to be between 75 and 90 μg/mL under standard CF dosing conditions [448]. While this concentration may be much higher than 10 μg/mL used in this study, only a small proportion of the tobramycin dose is bioavailable in the CF lung [449, 450]. In addition, long-term serum tobramycin concentrations of >4 μg/mL may be nephrotoxic and ototoxic [451]. Furthermore, 10 μg/mL tobramycin treatment of PAO1 cultures prior to the cultures reaching exponential growth resulted in complete killing of the bacteria and thus no rhPON2-dependent effects could be studied. Therefore, it would be informative if the treatment of PAO1 with rhPON2 combined with tobramycin was carried out with sub-

inhibitory concentrations of tobramycin, perhaps a concentration that is more relevant to that seen in the CF lung and even in conjunction with a second antibiotic. It is also essential that these experiments are repeated using clinically achievable levels of tobramycin and other relevant antibiotics, such as azithromycin. In addition, in this study rhPON2 was applied only once to bacterial cultures and was able to increase antibiotic susceptibility but did not eliminate the bacteria. However, in the therapeutic context, rhPON2 would be applied at regular intervals, perhaps even daily. It is likely that sustained treatment of rhPON2 may be more effective at completely clearing the infection than the application of a single dose.

7.4.3 Regulation of QS and virulence *in vivo* may differ to regulation of QS and virulence *in vitro*

The experiments in this study using rhPON2 to treat *P. aeruginosa* were carried out in nutrient-rich medium. However, the CF lung is known to be deficient in nutrients and inorganic ions such as iron [452]. Nutrient limitations may greatly affect how QS is regulated, and therefore, need to be investigated further. Furthermore, *P. aeruginosa* is often found in the CF lung growing in hypoxic niches [379]. As a consequence, the ability of rhPON2 to prevent QS and QS-associated virulence in anaerobically growing *P. aeruginosa* also requires further investigation.

Other studies with QS-inhibitors and QS knockout bacteria have shown that QSI typically results in inferior biofilms, that are easier to target with antibiotics [152, 273, 434, 435]. It is vital that future studies establish the ability of rhPON2 to interfere with biofilm formation both *in vitro* using defined media and artificial sputum and *in vivo* during both acute and chronic lung infection.

7.4.4 Therapeutic advantages of rhPON2 as an anti-Pseudomonal

There are a number of advantages of using PON2 as an anti-Pseudomonal therapy that were demonstrated by this study, as well as a number of perceived advantages:

i) rhPON2 caused prevention of accumulation of the major *P. aeruginosa* QS signal C12HSL and associated C12HSL-mediated virulence expression and should prevent robust biofilm formation;
ii) rhPON2 increased *P. aeruginosa* susceptibility to antibiotics;
iii) rhPON2 therapy by itself does not affect bacterial growth, and consequently there would be little selection pressure driving the development of resistance;
    a. rhPON2 is not internalised into bacterial cells, so efflux pumps could not contribute to resistance development;
    b. because rhPON2 does not interact with bacterial receptor proteins, mutations of bacterial receptors will not provide a resistance mechanism;
iv) a recombinant human enzyme is unlikely to elicit an immune response that would interfere with its function;
v) rhPON2 would prevent the proinflammatory effects of C12HSL on mammalian cells, decreasing host inflammatory cell-mediated lung damage

This type of therapy would add a new type of weapon to the arsenal of antimicrobials (whether antibiotics, anti-inflammatories, or other QS inhibitors) that could be used in combination to fight infectious disease.

7.4.5 Delivery of rhPON2

To efficiently deliver the rhPON2 to the airways, the recombinant protein will need to be nebulized or inhaled as a dry powder. CF patients are already subjected to inhaled antibiotics and recombinant protein therapy, for example Tobramycin and Dornase alfa respectively [5]. Dornase alfa is a licensed recombinant human DNase whose primary target is the high levels of neutrophil-derived DNA in the CF sputum to reduce sputum viscosity. Dornase alfa can also target the extracellular matrix surrounding the *P. aeruginosa* biofilms and the use of Dornase Alfa establishes a precedent for the delivery of a therapeutic recombinant human protein directly into the airways.

There are three important factors that would need to be considered during formulation of the rhPON2 for application to the lung (nebulized or in powdered form):

i) Accounting for the Ca^{2+}-dependence of rhPON2 lactonase activity. Dornase alfa stability is also dependent on calcium concentration [453]. The calcium composition of sputum is estimated to be ~3 mM [454], a concentration conducive to PON2 lactonase activity [262] and Dornase alfa stability [453]. However, Dornase alfa is still delivered to the airways with 0.15 mg/mL calcium chloride [455] to ensure stability. Requirement of supplementation of calcium will therefore need to be established when investigating the delivery of rhPON2 as a therapy.

ii) rhPON2 stability and activity in the lung environment. Our study found minimum detectable C12HSL 24 hours post-treatment in bacterial culture supernatants known to contain proteases, suggesting that rhPON2 is stable in this environment. Were there to be problems with rhPON2 stability, molecular dynamics simulations of PON2 structure may identify flexible regions that can be targeted for engineering to enhance stability and activity.

iii) Minimizing droplet particle size during nebulization, to efficiently deliver the rhPON2 peripherally to small airways.

All of these considerations can be investigated using *in vivo* infection models.

7.4.6 Testing rhPON2 therapy *in vivo* using animal models of infection

To date, there are no animal models that completely mimic the chronic *P. aeruginosa* infections in human CF [388] and the best representations of human CF disease are seen in transgenic *CFTR*-knockout pigs [386]. The *CFTR*-knockout pigs, unlike humans, do not spontaneously acquire *P. aeruginosa* lung infections, are expensive to house and time-consuming to rear and thus their use is restricted to specialized labs. For this reason, murine models feature prominently in the literature, because of their ease of use, availability and the increasing number of available transgenic variants. To allow the study of the effects of rhPON2 in an *in vivo* setting, this study demonstrated for the first time the development of sustained *P. aeruginosa* infection (>12 days post infection) in mice without installation of *P. aeruginosa* in agar or extracellular material mimicking a biofilm, but using

an intranasal challenge, a method similar to the one developed by Diavatopoulos and colleagues for investigating *S. aureus* infection [413]. Unlike the Diavatopoulos study, the method described in this thesis did not incorporate priming the murine host for *P. aeruginosa* infection by pre-infecting with human influenza virus. However the infections established were low-level (< 10^3 CFU detected) and priming the immune system may increase bacterial carriage. The intranasal challenge model of sustained *P. aeruginosa* infection has the advantages of ease of infection of the animal without the need for intubation, sedatives or a tracheotomy, cost-effectiveness and most importantly, the use of neonatal mice with an underdeveloped immune system that more closely represents the compromised immune function of the CF lung than do adult mice, increasing the likelihood of the development of a chronic infection.

Using *in vivo* models of chronic *P. aeruginosa* infection the efficacious dose of rhPON2,the ideal intervals of treatment and the best combinations of antibiotics that will maximise the therapeutic potential of rhPON2 can be elucidated. Additionally, using both acute and chronic infection models will help determine the effectiveness of rhPON2 in prevention and eradication of *P. aeruginosa* infections, respectively. Study of acute infection models will help elucidate the ability of rhPON2 to prevent the initial establishment of infections, while the study of chronic infection models will help determine whether rhPON2 can be successfully used to eradicate already-established *P. aeruginosa* infection.

7.5 FUTURE PROSPECTS

CF lung infections are polymicrobial and include a number of other Gram-negative pathogens that utilize AHLs for QS. This provides an opportunity to potentially extend beyond *P. aeruginosa,* the use of inhibition of QS by rhPON2. Bacteria belonging to the *Burkholderia cepacia* complex utilize AHLs (predominantly C8HSL) in a QS system homologous to that observed in *P. aeruginosa* [456, 457], while the emerging CF pathogen *Pandoraea pnomenusa* is also reported to utilise an AHL to regulate QS [458].

P. aeruginosa is a major opportunistic human pathogen and a significant source of bacteraemia. Its ability to cause infections is not restricted to people with CF. In the US, it is among the most common nosocomial pathogens and the second most frequently isolated pathogen from patients with ventilator-associated pneumonia [92]. Infections with *P. aeruginosa* are also commonly associated with burns [459], microbial keratitis in contact lens wearers [459], urinary tract infections in catheterized patients [459] and pulmonary infections in chronic obstructive pulmonary disease [460], HIV infections [461] and immunocompromised individuals such as patients on chemotherapy [462] and immunosuppressive drugs [459]. rhPON2 therapy may aid in the control of these infections. For pulmonary infections, nebulized rhPON2 therapy could be applied. For other infections, the method of delivery of rhPON2 may need to be adjusted: for example, in burns, topical application of rhPON2 in cream may be the most appropriate method of delivery.

PON2 needs much more research before it can be established as an anti-virulence therapy. However, there are multiple advantages of the therapy over other proposed anti-virulence therapies and in this light, PON2 warrants further attention and development.

7.6 CONCLUDING REMARKS

The work described in this thesis sheds new light on the potential of using the mammalian enzyme PON2 as a novel anti-Pseudomonal therapy. By investigating the effects of C12HSL on the airway, we confirmed and augmented established research on the effects that C12HSL has on infected host cells, thus allowing us to understand better the C12HSL-mediated modulation of host cell gene expression. Through further investigation of the regulation of human PON2 expression, this study was able to determine a mechanism through which endogenous, intracellular PON2 expression could be increased. This finding enabled us to suggest a mechanism by which the cells of *P. aeruginosa*-infected host could be protected from the detrimental effects of C12HSL. Using rhPON2 produced in this study, *in situ* lactonolysis of C12HSL by rhPON2 in actively growing *P. aeruginosa* cultures was demonstrated. This allowed us to investigate the effects that the unavailability of C12HSL in the bacterial cell environment has on QS by the bacteria, showing that the absence of C12HSL may attenuate *P. aeruginosa* pathogenicity. By treating bacteria with a combination of rhPON2 and a CF-relevant antibiotic, we were able to demonstrate a rhPON2-dose-dependent increase in *P. aeruginosa* antibiotic susceptibility. These findings strengthened the notion that rhPON2 can be effective when applied extracellularly as a recombinant protein. Finally, we described a novel mouse model, which, after further development, may be a useful tool for *in vivo* studies to further investigate PON2 as a therapy.

Taken together, the results suggest that treatment with PON2, in both its recombinant and native forms, offers substantial protection from *P. aeruginosa* by hydrolysing *P. aeruginosa*-produced AHL signals and decreasing C12HSL-mediated effects on host cells. Therefore, the work described in this thesis strongly indicates that PON2 should be further investigated as novel anti-Pseudomonal therapy.

REFERENCES

1. O'Sullivan, B.P. and S.D. Freedman, *Cystic fibrosis.* Lancet, 2009. **373**(9678): p. 1891-904.
2. Farrell, P., et al., *Diagnosis of cystic fibrosis in the Republic of Ireland: epidemiology and costs.* Ir Med J, 2007. **100**(8): p. 557-60.
3. Farrell, P.M., *The prevalence of cystic fibrosis in the European Union.* J Cyst Fibros, 2008. **7**(5): p. 450-3.
4. Bradbury, R., A. Champion, and D.W. Reid, *Poor clinical outcomes associated with a multi-drug resistant clonal strain of Pseudomonas aeruginosa in the Tasmanian cystic fibrosis population.* Respirology, 2008. **13**(6): p. 886-92.
5. Anon, *Patient Registry Annual Data Report, Cystic Fibrosis Foundation*. 2012.
6. Dodge, J.A., et al., *Cystic fibrosis mortality and survival in the UK: 1947-2003.* Eur Respir J, 2007. **29**(3): p. 522-6.
7. Dupuis, A., et al., *Cystic fibrosis birth rates in Canada: a decreasing trend since the onset of genetic testing.* J Pediatr, 2005. **147**(3): p. 312-5.
8. Yamashiro, Y., et al., *The estimated incidence of cystic fibrosis in Japan.* J Pediatr Gastroenterol Nutr, 1997. **24**(5): p. 544-7.
9. Lannefors, L. and A. Lindgren, *Demographic transition of the Swedish cystic fibrosis community--results of modern care.* Respir Med, 2002. **96**(9): p. 681-5.
10. Klaassen, T., et al., *Neonatal screening for the cystic fibrosis main mutation delta F508 in Estonia.* J Med Screen, 1998. **5**(1): p. 16-9.
11. Lucotte, G., S. Hazout, and M. De Braekeleer, *Complete map of cystic fibrosis mutation DF508 frequencies in Western Europe and correlation between mutation frequencies and incidence of disease.* Hum Biol, 1995. **67**(5): p. 797-803.
12. Bossi, A., et al., *What is the incidence of cystic fibrosis in Italy? Data from the National Registry (1988-2001).* Hum Biol, 2004. **76**(3): p. 455-67.
13. Nazer, H., et al., *Cystic fibrosis in Saudi Arabia.* Eur J Pediatr, 1989. **148**(4): p. 330-2.
14. Cruz-Coke, R. and R.S. Moreno, *Genetic epidemiology of single gene defects in Chile.* J Med Genet, 1994. **31**(9): p. 702-6.
15. Cabello, G.M., et al., *Cystic fibrosis: low frequency of DF508 mutation in 2 population samples from Rio de Janeiro, Brazil.* Hum Biol, 1999. **71**(2): p. 189-96.
16. Orozco, L., et al., *Frequency of delta F508 in a Mexican sample of cystic fibrosis patients.* J Med Genet, 1993. **30**(6): p. 501-2.
17. Padoa, C., et al., *Cystic fibrosis carrier frequencies in populations of African origin.* J Med Genet, 1999. **36**(1): p. 41-4.
18. Hurley, M.N., et al., *Rate of improvement of CF life expectancy exceeds that of general population--observational death registration study.* J Cyst Fibros, 2014. **13**(4): p. 410-5.
19. Emerson, J., et al., *Pseudomonas aeruginosa and other predictors of mortality and morbidity in young children with cystic fibrosis.* Pediatr Pulmonol, 2002. **34**(2): p. 91-100.
20. Langton Hewer, S.C. and A.R. Smyth, *Antibiotic strategies for eradicating Pseudomonas aeruginosa in people with cystic fibrosis.* Cochrane Database Syst Rev, 2014. **11**: p. CD004197.
21. Schelstraete, P., et al., *Eradication therapy for Pseudomonas aeruginosa colonization episodes in cystic fibrosis patients not chronically colonized by P. aeruginosa.* J Cyst Fibros, 2013. **12**(1): p. 1-8.
22. CFTR.info. *CFTR Stucture and Regulation*. 2015 17/04/2015]; Available from: http://www.cftr.info/home/about-this-website/.
23. Stutts, M.J., et al., *CFTR as a cAMP-dependent regulator of sodium channels.* Science, 1995. **269**(5225): p. 847-50.

24. Schwiebert, E.M., et al., *CFTR regulates outwardly rectifying chloride channels through an autocrine mechanism involving ATP.* Cell, 1995. **81**(7): p. 1063-73.
25. Reisin, I.L., et al., *The cystic fibrosis transmembrane conductance regulator is a dual ATP and chloride channel.* J Biol Chem, 1994. **269**(32): p. 20584-91.
26. Quinton, P.M., *Cystic fibrosis: impaired bicarbonate secretion and mucoviscidosis.* Lancet, 2008. **372**(9636): p. 415-7.
27. Rommens, J.M., et al., *Identification of the cystic fibrosis gene: chromosome walking and jumping.* Science, 1989. **245**(4922): p. 1059-65.
28. Rogan, M.P., D.A. Stoltz, and D.B. Hornick, *Cystic fibrosis transmembrane conductance regulator intracellular processing, trafficking, and opportunities for mutation-specific treatment.* Chest, 2011. **139**(6): p. 1480-90.
29. *Clinical and Functional Translation of CFTR*. 2014 07/05/14]; Available from: http://www.cftr2.org/progress.php.
30. Clancy, J.P. and M. Jain, *Personalized medicine in cystic fibrosis: dawning of a new era.* Am J Respir Crit Care Med, 2012. **186**(7): p. 593-7.
31. Bobadilla, J.L., et al., *Cystic fibrosis: a worldwide analysis of CFTR mutations--correlation with incidence data and application to screening.* Hum Mutat, 2002. **19**(6): p. 575-606.
32. Lao, O., et al., *Spatial patterns of cystic fibrosis mutation spectra in European populations.* Eur J Hum Genet, 2003. **11**(5): p. 385-94.
33. Rowe, S.M., S. Miller, and E.J. Sorscher, *Cystic fibrosis.* N Engl J Med, 2005. **352**(19): p. 1992-2001.
34. Gibson, L.E. and R.E. Cooke, *A test for concentration of electrolytes in sweat in cystic fibrosis of the pancreas utilizing pilocarpine by iontophoresis.* Pediatrics, 1959. **23**(3): p. 545-9.
35. Mishra, A., R. Greaves, and J. Massie, *The relevance of sweat testing for the diagnosis of cystic fibrosis in the genomic era.* Clin Biochem Rev, 2005. **26**(4): p. 135-53.
36. Khan, T.Z., et al., *Early pulmonary inflammation in infants with cystic fibrosis.* Am J Respir Crit Care Med, 1995. **151**(4): p. 1075-82.
37. Rowntree, R.K. and A. Harris, *The phenotypic consequences of CFTR mutations.* Ann Hum Genet, 2003. **67**(Pt 5): p. 471-85.
38. Cheng, S.H., et al., *Defective intracellular transport and processing of CFTR is the molecular basis of most cystic fibrosis.* Cell, 1990. **63**(4): p. 827-34.
39. McKone, E.F., et al., *Effect of genotype on phenotype and mortality in cystic fibrosis: a retrospective cohort study.* Lancet, 2003. **361**(9370): p. 1671-6.
40. Haardt, M., et al., *C-terminal truncations destabilize the cystic fibrosis transmembrane conductance regulator without impairing its biogenesis. A novel class of mutation.* J Biol Chem, 1999. **274**(31): p. 21873-7.
41. Derichs, N., *Targeting a genetic defect: cystic fibrosis transmembrane conductance regulator modulators in cystic fibrosis.* Eur Respir Rev, 2013. **22**(127): p. 58-65.
42. Mall, M., et al., *Increased airway epithelial Na+ absorption produces cystic fibrosis-like lung disease in mice.* Nat Med, 2004. **10**(5): p. 487-93.
43. Smith, J.J., et al., *Cystic fibrosis airway epithelia fail to kill bacteria because of abnormal airway surface fluid.* Cell, 1996. **85**(2): p. 229-36.
44. Boucher, R.C., *Airway surface dehydration in cystic fibrosis: pathogenesis and therapy.* Annu Rev Med, 2007. **58**: p. 157-70.
45. Goldman, M.J., et al., *Human beta-defensin-1 is a salt-sensitive antibiotic in lung that is inactivated in cystic fibrosis.* Cell, 1997. **88**(4): p. 553-60.
46. Zabner, J., et al., *Loss of CFTR chloride channels alters salt absorption by cystic fibrosis airway epithelia in vitro.* Mol Cell, 1998. **2**(3): p. 397-403.
47. Wilschanski, M. and P.R. Durie, *Patterns of GI disease in adulthood associated with mutations in the CFTR gene.* Gut, 2007. **56**(8): p. 1153-63.

48. Radpour, R., et al., *Genetic investigations of CFTR mutations in congenital absence of vas deferens, uterus, and vagina as a cause of infertility.* J Androl, 2008. **29**(5): p. 506-13.
49. Chan, H.C., et al., *The cystic fibrosis transmembrane conductance regulator in reproductive health and disease.* J Physiol, 2009. **587**(Pt 10): p. 2187-95.
50. Anderson, D.H., *CYSTIC FIBROSIS OF THE PANCREAS AND ITS RELATION TO CELIAC DISEASE.* Am J Dis Child, 1938. **2**(56): p. 344-399.
51. Riordan, J.R., et al., *Identification of the cystic fibrosis gene: cloning and characterization of complementary DNA.* Science, 1989. **245**(4922): p. 1066-73.
52. Lubsch, L., *Advances in the Management of Cystic Fibrosis.* US Pharmacist, 2007. **32**(7): p. HS-5-HS-16.
53. Corey, M., et al., *A comparison of survival, growth, and pulmonary function in patients with cystic fibrosis in Boston and Toronto.* J Clin Epidemiol, 1988. **41**(6): p. 583-91.
54. Peterson, M.L., D.R. Jacobs, Jr., and C.E. Milla, *Longitudinal changes in growth parameters are correlated with changes in pulmonary function in children with cystic fibrosis.* Pediatrics, 2003. **112**(3 Pt 1): p. 588-92.
55. Ratjen, F., *Restoring airway surface liquid in cystic fibrosis.* N Engl J Med, 2006. **354**(3): p. 291-3.
56. Braun, A.T. and C.A. Merlo, *Cystic fibrosis lung transplantation.* Curr Opin Pulm Med, 2011. **17**(6): p. 467-72.
57. Clancy, J.P., et al., *Evidence that systemic gentamicin suppresses premature stop mutations in patients with cystic fibrosis.* Am J Respir Crit Care Med, 2001. **163**(7): p. 1683-92.
58. Howard, M., R.A. Frizzell, and D.M. Bedwell, *Aminoglycoside antibiotics restore CFTR function by overcoming premature stop mutations.* Nat Med, 1996. **2**(4): p. 467-9.
59. Du, M., et al., *PTC124 is an orally bioavailable compound that promotes suppression of the human CFTR-G542X nonsense allele in a CF mouse model.* Proc Natl Acad Sci U S A, 2008. **105**(6): p. 2064-9.
60. Kerem, E., et al., *Effectiveness of PTC124 treatment of cystic fibrosis caused by nonsense mutations: a prospective phase II trial.* Lancet, 2008. **372**(9640): p. 719-27.
61. Wilschanski, M., et al., *Chronic ataluren (PTC124) treatment of nonsense mutation cystic fibrosis.* Eur Respir J, 2011. **38**(1): p. 59-69.
62. PTCTherapeutics. *Ataluren (PTC124) Clinical Trials*. 2014 13/05/14]; Available from: http://www.ptcbio.com/clinical_trials_ataluren.
63. Flume, P.A., et al., *Ivacaftor in subjects with cystic fibrosis who are homozygous for the F508del-CFTR mutation.* Chest, 2012. **142**(3): p. 718-24.
64. Ramsey, B.W., et al., *A CFTR potentiator in patients with cystic fibrosis and the G551D mutation.* N Engl J Med, 2011. **365**(18): p. 1663-72.
65. DepartmentofHealth. *Access to Kalydeco through the Pharmaceutical Benefits Scheme*. 2014 [cited 2015; Available from: http://www.health.gov.au/internet/main/publishing.nsf/Content/MC14-000305-pharmaceutical-benefits-scheme-listing-of-kalydeco.
66. Van Goor, F., et al., *Correction of the F508del-CFTR protein processing defect in vitro by the investigational drug VX-809.* Proc Natl Acad Sci U S A, 2011. **108**(46): p. 18843-8.
67. Clancy, J.P., et al., *Results of a phase IIa study of VX-809, an investigational CFTR corrector compound, in subjects with cystic fibrosis homozygous for the F508del-CFTR mutation.* Thorax, 2012. **67**(1): p. 12-8.
68. Wilschanski, M., *Novel therapeutic approaches for cystic fibrosis.* Discov Med, 2013. **15**(81): p. 127-33.
69. Grasemann, H., et al., *Inhalation of Moli1901 in patients with cystic fibrosis.* Chest, 2007. **131**(5): p. 1461-6.

70. Ratjen, F., et al., *Long term effects of denufosol tetrasodium in patients with cystic fibrosis.* J Cyst Fibros, 2012. **11**(6): p. 539-49.
71. Bonfield, T.L., M.W. Konstan, and M. Berger, *Altered respiratory epithelial cell cytokine production in cystic fibrosis.* J Allergy Clin Immunol, 1999. **104**(1): p. 72-8.
72. Gaggar, A., et al., *Matrix metalloprotease-9 dysregulation in lower airway secretions of cystic fibrosis patients.* Am J Physiol Lung Cell Mol Physiol, 2007. **293**(1): p. L96-L104.
73. Kettle, A.J., et al., *Myeloperoxidase and protein oxidation in the airways of young children with cystic fibrosis.* Am J Respir Crit Care Med, 2004. **170**(12): p. 1317-23.
74. Cohen-Cymberknoh, M., et al., *Airway inflammation in cystic fibrosis: molecular mechanisms and clinical implications.* Thorax, 2013. **68**(12): p. 1157-62.
75. Elizur, A., C.L. Cannon, and T.W. Ferkol, *Airway inflammation in cystic fibrosis.* Chest, 2008. **133**(2): p. 489-95.
76. Chroneos, Z.C., Z. Sever-Chroneos, and V.L. Shepherd, *Pulmonary surfactant: an immunological perspective.* Cell Physiol Biochem, 2010. **25**(1): p. 13-26.
77. LaFemina, M.J., et al., *Claudin-18 deficiency results in alveolar barrier dysfunction and impaired alveologenesis in mice.* Am J Respir Cell Mol Biol, 2014. **51**(4): p. 550-8.
78. Whitsett, J.A. and T. Alenghat, *Respiratory epithelial cells orchestrate pulmonary innate immunity.* Nat Immunol, 2015. **16**(1): p. 27-35.
79. Devine, D.A., *Antimicrobial peptides in defence of the oral and respiratory tracts.* Mol Immunol, 2003. **40**(7): p. 431-43.
80. Lipuma, J.J., *The changing microbial epidemiology in cystic fibrosis.* Clin Microbiol Rev, 2010. **23**(2): p. 299-323.
81. Hauser, A.R., et al., *Clinical significance of microbial infection and adaptation in cystic fibrosis.* Clin Microbiol Rev, 2011. **24**(1): p. 29-70.
82. Navarro, J., et al., *Factors associated with poor pulmonary function: cross-sectional analysis of data from the ERCF. European Epidemiologic Registry of Cystic Fibrosis.* Eur Respir J, 2001. **18**(2): p. 298-305.
83. Rosenfeld, M., et al., *Early pulmonary infection, inflammation, and clinical outcomes in infants with cystic fibrosis.* Pediatr Pulmonol, 2001. **32**(5): p. 356-66.
84. Soni, R., et al., *Effect of Burkholderia cepacia infection in the clinical course of patients with cystic fibrosis: a pilot study in a Sydney clinic.* Respirology, 2002. **7**(3): p. 241-5.
85. Whiteford, M.L., et al., *Outcome of Burkholderia (Pseudomonas) cepacia colonisation in children with cystic fibrosis following a hospital outbreak.* Thorax, 1995. **50**(11): p. 1194-8.
86. Rogers, G.B., et al., *Bacterial activity in cystic fibrosis lung infections.* Respir Res, 2005. **6**: p. 49.
87. Bakare, N., et al., *Prevalence of Aspergillus fumigatus and other fungal species in the sputum of adult patients with cystic fibrosis.* Mycoses, 2003. **46**(1-2): p. 19-23.
88. Hiatt, P.W., et al., *Effects of viral lower respiratory tract infection on lung function in infants with cystic fibrosis.* Pediatrics, 1999. **103**(3): p. 619-26.
89. Wark, P.A., et al., *Viral infections trigger exacerbations of cystic fibrosis in adults and children.* Eur Respir J, 2012. **40**(2): p. 510-2.
90. van Ewijk, B.E., et al., *Viral respiratory infections in cystic fibrosis.* J Cyst Fibros, 2005. **4 Suppl 2**: p. 31-6.
91. Goss, C.H. and J.L. Burns, *Exacerbations in cystic fibrosis. 1: Epidemiology and pathogenesis.* Thorax, 2007. **62**(4): p. 360-7.
92. Gellatly, S.L. and R.E. Hancock, *Pseudomonas aeruginosa: new insights into pathogenesis and host defenses.* Pathog Dis, 2013. **67**(3): p. 159-73.
93. Silby, M.W., et al., *Pseudomonas genomes: diverse and adaptable.* FEMS Microbiol Rev, 2011. **35**(4): p. 652-80.

94. Mathee, K., et al., *Dynamics of Pseudomonas aeruginosa genome evolution.* Proc Natl Acad Sci U S A, 2008. **105**(8): p. 3100-5.
95. Stover, C.K., et al., *Complete genome sequence of Pseudomonas aeruginosa PAO1, an opportunistic pathogen.* Nature, 2000. **406**(6799): p. 959-64.
96. Drake, D. and T.C. Montie, *Protection against Pseudomonas aeruginosa infection by passive transfer of anti-flagellar serum.* Can J Microbiol, 1987. **33**(9): p. 755-63.
97. Feldman, M., et al., *Role of flagella in pathogenesis of Pseudomonas aeruginosa pulmonary infection.* Infect Immun, 1998. **66**(1): p. 43-51.
98. Williams, B.J., J. Dehnbostel, and T.S. Blackwell, *Pseudomonas aeruginosa: host defence in lung diseases.* Respirology, 2010. **15**(7): p. 1037-56.
99. Miao, E.A., et al., *TLR5 and Ipaf: dual sensors of bacterial flagellin in the innate immune system.* Semin Immunopathol, 2007. **29**(3): p. 275-88.
100. Kohler, T., et al., *Swarming of Pseudomonas aeruginosa is dependent on cell-to-cell signaling and requires flagella and pili.* J Bacteriol, 2000. **182**(21): p. 5990-6.
101. Sriramulu, D.D., et al., *Microcolony formation: a novel biofilm model of Pseudomonas aeruginosa for the cystic fibrosis lung.* J Med Microbiol, 2005. **54**(Pt 7): p. 667-76.
102. Hauser, A.R., *The type III secretion system of Pseudomonas aeruginosa: infection by injection.* Nat Rev Microbiol, 2009. **7**(9): p. 654-65.
103. Laarman, A.J., et al., *Pseudomonas aeruginosa alkaline protease blocks complement activation via the classical and lectin pathways.* J Immunol, 2012. **188**(1): p. 386-93.
104. Malloy, J.L., et al., *Pseudomonas aeruginosa protease IV degrades surfactant proteins and inhibits surfactant host defense and biophysical functions.* Am J Physiol Lung Cell Mol Physiol, 2005. **288**(2): p. L409-18.
105. Bardoel, B.W., et al., *Pseudomonas evades immune recognition of flagellin in both mammals and plants.* PLoS Pathog, 2011. **7**(8): p. e1002206.
106. Matsumoto, K., *Role of bacterial proteases in pseudomonal and serratial keratitis.* Biol Chem, 2004. **385**(11): p. 1007-16.
107. Mariencheck, W.I., et al., *Pseudomonas aeruginosa elastase degrades surfactant proteins A and D.* Am J Respir Cell Mol Biol, 2003. **28**(4): p. 528-37.
108. King, J.D., et al., *Review: Lipopolysaccharide biosynthesis in Pseudomonas aeruginosa.* Innate Immun, 2009. **15**(5): p. 261-312.
109. Caiazza, N.C., R.M. Shanks, and G.A. O'Toole, *Rhamnolipids modulate swarming motility patterns of Pseudomonas aeruginosa.* J Bacteriol, 2005. **187**(21): p. 7351-61.
110. Boles, B.R., M. Thoendel, and P.K. Singh, *Rhamnolipids mediate detachment of Pseudomonas aeruginosa from biofilms.* Mol Microbiol, 2005. **57**(5): p. 1210-23.
111. Haba, E., et al., *Physicochemical characterization and antimicrobial properties of rhamnolipids produced by Pseudomonas aeruginosa 47T2 NCBIM 40044.* Biotechnol Bioeng, 2003. **81**(3): p. 316-22.
112. Jensen, P.O., et al., *Rapid necrotic killing of polymorphonuclear leukocytes is caused by quorum-sensing-controlled production of rhamnolipid by Pseudomonas aeruginosa.* Microbiology, 2007. **153**(Pt 5): p. 1329-38.
113. Zulianello, L., et al., *Rhamnolipids are virulence factors that promote early infiltration of primary human airway epithelia by Pseudomonas aeruginosa.* Infect Immun, 2006. **74**(6): p. 3134-47.
114. May, T.B., et al., *Alginate synthesis by Pseudomonas aeruginosa: a key pathogenic factor in chronic pulmonary infections of cystic fibrosis patients.* Clin Microbiol Rev, 1991. **4**(2): p. 191-206.
115. Wozniak, D.J., et al., *Alginate is not a significant component of the extracellular polysaccharide matrix of PA14 and PAO1 Pseudomonas aeruginosa biofilms.* Proc Natl Acad Sci U S A, 2003. **100**(13): p. 7907-12.
116. Hay, I.D., et al., *Genetics and regulation of bacterial alginate production.* Environ Microbiol, 2014. **16**(10): p. 2997-3011.

117. Kumon, H., et al., *A sandwich cup method for the penetration assay of antimicrobial agents through Pseudomonas exopolysaccharides.* Microbiol Immunol, 1994. **38**(8): p. 615-9.
118. Lau, G.W., et al., *The role of pyocyanin in Pseudomonas aeruginosa infection.* Trends Mol Med, 2004. **10**(12): p. 599-606.
119. Jimenez, P.N., et al., *The multiple signaling systems regulating virulence in Pseudomonas aeruginosa.* Microbiol Mol Biol Rev, 2012. **76**(1): p. 46-65.
120. Peek, M.E., et al., *Pyoverdine, the Major Siderophore in Pseudomonas aeruginosa, Evades NGAL Recognition.* Interdiscip Perspect Infect Dis, 2012. **2012**: p. 843509.
121. Schultz, M.J., et al., *The effect of pseudomonas exotoxin A on cytokine production in whole blood exposed to Pseudomonas aeruginosa.* FEMS Immunol Med Microbiol, 2000. **29**(3): p. 227-32.
122. Williams, H.D., J.E. Zlosnik, and B. Ryall, *Oxygen, cyanide and energy generation in the cystic fibrosis pathogen Pseudomonas aeruginosa.* Adv Microb Physiol, 2007. **52**: p. 1-71.
123. Cooper, M., G.R. Tavankar, and H.D. Williams, *Regulation of expression of the cyanide-insensitive terminal oxidase in Pseudomonas aeruginosa.* Microbiology, 2003. **149**(Pt 5): p. 1275-84.
124. Deep, A., U. Chaudhary, and V. Gupta, *Quorum sensing and Bacterial Pathogenicity: From Molecules to Disease.* J Lab Physicians, 2011. **3**(1): p. 4-11.
125. Drenkard, E., *Antimicrobial resistance of Pseudomonas aeruginosa biofilms.* Microbes Infect, 2003. **5**(13): p. 1213-9.
126. Li, Z., et al., *Longitudinal development of mucoid Pseudomonas aeruginosa infection and lung disease progression in children with cystic fibrosis.* JAMA, 2005. **293**(5): p. 581-8.
127. Taccetti, G., et al., *Early eradication therapy against Pseudomonas aeruginosa in cystic fibrosis patients.* The European respiratory journal : official journal of the European Society for Clinical Respiratory Physiology, 2005. **26**(3): p. 458-61.
128. Douglas, T.A., et al., *Acquisition and eradication of P. aeruginosa in young children with cystic fibrosis.* The European respiratory journal : official journal of the European Society for Clinical Respiratory Physiology, 2009. **33**(2): p. 305-11.
129. Okkotsu, Y., A.S. Little, and M.J. Schurr, *The Pseudomonas aeruginosa AlgZR two-component system coordinates multiple phenotypes.* Front Cell Infect Microbiol, 2014. **4**: p. 82.
130. Ratjen, F., G. Doring, and W.H. Nikolaizik, *Effect of inhaled tobramycin on early Pseudomonas aeruginosa colonisation in patients with cystic fibrosis.* Lancet, 2001. **358**(9286): p. 983-4.
131. Hartl, D., et al., *Innate immunity in cystic fibrosis lung disease.* J Cyst Fibros, 2012. **11**(5): p. 363-82.
132. Nealson, K.H., T. Platt, and J.W. Hastings, *Cellular control of the synthesis and activity of the bacterial luminescent system.* J Bacteriol, 1970. **104**(1): p. 313-22.
133. Hoang, T.T., et al., *Beta-ketoacyl acyl carrier protein reductase (FabG) activity of the fatty acid biosynthetic pathway is a determining factor of 3-oxo-homoserine lactone acyl chain lengths.* Microbiology, 2002. **148**(Pt 12): p. 3849-56.
134. Gambello, M.J., S. Kaye, and B.H. Iglewski, *LasR of Pseudomonas aeruginosa is a transcriptional activator of the alkaline protease gene (apr) and an enhancer of exotoxin A expression.* Infect Immun, 1993. **61**(4): p. 1180-4.
135. Pearson, J.P., E.C. Pesci, and B.H. Iglewski, *Roles of Pseudomonas aeruginosa las and rhl quorum-sensing systems in control of elastase and rhamnolipid biosynthesis genes.* J Bacteriol, 1997. **179**(18): p. 5756-67.

136. Tang, H.B., et al., *Contribution of specific Pseudomonas aeruginosa virulence factors to pathogenesis of pneumonia in a neonatal mouse model of infection.* Infect Immun, 1996. **64**(1): p. 37-43.
137. Pearson, J.P., et al., *Pseudomonas aeruginosa cell-to-cell signaling is required for virulence in a model of acute pulmonary infection.* Infect Immun, 2000. **68**(7): p. 4331-4.
138. Latifi, A., et al., *A hierarchical quorum-sensing cascade in Pseudomonas aeruginosa links the transcriptional activators LasR and RhIR (VsmR) to expression of the stationary-phase sigma factor RpoS.* Mol Microbiol, 1996. **21**(6): p. 1137-46.
139. Bleves, S., et al., *Quorum sensing negatively controls type III secretion regulon expression in Pseudomonas aeruginosa PAO1.* J Bacteriol, 2005. **187**(11): p. 3898-902.
140. Lazdunski, A.M., I. Ventre, and J.N. Sturgis, *Regulatory circuits and communication in Gram-negative bacteria.* Nat Rev Microbiol, 2004. **2**(7): p. 581-92.
141. Pesci, E.C., et al., *Quinolone signaling in the cell-to-cell communication system of Pseudomonas aeruginosa.* Proc Natl Acad Sci U S A, 1999. **96**(20): p. 11229-34.
142. Wade, D.S., et al., *Regulation of Pseudomonas quinolone signal synthesis in Pseudomonas aeruginosa.* J Bacteriol, 2005. **187**(13): p. 4372-80.
143. Chugani, S.A., et al., *QscR, a modulator of quorum-sensing signal synthesis and virulence in Pseudomonas aeruginosa.* Proc Natl Acad Sci U S A, 2001. **98**(5): p. 2752-7.
144. Ledgham, F., et al., *Global regulation in Pseudomonas aeruginosa: the regulatory protein AlgR2 (AlgQ) acts as a modulator of quorum sensing.* Res Microbiol, 2003. **154**(3): p. 207-13.
145. de Kievit, T., et al., *RsaL, a novel repressor of virulence gene expression in Pseudomonas aeruginosa.* J Bacteriol, 1999. **181**(7): p. 2175-84.
146. Siehnel, R., et al., *A unique regulator controls the activation threshold of quorum-regulated genes in Pseudomonas aeruginosa.* Proc Natl Acad Sci U S A, 2010. **107**(17): p. 7916-21.
147. Seet, Q. and L.H. Zhang, *Anti-activator QslA defines the quorum sensing threshold and response in Pseudomonas aeruginosa.* Mol Microbiol, 2011. **80**(4): p. 951-65.
148. Alhede, M., et al., *Pseudomonas aeruginosa biofilms: mechanisms of immune evasion.* Adv Appl Microbiol, 2014. **86**: p. 1-40.
149. Hoiby, N., et al., *Antibiotic resistance of bacterial biofilms.* Int J Antimicrob Agents, 2010. **35**(4): p. 322-32.
150. Wei, Q. and L.Z. Ma, *Biofilm matrix and its regulation in Pseudomonas aeruginosa.* Int J Mol Sci, 2013. **14**(10): p. 20983-1005.
151. Hickman, J.W., D.F. Tifrea, and C.S. Harwood, *A chemosensory system that regulates biofilm formation through modulation of cyclic diguanylate levels.* Proc Natl Acad Sci U S A, 2005. **102**(40): p. 14422-7.
152. Davies, D.G., et al., *The involvement of cell-to-cell signals in the development of a bacterial biofilm.* Science, 1998. **280**(5361): p. 295-8.
153. Wu, H., et al., *Detection of N-acylhomoserine lactones in lung tissues of mice infected with Pseudomonas aeruginosa.* Microbiology, 2000. **146 (Pt 10)**: p. 2481-93.
154. Pritt, B., L. O'Brien, and W. Winn, *Mucoid Pseudomonas in cystic fibrosis.* Am J Clin Pathol, 2007. **128**(1): p. 32-4.
155. Banin, E., M.L. Vasil, and E.P. Greenberg, *Iron and Pseudomonas aeruginosa biofilm formation.* Proc Natl Acad Sci U S A, 2005. **102**(31): p. 11076-81.
156. Monroe, D., *Looking for chinks in the armor of bacterial biofilms.* PLoS Biol, 2007. **5**(11): p. e307.
157. Singh, P.K., et al., *Quorum-sensing signals indicate that cystic fibrosis lungs are infected with bacterial biofilms.* Nature, 2000. **407**(6805): p. 762-4.

158. Ueda, A. and T.K. Wood, *Connecting quorum sensing, c-di-GMP, pel polysaccharide, and biofilm formation in Pseudomonas aeruginosa through tyrosine phosphatase TpbA (PA3885).* PLoS Pathog, 2009. **5**(6): p. e1000483.
159. Allesen-Holm, M., et al., *A characterization of DNA release in Pseudomonas aeruginosa cultures and biofilms.* Mol Microbiol, 2006. **59**(4): p. 1114-28.
160. Colvin, K.M., et al., *The pel polysaccharide can serve a structural and protective role in the biofilm matrix of Pseudomonas aeruginosa.* PLoS Pathog, 2011. **7**(1): p. e1001264.
161. Ma, L., et al., *Assembly and development of the Pseudomonas aeruginosa biofilm matrix.* PLoS Pathog, 2009. **5**(3): p. e1000354.
162. Mishra, M., et al., *Pseudomonas aeruginosa Psl polysaccharide reduces neutrophil phagocytosis and the oxidative response by limiting complement-mediated opsonization.* Cell Microbiol, 2012. **14**(1): p. 95-106.
163. Govan, J.R. and V. Deretic, *Microbial pathogenesis in cystic fibrosis: mucoid Pseudomonas aeruginosa and Burkholderia cepacia.* Microbiol Rev, 1996. **60**(3): p. 539-74.
164. Sutherland, I., *Biofilm exopolysaccharides: a strong and sticky framework.* Microbiology, 2001. **147**(Pt 1): p. 3-9.
165. Whitchurch, C.B., et al., *Extracellular DNA required for bacterial biofilm formation.* Science, 2002. **295**(5559): p. 1487.
166. Mulcahy, H., L. Charron-Mazenod, and S. Lewenza, *Extracellular DNA chelates cations and induces antibiotic resistance in Pseudomonas aeruginosa biofilms.* PLoS Pathog, 2008. **4**(11): p. e1000213.
167. Fuxman Bass, J.I., et al., *Extracellular DNA: a major proinflammatory component of Pseudomonas aeruginosa biofilms.* J Immunol, 2010. **184**(11): p. 6386-95.
168. Mann, E.E. and D.J. Wozniak, *Pseudomonas biofilm matrix composition and niche biology.* FEMS Microbiol Rev, 2012. **36**(4): p. 893-916.
169. Kaplan, J.B., *Biofilm dispersal: mechanisms, clinical implications, and potential therapeutic uses.* J Dent Res, 2010. **89**(3): p. 205-18.
170. Stewart, P.S. and J.W. Costerton, *Antibiotic resistance of bacteria in biofilms.* Lancet, 2001. **358**(9276): p. 135-8.
171. Bjarnsholt, T., et al., *Pseudomonas aeruginosa tolerance to tobramycin, hydrogen peroxide and polymorphonuclear leukocytes is quorum-sensing dependent.* Microbiology, 2005. **151**(Pt 2): p. 373-83.
172. Alhede, M., T. Bjarnsholt, and M. Givskov, *Pseudomonas aeruginosa biofilms: mechanisms of immune evasion.* Adv Appl Microbiol, 2014. **86**: p. 1-40.
173. Ren, C.L., et al., *Multiple antibiotic-resistant Pseudomonas aeruginosa and lung function decline in patients with cystic fibrosis.* J Cyst Fibros, 2012. **11**(4): p. 293-9.
174. Livermore, D.M., *Multiple mechanisms of antimicrobial resistance in Pseudomonas aeruginosa: our worst nightmare?* Clin Infect Dis, 2002. **34**(5): p. 634-40.
175. Gooderham, W.J. and R.E. Hancock, *Regulation of virulence and antibiotic resistance by two-component regulatory systems in Pseudomonas aeruginosa.* FEMS Microbiol Rev, 2009. **33**(2): p. 279-94.
176. Breidenstein, E.B., C. de la Fuente-Nunez, and R.E. Hancock, *Pseudomonas aeruginosa: all roads lead to resistance.* Trends Microbiol, 2011. **19**(8): p. 419-26.
177. Jacoby, G.A., *AmpC beta-lactamases.* Clin Microbiol Rev, 2009. **22**(1): p. 161-82, Table of Contents.
178. Ramsey, B.W., et al., *Intermittent administration of inhaled tobramycin in patients with cystic fibrosis. Cystic Fibrosis Inhaled Tobramycin Study Group.* N Engl J Med, 1999. **340**(1): p. 23-30.
179. Matz, G.J., *Aminoglycoside ototoxicity.* Am J Otolaryngol, 1986. **7**(2): p. 117-9.

180. Abramowsky, C.R. and G.L. Swinehart, *The nephropathy of cystic fibrosis: a human model of chronic nephrotoxicity.* Hum Pathol, 1982. **13**(10): p. 934-9.
181. Williams, S.C., et al., *Pseudomonas aeruginosa autoinducer enters and functions in mammalian cells.* J Bacteriol, 2004. **186**(8): p. 2281-7.
182. Hughes, D.T. and V. Sperandio, *Inter-kingdom signalling: communication between bacteria and their hosts.* Nat Rev Microbiol, 2008. **6**(2): p. 111-20.
183. Ritchie, A.J., et al., *The immunomodulatory Pseudomonas aeruginosa signalling molecule N-(3-oxododecanoyl)-L-homoserine lactone enters mammalian cells in an unregulated fashion.* Immunol Cell Biol, 2007. **85**(8): p. 596-602.
184. Chhabra, S.R., et al., *Synthetic analogues of the bacterial signal (quorum sensing) molecule N-(3-oxododecanoyl)-L-homoserine lactone as immune modulators.* J Med Chem, 2003. **46**(1): p. 97-104.
185. Hooi, D.S., et al., *Differential immune modulatory activity of Pseudomonas aeruginosa quorum-sensing signal molecules.* Infect Immun, 2004. **72**(11): p. 6463-70.
186. Ritchie, A.J., et al., *Modification of in vivo and in vitro T- and B-cell-mediated immune responses by the Pseudomonas aeruginosa quorum-sensing molecule N-(3-oxododecanoyl)-L-homoserine lactone.* Infect Immun, 2003. **71**(8): p. 4421-31.
187. Telford, G., et al., *The Pseudomonas aeruginosa quorum-sensing signal molecule N-(3-oxododecanoyl)-L-homoserine lactone has immunomodulatory activity.* Infect Immun, 1998. **66**(1): p. 36-42.
188. Kravchenko, V.V., et al., *Modulation of gene expression via disruption of NF-kappaB signaling by a bacterial small molecule.* Science, 2008. **321**(5886): p. 259-63.
189. Mayer, M.L., et al., *The Pseudomonas aeruginosa autoinducer 3O-C12 homoserine lactone provokes hyperinflammatory responses from cystic fibrosis airway epithelial cells.* PLoS One, 2011. **6**(1): p. e16246.
190. Smith, R.S., et al., *The Pseudomonas aeruginosa quorum-sensing molecule N-(3-oxododecanoyl)homoserine lactone contributes to virulence and induces inflammation in vivo.* J Bacteriol, 2002. **184**(4): p. 1132-9.
191. Li, H., et al., *Influence of Pseudomonas aeruginosa quorum sensing signal molecule N-(3-oxododecanoyl) homoserine lactone on mast cells.* Med Microbiol Immunol, 2009. **198**(2): p. 113-21.
192. Shiner, E.K., et al., *Pseudomonas aeruginosa autoinducer modulates host cell responses through calcium signalling.* Cell Microbiol, 2006. **8**(10): p. 1601-10.
193. DiMango, E., et al., *Diverse Pseudomonas aeruginosa gene products stimulate respiratory epithelial cells to produce interleukin-8.* J Clin Invest, 1995. **96**(5): p. 2204-10.
194. Smith, R.S., et al., *The Pseudomonas autoinducer N-(3-oxododecanoyl) homoserine lactone induces cyclooxygenase-2 and prostaglandin E2 production in human lung fibroblasts: implications for inflammation.* J Immunol, 2002. **169**(5): p. 2636-42.
195. Lu, Q., et al., *Regulation on expression of toll-like receptors on monocytes after stimulation with the 3-o-C12-HSL molecule from Pseudomonas aeruginosa.* Curr Microbiol, 2012. **65**(4): p. 384-9.
196. Vikstrom, E., K.E. Magnusson, and A. Pivoriunas, *The Pseudomonas aeruginosa quorum-sensing molecule N-(3-oxododecanoyl)-L-homoserine lactone stimulates phagocytic activity in human macrophages through the p38 MAPK pathway.* Microbes Infect, 2005. **7**(15): p. 1512-8.
197. Tateda, K., et al., *The Pseudomonas aeruginosa autoinducer N-3-oxododecanoyl homoserine lactone accelerates apoptosis in macrophages and neutrophils.* Infect Immun, 2003. **71**(10): p. 5785-93.
198. Horikawa, M., et al., *Synthesis of Pseudomonas quorum-sensing autoinducer analogs and structural entities required for induction of apoptosis in macrophages.* Bioorg Med Chem Lett, 2006. **16**(8): p. 2130-3.

199. Schwarzer, C., et al., *Pseudomonas aeruginosa homoserine lactone triggers apoptosis and Bak/Bax-independent release of mitochondrial cytochrome C in fibroblasts.* Cell Microbiol, 2014. **16**(7): p. 1094-104.
200. Li, L., et al., *Bacterial N-acylhomoserine lactone-induced apoptosis in breast carcinoma cells correlated with down-modulation of STAT3.* Oncogene, 2004. **23**(28): p. 4894-902.
201. Taguchi, R., et al., *Mucin 3 is involved in intestinal epithelial cell apoptosis via N-(3-oxododecanoyl)-L-homoserine lactone-induced suppression of Akt phosphorylation.* Am J Physiol Cell Physiol, 2014. **307**(2): p. C162-8.
202. Jacobi, C.A., et al., *Effects of bacterial N-acyl homoserine lactones on human Jurkat T lymphocytes-OdDHL induces apoptosis via the mitochondrial pathway.* Int J Med Microbiol, 2009. **299**(7): p. 509-19.
203. Schwarzer, C., et al., *Thapsigargin blocks Pseudomonas aeruginosa homoserine lactone-induced apoptosis in airway epithelia.* Am J Physiol Cell Physiol, 2014. **306**(9): p. C844-55.
204. Grabiner, M.A., et al., *Pseudomonas aeruginosa quorum-sensing molecule homoserine lactone modulates inflammatory signaling through PERK and eI-F2alpha.* J Immunol, 2014. **193**(3): p. 1459-67.
205. Kim, J.B., et al., *Paraoxonase-2 modulates stress response of endothelial cells to oxidized phospholipids and a bacterial quorum-sensing molecule.* Arterioscler Thromb Vasc Biol, 2011. **31**(11): p. 2624-33.
206. Zhang, J., et al., *Pseudomonas aeruginosa quorum-sensing molecule N-(3-oxododecanoyl) homoserine lactone attenuates lipopolysaccharide-induced inflammation by activating the unfolded protein response.* Biomed Rep, 2014. **2**(2): p. 233-238.
207. Eum, S.Y., et al., *Disruption of epithelial barrier by quorum-sensing N-3-(oxododecanoyl)-homoserine lactone is mediated by matrix metalloproteinases.* Am J Physiol Gastrointest Liver Physiol, 2014. **306**(11): p. G992-G1001.
208. Vikstrom, E., F. Tafazoli, and K.E. Magnusson, *Pseudomonas aeruginosa quorum sensing molecule N-(3 oxododecanoyl)-l-homoserine lactone disrupts epithelial barrier integrity of Caco-2 cells.* FEBS Lett, 2006. **580**(30): p. 6921-8.
209. Lawrence, R.N., et al., *The Pseudomonas aeruginosa quorum-sensing signal molecule, N-(3-oxododecanoyl)-L-homoserine lactone, inhibits porcine arterial smooth muscle contraction.* Br J Pharmacol, 1999. **128**(4): p. 845-8.
210. Gardiner, S.M., et al., *Haemodynamic effects of the bacterial quorum sensing signal molecule, N-(3-oxododecanoyl)-L-homoserine lactone, in conscious, normal and endotoxaemic rats.* Br J Pharmacol, 2001. **133**(7): p. 1047-54.
211. Rennemeier, C., et al., *Microbial quorum-sensing molecules induce acrosome loss and cell death in human spermatozoa.* Infect Immun, 2009. **77**(11): p. 4990-7.
212. Kravchenko, V.V., et al., *N-(3-oxo-acyl)homoserine lactones signal cell activation through a mechanism distinct from the canonical pathogen-associated molecular pattern recognition receptor pathways.* J Biol Chem, 2006. **281**(39): p. 28822-30.
213. Bryan, A., et al., *Human transcriptome analysis reveals a potential role for active transport in the metabolism of Pseudomonas aeruginosa autoinducers.* Microbes Infect, 2010. **12**(12-13): p. 1042-50.
214. Jahoor, A., et al., *Peroxisome proliferator-activated receptors mediate host cell proinflammatory responses to Pseudomonas aeruginosa autoinducer.* J Bacteriol, 2008. **190**(13): p. 4408-15.
215. Berger, J. and D.E. Moller, *The mechanisms of action of PPARs.* Annu Rev Med, 2002. **53**: p. 409-35.
216. Miyata, K.S., et al., *The peroxisome proliferator-activated receptor interacts with the retinoid X receptor in vivo.* Gene, 1994. **148**(2): p. 327-30.

217. Cooley, M., S.R. Chhabra, and P. Williams, *N-Acylhomoserine lactone-mediated quorum sensing: a twist in the tail and a blow for host immunity.* Chem Biol, 2008. **15**(11): p. 1141-7.
218. Cooley, M.A., C. Whittall, and M.S. Rolph, *Pseudomonas signal molecule 3-oxo-C12-homoserine lactone interferes with binding of rosiglitazone to human PPARgamma.* Microbes Infect, 2010. **12**(3): p. 231-7.
219. Pascual, G., et al., *A SUMOylation-dependent pathway mediates transrepression of inflammatory response genes by PPAR-gamma.* Nature, 2005. **437**(7059): p. 759-63.
220. Harmon, G.S., et al., *Pharmacological correction of a defect in PPAR-gamma signaling ameliorates disease severity in Cftr-deficient mice.* Nat Med, 2010. **16**(3): p. 313-8.
221. Ollero, M., et al., *Decreased expression of peroxisome proliferator activated receptor gamma in cftr-/- mice.* J Cell Physiol, 2004. **200**(2): p. 235-44.
222. Perez, A., et al., *Peroxisome proliferator-activated receptor-gamma in cystic fibrosis lung epithelium.* Am J Physiol Lung Cell Mol Physiol, 2008. **295**(2): p. L303-13.
223. Griffin, P.E., et al., *Expression of PPARgamma and paraoxonase 2 correlated with Pseudomonas aeruginosa infection in cystic fibrosis.* PLoS One, 2012. **7**(7): p. e42241.
224. Luciani, A., et al., *SUMOylation of tissue transglutaminase as link between oxidative stress and inflammation.* J Immunol, 2009. **183**(4): p. 2775-84.
225. Karlsson, T., et al., *The Pseudomonas aeruginosa N-acylhomoserine lactone quorum sensing molecules target IQGAP1 and modulate epithelial cell migration.* PLoS Pathog, 2012. **8**(10): p. e1002953.
226. Bensenor, L.B., et al., *IQGAP1 regulates cell motility by linking growth factor signaling to actin assembly.* J Cell Sci, 2007. **120**(Pt 4): p. 658-69.
227. Briggs, M.W. and D.B. Sacks, *IQGAP proteins are integral components of cytoskeletal regulation.* EMBO Rep, 2003. **4**(6): p. 571-4.
228. Skindersoe, M.E., et al., *Effects of antibiotics on quorum sensing in Pseudomonas aeruginosa.* Antimicrob Agents Chemother, 2008. **52**(10): p. 3648-63.
229. Hoffmann, N., et al., *Azithromycin blocks quorum sensing and alginate polymer formation and increases the sensitivity to serum and stationary-growth-phase killing of Pseudomonas aeruginosa and attenuates chronic P. aeruginosa lung infection in Cftr(-/-) mice.* Antimicrob Agents Chemother, 2007. **51**(10): p. 3677-87.
230. Kabra, S.K., et al., *Long-term daily high and low doses of azithromycin in children with cystic fibrosis: a randomized controlled trial.* J Cyst Fibros, 2010. **9**(1): p. 17-23.
231. Equi, A., et al., *Long term azithromycin in children with cystic fibrosis: a randomised, placebo-controlled crossover trial.* Lancet, 2002. **360**(9338): p. 978-84.
232. Hentzer, M., et al., *Inhibition of quorum sensing in Pseudomonas aeruginosa biofilm bacteria by a halogenated furanone compound.* Microbiology, 2002. **148**(Pt 1): p. 87-102.
233. Bottomley, M.J., et al., *Molecular insights into quorum sensing in the human pathogen Pseudomonas aeruginosa from the structure of the virulence regulator LasR bound to its autoinducer.* J Biol Chem, 2007. **282**(18): p. 13592-600.
234. Wu, H., et al., *Synthetic furanones inhibit quorum-sensing and enhance bacterial clearance in Pseudomonas aeruginosa lung infection in mice.* J Antimicrob Chemother, 2004. **53**(6): p. 1054-61.
235. Garcia-Contreras, R., T. Maeda, and T.K. Wood, *Resistance to quorum-quenching compounds.* Appl Environ Microbiol, 2013. **79**(22): p. 6840-6.
236. Maeda, T., et al., *Quorum quenching quandary: resistance to antivirulence compounds.* ISME J, 2012. **6**(3): p. 493-501.
237. O'Loughlin, C.T., et al., *A quorum-sensing inhibitor blocks Pseudomonas aeruginosa virulence and biofilm formation.* Proc Natl Acad Sci U S A, 2013. **110**(44): p. 17981-6.
238. Kaufmann, G.F., et al., *Antibody interference with N-acyl homoserine lactone-mediated bacterial quorum sensing.* J Am Chem Soc, 2006. **128**(9): p. 2802-3.

239. Miyairi, S., et al., *Immunization with 3-oxododecanoyl-L-homoserine lactone-protein conjugate protects mice from lethal Pseudomonas aeruginosa lung infection.* J Med Microbiol, 2006. **55**(Pt 10): p. 1381-7.
240. Papaioannou, E., et al., *Quorum-Quenching Acylase Reduces the Virulence of Pseudomonas aeruginosa in a Caenorhabditis elegans Infection Model.* Antimicrobial Agents and Chemotherapy, 2009. **53**(11): p. 4891-4897.
241. Chowdhary, P.K., et al., *Bacillus megaterium CYP102A1 oxidation of acyl homoserine lactones and acyl homoserines.* Biochemistry, 2007. **46**(50): p. 14429-37.
242. Dong, Y.H., et al., *Quenching quorum-sensing-dependent bacterial infection by an N-acyl homoserine lactonase.* Nature, 2001. **411**(6839): p. 813-7.
243. Yates, E.A., et al., *N-acylhomoserine lactones undergo lactonolysis in a pH-, temperature-, and acyl chain length-dependent manner during growth of Yersinia pseudotuberculosis and Pseudomonas aeruginosa.* Infect Immun, 2002. **70**(10): p. 5635-46.
244. Carlier, A., et al., *The Ti plasmid of Agrobacterium tumefaciens harbors an attM-paralogous gene, aiiB, also encoding N-Acyl homoserine lactonase activity.* Appl Environ Microbiol, 2003. **69**(8): p. 4989-93.
245. Mei, G.Y., et al., *AidH, an alpha/beta-hydrolase fold family member from an Ochrobactrum sp. strain, is a novel N-acylhomoserine lactonase.* Appl Environ Microbiol, 2010. **76**(15): p. 4933-42.
246. Wang, W.Z., et al., *AiiM, a novel class of N-acylhomoserine lactonase from the leaf-associated bacterium Microbacterium testaceum.* Appl Environ Microbiol, 2010. **76**(8): p. 2524-30.
247. Ozer, E.A., et al., *Human and murine paraoxonase 1 are host modulators of Pseudomonas aeruginosa quorum-sensing.* Fems Microbiology Letters, 2005. **253**(1): p. 29-37.
248. Draganov, D.I., et al., *Human paraoxonases (PON1, PON2, and PON3) are lactonases with overlapping and distinct substrate specificities.* J Lipid Res, 2005. **46**(6): p. 1239-47.
249. Devarajan, A., et al., *Role of PON2 in innate immune response in an acute infection model.* Mol Genet Metab, 2013. **110**(3): p. 362-70.
250. Stoltz, D.A., et al., *Drosophila are protected from Pseudomonas aeruginosa lethality by transgenic expression of paraoxonase-1.* J Clin Invest, 2008. **118**(9): p. 3123-31.
251. Mazur, A., *An enzyme in animal tissue capable of hydrolyzing the phosphorus-fluorine bond of alkyl fluorophosphates.* Journal of Biological Chemistry, 1946. **164**: p. 271-289.
252. Aldridge, W.N., *Serum esterases. II. An enzyme hydrolysing diethyl p-nitrophenyl phosphate (E600) and its identity with the A-esterase of mammalian sera.* Biochem J, 1953. **53**(1): p. 117-24.
253. Primo-Parmo, S.L., et al., *The human serum paraoxonase/arylesterase gene (PON1) is one member of a multigene family.* Genomics, 1996. **33**(3): p. 498-507.
254. Harel, M., et al., *Structure and evolution of the serum paraoxonase family of detoxifying and anti-atherosclerotic enzymes.* Nat Struct Mol Biol, 2004. **11**(5): p. 412-9.
255. Hassett, C., et al., *Characterization of cDNA clones encoding rabbit and human serum paraoxonase: the mature protein retains its signal sequence.* Biochemistry, 1991. **30**(42): p. 10141-9.
256. Blatter, M.C., et al., *Identification of a distinct human high-density lipoprotein subspecies defined by a lipoprotein-associated protein, K-45. Identity of K-45 with paraoxonase.* Eur J Biochem, 1993. **211**(3): p. 871-9.

257. Reddy, S.T., et al., *Human paraoxonase-3 is an HDL-associated enzyme with biological activity similar to paraoxonase-1 protein but is not regulated by oxidized lipids.* Arterioscler Thromb Vasc Biol, 2001. **21**(4): p. 542-7.
258. Ng, C.J., et al., *Paraoxonase-2 is a ubiquitously expressed protein with antioxidant properties and is capable of preventing cell-mediated oxidative modification of low density lipoprotein.* J Biol Chem, 2001. **276**(48): p. 44444-9.
259. Horke, S., et al., *Paraoxonase-2 reduces oxidative stress in vascular cells and decreases endoplasmic reticulum stress-induced caspase activation.* Circulation, 2007. **115**(15): p. 2055-64.
260. Chun, C.K., et al., *Inactivation of a Pseudomonas aeruginosa quorum-sensing signal by human airway epithelia.* Proc Natl Acad Sci U S A, 2004. **101**(10): p. 3587-90.
261. Yang, F., et al., *Quorum quenching enzyme activity is widely conserved in the sera of mammalian species.* FEBS Lett, 2005. **579**(17): p. 3713-7.
262. Teiber, J.F., et al., *Dominant role of paraoxonases in inactivation of the Pseudomonas aeruginosa quorum-sensing signal N-(3-oxododecanoyl)-L-homoserine lactone.* Infect Immun, 2008. **76**(6): p. 2512-9.
263. Estin, M.L., D.A. Stoltz, and J. Zabner, *Paraoxonase 1, quorum sensing, and P. aeruginosa infection: a novel model.* Adv Exp Med Biol, 2010. **660**: p. 183-93.
264. Stoltz, D.A., et al., *Paraoxonase-2 deficiency enhances Pseudomonas aeruginosa quorum sensing in murine tracheal epithelia.* Am J Physiol Lung Cell Mol Physiol, 2007. **292**(4): p. L852-60.
265. Horke, S., et al., *Paraoxonase 2 is down-regulated by the Pseudomonas aeruginosa quorumsensing signal N-(3-oxododecanoyl)-L-homoserine lactone and attenuates oxidative stress induced by pyocyanin.* Biochem J, 2010. **426**(1): p. 73-83.
266. Simanski, M., et al., *Paraoxonase 2 acts as a quorum sensing-quenching factor in human keratinocytes.* J Invest Dermatol, 2012. **132**(9): p. 2296-9.
267. Horke, S., et al., *A novel paraoxonase 2-dependent mechanism mediating the biological effects of the Pseudomonas aeruginosa quorum-sensing molecule N-(3-oxo-dodecanoyl)-L-homoserine lactone.* Infect Immun, 2015.
268. Shiner, M., B. Fuhrman, and M. Aviram, *Macrophage paraoxonase 2 (PON2) expression is up-regulated by pomegranate juice phenolic anti-oxidants via PPAR gamma and AP-1 pathway activation.* Atherosclerosis, 2007. **195**(2): p. 313-21.
269. Rosenblat, M., et al., *Mouse macrophage paraoxonase 2 activity is increased whereas cellular paraoxonase 3 activity is decreased under oxidative stress.* Arterioscler Thromb Vasc Biol, 2003. **23**(3): p. 468-74.
270. Rosenblat, M., et al., *Triglyceride accumulation in macrophages upregulates paraoxonase 2 (PON2) expression via ROS-mediated JNK/c-Jun signaling pathway activation.* Biofactors, 2012. **38**(6): p. 458-69.
271. Shiner, M., B. Fuhrman, and M. Aviram, *A biphasic U-shape effect of cellular oxidative stress on the macrophage anti-oxidant paraoxonase 2 (PON2) enzymatic activity.* Biochem Biophys Res Commun, 2006. **349**(3): p. 1094-9.
272. Devarajan, A., et al., *Paraoxonase 2 deficiency alters mitochondrial function and exacerbates the development of atherosclerosis.* Antioxid Redox Signal, 2011. **14**(3): p. 341-51.
273. Altenhofer, S., et al., *One enzyme, two functions: PON2 prevents mitochondrial superoxide formation and apoptosis independent from its lactonase activity.* J Biol Chem, 2010. **285**(32): p. 24398-403.
274. Devarajan, A., et al., *Macrophage paraoxonase 2 regulates calcium homeostasis and cell survival under endoplasmic reticulum stress conditions and is sufficient to prevent the development of aggravated atherosclerosis in paraoxonase 2 deficiency/apoE-/- mice on a Western diet.* Mol Genet Metab, 2012. **107**(3): p. 416-27.

275. Technologies, L., *Bac-to-Bac Baculovirus Expression System User Guide*. 2013: Life Technologies.
276. Matsuda, K., et al., *Sensitive quantitative detection of commensal bacteria by rRNA-targeted reverse transcription-PCR.* Appl Environ Microbiol, 2007. **73**(1): p. 32-9.
277. Joly, B., et al., *Relative expression of Pseudomonas aeruginosa virulence genes analyzed by a real time RT-PCR method during lung infection in rats.* FEMS Microbiol Lett, 2005. **243**(1): p. 271-8.
278. Gargalovic, P.S., et al., *The unfolded protein response is an important regulator of inflammatory genes in endothelial cells.* Arterioscler Thromb Vasc Biol, 2006. **26**(11): p. 2490-6.
279. Grootjans, J., et al., *Ischaemia-induced mucus barrier loss and bacterial penetration are rapidly counteracted by increased goblet cell secretory activity in human and rat colon.* Gut, 2013. **62**(2): p. 250-8.
280. Livak, K.J. and T.D. Schmittgen, *Analysis of relative gene expression data using real-time quantitative PCR and the 2(-Delta Delta C(T)) Method.* Methods, 2001. **25**(4): p. 402-8.
281. O'Reilly, D.R., Miller, L.K. and Luckow, V.A., *Baculovirus Expression Vectors: A laboratory Guide*. 1992, New York: W.H. Freeman and Company.
282. Davis, T.R., et al., *Baculovirus expression of alkaline phosphatase as a reporter gene for evaluation of production, glycosylation and secretion.* Biotechnology (N Y), 1992. **10**(10): p. 1148-50.
283. Charlton, T.S., et al., *A novel and sensitive method for the quantification of N-3-oxoacyl homoserine lactones using gas chromatography-mass spectrometry: application to a model bacterial biofilm.* Environ Microbiol, 2000. **2**(5): p. 530-41.
284. Williams, P., *Quorum sensing, communication and cross-kingdom signalling in the bacterial world.* Microbiology, 2007. **153**(Pt 12): p. 3923-38.
285. Saleh, A., et al., *Pseudomonas aeruginosa quorum-sensing signal molecule N-(3-oxododecanoyl)-L-homoserine lactone inhibits expression of P2Y receptors in cystic fibrosis tracheal gland cells.* Infect Immun, 1999. **67**(10): p. 5076-82.
286. Kitchener, J., *Important human genes and signal pathways are modulated by low concentrations of Pseudomonas aeruginosa signalling molecule*, in *School of Medicine*. 2013, University of Tasmania: Hobart.
287. Zabner, J., et al., *Development of cystic fibrosis and noncystic fibrosis airway cell lines.* Am J Physiol Lung Cell Mol Physiol, 2003. **284**(5): p. L844-54.
288. Schwarzer, C., et al., *Pseudomonas aeruginosa biofilm-associated homoserine lactone C12 rapidly activates apoptosis in airway epithelia.* Cell Microbiol, 2012. **14**(5): p. 698-709.
289. Andersen, J.L. and S. Kornbluth, *The tangled circuitry of metabolism and apoptosis.* Mol Cell, 2013. **49**(3): p. 399-410.
290. Mason, E.F. and J.C. Rathmell, *Cell metabolism: an essential link between cell growth and apoptosis.* Biochim Biophys Acta, 2011. **1813**(4): p. 645-54.
291. Pradelli, L.A., M. Beneteau, and J.E. Ricci, *Mitochondrial control of caspase-dependent and -independent cell death.* Cell Mol Life Sci, 2010. **67**(10): p. 1589-97.
292. Pradelli, L.A., et al., *Glucose metabolism is inhibited by caspases upon the induction of apoptosis.* Cell Death Dis, 2014. **5**: p. e1406.
293. Freeman, W.M., S.J. Walker, and K.E. Vrana, *Quantitative RT-PCR: pitfalls and potential.* Biotechniques, 1999. **26**(1): p. 112-22, 124-5.
294. Chuaqui, R.F., et al., *Post-analysis follow-up and validation of microarray experiments.* Nat Genet, 2002. **32 Suppl**: p. 509-14.
295. Leek, J.T., M.A. Taub, and J.L. Rasgon, *A statistical approach to selecting and confirming validation targets in -omics experiments.* BMC Bioinformatics, 2012. **13**: p. 150.

296. Rajeevan, M.S., et al., *Use of real-time quantitative PCR to validate the results of cDNA array and differential display PCR technologies.* Methods, 2001. **25**(4): p. 443-51.
297. Morey, J.S., J.C. Ryan, and F.M. Van Dolah, *Microarray validation: factors influencing correlation between oligonucleotide microarrays and real-time PCR.* Biol Proced Online, 2006. **8**: p. 175-93.
298. Pomerantz, J.L. and D. Baltimore, *NF-kappaB activation by a signaling complex containing TRAF2, TANK and TBK1, a novel IKK-related kinase.* EMBO J, 1999. **18**(23): p. 6694-704.
299. Smith, R.S., et al., *IL-8 production in human lung fibroblasts and epithelial cells activated by the Pseudomonas autoinducer N-3-oxododecanoyl homoserine lactone is transcriptionally regulated by NF-kappa B and activator protein-2.* J Immunol, 2001. **167**(1): p. 366-74.
300. Luo, Y.M., et al., *[Effects of PPAR-gamma agonist rosiglitazone on MMP-9 and TIMP-1 expression of monocyte-derived macrophages isolated from patients with acute coronary syndrome].* Zhonghua Xin Xue Guan Bing Za Zhi, 2009. **37**(8): p. 739-45.
301. Amerik, A.Y. and M. Hochstrasser, *Mechanism and function of deubiquitinating enzymes.* Biochim Biophys Acta, 2004. **1695**(1-3): p. 189-207.
302. Nijman, S.M., et al., *A genomic and functional inventory of deubiquitinating enzymes.* Cell, 2005. **123**(5): p. 773-86.
303. Antigny, F., et al., *CFTR and Ca Signaling in Cystic Fibrosis.* Front Pharmacol, 2011. **2**: p. 67.
304. Martins, J.R., et al., *F508del-CFTR increases intracellular Ca(2+) signaling that causes enhanced calcium-dependent Cl(-) conductance in cystic fibrosis.* Biochim Biophys Acta, 2011. **1812**(11): p. 1385-92.
305. Schwarzer, C., et al., *Pseudomonas aeruginosa Homoserine lactone activates store-operated cAMP and cystic fibrosis transmembrane regulator-dependent Cl- secretion by human airway epithelia.* J Biol Chem, 2010. **285**(45): p. 34850-63.
306. Weber, S.M., et al., *PPARgamma ligands induce ER stress in pancreatic beta-cells: ER stress activation results in attenuation of cytokine signaling.* Am J Physiol Endocrinol Metab, 2004. **287**(6): p. E1171-7.
307. Schroder, M. and R.J. Kaufman, *The mammalian unfolded protein response.* Annu Rev Biochem, 2005. **74**: p. 739-89.
308. Hybiske, K., et al., *Effects of cystic fibrosis transmembrane conductance regulator and DeltaF508CFTR on inflammatory response, ER stress, and Ca2+ of airway epithelia.* Am J Physiol Lung Cell Mol Physiol, 2007. **293**(5): p. L1250-60.
309. Voisin, G., et al., *Oxidative stress modulates the expression of genes involved in cell survival in DeltaF508 cystic fibrosis airway epithelial cells.* Physiol Genomics, 2014. **46**(17): p. 634-46.
310. Primo-Parmo, S.L., et al., *Characterization of 12 silent alleles of the human butyrylcholinesterase (BCHE) gene.* Am J Hum Genet, 1996. **58**(1): p. 52-64.
311. Sorenson, R.C., et al., *Human serum Paraoxonase/Arylesterase's retained hydrophobic N-terminal leader sequence associates with HDLs by binding phospholipids : apolipoprotein A-I stabilizes activity.* Arterioscler Thromb Vasc Biol, 1999. **19**(9): p. 2214-25.
312. Ng, C.J., et al., *Paraoxonase-2 deficiency aggravates atherosclerosis in mice despite lower apolipoprotein-B-containing lipoproteins: anti-atherogenic role for paraoxonase-2.* J Biol Chem, 2006. **281**(40): p. 29491-500.
313. Shih, D.M., et al., *Mice lacking serum paraoxonase are susceptible to organophosphate toxicity and atherosclerosis.* Nature, 1998. **394**(6690): p. 284-7.
314. Shih, D.M., et al., *Decreased obesity and atherosclerosis in human paraoxonase 3 transgenic mice.* Circ Res, 2007. **100**(8): p. 1200-7.

315. Witte, I., et al., *Beyond reduction of atherosclerosis: PON2 provides apoptosis resistance and stabilizes tumor cells.* Cell Death Dis, 2011. **2**: p. e112.
316. Wagner, V.E., et al., *Microarray analysis of Pseudomonas aeruginosa quorum-sensing regulons: effects of growth phase and environment.* J Bacteriol, 2003. **185**(7): p. 2080-95.
317. Schuster, M., et al., *Identification, timing, and signal specificity of Pseudomonas aeruginosa quorum-controlled genes: a transcriptome analysis.* J Bacteriol, 2003. **185**(7): p. 2066-79.
318. Gardner, O.S., B.J. Dewar, and L.M. Graves, *Activation of mitogen-activated protein kinases by peroxisome proliferator-activated receptor ligands: an example of nongenomic signaling.* Mol Pharmacol, 2005. **68**(4): p. 933-41.
319. De Bosscher, K., W. Vanden Berghe, and G. Haegeman, *Cross-talk between nuclear receptors and nuclear factor kappaB.* Oncogene, 2006. **25**(51): p. 6868-86.
320. Ali, N., *PON2 and PPARgamma in Cystic Fibrosis*, in *School of Medicine*. 2010, UTAS: Hobart.
321. Fuhrman, B., et al., *Urokinase activates macrophage PON2 gene transcription via the PI3K/ROS/MEK/SREBP-2 signalling cascade mediated by the PDGFR-beta.* Cardiovasc Res, 2009. **84**(1): p. 145-54.
322. Rosenblat, M., et al., *Increased macrophage cholesterol biosynthesis and decreased cellular paraoxonase 2 (PON2) expression in Delta6-desaturase knockout (6-DS KO) mice: beneficial effects of arachidonic acid.* Atherosclerosis, 2010. **210**(2): p. 414-21.
323. Tomas, M., et al., *Effect of simvastatin therapy on paraoxonase activity and related lipoproteins in familial hypercholesterolemic patients.* Arterioscler Thromb Vasc Biol, 2000. **20**(9): p. 2113-9.
324. Wang, Q., et al., *Statins: multiple neuroprotective mechanisms in neurodegenerative diseases.* Exp Neurol, 2011. **230**(1): p. 27-34.
325. Khateeb, J., et al., *Paraoxonase 1 (PON1) expression in hepatocytes is upregulated by pomegranate polyphenols: a role for PPAR-gamma pathway.* Atherosclerosis, 2010. **208**(1): p. 119-25.
326. Fuhrman, B., *Regulation of hepatic paraoxonase-1 expression.* J Lipids, 2012. **2012**: p. 684010.
327. Pawliczak, R., et al., *85-kDa cytosolic phospholipase A2 mediates peroxisome proliferator-activated receptor gamma activation in human lung epithelial cells.* J Biol Chem, 2002. **277**(36): p. 33153-63.
328. Wang, A.C., et al., *Peroxisome proliferator-activated receptor-gamma regulates airway epithelial cell activation.* Am J Respir Cell Mol Biol, 2001. **24**(6): p. 688-93.
329. Nordeen, S.K., *Luciferase reporter gene vectors for analysis of promoters and enhancers.* Biotechniques, 1988. **6**(5): p. 454-8.
330. Forman, B.M., et al., *15-Deoxy-delta 12, 14-prostaglandin J2 is a ligand for the adipocyte determination factor PPAR gamma.* Cell, 1995. **83**(5): p. 803-12.
331. Gurnell, M., et al., *A dominant-negative peroxisome proliferator-activated receptor gamma (PPARgamma) mutant is a constitutive repressor and inhibits PPARgamma-mediated adipogenesis.* J Biol Chem, 2000. **275**(8): p. 5754-9.
332. Leesnitzer, L.M., et al., *Functional consequences of cysteine modification in the ligand binding sites of peroxisome proliferator activated receptors by GW9662.* Biochemistry, 2002. **41**(21): p. 6640-50.
333. Kahn, C.R., L. Chen, and S.E. Cohen, *Unraveling the mechanism of action of thiazolidinediones.* J Clin Invest, 2000. **106**(11): p. 1305-7.
334. Nagasawa, M., et al., *Identification of a functional peroxisome proliferator-activated receptor (PPAR) response element (PPRE) in the human apolipoprotein A-IV gene.* Biochem Pharmacol, 2009. **78**(5): p. 523-30.

335. Bulger, M. and M. Groudine, *Functional and mechanistic diversity of distal transcription enhancers.* Cell, 2011. **144**(3): p. 327-39.
336. Lettice, L.A., et al., *A long-range Shh enhancer regulates expression in the developing limb and fin and is associated with preaxial polydactyly.* Hum Mol Genet, 2003. **12**(14): p. 1725-35.
337. Welch, J.S., et al., *PPARgamma and PPARdelta negatively regulate specific subsets of lipopolysaccharide and IFN-gamma target genes in macrophages.* Proc Natl Acad Sci U S A, 2003. **100**(11): p. 6712-7.
338. Seargent, J.M., E.A. Yates, and J.H. Gill, *GW9662, a potent antagonist of PPARgamma, inhibits growth of breast tumour cells and promotes the anticancer effects of the PPARgamma agonist rosiglitazone, independently of PPARgamma activation.* Br J Pharmacol, 2004. **143**(8): p. 933-7.
339. Derlacz, R.A., et al., *PPAR-gamma-independent inhibitory effect of rosiglitazone on glucose synthesis in primary cultured rabbit kidney-cortex tubules.* Biochem Cell Biol, 2008. **86**(5): p. 396-404.
340. Scatena, R., et al., *Mitochondrial respiratory chain dysfunction, a non-receptor-mediated effect of synthetic PPAR-ligands: biochemical and pharmacological implications.* Biochem Biophys Res Commun, 2004. **319**(3): p. 967-73.
341. Perez-Ortiz, J.M., et al., *Glitazones differentially regulate primary astrocyte and glioma cell survival. Involvement of reactive oxygen species and peroxisome proliferator-activated receptor-gamma.* J Biol Chem, 2004. **279**(10): p. 8976-85.
342. Andersson, C., et al., *Alterations in immune response and PPAR/LXR regulation in cystic fibrosis macrophages.* J Cyst Fibros, 2008. **7**(1): p. 68-78.
343. van Heeckeren, A.M., et al., *Response to acute lung infection with mucoid Pseudomonas aeruginosa in cystic fibrosis mice.* Am J Respir Crit Care Med, 2006. **173**(3): p. 288-96.
344. Watkins, P.B., *Idiosyncratic liver injury: challenges and approaches.* Toxicol Pathol, 2005. **33**(1): p. 1-5.
345. Nissen, S.E. and K. Wolski, *Effect of rosiglitazone on the risk of myocardial infarction and death from cardiovascular causes.* N Engl J Med, 2007. **356**(24): p. 2457-71.
346. Lincoff, A.M., et al., *Pioglitazone and risk of cardiovascular events in patients with type 2 diabetes mellitus: a meta-analysis of randomized trials.* JAMA, 2007. **298**(10): p. 1180-8.
347. FDA. *FDA Drug Safety Communication: FDA requires removal of some prescribing and dispensing restrictions for rosiglitazone-containing diabetes medicines*. 2013 [cited 2014 17/10]; Available from: http://www.fda.gov/downloads/Drugs/DrugSafety/UCM381108.pdf.
348. Williams, P., et al., *Look who's talking: communication and quorum sensing in the bacterial world.* Philos Trans R Soc Lond B Biol Sci, 2007. **362**(1483): p. 1119-34.
349. Stoltz, D.A., et al., *A common mutation in paraoxonase-2 results in impaired lactonase activity.* J Biol Chem, 2009. **284**(51): p. 35564-71.
350. Ng, C.J., et al., *Adenovirus mediated expression of human paraoxonase 2 protects against the development of atherosclerosis in apolipoprotein E-deficient mice.* Mol Genet Metab, 2006. **89**(4): p. 368-73.
351. Huang, J.J., et al., *Identification of QuiP, the product of gene PA1032, as the second acyl-homoserine lactone acylase of Pseudomonas aeruginosa PAO1.* Appl Environ Microbiol, 2006. **72**(2): p. 1190-7.
352. Papaioannou, E., et al., *Quorum-quenching acylase reduces the virulence of Pseudomonas aeruginosa in a Caenorhabditis elegans infection model.* Antimicrob Agents Chemother, 2009. **53**(11): p. 4891-7.

353. Wahjudi, M., et al., *PA0305 of Pseudomonas aeruginosa is a quorum quenching acylhomoserine lactone acylase belonging to the Ntn hydrolase superfamily.* Microbiology, 2011. **157**(Pt 7): p. 2042-55.
354. Chen, C.N., et al., *A probable aculeacin A acylase from the Ralstonia solanacearum GMI1000 is N-acyl-homoserine lactone acylase with quorum-quenching activity.* BMC Microbiol, 2009. **9**: p. 89.
355. Sio, C.F., et al., *Quorum quenching by an N-acyl-homoserine lactone acylase from Pseudomonas aeruginosa PAO1.* Infect Immun, 2006. **74**(3): p. 1673-82.
356. Brushia, R.J., et al., *Baculovirus-mediated expression and purification of human serum paraoxonase 1A.* J Lipid Res, 2001. **42**(6): p. 951-8.
357. Aharoni, A., et al., *Directed evolution of mammalian paraoxonases PON1 and PON3 for bacterial expression and catalytic specialization.* Proc Natl Acad Sci U S A, 2004. **101**(2): p. 482-7.
358. Josse, D., et al., *Identification of residues essential for human paraoxonase (PON1) arylesterase/organophosphatase activities.* Biochemistry, 1999. **38**(9): p. 2816-25.
359. Teiber, J. and D. Draganov, *High-performance Liquid Chromatography analysis of N-acyl Homoserine Lactone hydrolysis by Paraoxonases*, in *Quorum Sensing: Methods and Protocols*, K.P. Rumbaugh, Editor. 2011, Springer Science+Business Media. p. 291-298.
360. Hong, K.W., et al., *Quorum quenching revisited--from signal decays to signalling confusion.* Sensors (Basel), 2012. **12**(4): p. 4661-96.
361. Huang, J.J., et al., *Utilization of acyl-homoserine lactone quorum signals for growth by a soil pseudomonad and Pseudomonas aeruginosa PAO1.* Appl Environ Microbiol, 2003. **69**(10): p. 5941-9.
362. Lazenby, J.J., et al., *A quadruple knockout of lasIR and rhlIR of Pseudomonas aeruginosa PAO1 that retains wild-type twitching motility has equivalent infectivity and persistence to PAO1 in a mouse model of lung infection.* PLoS One, 2013. **8**(4): p. e60973.
363. Schaber, J.A., et al., *Analysis of quorum sensing-deficient clinical isolates of Pseudomonas aeruginosa.* J Med Microbiol, 2004. **53**(Pt 9): p. 841-53.
364. Davies, J. and B.D. Davis, *Misreading of ribonucleic acid code words induced by aminoglycoside antibiotics. The effect of drug concentration.* J Biol Chem, 1968. **243**(12): p. 3312-6.
365. Morita, Y., M.L. Sobel, and K. Poole, *Antibiotic inducibility of the MexXY multidrug efflux system of Pseudomonas aeruginosa: involvement of the antibiotic-inducible PA5471 gene product.* J Bacteriol, 2006. **188**(5): p. 1847-55.
366. Jeannot, K., et al., *Induction of the MexXY efflux pump in Pseudomonas aeruginosa is dependent on drug-ribosome interaction.* J Bacteriol, 2005. **187**(15): p. 5341-6.
367. Evans, K., et al., *Influence of the MexAB-OprM multidrug efflux system on quorum sensing in Pseudomonas aeruginosa.* J Bacteriol, 1998. **180**(20): p. 5443-7.
368. Hassett, D.J., et al., *Quorum sensing in Pseudomonas aeruginosa controls expression of catalase and superoxide dismutase genes and mediates biofilm susceptibility to hydrogen peroxide.* Mol Microbiol, 1999. **34**(5): p. 1082-93.
369. Erickson, D.L., et al., *Pseudomonas aeruginosa relA contributes to virulence in Drosophila melanogaster.* Infect Immun, 2004. **72**(10): p. 5638-45.
370. Kayama, S., et al., *The role of rpoS gene and quorum-sensing system in ofloxacin tolerance in Pseudomonas aeruginosa.* FEMS Microbiol Lett, 2009. **298**(2): p. 184-92.
371. Balasubramanian, D., et al., *Deep sequencing analyses expands the Pseudomonas aeruginosa AmpR regulon to include small RNA-mediated regulation of iron acquisition, heat shock and oxidative stress response.* Nucleic Acids Res, 2014. **42**(2): p. 979-98.

372. Balasubramanian, D., et al., *Co-regulation of {beta}-lactam resistance, alginate production and quorum sensing in Pseudomonas aeruginosa.* J Med Microbiol, 2011. **60**(Pt 2): p. 147-56.
373. Hoffman, L.R., et al., *Aminoglycoside antibiotics induce bacterial biofilm formation.* Nature, 2005. **436**(7054): p. 1171-5.
374. Brackman, G., et al., *Quorum sensing inhibitors increase the susceptibility of bacterial biofilms to antibiotics in vitro and in vivo.* Antimicrob Agents Chemother, 2011. **55**(6): p. 2655-61.
375. Rampioni, G., et al., *RsaL provides quorum sensing homeostasis and functions as a global regulator of gene expression in Pseudomonas aeruginosa.* Mol Microbiol, 2007. **66**(6): p. 1557-65.
376. Lee, J., et al., *A cell-cell communication signal integrates quorum sensing and stress response.* Nat Chem Biol, 2013. **9**(5): p. 339-43.
377. Davidson, D.J., et al., *Lung disease in the cystic fibrosis mouse exposed to bacterial pathogens.* Nat Genet, 1995. **9**(4): p. 351-7.
378. Matsui, H., et al., *Evidence for periciliary liquid layer depletion, not abnormal ion composition, in the pathogenesis of cystic fibrosis airways disease.* Cell, 1998. **95**(7): p. 1005-15.
379. Worlitzsch, D., et al., *Effects of reduced mucus oxygen concentration in airway Pseudomonas infections of cystic fibrosis patients.* J Clin Invest, 2002. **109**(3): p. 317-25.
380. Machen, T.E., *Innate immune response in CF airway epithelia: hyperinflammatory?* Am J Physiol Cell Physiol, 2006. **291**(2): p. C218-30.
381. Lau, G.W., D.J. Hassett, and B.E. Britigan, *Modulation of lung epithelial functions by Pseudomonas aeruginosa.* Trends Microbiol, 2005. **13**(8): p. 389-97.
382. Cheung, A.T., et al., *Chronic Pseudomonas aeruginosa endobronchitis in rhesus monkeys: I. Effects of pentoxifylline on neutrophil influx.* J Med Primatol, 1992. **21**(7-8): p. 357-62.
383. Winnie, G.B., et al., *Induction of phagocytic inhibitory activity in cats with chronic Pseudomonas aeruginosa pulmonary infection.* Infect Immun, 1982. **38**(3): p. 1088-93.
384. Pennington, J.E., et al., *Active immunization with lipopolysaccharide Pseudomonas antigen for chronic Pseudomonas bronchopneumonia in guinea pigs.* J Clin Invest, 1981. **68**(5): p. 1140-8.
385. Sun, X., et al., *Disease phenotype of a ferret CFTR-knockout model of cystic fibrosis.* J Clin Invest, 2010. **120**(9): p. 3149-60.
386. Rogers, C.S., et al., *Production of CFTR-null and CFTR-DeltaF508 heterozygous pigs by adeno-associated virus-mediated gene targeting and somatic cell nuclear transfer.* J Clin Invest, 2008. **118**(4): p. 1571-7.
387. Stoltz, D.A., et al., *Cystic fibrosis pigs develop lung disease and exhibit defective bacterial eradication at birth.* Sci Transl Med, 2010. **2**(29): p. 29ra31.
388. Glavac, D., et al., *Screening methods for cystic fibrosis transmembrane conductance regulator (CFTR) gene mutations in non-human primates.* Pflugers Arch, 2000. **439**(3 Suppl): p. R12-3.
389. Tata, F., et al., *Cloning the mouse homolog of the human cystic fibrosis transmembrane conductance regulator gene.* Genomics, 1991. **10**(2): p. 301-7.
390. Snouwaert, J.N., et al., *An animal model for cystic fibrosis made by gene targeting.* Science, 1992. **257**(5073): p. 1083-8.
391. Ratcliff, R., et al., *Production of a severe cystic fibrosis mutation in mice by gene targeting.* Nat Genet, 1993. **4**(1): p. 35-41.
392. O'Neal, W.K., et al., *A severe phenotype in mice with a duplication of exon 3 in the cystic fibrosis locus.* Hum Mol Genet, 1993. **2**(10): p. 1561-9.

393. Rozmahel, R., et al., *Modulation of disease severity in cystic fibrosis transmembrane conductance regulator deficient mice by a secondary genetic factor.* Nat Genet, 1996. **12**(3): p. 280-7.
394. van Doorninck, J.H., et al., *A mouse model for the cystic fibrosis delta F508 mutation.* EMBO J, 1995. **14**(18): p. 4403-11.
395. Delaney, S.J., et al., *Cystic fibrosis mice carrying the missense mutation G551D replicate human genotype-phenotype correlations.* EMBO J, 1996. **15**(5): p. 955-63.
396. Dickinson, P., et al., *Enhancing the efficiency of introducing precise mutations into the mouse genome by hit and run gene targeting.* Transgenic Res, 2000. **9**(1): p. 55-66.
397. Zhou, L., et al., *Correction of lethal intestinal defect in a mouse model of cystic fibrosis by human CFTR.* Science, 1994. **266**(5191): p. 1705-8.
398. McCray, P.B., Jr., et al., *Efficient killing of inhaled bacteria in DeltaF508 mice: role of airway surface liquid composition.* Am J Physiol, 1999. **277**(1 Pt 1): p. L183-90.
399. Kent, G., et al., *Lung disease in mice with cystic fibrosis.* J Clin Invest, 1997. **100**(12): p. 3060-9.
400. Grubb, B.R. and R.C. Boucher, *Pathophysiology of gene-targeted mouse models for cystic fibrosis.* Physiol Rev, 1999. **79**(1 Suppl): p. S193-214.
401. Southern, P.M., Jr., A.K. Pierce, and J.P. Sanford, *Exposure chamber for 66 mice suitable for use with the henderson aerosol apparatus.* Appl Microbiol, 1968. **16**(3): p. 540-2.
402. Tang, H., M. Kays, and A. Prince, *Role of Pseudomonas aeruginosa pili in acute pulmonary infection.* Infect Immun, 1995. **63**(4): p. 1278-85.
403. Guilbault, C., et al., *Cystic fibrosis lung disease following infection with Pseudomonas aeruginosa in Cftr knockout mice using novel non-invasive direct pulmonary infection technique.* Lab Anim, 2005. **39**(3): p. 336-52.
404. Johansen, H.K., *Potential of preventing Pseudomonas aeruginosa lung infections in cystic fibrosis patients: experimental studies in animals.* APMIS Suppl, 1996. **63**: p. 5-42.
405. Yu, H., et al., *Microbial pathogenesis in cystic fibrosis: pulmonary clearance of mucoid Pseudomonas aeruginosa and inflammation in a mouse model of repeated respiratory challenge.* Infect Immun, 1998. **66**(1): p. 280-8.
406. Yu, H., S.Z. Nasr, and V. Deretic, *Innate lung defenses and compromised Pseudomonas aeruginosa clearance in the malnourished mouse model of respiratory infections in cystic fibrosis.* Infect Immun, 2000. **68**(4): p. 2142-7.
407. Cash, H.A., et al., *A rat model of chronic respiratory infection with Pseudomonas aeruginosa.* Am Rev Respir Dis, 1979. **119**(3): p. 453-9.
408. Stevenson, M.M., et al., *In vitro and in vivo T cell responses in mice during bronchopulmonary infection with mucoid Pseudomonas aeruginosa.* Clin Exp Immunol, 1995. **99**(1): p. 98-105.
409. Morissette, C., E. Skamene, and F. Gervais, *Endobronchial inflammation following Pseudomonas aeruginosa infection in resistant and susceptible strains of mice.* Infect Immun, 1995. **63**(5): p. 1718-24.
410. Hoffmann, N., et al., *Novel mouse model of chronic Pseudomonas aeruginosa lung infection mimicking cystic fibrosis.* Infect Immun, 2005. **73**(4): p. 2504-14.
411. Starke, J.R., et al., *A mouse model of chronic pulmonary infection with Pseudomonas aeruginosa and Pseudomonas cepacia.* Pediatr Res, 1987. **22**(6): p. 698-702.
412. Weiss, A.A. and M.S. Goodwin, *Lethal infection by Bordetella pertussis mutants in the infant mouse model.* Infect Immun, 1989. **57**(12): p. 3757-64.
413. Diavatopoulos, D.A., et al., *Influenza A virus facilitates Streptococcus pneumoniae transmission and disease.* FASEB J, 2010. **24**(6): p. 1789-98.

414. Munder, A., et al., *Pulmonary microbial infection in mice: comparison of different application methods and correlation of bacterial numbers and histopathology.* Exp Toxicol Pathol, 2002. **54**(2): p. 127-33.
415. Tam, M., G.J. Snipes, and M.M. Stevenson, *Characterization of chronic bronchopulmonary Pseudomonas aeruginosa infection in resistant and susceptible inbred mouse strains.* Am J Respir Cell Mol Biol, 1999. **20**(4): p. 710-9.
416. Gosselin, D., et al., *Role of tumor necrosis factor alpha in innate resistance to mouse pulmonary infection with Pseudomonas aeruginosa.* Infect Immun, 1995. **63**(9): p. 3272-8.
417. Sapru, K., P.K. Stotland, and M.M. Stevenson, *Quantitative and qualitative differences in bronchoalveolar inflammatory cells in Pseudomonas aeruginosa-resistant and -susceptible mice.* Clin Exp Immunol, 1999. **115**(1): p. 103-9.
418. Soudi, S., et al., *Comparative study of the effect of LPS on the function of BALB/c and C57BL/6 peritoneal macrophages.* Cell J, 2013. **15**(1): p. 45-54.
419. Raoust, E., et al., *Pseudomonas aeruginosa LPS or flagellin are sufficient to activate TLR-dependent signaling in murine alveolar macrophages and airway epithelial cells.* PLoS One, 2009. **4**(10): p. e7259.
420. Lavenir, R., et al., *Improved reliability of Pseudomonas aeruginosa PCR detection by the use of the species-specific ecfX gene target.* J Microbiol Methods, 2007. **70**(1): p. 20-9.
421. da Silva Filho, L.V., et al., *The combination of PCR and serology increases the diagnosis of Pseudomonas aeruginosa colonization/infection in cystic fibrosis.* Pediatr Pulmonol, 2007. **42**(10): p. 938-44.
422. Xu, J., et al., *Early detection of Pseudomonas aeruginosa--comparison of conventional versus molecular (PCR) detection directly from adult patients with cystic fibrosis (CF).* Ann Clin Microbiol Antimicrob, 2004. **3**: p. 21.
423. Qin, X., et al., *Use of real-time PCR with multiple targets to identify Pseudomonas aeruginosa and other nonfermenting gram-negative bacilli from patients with cystic fibrosis.* J Clin Microbiol, 2003. **41**(9): p. 4312-7.
424. Munder, A., et al., *In vivo imaging of bioluminescent Pseudomonas aeruginosa in an acute murine airway infection model.* Pathog Dis, 2014.
425. Hamblin, M.R., et al., *Optical monitoring and treatment of potentially lethal wound infections in vivo.* J Infect Dis, 2003. **187**(11): p. 1717-25.
426. Rasko, D.A. and V. Sperandio, *Anti-virulence strategies to combat bacteria-mediated disease.* Nat Rev Drug Discov, 2010. **9**(2): p. 117-28.
427. Rumbaugh, K.P., et al., *Contribution of quorum sensing to the virulence of Pseudomonas aeruginosa in burn wound infections.* Infect Immun, 1999. **67**(11): p. 5854-62.
428. Rumbaugh, K.P., J.A. Griswold, and A.N. Hamood, *Contribution of the regulatory gene lasR to the pathogenesis of Pseudomonas aeruginosa infection of burned mice.* J Burn Care Rehabil, 1999. **20**(1 Pt 1): p. 42-9.
429. Stoodley, P., et al., *The formation of migratory ripples in a mixed species bacterial biofilm growing in turbulent flow.* Environ Microbiol, 1999. **1**(5): p. 447-55.
430. Heydorn, A., et al., *Statistical analysis of Pseudomonas aeruginosa biofilm development: impact of mutations in genes involved in twitching motility, cell-to-cell signaling, and stationary-phase sigma factor expression.* Appl Environ Microbiol, 2002. **68**(4): p. 2008-17.
431. Juhas, M., L. Eberl, and B. Tummler, *Quorum sensing: the power of cooperation in the world of Pseudomonas.* Environ Microbiol, 2005. **7**(4): p. 459-71.
432. Hentzer, M., et al., *Attenuation of Pseudomonas aeruginosa virulence by quorum sensing inhibitors.* EMBO J, 2003. **22**(15): p. 3803-15.

433. Tan, S.Y., et al., *Identification of five structurally unrelated quorum-sensing inhibitors of Pseudomonas aeruginosa from a natural-derivative database.* Antimicrob Agents Chemother, 2013. **57**(11): p. 5629-41.
434. Kiran, S., et al., *Enzymatic quorum quenching increases antibiotic susceptibility of multidrug resistant Pseudomonas aeruginosa.* Iran J Microbiol, 2011. **3**(1): p. 1-12.
435. Schipper, C., et al., *Metagenome-derived clones encoding two novel lactonase family proteins involved in biofilm inhibition in Pseudomonas aeruginosa.* Appl Environ Microbiol, 2009. **75**(1): p. 224-33.
436. Struss, A.K., et al., *Toward implementation of quorum sensing autoinducers as biomarkers for infectious disease states.* Anal Chem, 2013. **85**(6): p. 3355-62.
437. Favre-Bonte, S., et al., *Detection of Pseudomonas aeruginosa cell-to-cell signals in lung tissue of cystic fibrosis patients.* Microb Pathog, 2002. **32**(3): p. 143-7.
438. Winstanley, C. and J.L. Fothergill, *The role of quorum sensing in chronic cystic fibrosis Pseudomonas aeruginosa infections.* FEMS Microbiol Lett, 2009. **290**(1): p. 1-9.
439. Smith, E.E., et al., *Genetic adaptation by Pseudomonas aeruginosa to the airways of cystic fibrosis patients.* Proc Natl Acad Sci U S A, 2006. **103**(22): p. 8487-92.
440. D'Argenio, D.A., et al., *Growth phenotypes of Pseudomonas aeruginosa lasR mutants adapted to the airways of cystic fibrosis patients.* Mol Microbiol, 2007. **64**(2): p. 512-33.
441. Bjarnsholt, T., et al., *Quorum sensing and virulence of Pseudomonas aeruginosa during lung infection of cystic fibrosis patients.* PLoS One, 2010. **5**(4): p. e10115.
442. Wilder, C.N., S.P. Diggle, and M. Schuster, *Cooperation and cheating in Pseudomonas aeruginosa: the roles of the las, rhl and pqs quorum-sensing systems.* ISME J, 2011. **5**(8): p. 1332-43.
443. Diggle, S.P., et al., *Cooperation and conflict in quorum-sensing bacterial populations.* Nature, 2007. **450**(7168): p. 411-4.
444. Ricote, M. and C.K. Glass, *PPARs and molecular mechanisms of transrepression.* Biochim Biophys Acta, 2007. **1771**(8): p. 926-35.
445. Bartoszewski, R., et al., *Activation of the unfolded protein response by deltaF508 CFTR.* Am J Respir Cell Mol Biol, 2008. **39**(4): p. 448-57.
446. Ntimbane, T., et al., *Cystic fibrosis-related diabetes: from CFTR dysfunction to oxidative stress.* Clin Biochem Rev, 2009. **30**(4): p. 153-77.
447. Vic, P., et al., *Efficacy, tolerance, and pharmacokinetics of once daily tobramycin for pseudomonas exacerbations in cystic fibrosis.* Arch Dis Child, 1998. **78**(6): p. 536-9.
448. Rosenfeld, M., et al., *Serum and lower respiratory tract drug concentrations after tobramycin inhalation in young children with cystic fibrosis.* J Pediatr, 2001. **139**(4): p. 572-7.
449. Contrepois, A., et al., *Renal disposition of gentamicin, dibekacin, tobramycin, netilmicin, and amikacin in humans.* Antimicrob Agents Chemother, 1985. **27**(4): p. 520-4.
450. Town, D.J., et al., *Creatinine clearance as predictor of tobramycin elimination in adult patients with cystic fibrosis.* Ther Drug Monit, 1996. **18**(5): p. 562-9.
451. Rodman, D.P., A.J. Maxwell, and J.T. McKnight, *Extended dosage intervals for aminoglycosides.* Am J Hosp Pharm, 1994. **51**(16): p. 2016-21.
452. Stintzi, A., et al., *Quorum-sensing and siderophore biosynthesis in Pseudomonas aeruginosa: lasR/lasI mutants exhibit reduced pyoverdine biosynthesis.* FEMS Microbiol Lett, 1998. **166**(2): p. 341-5.
453. Chen, B., et al., *Influence of calcium ions on the structure and stability of recombinant human deoxyribonuclease I in the aqueous and lyophilized states.* J Pharm Sci, 1999. **88**(4): p. 477-82.
454. Sanders, N.N., et al., *Role of magnesium in the failure of rhDNase therapy in patients with cystic fibrosis.* Thorax, 2006. **61**(11): p. 962-8.

455. Roche, *Pulmozyme data Sheet*. 2014, Roche.
456. Lewenza, S., et al., *Quorum sensing in Burkholderia cepacia: identification of the LuxRI homologs CepRI.* J Bacteriol, 1999. **181**(3): p. 748-56.
457. Gotschlich, A., et al., *Synthesis of multiple N-acylhomoserine lactones is wide-spread among the members of the Burkholderia cepacia complex.* Syst Appl Microbiol, 2001. **24**(1): p. 1-14.
458. Ee, R., et al., *Quorum sensing activity in Pandoraea pnomenusa RB38.* Sensors (Basel), 2014. **14**(6): p. 10177-86.
459. Bodey, G.P., et al., *Infections caused by Pseudomonas aeruginosa.* Rev Infect Dis, 1983. **5**(2): p. 279-313.
460. Murphy, T.F., *The many faces of Pseudomonas aeruginosa in chronic obstructive pulmonary disease.* Clin Infect Dis, 2008. **47**(12): p. 1534-6.
461. Schuster, M.G. and A.H. Norris, *Community-acquired Pseudomonas aeruginosa pneumonia in patients with HIV infection.* AIDS, 1994. **8**(10): p. 1437-41.
462. Hachem, R.Y., et al., *Colistin is effective in treatment of infections caused by multidrug-resistant Pseudomonas aeruginosa in cancer patients.* Antimicrob Agents Chemother, 2007. **51**(6): p. 1905-11.

APPENDIX

8.1 EXAMPLE CALCULATION OF BACULOVIRUS TITRE BY END-POINT DILUTION METHOD

Dilution	Infected wells	Uninfected wells
10^{-5}	12	0
10^{-6}	8	4
10^{-7}	1	11
10^{-8}	0	12

At the 10^{-5}, all 12 wells were infected. However, at the 10^{-6} dilution, 8 weeks were infected and only one well at 10^{-7}. Assuming that these wells would also have been infected by 10^{-5} dilution, the total number of infected wells is taken to be 21 (12 + 8 + 1). Similarly, the same could be said about the uninfected cells and hence the total number of uninfected wells at 10^{-8} would be 27 (4+11+12). Extending this, the following results were obtained.

Dilution	Infected	Uninfected	% Infected
10^{-5}	21	0	100.0
10^{-6}	9	4	69.2
10^{-7}	1	15	6.3
10^{-8}	0	27	0.0

In this case, the dilution that would have given 50% infection lies between 10^{-6} and 10^{-7}. This dilution is calculated by linear interpolation between infection rates observed at these dilutions.

First, the proportionate distance (PD) of a 50% response from the response above 50% is calculated using the following formula:

PD = (A-50)/(A-B)

Where A is the % response above 50%, and B is the % response below 50%. In the above example,

PD = (69.2-50)/(69.2-6.3)

= 0.305

The dose that would give a 50% response, the $TCID_{50}$, is then calculated using the following formula:

Log $TCID_{50}$ = log of the dilution giving a response greater than 50% - PD of that response

Thus,

Log $TCID_{50}$ = - 6 - 0.305

= - 6.305

Therefore, $TCID_{50} = 4.95 \times 10^{-7}$

The titre of virus ($TCID_{50}$ / 10 µL) =(1/ $TCID_{50}$) = 1 / 4.95×10^{-7} = 2.02×10^{6} $TCID_{50}$ / µL

The titre of virus ($TCID_{50}$ / 10 mL) = 2.02×10^{6} $TCID_{50}$ / µL X 100 = 2.02×10^{8} $TCID_{50}$ / mL

Next,

The titre of virus (pfu/ mL) = The titre of virus ($TCID_{50}$ / mL) x 0.69 (constant based on Poisson distribution), therefore

The titre of virus (pfu/ mL) = 2.02×10^{8} $TCID_{50}$ / mL x 0.69

= 1.4×10^{8} pfu/mL

Figure 8.1 Example calculation of baculovirus titre by end-point dilution method. Example adapted from O'Reilly et al. 1992.

8.2 COMPLETE TRANSCRIPTOM ARRAY GENE EXPRESSION DATA SET

Table 8.2 Complete transcriptome array gene expression data.

Array data arranged from highest fold change to lowest. The Affymetrix GeneChip Human Transcriptome array 2.0 platform was used.

Gene Symbol	Description	Fold Change
CHD5	chromodomain helicase DNA binding protein 5	9.94
POLN	polymerase (DNA directed) nu	9.85
PRAM1	PML-RARA regulated adaptor molecule 1	8.62
RC3H1	ring finger and CCCH-type domains 1	8.12
FRMD4B	FERM domain containing 4B	7.77
MUC19	mucin 19, oligomeric	7.43
SORBS2	sorbin and SH3 domain containing 2	7.38
LDHB	lactate dehydrogenase B	7.34
VPS13A	vacuolar protein sorting 13 homolog A (S. cerevisiae)	7.15
TDRKH	tudor and KH domain containing	7.09
PNPT1	polyribonucleotide nucleotidyltransferase 1	7
ASIC4	acid-sensing (proton-gated) ion channel family member 4	6.76
RCOR3	REST corepressor 3	6.41
NIPBL	Nipped-B homolog (Drosophila)	6.35
TAPT1	transmembrane anterior posterior transformation 1	6.33
CCDC38	coiled-coil domain containing 38	6.12
SLC3A1	solute carrier family 3 member 1	6.08
LRRCC1	leucine rich repeat and coiled-coil centrosomal protein 1	5.9
FAM82A1	family with sequence similarity 82, member A1	5.81
ZFAND6	zinc finger, AN1-type domain 6	5.7
SLC30A8	solute carrier family 30 (zinc transporter), member 8	5.65
NRCAM	neuronal cell adhesion molecule	5.62
MEIS1	Meis homeobox 1	5.53
SERPINI1	serpin peptidase inhibitor, clade I (neuroserpin), member 1	5.5
UVSSA	UV-stimulated scaffold protein A	5.45
ADAM2	ADAM metallopeptidase domain 2	5.43
GRHL1	grainyhead-like 1 (Drosophila)	5.42
AK5	adenylate kinase 5	5.41
MAP3K2	mitogen-activated protein kinase kinase kinase 2	5.41
RBM26-AS1	RBM26 antisense RNA 1 (non-protein coding)	5.38
POLN	polymerase (DNA directed) nu	5.37
PLCB4	phospholipase C, beta 4	5.31
KRT6A	keratin 6A	5.27

RERE	arginine-glutamic acid dipeptide (RE) repeats	5.27
C1orf222, KIAA1751	chromosome 1 open reading frame 222, KIAA1751	5.17
TTLL5	tubulin tyrosine ligase-like family, member 5	5.15
KLRG1	killer cell lectin-like receptor subfamily G, member 1	5.14
DNAH6	dynein, axonemal, heavy chain 6	5.1
WNK3	WNK lysine deficient protein kinase 3	5.08
C1orf222, KIAA1751	chromosome 1 open reading frame 222, KIAA1751	5.04
RAD17	RAD17 homolog (S. pombe)	5.03
ATP13A2	ATPase type 13A2	5.01
GSTCD	glutathione S-transferase, C-terminal domain containing	5.01
PDE8A	phosphodiesterase 8A	4.99
TRHDE-AS1	TRHDE antisense RNA 1 (non-protein coding)	4.94
CSTF2	cleavage stimulation factor, 3' pre-RNA, subunit 2, 64kDa	4.92
AKAP7	A kinase (PRKA) anchor protein 7	4.85
DDHD2	DDHD domain containing 2	4.82
GPR97	G protein-coupled receptor 97	4.82
MDH1B	malate dehydrogenase 1B, NAD (soluble)	4.79
NGFR	nerve growth factor receptor	4.77
ARHGEF6	Rac/Cdc42 guanine nucleotide exchange factor (GEF) 6	4.76
C17orf104	chromosome 17 open reading frame 104	4.75
VPS13B	vacuolar protein sorting 13 homolog B (yeast)	4.72
CGN	cingulin	4.65
FRYL	FRY-like	4.64
FSD1L	fibronectin type III and SPRY domain containing 1-like	4.64
MTUS1	microtubule associated tumor suppressor 1	4.61
CASP3	caspase 3, apoptosis-related cysteine peptidase	4.55
NEDD1	neural precursor cell expressed, developmentally down-regulated 1	4.54
FSD2	fibronectin type III and SPRY domain containing 2	4.5
LOC100302640	uncharacterized LOC100302640	4.5
SNCAIP	synuclein, alpha interacting protein	4.5
KANK1	KN motif and ankyrin repeat domains 1	4.48
MLLT4	myeloid/lymphoid or mixed-lineage leukemia 4	4.47
FAM135A	family with sequence similarity 135, member A	4.44
LAMA4	laminin, alpha 4	4.44
TOP2B	topoisomerase (DNA) II beta 180kDa	4.42
LARP7	La ribonucleoprotein domain family, member 7	4.41
SORBS2	sorbin and SH3 domain containing 2	4.38
MARK1	MAP/microtubule affinity-regulating kinase 1	4.37
TM9SF4	transmembrane 9 superfamily protein member 4	4.37
LAMA2	laminin, alpha 2	4.36
F8	coagulation factor VIII, procoagulant component	4.35
SCLY, UBE2F	selenocysteine lyase, ubiquitin-conjugating enzyme E2F (putative), UBE2F-SCLY readthrough	4.35

NLGN1	neuroligin 1	4.34
EPHA7	EPH receptor A7	4.33
TPTE2P5	transmembrane phosphoinositide 3-phosphatase and tensin homolog 2 pseudogene 5	4.33
AGBL5	ATP/GTP binding protein-like 5	4.3
DMXL1	Dmx-like 1	4.29
ZNF277	zinc finger protein 277	4.24
CEACAM5	carcinoembryonic antigen-related cell adhesion molecule 5	4.23
ENPP1	ectonucleotide pyrophosphatase/phosphodiesterase 1	4.23
UBE2E1	ubiquitin-conjugating enzyme E2E 1	4.22
DST	dystonin, dystonin-like	4.21
CEP170,171	centrosomal protein 170kDa, centrosomal protein 170kDa pseudogene 1	4.2
KIAA0319L	KIAA0319-like	4.17
EPS8	epidermal growth factor receptor pathway substrate 8	4.14
ME3	malic enzyme 3, NADP(+)-dependent, mitochondrial	4.14
GANC, CAPN3	glucosidase, alpha; neutral C, calpain 3, (p94)	4.12
NF1	neurofibromin 1	4.1
ZC3H6	zinc finger CCCH-type containing 6	4.1
LTA4H	leukotriene A4 hydrolase	4.09
MYO5B	myosin VB	4.07
TAS1R1	taste receptor, type 1, member 1	4.07
ARAP2	ArfGAP with RhoGAP domain, ankyrin repeat and PH domain 2	4.05
FAM160B1	family with sequence similarity 160, member B1	4.04
PNPT1	polyribonucleotide nucleotidyltransferase 1	4.04
Mar-01	mitochondrial amidoxime reducing component 1	4.02
HCLS1	hematopoietic cell-specific Lyn substrate 1	4.01
POU2F1	POU class 2 homeobox 1	4.01
C10orf57	chromosome 10 open reading frame 57	4
CDKL4	cyclin-dependent kinase-like 4	4
LRP2	low density lipoprotein receptor-related protein 2	4
CEP192	centrosomal protein 192kDa	3.99
FNTA	farnesyltransferase, CAAX box, alpha	3.99
DDX43	DEAD (Asp-Glu-Ala-Asp) box polypeptide 43	3.98
ANKRD11	ankyrin repeat domain 11	3.97
LDB2	LIM domain binding 2	3.94
FAM114A2	family with sequence similarity 114, member A2	3.93
TTC8	tetratricopeptide repeat domain 8	3.93
SLC12A2	solute carrier family 12 (sodium/potassium/chloride transporters), member 2	3.92
EP400	E1A binding protein p400	3.91
FBN1	fibrillin 1	3.89
KIAA0146	KIAA0146	3.89
POLA1	polymerase (DNA directed), alpha 1, catalytic subunit	3.89
ARFGEF2	ADP-ribosylation factor guanine nucleotide-exchange factor 2 (brefeldin A-inhibited)	3.88

CDKL5	cyclin-dependent kinase-like 5	3.87
SLA	Src-like-adaptor	3.87
STAT4	signal transducer and activator of transcription 4	3.87
ZCCHC11	zinc finger, CCHC domain containing 11	3.87
SLC19A3	solute carrier family 19, member 3	3.86
KCNH7	potassium voltage-gated channel, subfamily H (eag-related), member 7	3.85
NEMF	nuclear export mediator factor	3.85
SUN1	Sad1 and UNC84 domain containing 1	3.85
CAB39L	calcium binding protein 39-like	3.84
SYNE1	spectrin repeat containing, nuclear envelope 1	3.84
ACAA1	acetyl-CoA acyltransferase 1	3.83
CYP2F1	cytochrome P450, family 2, subfamily F, polypeptide 1	3.83
PARVB	parvin, beta	3.83
ADAM7	ADAM metallopeptidase domain 7	3.82
ATXN7	ataxin 7	3.81
DECR1	2,4-dienoyl CoA reductase 1, mitochondrial	3.81
FBXL13	F-box and leucine-rich repeat protein 13	3.81
CA7	carbonic anhydrase VII	3.8
BIN3	bridging integrator 3	3.78
RUFY2	RUN and FYVE domain containing 2	3.77
SLC9A9	solute carrier family 9, subfamily A (NHE9, cation proton antiporter 9), member 9	3.77
STC1	stanniocalcin 1	3.77
ALOX15B	arachidonate 15-lipoxygenase, type B	3.76
DNAH8	dynein, axonemal, heavy chain 8	3.76
ZNF451	zinc finger protein 451	3.76
FLJ37644	uncharacterized LOC400618	3.75
OSBPL5	oxysterol binding protein-like 5	3.75
TMX3	thioredoxin-related transmembrane protein 3	3.74
WNK3	WNK lysine deficient protein kinase 3	3.74
COL14A1	collagen, type XIV, alpha 1	3.73
FLJ22763	uncharacterized LOC401081	3.73
C17orf57, ITGB3	chromosome 17 open reading frame 57, integrin, beta 3 (platelet glycoprotein IIIa, antigen CD61)	3.72
LRRCC1	leucine rich repeat and coiled-coil centrosomal protein 1	3.72
DIAPH3	diaphanous homolog 3 (Drosophila)	3.71
PPM1L	protein phosphatase, Mg2+/Mn2+ dependent, 1L	3.71
SMARCE1	SWI/SNF related, actin dependent regulator of chromatin, subfamily e, member 1	3.71
TAB3	TGF-beta activated kinase 1/MAP3K7 binding protein 3	3.71
ZSWIM5	zinc finger, SWIM-type containing 5	3.71
GAL	galanin prepropeptide	3.7
RNF32	ring finger protein 32	3.7
ANTXR2	anthrax toxin receptor 2	3.69
NPNT	nephronectin	3.68

RAD21, MIR3610	RAD21 homolog (S. pombe), microRNA 3610	3.68
UACA	uveal autoantigen with coiled-coil domains and ankyrin repeats	3.68
EPB41L3	erythrocyte membrane protein band 4.1-like 3	3.66
KIAA0368	KIAA0368	3.66
KIF27	kinesin family member 27	3.66
VGLL4	vestigial like 4 (Drosophila)	3.66
RNF150	ring finger protein 150	3.64
SYNE2	spectrin repeat containing, nuclear envelope 2	3.64
ADAM2	ADAM metallopeptidase domain 2	3.63
STAT5B	signal transducer and activator of transcription 5B	3.63
SYTL2	synaptotagmin-like 2	3.63
TMOD3	tropomodulin 3 (ubiquitous)	3.63
HERC5	HECT and RLD domain containing E3 ubiquitin protein ligase 5	3.62
ADAM7	ADAM metallopeptidase domain 7	3.61
CALB1	calbindin 1, 28kDa	3.59
KIAA1199	KIAA1199	3.59
NEO1	neogenin 1	3.59
CADPS2	Ca++-dependent secretion activator 2	3.58
LYST	lysosomal trafficking regulator	3.58
NUMA1	nuclear mitotic apparatus protein 1	3.58
AP1S3	adaptor-related protein complex 1, sigma 3 subunit	3.57
ZCCHC4	zinc finger, CCHC domain containing 4	3.56
AKNAD1	AKNA domain containing 1	3.55
ARHGAP22	Rho GTPase activating protein 22	3.55
CCDC39	coiled-coil domain containing 39	3.55
CACNA2D2	calcium channel, voltage-dependent, alpha 2/delta subunit 2	3.54
GRIN3A	glutamate receptor, ionotropic, N-methyl-D-aspartate 3A	3.54
SLC28A1	solute carrier family 28 (sodium-coupled nucleoside transporter), member 1	3.54
YPEL1	yippee-like 1 (Drosophila)	3.54
AEBP2	AE binding protein 2	3.53
MYH15	myosin, heavy chain 15	3.53
PLXDC1	plexin domain containing 1	3.51
TPTE	transmembrane phosphatase with tensin homology	3.51
LARP4	La ribonucleoprotein domain family, member 4	3.5
SLC6A5	solute carrier family 6 (neurotransmitter transporter, glycine), member 5	3.5
APBB3	amyloid beta (A4) precursor protein-binding, family B, member 3	3.49
ATM, NPAT	ataxia telangiectasia mutated, nuclear protein, ataxia-telangiectasia locus	3.49
PPP1R9A	protein phosphatase 1, regulatory subunit 9A	3.49
ADAM7	ADAM metallopeptidase domain 7	3.48
C1orf228	chromosome 1 open reading frame 228	3.48
CAGE1	cancer antigen 1	3.48
ODZ1	odz, odd Oz/ten-m homolog 1 (Drosophila)	3.48
PCLO	piccolo (presynaptic cytomatrix protein)	3.48

PCSK6,	proprotein convertase subtilisin/kexin type 6	3.48
PCLO	piccolo (presynaptic cytomatrix protein)	3.47
CCDC144C, B	coiled-coil domain containing 144C, coiled-coil domain containing 144B (pseudogene)	3.46
FBXO41	F-box protein 41	3.46
NELL2	NEL-like 2 (chicken)	3.46
RAP1B	RAP1B, member of RAS oncogene family	3.46
LRP2BP	LRP2 binding protein	3.45
TSPAN9	tetraspanin 9	3.45
ANKH	ankylosis, progressive homolog (mouse)	3.44
CCDC11	coiled-coil domain containing 11	3.44
MAST4	microtubule associated serine/threonine kinase family member 4	3.44
ATP2A2	ATPase, Ca++ transporting, cardiac muscle, slow twitch 2	3.43
COL28A1	collagen, type XXVIII, alpha 1	3.43
PLXNC1	plexin C1	3.43
PPARG	peroxisome proliferator-activated receptor gamma	3.43
COL22A1	collagen, type XXII, alpha 1	3.42
FAM190A	family with sequence similarity 190, member A	3.42
FAM227B	family with sequence similarity 227, member B	3.42
LRRC34	leucine rich repeat containing 34	3.42
CLEC16A	C-type lectin domain family 16, member A	3.41
ITGAX	integrin, alpha X (complement component 3 receptor 4 subunit)	3.41
KAT7	K(lysine) acetyltransferase 7	3.4
PTCHD2	patched domain containing 2	3.4
SYNE1	spectrin repeat containing, nuclear envelope 1	3.4
TARBP1	TAR (HIV-1) RNA binding protein 1	3.4
ZNF345	zinc finger protein 345	3.39
NTRK2	neurotrophic tyrosine kinase, receptor, type 2	3.38
SKAP2	src kinase associated phosphoprotein 2	3.38
SSBP3	single stranded DNA binding protein 3	3.38
DNAH1	dynein, axonemal, heavy chain 1	3.37
PWRN1	Prader-Willi region non-protein coding RNA 1	3.36
CP	ceruloplasmin (ferroxidase)	3.35
SLC1A3	solute carrier family 1 (glial high affinity glutamate transporter), member 3	3.35
ZEB1	zinc finger E-box binding homeobox 1	3.35
F7	coagulation factor VII (serum prothrombin conversion accelerator)	3.34
RPS23	ribosomal protein S23	3.34
CNTRL	centriolin	3.33
ENTPD5	ectonucleoside triphosphate diphosphohydrolase 5	3.33
TTC17	tetratricopeptide repeat domain 17	3.33
CSGALNACT1	chondroitin sulfate N-acetylgalactosaminyltransferase 1	3.32
DUSP11	dual specificity phosphatase 11 (RNA/RNP complex 1-interacting)	3.32
HIVEP1	human immunodeficiency virus type I enhancer binding protein 1	3.32
INO80D	INO80 complex subunit D	3.32

COL24A1	collagen, type XXIV, alpha 1	3.31
GTF2I	general transcription factor IIi	3.31
NPAS2	neuronal PAS domain protein 2	3.3
SNX2	sorting nexin 2	3.3
DOCK5	dedicator of cytokinesis 5	3.29
NAB1	NGFI-A binding protein 1 (EGR1 binding protein 1)	3.29
WDR17	WD repeat domain 17	3.29
DLEU2	deleted in lymphocytic leukemia 2 (non-protein coding)	3.27
LRSAM1	leucine rich repeat and sterile alpha motif containing 1	3.27
LRTOMT	leucine rich transmembrane and 0-methyltransferase domain containing	3.27
ATG13	autophagy related 13	3.26
KALRN	kalirin, RhoGEF kinase	3.25
FAM135A	family with sequence similarity 135, member A	3.24
TFAP2A	transcription factor AP-2 alpha (activating enhancer binding protein 2 alpha)	3.23
ACOXL	acyl-CoA oxidase-like	3.22
C14orf118	chromosome 14 open reading frame 118	3.22
F8	coagulation factor VIII, procoagulant component	3.22
GAD2	glutamate decarboxylase 2 (pancreatic islets and brain, 65kDa)	3.22
PPFIA3	protein tyrosine phosphatase, receptor type, f polypeptide (PTPRF), interacting protein (liprin), alpha 3	3.22
CYFIP2	cytoplasmic FMR1 interacting protein 2	3.2
KMO	kynurenine 3-monooxygenase (kynurenine 3-hydroxylase)	3.2
PIK3C3	phosphoinositide-3-kinase, class 3	3.2
PLA2G4A	phospholipase A2, group IVA (cytosolic, calcium-dependent)	3.2
POLK	polymerase (DNA directed) kappa	3.2
TNS1	tensin 1	3.2
ADAM22	ADAM metallopeptidase domain 22	3.19
BRE, MRPL33	brain and reproductive organ-expressed (TNFRSF1A modulator), mitochondrial ribosomal protein L33	3.19
C9orf84	chromosome 9 open reading frame 84	3.19
GLT8D2	glycosyltransferase 8 domain containing 2	3.19
MST1	macrophage stimulating 1 (hepatocyte growth factor-like)	3.19
NDRG2	NDRG family member 2	3.19
ARHGAP9	Rho GTPase activating protein 9	3.18
FAM198B	family with sequence similarity 198, member B	3.18
FN1	fibronectin 1	3.18
GYS2	glycogen synthase 2 (liver)	3.18
QARS	glutaminyl-tRNA synthetase	3.18
REV1	REV1, polymerase (DNA directed)	3.18
APBB1IP	amyloid beta (A4) precursor protein-binding, family B, member 1 interacting protein	3.17
CLOCK	clock homolog (mouse)	3.17
KLRF1	killer cell lectin-like receptor subfamily F, member 1	3.17
TMEM218	transmembrane protein 218	3.17
UBE3D	ubiquitin protein ligase E3D	3.17

MGAT4A	mannosyl (alpha-1,3-)-glycoprotein beta-1,4-N-acetylglucosaminyltransferase, isozyme A	3.16
POLR3B	polymerase (RNA) III (DNA directed) polypeptide B	3.16
SUCLA2	succinate-CoA ligase, ADP-forming, beta subunit	3.16
XYLB	xylulokinase homolog (H. influenzae)	3.16
C17orf57, ITGB3	chromosome 17 open reading frame 57, integrin, beta 3 (platelet glycoprotein IIIa, antigen CD61)	3.15
NOS2	nitric oxide synthase 2, inducible	3.15
PIK3C2G	phosphoinositide-3-kinase, class 2, gamma polypeptide	3.15
SLC12A1	solute carrier family 12 (sodium/potassium/chloride transporters), member 1	3.15
USO1	USO1 vesicle docking protein homolog (yeast)	3.15
MTA3	metastasis associated 1 family, member 3, uncharacterized LOC100130921	3.14
ODZ1	odz, odd Oz/ten-m homolog 1 (Drosophila)	3.14
SLFN11	schlafen family member 11	3.14
TEX11	testis expressed 11	3.14
IYD	iodotyrosine deiodinase	3.13
RGS8	regulator of G-protein signaling 8	3.13
SI	sucrase-isomaltase (alpha-glucosidase)	3.13
DOCK5	dedicator of cytokinesis 5	3.12
NCALD	neurocalcin delta	3.12
TNFRSF19	tumor necrosis factor receptor superfamily, member 19	3.12
ARID2	AT rich interactive domain 2 (ARID, RFX-like)	3.11
PDE6C	phosphodiesterase 6C, cGMP-specific, cone, alpha prime	3.11
IGHMBP2	immunoglobulin mu binding protein 2	3.1
PLEKHG4	pleckstrin homology domain containing, family G (with RhoGef domain) member 4	3.1
SIPA1L2	signal-induced proliferation-associated 1 like 2	3.1
AMY2A	amylase, alpha 2A (pancreatic)	3.09
MEF2BNB	MEF2BNB-MEF2B readthrough, myocyte enhancer factor 2B	3.09
PDK2	pyruvate dehydrogenase kinase, isozyme 2	3.09
ENDOV	endonuclease V	3.08
FAM176A	family with sequence similarity 176, member A	3.08
RIPK2	receptor-interacting serine-threonine kinase 2	3.07
USH1C	Usher syndrome 1C (autosomal recessive, severe)	3.07
KHDRBS3	KH domain containing, RNA binding, signal transduction associated 3	3.06
SCUBE2	signal peptide, CUB domain, EGF-like 2	3.06
UNC45B	unc-45 homolog B (C. elegans)	3.06
AP2A2	adaptor-related protein complex 2, alpha 2 subunit	3.05
C3orf62, MIR4271	chromosome 3 open reading frame 62, microRNA 4271	3.05
CYP3A43	cytochrome P450, family 3, subfamily A, polypeptide 43	3.05
SSBP3	single stranded DNA binding protein 3	3.05
TMTC1	transmembrane and tetratricopeptide repeat containing 1	3.05
TP53BP2	tumor protein p53 binding protein, 2	3.05
PRDM7	PR domain containing 7	3.04

SYT1	synaptotagmin I	3.04
CADPS2	Ca++-dependent secretion activator 2	3.03
DYNC2H1	dynein, cytoplasmic 2, heavy chain 1	3.03
PLS1	plastin 1	3.03
SETD9	SET domain containing 9	3.03
TBCK	TBC1 domain containing kinase	3.03
UTRN	utrophin	3.03
ARHGEF6	Rac/Cdc42 guanine nucleotide exchange factor (GEF) 6	3.02
ARID2	AT rich interactive domain 2 (ARID, RFX-like)	3.02
DMD	dystrophin	3.02
FAM76B	family with sequence similarity 76, member B	3.02
LINC00277	long intergenic non-protein coding RNA 277	3.02
LRRC7	leucine rich repeat containing 7	3.02
SUCLA2	succinate-CoA ligase, ADP-forming, beta subunit	3.02
CCDC152	coiled-coil domain containing 152	3.01
OLAH	oleoyl-ACP hydrolase	3.01
RAET1E	retinoic acid early transcript 1E	3.01
DKFZp686O1327	uncharacterized LOC401014	3
KRT79	keratin 79	3
PAWR	PRKC, apoptosis, WT1, regulator	3
PECR	peroxisomal trans-2-enoyl-CoA reductase	3
SCN5A	sodium channel, voltage-gated, type V, alpha subunit	3
TMEM68	transmembrane protein 68	3
ABCC12	ATP-binding cassette, sub-family C (CFTR/MRP), member 12	2.99
AKD1	adenylate kinase domain containing 1	2.99
ALB	albumin	2.99
LOC728978	uncharacterized LOC728978	2.99
ODF2L	outer dense fiber of sperm tails 2-like	2.99
TMED8	transmembrane emp24 protein transport domain containing 8	2.99
ADCY1	adenylate cyclase 1 (brain)	2.98
CDK7	cyclin-dependent kinase 7	2.98
MADD	MAP-kinase activating death domain	2.98
PFKFB4	6-phosphofructo-2-kinase/fructose-2,6-biphosphatase 4	2.98
PLEKHG1	pleckstrin homology domain containing, family G (with RhoGef domain) member 1	2.98
SLC7A8	solute carrier family 7 (amino acid transporter light chain, L system), member 8	2.98
CABIN1	calcineurin binding protein 1	2.97
FAM46A	family with sequence similarity 46, member A	2.97
KIAA1244	KIAA1244	2.97
ZCCHC17	zinc finger, CCHC domain containing 17	2.97
AKD1	adenylate kinase domain containing 1	2.96
APEX1	APEX nuclease (multifunctional DNA repair enzyme) 1	2.96
ARHGAP15	Rho GTPase activating protein 15	2.96

AUTS2	autism susceptibility candidate 2	2.96
KIAA0100	KIAA0100	2.96
LRBA	LPS-responsive vesicle trafficking, beach and anchor containing	2.96
ABTB1	ankyrin repeat and BTB (POZ) domain containing 1	2.95
ARHGAP42	Rho GTPase activating protein 42	2.95
C14orf133	chromosome 14 open reading frame 133	2.95
DMXL2	Dmx-like 2	2.95
KTN1	kinectin 1 (kinesin receptor)	2.95
PPIL2	peptidylprolyl isomerase (cyclophilin)-like 2	2.95
RGS4	regulator of G-protein signaling 4	2.95
RNF150	ring finger protein 150	2.95
UBE4B	ubiquitination factor E4B	2.95
WDR93	WD repeat domain 93	2.95
BMP4	bone morphogenetic protein 4	2.94
IZUMO2	IZUMO family member 2	2.94
MYOM2	myomesin (M-protein) 2, 165kDa	2.94
C6orf170	chromosome 6 open reading frame 170	2.93
KANSL1L	KAT8 regulatory NSL complex subunit 1-like	2.93
WDR41	WD repeat domain 41	2.93
ZNF284	zinc finger protein 284	2.93
F11	coagulation factor XI	2.92
FREM1	FRAS1 related extracellular matrix 1	2.91
LRRC37B	leucine rich repeat containing 37B	2.91
MACC1	metastasis associated in colon cancer 1	2.91
SLC4A4	solute carrier family 4, sodium bicarbonate cotransporter, member 4	2.91
WDR48	WD repeat domain 48	2.91
ERO1LB	ERO1-like beta (S. cerevisiae)	2.9
FAS	Fas (TNF receptor superfamily, member 6)	2.9
SPINK4	serine peptidase inhibitor, Kazal type 4	2.9
XRN2	5'-3' exoribonuclease 2	2.9
DOCK2	dedicator of cytokinesis 2	2.89
FRMD5	FERM domain containing 5	2.89
IL2RB	interleukin 2 receptor, beta	2.89
LIMCH1	LIM and calponin homology domains 1	2.89
LRIG2	leucine-rich repeats and immunoglobulin-like domains 2	2.89
MCM10	minichromosome maintenance complex component 10	2.89
PPP2R5C	protein phosphatase 2, regulatory subunit B', gamma	2.89
STK32B	serine/threonine kinase 32B	2.89
ZCWPW1	zinc finger, CW type with PWWP domain 1	2.89
ATP11C	ATPase, class VI, type 11C	2.88
CCDC66	coiled-coil domain containing 66	2.88
CTPS2	CTP synthase 2	2.88
KLHL7	kelch-like 7 (Drosophila)	2.88

SGK1	serum/glucocorticoid regulated kinase 1	2.88
TMEM150C	transmembrane protein 150C	2.88
TMEM212	transmembrane protein 212	2.88
VPS39	vacuolar protein sorting 39 homolog (S. cerevisiae)	2.88
ATP11A	ATPase, class VI, type 11A	2.87
CPNE8	copine VIII	2.87
DUSP15, C20orf57	dual specificity phosphatase 15, chromosome 20 open reading frame 57	2.87
JMJD1C	jumonji domain containing 1C	2.87
MACF1	microtubule-actin crosslinking factor 1	2.87
NEK10	NIMA (never in mitosis gene a)- related kinase 10	2.87
NKTR	natural killer-tumor recognition sequence	2.87
TBC1D25	TBC1 domain family, member 25	2.87
USP9Y	ubiquitin specific peptidase 9, Y-linked	2.87
ZNF568	zinc finger protein 568	2.86
ANK2	ankyrin 2, neuronal	2.85
ASPRV1	aspartic peptidase, retroviral-like 1, PCBP1 antisense RNA 1 (non-protein coding)	2.85
MANSC1	MANSC domain containing 1	2.85
OFCC1	orofacial cleft 1 candidate 1	2.85
PIEZO2	piezo-type mechanosensitive ion channel component 2	2.85
ZNF277	zinc finger protein 277	2.85
ARID1A	AT rich interactive domain 1A (SWI-like)	2.84
ERC2	ELKS/RAB6-interacting/CAST family member 2	2.84
PGD	phosphogluconate dehydrogenase	2.84
RAB36	RAB36, member RAS oncogene family	2.84
ZFYVE26	zinc finger, FYVE domain containing 26	2.84
CADPS	Ca++-dependent secretion activator	2.83
LARGE	like-glycosyltransferase	2.83
SUPT16H	suppressor of Ty 16 homolog (S. cerevisiae)	2.83
TNFSF10	tumor necrosis factor (ligand) superfamily, member 10	2.83
CTBP2	C-terminal binding protein 2	2.82
F13B	coagulation factor XIII, B polypeptide	2.82
GCNT3	glucosaminyl (N-acetyl) transferase 3, mucin type	2.82
TEX14	testis expressed 14	2.82
AGTR1	angiotensin II receptor, type 1	2.81
C9orf85	chromosome 9 open reading frame 85	2.81
HECW2	HECT, C2 and WW domain containing E3 ubiquitin protein ligase 2	2.81
JHDM1D	jumonji C domain containing histone demethylase 1 homolog D (S. cerevisiae)	2.81
RGS6	regulator of G-protein signaling 6	2.81
SPTLC3	serine palmitoyltransferase, long chain base subunit 3	2.81
DOK5	docking protein 5	2.8
SLC16A14	solute carrier family 16, member 14 (monocarboxylic acid transporter 14)	2.8
C10orf137	chromosome 10 open reading frame 137	2.79

FCHSD2	FCH and double SH3 domains 2	2.79
THRA, NR1D1	thyroid hormone receptor, alpha, nuclear receptor subfamily 1, group D, member 1	2.79
TNIP1	TNFAIP3 interacting protein 1	2.79
DZANK1	double zinc ribbon and ankyrin repeat domains 1	2.78
ERGIC1	endoplasmic reticulum-golgi intermediate compartment (ERGIC) 1	2.78
LYST	lysosomal trafficking regulator	2.78
MCM8	minichromosome maintenance complex component 8	2.78
ASB15	ankyrin repeat and SOCS box containing 15	2.77
FRAS1	Fraser syndrome 1	2.77
FSD2	fibronectin type III and SPRY domain containing 2	2.77
MYO18A, TIAF1	myosin XVIIIA, TGFB1-induced anti-apoptotic factor 1	2.77
WDR33, SFT2D3	WD repeat domain 33, SFT2 domain containing 3	2.77
ZNF211	zinc finger protein 211	2.77
MYH15	myosin, heavy chain 15	2.76
ZNF518A	zinc finger protein 518A	2.76
ACACB	acetyl-CoA carboxylase beta	2.75
ALB	albumin	2.75
C14orf45	chromosome 14 open reading frame 45	2.75
C5orf4	chromosome 5 open reading frame 4	2.75
CALCOCO2	calcium binding and coiled-coil domain 2	2.75
HAUS3, POLN	HAUS augmin-like complex, subunit 3, polymerase (DNA directed) nu	2.75
MCOLN3	mucolipin 3	2.75
OCA2	oculocutaneous albinism II	2.75
PPIG	peptidylprolyl isomerase G (cyclophilin G)	2.75
UBE3C	ubiquitin protein ligase E3C	2.75
UIMC1	ubiquitin interaction motif containing 1	2.75
DFNB59	deafness, autosomal recessive 59	2.74
GIGYF2	GRB10 interacting GYF protein 2	2.74
MTMR7	myotubularin related protein 7	2.74
MYO5C	myosin VC	2.74
MYOM3	myomesin family, member 3	2.74
DAPK1	death-associated protein kinase 1	2.73
NOVA1-AS1	NOVA1 antisense RNA 1 (non-protein coding)	2.73
RPGRIP1L	RPGRIP1-like	2.73
SART3	squamous cell carcinoma antigen recognized by T cells 3	2.73
SYP	synaptophysin	2.73
ZC4H2	zinc finger, C4H2 domain containing	2.73
ARHGAP42	Rho GTPase activating protein 42	2.72
CLIP4	CAP-GLY domain containing linker protein family, member 4	2.72
CREM	cAMP responsive element modulator	2.72
GLIPR2	GLI pathogenesis-related 2	2.72
HELQ	helicase, POLQ-like	2.72

KRT32	keratin 32	2.72
NEB	nebulin	2.72
PSD3	pleckstrin and Sec7 domain containing 3	2.72
RAD54L2	RAD54-like 2 (S. cerevisiae)	2.72
STK11IP	serine/threonine kinase 11 interacting protein	2.72
TDP2	tyrosyl-DNA phosphodiesterase 2	2.72
ATP1A1	ATPase, Na+/K+ transporting, alpha 1 polypeptide	2.71
C12orf26	chromosome 12 open reading frame 26	2.71
C2orf65	chromosome 2 open reading frame 65	2.71
DUS4L	dihydrouridine synthase 4-like (S. cerevisiae)	2.71
PALLD	palladin, cytoskeletal associated protein	2.71
ZNF124	zinc finger protein 124	2.71
DGKG	diacylglycerol kinase, gamma 90kDa	2.7
MRVI1	murine retrovirus integration site 1 homolog	2.7
RPL34-AS1	RPL34 antisense RNA 1 (non-protein coding)	2.7
UCP3	uncoupling protein 3 (mitochondrial, proton carrier)	2.7
VPS13D	vacuolar protein sorting 13 homolog D (S. cerevisiae)	2.7
CNOT2	CCR4-NOT transcription complex, subunit 2	2.69
COL2A1	collagen, type II, alpha 1	2.69
COL4A3BP	collagen, type IV, alpha 3 (Goodpasture antigen) binding protein	2.69
MTND2P2B	MT-ND2 pseudogene 28, NADH-ubiquinone oxidoreductase chain 2-like	2.69
PARP2	poly (ADP-ribose) polymerase 2	2.69
PRR4, PRH1	proline rich 4 (lacrimal), PRH1-PRR4 readthrough, proline-rich protein HaeIII subfamily 1	2.69
RAD51B	RAD51 homolog B (S. cerevisiae)	2.69
RUNDC3B	RUN domain containing 3B	2.69
TTC37	tetratricopeptide repeat domain 37	2.69
DEDD	death effector domain containing	2.68
NMD3	NMD3 homolog (S. cerevisiae)	2.68
ATRX	alpha thalassemia/mental retardation syndrome X-linked	2.67
CCT6P1	chaperonin containing TCP1, subunit 6 (zeta) pseudogene 1	2.67
CEP192	centrosomal protein 192kDa	2.67
NAV3	neuron navigator 3	2.67
SERPINB9	serpin peptidase inhibitor, clade B (ovalbumin), member 9	2.67
SLC24A1	solute carrier family 24 (sodium/potassium/calcium exchanger), member 1	2.67
SLC43A2	solute carrier family 43, member 2	2.67
DOCK10	dedicator of cytokinesis 10	2.66
KHDRBS3	KH domain containing, RNA binding, signal transduction associated 3	2.66
LAMA2	laminin, alpha 2	2.66
LOC647859	occludin pseudogene	2.66
PARP1	poly (ADP-ribose) polymerase 1	2.66
REPS2	RALBP1 associated Eps domain containing 2	2.66
WDR48	WD repeat domain 48	2.66
ZNF236	zinc finger protein 236	2.66

BCO2	beta-carotene oxygenase 2	2.65
CEP85L	centrosomal protein 85kDa-like	2.65
ERGIC2	ERGIC and golgi 2	2.65
FLJ40852	uncharacterized LOC285962	2.65
KIAA1033	KIAA1033	2.65
NAV3	neuron navigator 3	2.65
PION	pigeon homolog (Drosophila)	2.65
SPTA1	spectrin, alpha, erythrocytic 1 (elliptocytosis 2)	2.65
ATP6V0A2	ATPase, H+ transporting, lysosomal V0 subunit a2	2.64
MAPKAPK5	mitogen-activated protein kinase-activated protein kinase 5	2.64
ZNF148	zinc finger protein 148	2.64
C5orf42	chromosome 5 open reading frame 42	2.63
C9orf174	chromosome 9 open reading frame 174, pseudogene	2.63
CHD8	chromodomain helicase DNA binding protein 8	2.63
FMN1	formin 1, formin-1-like	2.63
LZTFL1	leucine zipper transcription factor-like 1	2.63
NUP54	nucleoporin 54kDa	2.63
PHACTR4	phosphatase and actin regulator 4	2.63
TBC1D8B	TBC1 domain family, member 8B (with GRAM domain)	2.63
EPHB3	EPH receptor B3	2.62
NAP1L1	nucleosome assembly protein 1-like 1	2.62
PSD3	pleckstrin and Sec7 domain containing 3	2.62
RAP1B	RAP1B, member of RAS oncogene family	2.62
TRPM3	transient receptor potential cation channel, subfamily M, member 3	2.62
VASH2	vasohibin 2	2.62
ZNF552	zinc finger protein 552	2.62
ADK	adenosine kinase	2.61
AKD1	adenylate kinase domain containing 1	2.61
CACNA2D4	calcium channel, voltage-dependent, alpha 2/delta subunit 4	2.61
COL15A1	collagen, type XV, alpha 1	2.61
EVC	Ellis van Creveld syndrome	2.61
KIAA1841	KIAA1841	2.61
LRRK2	leucine-rich repeat kinase 2	2.61
MDH1B	malate dehydrogenase 1B, NAD (soluble)	2.61
MYCBP2	MYC binding protein 2, E3 ubiquitin protein ligase	2.61
NXF2B, NXF2	nuclear RNA export factor 2B, nuclear RNA export factor 2	2.61
NXF2B, NXF2	nuclear RNA export factor 2B, nuclear RNA export factor 2	2.61
PPP4R1L	protein phosphatase 4, regulatory subunit 1-like	2.61
RFX8	regulatory factor X, 8	2.61
USP8	ubiquitin specific peptidase 8	2.61
AKAP9	A kinase (PRKA) anchor protein (yotiao) 9	2.6
CAMK2G	calcium/calmodulin-dependent protein kinase II gamma	2.6
CATSPER4	cation channel, sperm associated 4	2.6

FAM91A2	family with sequence similarity 91, member A2	2.6
KCNAB2	potassium voltage-gated channel, shaker-related subfamily, beta member 2	2.6
NHSL1	NHS-like 1	2.6
PLEKHH2	pleckstrin homology domain containing, family H (with MyTH4 domain) member 2	2.6
PPIL3	peptidylprolyl isomerase (cyclophilin)-like 3	2.6
SPEG	SPEG complex locus	2.6
TNNC2	troponin C type 2 (fast)	2.6
XRRA1	X-ray radiation resistance associated 1	2.6
ZBTB20	zinc finger and BTB domain containing 20	2.6
ZNF333	zinc finger protein 333	2.6
C11orf45	chromosome 11 open reading frame 45	2.59
GCM1	glial cells missing homolog 1 (Drosophila)	2.59
INADL	InaD-like (Drosophila)	2.59
ODZ4	odz, odd Oz/ten-m homolog 4 (Drosophila)	2.59
TPH2	tryptophan hydroxylase 2	2.59
TRPM3	transient receptor potential cation channel, subfamily M, member 3	2.59
FAM206A	family with sequence similarity 206, member A	2.58
HECTD1	HECT domain containing E3 ubiquitin protein ligase 1	2.58
JARID2	jumonji, AT rich interactive domain 2	2.58
MPP3	membrane protein, palmitoylated 3 (MAGUK p55 subfamily member 3)	2.58
PLAC8	placenta-specific 8	2.58
TBL2	transducin (beta)-like 2	2.58
TRPV2	transient receptor potential cation channel, subfamily V, member 2	2.58
CNOT10	CCR4-NOT transcription complex, subunit 10	2.57
DUSP16	dual specificity phosphatase 16	2.57
EFR3A	EFR3 homolog A (S. cerevisiae)	2.57
MYOM2	myomesin (M-protein) 2, 165kDa	2.57
NR2C1	nuclear receptor subfamily 2, group C, member 1	2.57
RBM23	RNA binding motif protein 23	2.57
SH3BGR	SH3 domain binding glutamic acid-rich protein	2.57
ZSCAN16	zinc finger and SCAN domain containing 16	2.57
BPIFA2	BPI fold containing family A, member 2	2.56
C12orf76	chromosome 12 open reading frame 76	2.56
FAM194A	family with sequence similarity 194, member A	2.56
LARP1B	La ribonucleoprotein domain family, member 1B	2.56
MLLT4	myeloid/lymphoid or mixed-lineage leukemia (trithorax homolog, Drosophila); translocated to, 4	2.56
PDE8B	phosphodiesterase 8B	2.56
SETD5	SET domain containing 5	2.56
SYT1	synaptotagmin I	2.56
CCDC92	coiled-coil domain containing 92	2.55
FAM105B	family with sequence similarity 105, member B	2.55
GIPC2	GIPC PDZ domain containing family, member 2	2.55

HELZ	helicase with zinc finger	2.55
MYH10	myosin, heavy chain 10, non-muscle	2.55
NYNRIN	NYN domain and retroviral integrase containing	2.55
TMBIM6	transmembrane BAX inhibitor motif containing 6	2.55
ZNF260	zinc finger protein 260	2.55
ZNF519	zinc finger protein 519	2.55
ZNF615	zinc finger protein 615	2.55
ATP13A4	ATPase type 13A4	2.54
C17orf76-AS1	C17orf76 antisense RNA 1 (non-protein coding), small nucleolar RNA, C/D box 65	2.54
CCDC88C	coiled-coil domain containing 88C	2.54
DOCK4	dedicator of cytokinesis 4	2.54
KIAA0586	KIAA0586	2.54
L3MBTL3	l(3)mbt-like 3 (Drosophila)	2.54
LIN52	lin-52 homolog (C. elegans)	2.54
MTHFD2L	methylenetetrahydrofolate dehydrogenase (NADP+ dependent) 2-like	2.54
PHLPP1	PH domain and leucine rich repeat protein phosphatase 1	2.54
PRR4, PRH1	proline rich 4 (lacrimal), PRH1-PRR4 readthrough, proline-rich protein HaeIII subfamily 1	2.54
ADGB	androglobin	2.53
CHN1	chimerin (chimaerin) 1	2.53
EYS	eyes shut homolog (Drosophila)	2.53
IQCH	IQ motif containing H	2.53
MSR1	macrophage scavenger receptor 1	2.53
PLAG1	pleiomorphic adenoma gene 1	2.53
SPOCK3	sparc/osteonectin, cwcv and kazal-like domains proteoglycan (testican) 3	2.53
VOPP1	vesicular, overexpressed in cancer, prosurvival protein 1	2.53
ZC3H13	zinc finger CCCH-type containing 13	2.53
ZC3H8	zinc finger CCCH-type containing 8	2.53
APPL1	adaptor protein, phosphotyrosine interaction, PH domain and leucine zipper containing 1	2.52
ARG2	arginase, type II	2.52
ARHGAP25	Rho GTPase activating protein 25	2.52
DENND4A	DENN/MADD domain containing 4A	2.52
FAM183A	family with sequence similarity 183, member A	2.52
FAM70A	family with sequence similarity 70, member A	2.52
FUCA1	fucosidase, alpha-L- 1, tissue	2.52
GUCY2C	guanylate cyclase 2C (heat stable enterotoxin receptor)	2.52
IKZF5	IKAROS family zinc finger 5 (Pegasus)	2.52
ITM2A	integral membrane protein 2A	2.52
KDM4C	lysine (K)-specific demethylase 4C	2.52
KIF22	kinesin family member 22	2.52
PTPN13	protein tyrosine phosphatase, non-receptor type 13 (APO-1/CD95 (Fas)-associated phosphatase)	2.52
TBL1XR1	transducin (beta)-like 1 X-linked receptor 1	2.52
BMP4	bone morphogenetic protein 4	2.51

C3orf33	chromosome 3 open reading frame 33	2.51
CCNG1	cyclin G1	2.51
CDC42BPG	CDC42 binding protein kinase gamma (DMPK-like)	2.51
NUDT22	nudix (nucleoside diphosphate linked moiety X)-type motif 22	2.51
SH3GL3	SH3-domain GRB2-like 3	2.51
SPRR1B	small proline-rich protein 1B	2.51
STRN3	striatin, calmodulin binding protein 3	2.51
TCF4	transcription factor 4	2.51
BLNK	B-cell linker	2.5
COG4	component of oligomeric golgi complex 4	2.5
CORO7-PAM16	CORO7-PAM16 readthrough, coronin 7, presequence translocase-associated motor 16 homolog	2.5
KIF5C	kinesin family member 5C	2.5
MUC12	mucin 12, cell surface associated	2.5
MUSK	muscle, skeletal, receptor tyrosine kinase	2.5
NCK1	NCK adaptor protein 1	2.5
NLRC5	NLR family, CARD domain containing 5	2.5
PLAGL1	pleiomorphic adenoma gene-like 1	2.5
PM20D1	peptidase M20 domain containing 1	2.5
PON3, PON1	paraoxonase 3, paraoxonase 1	2.5
PRMT5	protein arginine methyltransferase 5	2.5
PSEN2	presenilin 2 (Alzheimer disease 4)	2.5
RABEP1	rabaptin, RAB GTPase binding effector protein 1	2.5
SLC44A5	solute carrier family 44, member 5	2.5
USH2A	Usher syndrome 2A (autosomal recessive, mild)	2.5
CNOT7	CCR4-NOT transcription complex, subunit 7	2.49
CPNE6	copine VI (neuronal)	2.49
FAM153A, FAM153B	family with sequence similarity 153, members A-B	2.49
IQCA1	IQ motif containing with AAA domain 1	2.49
PDE8A	phosphodiesterase 8A	2.49
PFKM	phosphofructokinase, muscle	2.49
RERG	RAS-like, estrogen-regulated, growth inhibitor	2.49
SLC9A5	solute carrier family 9, subfamily A (NHE5, cation proton antiporter 5), member 5	2.49
TLR3	toll-like receptor 3	2.49
TMEM199, MIR4723	transmembrane protein 199, microRNA 4723	2.49
VEZT	vezatin, adherens junctions transmembrane protein	2.49
WTAP	Wilms tumor 1 associated protein	2.49
ABCA8	ATP-binding cassette, sub-family A (ABC1), member 8	2.48
AFF1	AF4/FMR2 family, member 1	2.48
C5orf47	chromosome 5 open reading frame 47	2.48
DCP1B	DCP1 decapping enzyme homolog B (S. cerevisiae)	2.48
DMRT3	doublesex and mab-3 related transcription factor 3	2.48
ERI3	ERI1 exoribonuclease family member 3	2.48

GALC	galactosylceramidase	2.48
KDM5D	lysine (K)-specific demethylase 5D	2.48
MRPS11	mitochondrial ribosomal protein S11	2.48
NOSTRIN	nitric oxide synthase trafficker	2.48
PCYT1A, TCTEX1D2	phosphate cytidylyltransferase 1, choline, alpha, Tctex1 domain containing 2	2.48
PRDM14	PR domain containing 14	2.48
RYK	receptor-like tyrosine kinase	2.48
SERPINB5	serpin peptidase inhibitor, clade B (ovalbumin), member 5	2.48
SUPT3H	suppressor of Ty 3 homolog (S. cerevisiae)	2.48
TP73	tumor protein p73	2.48
ZNF675	zinc finger protein 675	2.48
BRWD1	bromodomain and WD repeat domain containing 1	2.47
CACNA1I	calcium channel, voltage-dependent, T type, alpha 1I subunit	2.47
COL13A1	collagen, type XIII, alpha 1	2.47
DIP2A	DIP2 disco-interacting protein 2 homolog A (Drosophila)	2.47
FEZ2	fasciculation and elongation protein zeta 2 (zygin II)	2.47
FMO5	flavin containing monooxygenase 5	2.47
PPP1R12A	protein phosphatase 1, regulatory subunit 12A	2.47
SAA2, SAA4	serum amyloid A2, serum amyloid A4, constitutive, SAA2-SAA4 readthrough	2.47
STK33	serine/threonine kinase 33	2.47
VPS39	vacuolar protein sorting 39 homolog (S. cerevisiae)	2.47
ZNHIT6	zinc finger, HIT-type containing 6	2.47
AFF1	AF4/FMR2 family, member 1	2.46
DNM3	dynamin 3	2.46
GRTP1	growth hormone regulated TBC protein 1	2.46
HERC3	HECT and RLD domain containing E3 ubiquitin protein ligase 3	2.46
IFT43	intraflagellar transport 43 homolog (Chlamydomonas)	2.46
ITGA1, PELO	integrin, alpha 1, pelota homolog (Drosophila)	2.46
ITPA	inosine triphosphatase (nucleoside triphosphate pyrophosphatase)	2.46
KIAA1109	KIAA1109	2.46
LAMA3	laminin, alpha 3	2.46
LOC100506674	uncharacterized LOC100506674	2.46
SMC6	structural maintenance of chromosomes 6	2.46
SPEF2	sperm flagellar 2	2.46
TTC21A	tetratricopeptide repeat domain 21A	2.46
ZDHHC23	zinc finger, DHHC-type containing 23	2.46
ZNF487P	zinc finger protein 487, pseudogene	2.46
AHCYL1	adenosylhomocysteinase-like 1	2.45
CDKN2AIP	CDKN2A interacting protein	2.45
HERC3	HECT and RLD domain containing E3 ubiquitin protein ligase 3	2.45
IL4R	interleukin 4 receptor	2.45
LINC00461, MIR9-2	long intergenic non-protein coding RNA 461, microRNA 9-2	2.45

RARB	retinoic acid receptor, beta	2.45
ROS1, GOPC	c-ros oncogene 1 , receptor tyrosine kinase, golgi-associated PDZ and coiled-coil motif containing	2.45
RXFP2	relaxin/insulin-like family peptide receptor 2	2.45
SLC25A36	solute carrier family 25 (pyrimidine nucleotide carrier), member 36	2.45
SND1	staphylococcal nuclease and tudor domain containing 1	2.45
STAG1	stromal antigen 1	2.45
TMEM130	transmembrane protein 130	2.45
TXLNB	taxilin beta	2.45
ZBTB33	zinc finger and BTB domain containing 33	2.45
AGPAT4	1-acylglycerol-3-phosphate O-acyltransferase 4 (lysophosphatidic acid acyltransferase, delta)	2.44
ALG10B, ALG10	asparagine-linked glycosylation 10, alpha-1,2-glucosyltransferase homolog	2.44
ASPRV1	aspartic peptidase, retroviral-like 1, PCBP1 antisense RNA 1 (non-protein coding)	2.44
ATP13A5	ATPase type 13A5	2.44
C10orf90	chromosome 10 open reading frame 90	2.44
EML6	echinoderm microtubule associated protein like 6	2.44
GPR180	G protein-coupled receptor 180	2.44
IKZF5	IKAROS family zinc finger 5 (Pegasus)	2.44
LANCL1	LanC lantibiotic synthetase component C-like 1 (bacterial)	2.44
LHCGR	luteinizing hormone/choriogonadotropin receptor	2.44
MED15	mediator complex subunit 15	2.44
MKL1	megakaryoblastic leukemia (translocation) 1	2.44
MRO	maestro	2.44
PDK3	pyruvate dehydrogenase kinase, isozyme 3	2.44
RBM23	RNA binding motif protein 23	2.44
SEC24B	SEC24 family, member B (S. cerevisiae)	2.44
SSH3	slingshot homolog 3 (Drosophila)	2.44
ST6GAL1	ST6 beta-galactosamide alpha-2,6-sialyltranferase 1	2.44
TEC	tec protein tyrosine kinase	2.44
TULP2	tubby like protein 2	2.44
ABHD12B, MIR4454	abhydrolase domain containing 12B, microRNA 4454	2.43
AHI1	Abelson helper integration site 1	2.43
CACNA1F	calcium channel, voltage-dependent, L type, alpha 1F subunit	2.43
CARS	cysteinyl-tRNA synthetase	2.43
KIF1B	kinesin family member 1B	2.43
KIRREL	kin of IRRE like (Drosophila)	2.43
MTMR8, ASB12	myotubularin related protein 8, ankyrin repeat and SOCS box containing 12	2.43
RAB38	RAB38, member RAS oncogene family	2.43
RCOR3	REST corepressor 3	2.43
RFX7	regulatory factor X, 7	2.43
TRIM36	tripartite motif containing 36	2.43
UBE3D	ubiquitin protein ligase E3D	2.43
ZFP90	zinc finger protein 90 homolog (mouse)	2.43

EIF2C3	eukaryotic translation initiation factor 2C, 3	2.42
FANCB	Fanconi anemia, complementation group B	2.42
PTPN6	protein tyrosine phosphatase, non-receptor type 6	2.42
PTPRE	protein tyrosine phosphatase, receptor type, E	2.42
SGK494	uncharacterized serine/threonine-protein kinase SgK494	2.42
ST7L	suppression of tumorigenicity 7 like	2.42
TTC6	tetratricopeptide repeat domain 6, tetratricopeptide repeat protein 6-like	2.42
ZBTB41	zinc finger and BTB domain containing 41	2.42
AQPEP	laeverin	2.41
ARHGAP26	Rho GTPase activating protein 26	2.41
GRB14	growth factor receptor-bound protein 14	2.41
LIPM	lipase, family member M	2.41
NAA16	N(alpha)-acetyltransferase 16, NatA auxiliary subunit	2.41
ATP11B	ATPase, class VI, type 11B	2.4
CCDC150	coiled-coil domain containing 150	2.4
GTF2B	general transcription factor IIB	2.4
HERC5	HECT and RLD domain containing E3 ubiquitin protein ligase 5	2.4
NBEAL1	neurobeachin-like 1, 60S ribosomal protein L12-like	2.4
NIPAL1	NIPA-like domain containing 1	2.4
NNT	nicotinamide nucleotide transhydrogenase	2.4
PAK3	p21 protein (Cdc42/Rac)-activated kinase 3	2.4
RFX3	regulatory factor X, 3 (influences HLA class II expression)	2.4
RGL1	ral guanine nucleotide dissociation stimulator-like 1	2.4
TRIM29	tripartite motif containing 29	2.4
CLEC16A	C-type lectin domain family 16, member A	2.39
DYRK3	dual-specificity tyrosine-(Y)-phosphorylation regulated kinase 3	2.39
FBXO36	F-box protein 36	2.39
HORMAD2	HORMA domain containing 2	2.39
HTR3D	5-hydroxytryptamine (serotonin) receptor 3D, ionotropic	2.39
LOC100132891	uncharacterized LOC100132891	2.39
SH3BP5	SH3-domain binding protein 5 (BTK-associated)	2.39
USP34	ubiquitin specific peptidase 34	2.39
AHCYL2	adenosylhomocysteinase-like 2	2.38
EPHA3	EPH receptor A3	2.38
FER1L5	fer-1-like 5 (C. elegans)	2.38
FXYD6, FXYD6	FXYD domain containing ion transport regulator 2 & 6, FXYD6-FXYD2 readthrough	2.38
HHIP	hedgehog interacting protein	2.38
IFIT3	interferon-induced protein with tetratricopeptide repeats 3	2.38
SORBS2	sorbin and SH3 domain containing 2	2.38
SPAG17	sperm associated antigen 17	2.38
TLR6	toll-like receptor 6	2.38
USP54	ubiquitin specific peptidase 54	2.38
ADPGK	ADP-dependent glucokinase	2.37

ANKRD20A1-7/P	ankyrin repeat domain 20 family, members A1-A7	2.37
FLJ39653	uncharacterized FLJ39653	2.37
FMN2	formin 2	2.37
HARS2	histidyl-tRNA synthetase 2, mitochondrial (putative)	2.37
HSPA4L	heat shock 70kDa protein 4-like	2.37
IL15	interleukin 15	2.37
MED23	mediator complex subunit 23	2.37
NFE2L2	nuclear factor (erythroid-derived 2)-like 2	2.37
PHLPP1	PH domain and leucine rich repeat protein phosphatase 1	2.37
PNPLA7	patatin-like phospholipase domain containing 7	2.37
SLC43A2	solute carrier family 43, member 2	2.37
SPAG17	sperm associated antigen 17	2.37
TAPT1	transmembrane anterior posterior transformation 1	2.37
TSHR	thyroid stimulating hormone receptor	2.37
UTY	ubiquitously transcribed tetratricopeptide repeat gene, Y-linked	2.37
ZNF780B	zinc finger protein 780B	2.37
ITGAV	integrin, alpha V	2.36
PPP1R7	protein phosphatase 1, regulatory subunit 7	2.36
RELN	reelin	2.36
UGGT2	UDP-glucose glycoprotein glucosyltransferase 2	2.36
WAC	WW domain containing adaptor with coiled-coil	2.36
ZCCHC2	zinc finger, CCHC domain containing 2	2.36
ADAL	adenosine deaminase-like	2.35
AFAP1L2	actin filament associated protein 1-like 2	2.35
CD101	CD101 molecule	2.35
CDHR3	cadherin-related family member 3	2.35
CREG1	cellular repressor of E1A-stimulated genes 1	2.35
CRYZ	crystallin, zeta (quinone reductase)	2.35
IQCB1	IQ motif containing B1	2.35
KRT10	keratin 10	2.35
LTBR	lymphotoxin beta receptor (TNFR superfamily, member 3)	2.35
MS4A3	membrane-spanning 4-domains, subfamily A, member 3 (hematopoietic cell-specific)	2.35
PDE6C	phosphodiesterase 6C, cGMP-specific, cone, alpha prime	2.35
PDS5B	PDS5, regulator of cohesion maintenance, homolog B (S. cerevisiae)	2.35
SLC25A26	solute carrier family 25 (S-adenosylmethionine carrier), member 26	2.35
STAG2	stromal antigen 2	2.35
STXBP5	syntaxin binding protein 5 (tomosyn)	2.35
TRAPPC9	trafficking protein particle complex 9	2.35
ZMYM3	zinc finger, MYM-type 3	2.35
C5	complement component 5	2.34
CARD9	caspase recruitment domain family, member 9	2.34
CERS2	ceramide synthase 2	2.34

DDX26B	DEAD/H (Asp-Glu-Ala-Asp/His) box polypeptide 26B	2.34
EDARADD	EDAR-associated death domain	2.34
FAM65B	family with sequence similarity 65, member B	2.34
FLJ42351	uncharacterized LOC400999	2.34
GMPS	guanine monphosphate synthetase	2.34
IL13RA2	interleukin 13 receptor, alpha 2	2.34
LMLN	leishmanolysin-like (metallopeptidase M8 family)	2.34
MECOM	MDS1 and EVI1 complex locus	2.34
MICAL2	microtubule associated monoxygenase, calponin and LIM domain containing 2	2.34
MTX2	metaxin 2	2.34
PRDM15	PR domain containing 15	2.34
PTPN12	protein tyrosine phosphatase, non-receptor type 12	2.34
RAPGEF4	Rap guanine nucleotide exchange factor (GEF) 4	2.34
RNF175	ring finger protein 175	2.34
TAB3	TGF-beta activated kinase 1/MAP3K7 binding protein 3	2.34
TRMT1	tRNA methyltransferase 1 homolog (S. cerevisiae)	2.34
ZNF638	zinc finger protein 638	2.34
CDKL5	cyclin-dependent kinase-like 5	2.33
CLDND1	a domain containing 1	2.33
EIF2C3	eukaryotic translation initiation factor 2C, 3	2.33
GPR112	G protein-coupled receptor 112	2.33
MRPS27	mitochondrial ribosomal protein S27	2.33
MTMR4	myotubularin related protein 4	2.33
PTPN14	protein tyrosine phosphatase, non-receptor type 14	2.33
PTPRQ	protein tyrosine phosphatase, receptor type, Q	2.33
SASH1	SAM and SH3 domain containing 1	2.33
SSX2IP	synovial sarcoma, X breakpoint 2 interacting protein	2.33
STK31	serine/threonine kinase 31	2.33
TINAG	tubulointerstitial nephritis antigen	2.33
TTLL7	tubulin tyrosine ligase-like family, member 7	2.33
ZNF577	zinc finger protein 577	2.33
ABCA10	ATP-binding cassette, sub-family A (ABC1), member 10	2.32
ARSK	arylsulfatase family, member K	2.32
EPB41L5	erythrocyte membrane protein band 4.1 like 5	2.32
EVI5	ecotropic viral integration site 5	2.32
FAM135A	family with sequence similarity 135, member A	2.32
HDAC4	histone deacetylase 4	2.32
PCYT1B	phosphate cytidylyltransferase 1, choline, beta	2.32
UNC5B	unc-5 homolog B (C. elegans)	2.32
WFDC8	WAP four-disulfide core domain 8	2.32
ATP10A	ATPase, class V, type 10A	2.31
DEPDC4	DEP domain containing 4	2.31
ENTPD3	ectonucleoside triphosphate diphosphohydrolase 3	2.31

FGD6	FYVE, RhoGEF and PH domain containing 6	2.31
GALNT14	UDP-N-acetyl-alpha-D-galactosamine:polypeptide N-acetylgalactosaminyltransferase 14 (GalNAc-T14)	2.31
GRIA2	glutamate receptor, ionotropic, AMPA 2	2.31
IL1RL2	interleukin 1 receptor-like 2	2.31
LTBP3	latent transforming growth factor beta binding protein 3	2.31
MX1	myxovirus (influenza virus) resistance 1, interferon-inducible protein p78 (mouse)	2.31
MYD88	myeloid differentiation primary response gene (88)	2.31
OSBPL6	oxysterol binding protein-like 6	2.31
OTX2-AS1	OTX2 antisense RNA 1 (non-protein coding)	2.31
PHKG1	phosphorylase kinase, gamma 1 (muscle)	2.31
PVR	poliovirus receptor	2.31
RASGRP4	RAS guanyl releasing protein 4	2.31
SMCHD1	structural maintenance of chromosomes flexible hinge domain containing 1	2.31
TEX35	testis expressed 35	2.31
THADA	thyroid adenoma associated	2.31
TNIP3	TNFAIP3 interacting protein 3	2.31
UBE2E1	ubiquitin-conjugating enzyme E2E 1	2.31
WDR11	WD repeat domain 11	2.31
ACVR1C	activin A receptor, type IC	2.3
BOLL	bol, boule-like (Drosophila)	2.3
CAMK2G	calcium/calmodulin-dependent protein kinase II gamma	2.3
CEACAM19	carcinoembryonic antigen-related cell adhesion molecule 19	2.3
DGCR14, TSSK2	DiGeorge syndrome critical region gene 14, testis-specific serine kinase 2	2.3
EPC1	enhancer of polycomb homolog 1 (Drosophila)	2.3
GRB10	growth factor receptor-bound protein 10	2.3
KIAA1210	KIAA1210	2.3
LHFP	lipoma HMGIC fusion partner	2.3
LRRC37B	leucine rich repeat containing 37B	2.3
MREG	melanoregulin	2.3
RAB3A	RAB3A, member RAS oncogene family	2.3
RSPH3	radial spoke 3 homolog (Chlamydomonas)	2.3
SCIN	scinderin	2.3
SLCO1C1	solute carrier organic anion transporter family, member 1C1	2.3
STX2	syntaxin 2	2.3
TTN	titin	2.3
ABCB11	ATP-binding cassette, sub-family B (MDR/TAP), member 11	2.29
ACAA2	acetyl-CoA acyltransferase 2	2.29
ALG9	asparagine-linked glycosylation 9, alpha-1,2-mannosyltransferase homolog (S. cerevisiae)	2.29
ARHGAP32	Rho GTPase activating protein 32	2.29
C21orf49	chromosome 21 open reading frame 49	2.29
DLG3	discs, large homolog 3 (Drosophila)	2.29
GNAT2	guanine nucleotide binding protein (G protein), alpha transducing activity polypeptide 2	2.29

LOC284930	uncharacterized LOC284930	2.29
SKIV2L2	superkiller viralicidic activity 2-like 2 (S. cerevisiae)	2.29
STC1	stanniocalcin 1	2.29
TEKT4P2, MAFIP	tektin 4 pseudogene 2, tektin 4 pseudogene, MAFF interacting protein (pseudogene)	2.29
ZNF599	zinc finger protein 599	2.29
ANKS1B	ankyrin repeat and sterile alpha motif domain containing 1B	2.28
ATAD2B	ATPase family, AAA domain containing 2B	2.28
CTNNBL1	catenin, beta like 1	2.28
DHRS1	dehydrogenase/reductase (SDR family) member 1	2.28
FUBP3	far upstream element (FUSE) binding protein 3	2.28
POT1	protection of telomeres 1 homolog (S. pombe)	2.28
SEC31A	SEC31 homolog A (S. cerevisiae)	2.28
SH3TC1	SH3 domain and tetratricopeptide repeats 1	2.28
VSTM2A	V-set and transmembrane domain containing 2A	2.28
ADD3	adducin 3 (gamma)	2.27
ASIC2	acid-sensing (proton-gated) ion channel 2	2.27
C12orf39	chromosome 12 open reading frame 39	2.27
C15orf41	chromosome 15 open reading frame 41	2.27
C4orf21	chromosome 4 open reading frame 21	2.27
CLIP4	CAP-GLY domain containing linker protein family, member 4	2.27
DNAJB5	DnaJ (Hsp40) homolog, subfamily B, member 5	2.27
FCER1A	Fc fragment of IgE, high affinity I, receptor for; alpha polypeptide	2.27
MCTP1	multiple C2 domains, transmembrane 1	2.27
MTUS1	microtubule associated tumor suppressor 1	2.27
MYH10	myosin, heavy chain 10, non-muscle	2.27
SLC4A7	solute carrier family 4, sodium bicarbonate cotransporter, member 7	2.27
SMARCE1	SWI/SNF related, matrix associated, actin dependent regulator of chromatin, subfamily e, member 1	2.27
STIM2	stromal interaction molecule 2	2.27
ULBP3	UL16 binding protein 3	2.27
VPS11	vacuolar protein sorting 11 homolog (S. cerevisiae)	2.27
ZBTB41	zinc finger and BTB domain containing 41	2.27
ZNF143	zinc finger protein 143	2.27
CEP170, CEP170P1	centrosomal protein 170kDa, centrosomal protein 170kDa pseudogene 1	2.26
GZMB	granzyme B (granzyme 2, cytotoxic T-lymphocyte-associated serine esterase 1)	2.26
KDM6B	lysine (K)-specific demethylase 6B	2.26
L2HGDH	L-2-hydroxyglutarate dehydrogenase	2.26
MAGI3	membrane associated guanylate kinase, WW and PDZ domain containing 3	2.26
MLLT4	myeloid/lymphoid or mixed-lineage leukemia (trithorax homolog, Drosophila); translocated to, 4	2.26
PSMD11	proteasome (prosome, macropain) 26S subunit, non-ATPase, 11	2.26
RUNX1T1	runt-related transcription factor 1; translocated to, 1 (cyclin D-related)	2.26
SAMM50, PNPLA3	sorting and assembly machinery component 50 homolog, patatin-like phospholipase domain containing 3	2.26

SETD5	SET domain containing 5	2.26
SLFN11	schlafen family member 11	2.26
SRRM1	serine/arginine repetitive matrix 1	2.26
SVEP1	sushi, von Willebrand factor type A, EGF and pentraxin domain containing 1	2.26
ZMYM6	zinc finger, MYM-type 6	2.26
ACOX2	acyl-CoA oxidase 2, branched chain	2.25
ARHGAP31	Rho GTPase activating protein 31	2.25
BAIAP2	BAI1-associated protein 2	2.25
CNOT4	CCR4-NOT transcription complex, subunit 4	2.25
CPT1C	carnitine palmitoyltransferase 1C	2.25
FOXRED1	FAD-dependent oxidoreductase domain containing 1	2.25
FUBP1	far upstream element (FUSE) binding protein 1	2.25
GFM1	G elongation factor, mitochondrial 1	2.25
HIBCH	3-hydroxyisobutyryl-CoA hydrolase	2.25
HSPBAP1	HSPB (heat shock 27kDa) associated protein 1	2.25
IGSF9B	immunoglobulin superfamily, member 9B	2.25
LOC152586	glycosyltransferase 54 domain-containing protein	2.25
MLF1IP	MLF1 interacting protein	2.25
PACS1	phosphofurin acidic cluster sorting protein 1	2.25
PCBD2	pterin-4 alpha-carbinolamine dehydratase/dimerization nuclear factor 1 alpha (TCF1) 2	2.25
PRIC285	peroxisomal proliferator-activated receptor A interacting complex 285	2.25
RFX7	regulatory factor X, 7	2.25
RHOBTB2	Rho-related BTB domain containing 2	2.25
STAT2	signal transducer and activator of transcription 2, 113kDa	2.25
AP1G1	adaptor-related protein complex 1, gamma 1 subunit	2.24
ASB6	ankyrin repeat and SOCS box containing 6	2.24
C10orf88	chromosome 10 open reading frame 88	2.24
CACNB1	calcium channel, voltage-dependent, beta 1 subunit	2.24
CAPN3	calpain 3, (p94)	2.24
COL19A1	collagen, type XIX, alpha 1	2.24
DGKD	diacylglycerol kinase, delta 130kDa	2.24
FAM178B	family with sequence similarity 178, member B	2.24
HEATR7B2	HEAT repeat family member 7B2	2.24
KANSL1L	KAT8 regulatory NSL complex subunit 1-like	2.24
MYOF	myoferlin	2.24
NPC2, MIR4709	Niemann-Pick disease, type C2, microRNA 4709	2.24
PPME1	protein phosphatase methylesterase 1	2.24
UAP1L1	UDP-N-acteylglucosamine pyrophosphorylase 1-like 1	2.24
ADAMTS2	ADAM metallopeptidase with thrombospondin type 1 motif, 2	2.23
C2orf56	chromosome 2 open reading frame 56	2.23
CLIC6	chloride intracellular channel 6	2.23
CTSB	cathepsin B	2.23

ERCC6L2	excision repair cross-complementing rodent repair deficiency, complementation group 6-like 2	2.23
FAM133B	family with sequence similarity 133, member B	2.23
FMNL2	formin-like 2	2.23
GNPDA2	glucosamine-6-phosphate deaminase 2	2.23
GSTT2B, GSTT2	glutathione S-transferase theta 2B (gene/pseudogene), glutathione S-transferase theta 2	2.23
HDAC8	histone deacetylase 8	2.23
HMBOX1	homeobox containing 1	2.23
IBTK	inhibitor of Bruton agammaglobulinemia tyrosine kinase	2.23
KAL1	Kallmann syndrome 1 sequence	2.23
LARP4	La ribonucleoprotein domain family, member 4	2.23
POLR3G	polymerase (RNA) III (DNA directed) polypeptide G (32kD)	2.23
RTTN	rotatin	2.23
ST8SIA6	ST8 alpha-N-acetyl-neuraminide alpha-2,8-sialyltransferase 6	2.23
TMEM150C	transmembrane protein 150C	2.23
ZBTB38	zinc finger and BTB domain containing 38	2.23
ZCCHC8	zinc finger, CCHC domain containing 8	2.23
ZNF512	zinc finger protein 512	2.23
ABCC2	ATP-binding cassette, sub-family C (CFTR/MRP), member 2	2.22
ANKRD12	ankyrin repeat domain 12	2.22
BAZ2B	bromodomain adjacent to zinc finger domain, 2B	2.22
CAMK2B	calcium/calmodulin-dependent protein kinase II beta	2.22
CD1B	CD1b molecule	2.22
CLDND1	claudin domain containing 1	2.22
DOCK11	dedicator of cytokinesis 11	2.22
EP400	E1A binding protein p400	2.22
FGFR1	fibroblast growth factor receptor 1	2.22
FRMD3	FERM domain containing 3	2.22
IL1RAP	interleukin 1 receptor accessory protein	2.22
LOC100506942	uncharacterized LOC100506942	2.22
LPP	LIM domain containing preferred translocation partner in lipoma	2.22
LRRK1	leucine-rich repeat kinase 1	2.22
LTBP1	latent transforming growth factor beta binding protein 1	2.22
MGA	MAX gene associated	2.22
NCOA6	nuclear receptor coactivator 6	2.22
NID2	nidogen 2 (osteonidogen)	2.22
NOC3L	nucleolar complex associated 3 homolog (S. cerevisiae)	2.22
NUP155	nucleoporin 155kDa	2.22
PTPN14	protein tyrosine phosphatase, non-receptor type 14	2.22
RPH3AL	rabphilin 3A-like (without C2 domains)	2.22
SEL1L3	sel-1 suppressor of lin-12-like 3 (C. elegans)	2.22
SMG7	smg-7 homolog, nonsense mediated mRNA decay factor (C. elegans)	2.22
ST3GAL5	ST3 beta-galactoside alpha-2,3-sialyltransferase 5	2.22

TPP2	tripeptidyl peptidase II	2.22
ACSF2	acyl-CoA synthetase family member 2	2.21
ASTE1	asteroid homolog 1 (Drosophila)	2.21
ASTE1	asteroid homolog 1 (Drosophila)	2.21
ATP9B	ATPase, class II, type 9B	2.21
C10orf76	chromosome 10 open reading frame 76	2.21
CCDC150	coiled-coil domain containing 150	2.21
CDC14A	CDC14 cell division cycle 14 homolog A (S. cerevisiae)	2.21
CYFIP2	cytoplasmic FMR1 interacting protein 2	2.21
D21S2088E	D21S2088E	2.21
EBAG9	estrogen receptor binding site associated, antigen, 9	2.21
ESR1	estrogen receptor 1	2.21
FAM189A1	family with sequence similarity 189, member A1	2.21
GALNT1	UDP-N-acetyl-alpha-D-galactosamine:polypeptide N-acetylgalactosaminyltransferase 1 (GalNAc-T1)	2.21
GALNT14	UDP-N-acetyl-alpha-D-galactosamine:polypeptide N-acetylgalactosaminyltransferase 14 (GalNAc-T14)	2.21
GKAP1	G kinase anchoring protein 1	2.21
GLOD4	glyoxalase domain containing 4	2.21
KATNAL1	katanin p60 subunit A-like 1	2.21
KDR	kinase insert domain receptor (a type III receptor tyrosine kinase)	2.21
KIAA0528	KIAA0528	2.21
KIAA1109	KIAA1109	2.21
MAEA	macrophage erythroblast attacher	2.21
MYO5A	myosin VA (heavy chain 12, myoxin)	2.21
PCDHGA/B/C1-12	protocadherin gamma subfamily A-C/1-12	2.21
PTPN3	protein tyrosine phosphatase, non-receptor type 3	2.21
SQLE	squalene epoxidase	2.21
TSNAX-DISC1	TSNAX-DISC1 readthrough, disrupted in schizophrenia 1, translin-associated factor X	2.21
TTLL7	tubulin tyrosine ligase-like family, member 7	2.21
ABCC9	ATP-binding cassette, sub-family C (CFTR/MRP), member 9	2.2
ANK3	ankyrin 3, node of Ranvier (ankyrin G)	2.2
CAPRIN1	cell cycle associated protein 1	2.2
DENND4C	DENN/MADD domain containing 4C	2.2
DGCR5	DiGeorge syndrome critical region gene 5 (non-protein coding)	2.2
DNAJC6	DnaJ (Hsp40) homolog, subfamily C, member 6	2.2
ERGIC2	ERGIC and golgi 2	2.2
FAM228B	family with sequence similarity 228, member B	2.2
GMPS	guanine monphosphate synthetase	2.2
LRRK2	leucine-rich repeat kinase 2	2.2
MLH3	mutL homolog 3 (E. coli)	2.2
NAALAD2	N-acetylated alpha-linked acidic dipeptidase 2	2.2
PLD5	phospholipase D family, member 5	2.2
PRDM10	PR domain containing 10	2.2

RBM26-AS1	RBM26 antisense RNA 1 (non-protein coding)	2.2
RBM4B	RNA binding motif protein 4B	2.2
SCARA3	scavenger receptor class A, member 3	2.2
SYNM	synemin, intermediate filament protein	2.2
TMEM25	transmembrane protein 25	2.2
TRPS1	trichorhinophalangeal syndrome I	2.2
AKAP13	A kinase (PRKA) anchor protein 13	2.19
ANKRD26P3	ankyrin repeat domain 26 pseudogene 3	2.19
C11orf24	chromosome 11 open reading frame 24	2.19
C1QTNF5, MFRP	C1q and tumor necrosis factor related protein 5, membrane frizzled-related protein	2.19
CEP192	centrosomal protein 192kDa	2.19
CEP290	centrosomal protein 290kDa	2.19
CXorf57	chromosome X open reading frame 57	2.19
FAM228B	family with sequence similarity 228, member B	2.19
GABRA3	gamma-aminobutyric acid (GABA) A receptor, alpha 3	2.19
HNRNPU	heterogeneous nuclear ribonucleoprotein U (scaffold attachment factor A)	2.19
KIAA0317	KIAA0317	2.19
LDHA	lactate dehydrogenase A	2.19
LRRC48	leucine rich repeat containing 48	2.19
LRRIQ1	leucine-rich repeats and IQ motif containing 1	2.19
PPFIA2	protein tyrosine phosphatase, receptor type, f polypeptide (PTPRF), interacting protein (liprin), alpha 2	2.19
RRH	retinal pigment epithelium-derived rhodopsin homolog	2.19
TUBGCP2	tubulin, gamma complex associated protein 2	2.19
UBAP2	ubiquitin associated protein 2	2.19
XPR1	xenotropic and polytropic retrovirus receptor 1	2.19
ABCC9	ATP-binding cassette, sub-family C (CFTR/MRP), member 9	2.18
APBB1IP	amyloid beta (A4) precursor protein-binding, family B, member 1 interacting protein	2.18
CEP41	centrosomal protein 41kDa	2.18
CUL4B	cullin 4B	2.18
DENND1B	DENN/MADD domain containing 1B	2.18
DNAJC1	DnaJ (Hsp40) homolog, subfamily C, member 1	2.18
ESYT2	extended synaptotagmin-like protein 2	2.18
GANC, CAPN3	glucosidase, alpha; neutral C, calpain 3, (p94)	2.18
HTRA4	HtrA serine peptidase 4	2.18
KIAA1324L	KIAA1324-like	2.18
KIF27	kinesin family member 27	2.18
MAN1B1	mannosidase, alpha, class 1B, member 1	2.18
NDUFA12	NADH dehydrogenase (ubiquinone) 1 alpha subcomplex, 12	2.18
NF1	neurofibromin 1	2.18
NF1	neurofibromin 1	2.18
NUCB1	nucleobindin 1	2.18
PLCL1	phospholipase C-like 1	2.18

SLC25A20	solute carrier family 25 (carnitine/acylcarnitine translocase), member 20	2.18
SNX25	sorting nexin 25	2.18
SPTLC3	serine palmitoyltransferase, long chain base subunit 3	2.18
TFDP1	transcription factor Dp-1	2.18
TXNDC16	thioredoxin domain containing 16	2.18
WASL	Wiskott-Aldrich syndrome-like	2.18
ABCB7	ATP-binding cassette, sub-family B (MDR/TAP), member 7	2.17
BRWD1	bromodomain and WD repeat domain containing 1	2.17
C17orf81	chromosome 17 open reading frame 81	2.17
CASP7	caspase 7, apoptosis-related cysteine peptidase	2.17
CLCA4	chloride channel accessory 4	2.17
CLEC3A	C-type lectin domain family 3, member A	2.17
DHX36	DEAH (Asp-Glu-Ala-His) box polypeptide 36	2.17
FAM102B	family with sequence similarity 102, member B	2.17
IL1RAP	interleukin 1 receptor accessory protein	2.17
LAT	linker for activation of T cells	2.17
LRRC27	leucine rich repeat containing 27	2.17
MAP3K15	mitogen-activated protein kinase kinase kinase 15	2.17
MSL3	male-specific lethal 3 homolog (Drosophila)	2.17
NCOA6	nuclear receptor coactivator 6	2.17
PRKAR2B	protein kinase, cAMP-dependent, regulatory, type II, beta	2.17
PTK2B	PTK2B protein tyrosine kinase 2 beta	2.17
RBM23	RNA binding motif protein 23	2.17
SLC28A3	solute carrier family 28 (sodium-coupled nucleoside transporter), member 3	2.17
SNORD113-4	small nucleolar RNA, C/D box 113-4	2.17
SRSF4	serine/arginine-rich splicing factor 4	2.17
STX16-NPEPL1	STX16-NPEPL1 readthrough (non-protein coding), syntaxin 16, aminopeptidase-like 1	2.17
SULF1	sulfatase 1	2.17
TAF1D, MIR1304	TATA box binding protein (TBP)-associated factor, RNA polymerase I, microRNA 1304	2.17
TCEANC2	transcription elongation factor A (SII) N-terminal and central domain containing 2	2.17
UPK1B	uroplakin 1B	2.17
ANKRD46	ankyrin repeat domain 46, glyceraldehyde 3 phosphate dehydrogenase pseudogene 62	2.16
BIRC3	baculoviral IAP repeat containing 3	2.16
C2CD3	C2 calcium-dependent domain containing 3	2.16
CCDC9	coiled-coil domain containing 9	2.16
CD2AP	CD2-associated protein	2.16
CDKL3	cyclin-dependent kinase-like 3	2.16
CLDN10	claudin 10	2.16
COG7	component of oligomeric golgi complex 7	2.16
DGKE	diacylglycerol kinase, epsilon 64kDa	2.16
EEF2K	eukaryotic elongation factor-2 kinase	2.16
FRYL	FRY-like	2.16

GTF2I	general transcription factor IIi	2.16
LEF1	lymphoid enhancer-binding factor 1	2.16
LMOD3	leiomodin 3 (fetal)	2.16
LOC644135	uncharacterized LOC644135	2.16
MLL	myeloid/lymphoid or mixed-lineage leukemia (trithorax homolog, Drosophila)	2.16
NEDD4	neural precursor cell expressed, developmentally down-regulated 4, E3 ubiquitin protein ligase	2.16
NFX1	nuclear transcription factor, X-box binding 1	2.16
PLEKHH2	pleckstrin homology domain containing, family H (with MyTH4 domain) member 2	2.16
RC3H1	ring finger and CCCH-type domains 1	2.16
ROBO1	roundabout, axon guidance receptor, homolog 1 (Drosophila)	2.16
SERPINB4,3	serpin peptidase inhibitor, clade B (ovalbumin), member 3 & 4	2.16
SFSWAP	splicing factor, suppressor of white-apricot homolog (Drosophila)	2.16
SYCP2	synaptonemal complex protein 2	2.16
TMBIM6	transmembrane BAX inhibitor motif containing 6	2.16
ZNF566	zinc finger protein 566	2.16
ALB	albumin	2.15
ANO3	anoctamin 3	2.15
CCDC51	coiled-coil domain containing 51	2.15
CCNK	cyclin K	2.15
CDK5RAP2	CDK5 regulatory subunit associated protein 2	2.15
CHMP7	charged multivesicular body protein 7	2.15
EPC2	enhancer of polycomb homolog 2 (Drosophila)	2.15
FAM54A	family with sequence similarity 54, member A	2.15
FANK1	fibronectin type III and ankyrin repeat domains 1	2.15
HMBOX1	homeobox containing 1	2.15
INO80D	INO80 complex subunit D	2.15
MON1A	MON1 homolog A (yeast)	2.15
NEB	nebulin	2.15
PACSIN2	protein kinase C and casein kinase substrate in neurons 2	2.15
PCP4	Purkinje cell protein 4	2.15
PPP1R3E	protein phosphatase 1, regulatory subunit 3E	2.15
PRKAA2	protein kinase, AMP-activated, alpha 2 catalytic subunit	2.15
SASH1	SAM and SH3 domain containing 1	2.15
SASH1	SAM and SH3 domain containing 1	2.15
SNX2	sorting nexin 2	2.15
USP49	ubiquitin specific peptidase 49	2.15
ZBTB16	zinc finger and BTB domain containing 16	2.15
ZNF487P	zinc finger protein 487, pseudogene	2.15
ARHGAP20	Rho GTPase activating protein 20	2.14
ARHGEF11	Rho guanine nucleotide exchange factor (GEF) 11	2.14
ARMC8	armadillo repeat containing 8	2.14
C15orf41	chromosome 15 open reading frame 41	2.14

DNAJC3	DnaJ (Hsp40) homolog, subfamily C, member 3	2.14
EXTL2	exostoses (multiple)-like 2	2.14
GCOM1	GRINL1A complex locus 1 & 2, myocardial zonula adherens protein	2.14
GDAP1	ganglioside induced differentiation associated protein 1	2.14
HBE1	hemoglobin, epsilon 1	2.14
IMPAD1	inositol monophosphatase domain containing 1	2.14
HLA-DQB1	HLA class II histocompatibility antigen, DQ beta 1	2.14
LUZP2	leucine zipper protein 2	2.14
LYPLA1	lysophospholipase I	2.14
NAE1	NEDD8 activating enzyme E1 subunit 1	2.14
NAV3	neuron navigator 3	2.14
PAPOLG	poly(A) polymerase gamma	2.14
PTBP1	polypyrimidine tract binding protein 1	2.14
RGL2	ral guanine nucleotide dissociation stimulator-like 2	2.14
RGL2	ral guanine nucleotide dissociation stimulator-like 2	2.14
RGL2	ral guanine nucleotide dissociation stimulator-like 2	2.14
RGL2	ral guanine nucleotide dissociation stimulator-like 2	2.14
RGL2	ral guanine nucleotide dissociation stimulator-like 2	2.14
SLC47A1	solute carrier family 47, member 1	2.14
SUSD1	sushi domain containing 1	2.14
TANC2	tetratricopeptide repeat, ankyrin repeat and coiled-coil containing 2	2.14
TSHZ2	teashirt zinc finger homeobox 2	2.14
UBR3	ubiquitin protein ligase E3 component n-recognin 3 (putative)	2.14
VWA3A	von Willebrand factor A domain containing 3A	2.14
YWHAQ	tyrosine 3-monooxygenase/tryptophan 5-monooxygenase activation protein	2.14
ANKS6	ankyrin repeat and sterile alpha motif domain containing 6	2.13
ARHGAP5	Rho GTPase activating protein 5	2.13
C11orf74	chromosome 11 open reading frame 74	2.13
C9orf153	chromosome 9 open reading frame 153	2.13
CSTF1	cleavage stimulation factor, 3' pre-RNA, subunit 1, 50kDa	2.13
ECT2	epithelial cell transforming sequence 2 oncogene	2.13
GUCY2F	guanylate cyclase 2F, retinal	2.13
KIAA1244	KIAA1244	2.13
KIAA1377	KIAA1377	2.13
KIF5C	kinesin family member 5C	2.13
KPNA5	karyopherin alpha 5 (importin alpha 6)	2.13
PIKFYVE	phosphoinositide kinase, FYVE finger containing	2.13
SENP2	SUMO1/sentrin/SMT3 specific peptidase 2	2.13
WWC1	WW and C2 domain containing 1	2.13
ZBTB40	zinc finger and BTB domain containing 40	2.13
ANKRD13B	ankyrin repeat domain 13B	2.12
BACE2	beta-site APP-cleaving enzyme 2	2.12
BTN2A2	butyrophilin, subfamily 2, member A2	2.12

CABLES2	Cdk5 and Abl enzyme substrate 2	2.12
CITED2	Cbp/p300-interacting transactivator, with Glu/Asp-rich carboxy-terminal domain, 2	2.12
CMTM8	CKLF-like MARVEL transmembrane domain containing 8	2.12
DDX23	DEAD (Asp-Glu-Ala-Asp) box polypeptide 23	2.12
ELOVL6	ELOVL fatty acid elongase 6	2.12
FAM193B	family with sequence similarity 193, member B	2.12
FNDC5	fibronectin type III domain containing 5	2.12
GALC	galactosylceramidase	2.12
GEMIN5	gem (nuclear organelle) associated protein 5	2.12
GFAP	glial fibrillary acidic protein	2.12
GUCY2F	guanylate cyclase 2F, retinal	2.12
HDAC8	histone deacetylase 8	2.12
LOC729970	hCG2028352-like	2.12
MCM8	minichromosome maintenance complex component 8	2.12
MESDC2	mesoderm development candidate 2	2.12
NALCN	sodium leak channel, non-selective	2.12
NFRKB	nuclear factor related to kappaB binding protein	2.12
PLXNA1	plexin A1	2.12
REPS1	RALBP1 associated Eps domain containing 1	2.12
RPAP3	RNA polymerase II associated protein 3	2.12
RPUSD3	RNA pseudouridylate synthase domain containing 3	2.12
SCN10A	sodium channel, voltage-gated, type X, alpha subunit	2.12
SNX4	sorting nexin 4	2.12
SSBP2	single-stranded DNA binding protein 2	2.12
STIM1, MIR4687	stromal interaction molecule 1, microRNA 4687	2.12
TPCN1	two pore segment channel 1	2.12
Mar-02	membrane-associated ring finger (C3HC4) 2, E3 ubiquitin protein ligase	2.11
BTBD7	BTB (POZ) domain containing 7	2.11
C12orf76	chromosome 12 open reading frame 76	2.11
CNOT1	CCR4-NOT transcription complex, subunit 1	2.11
DDX23	DEAD (Asp-Glu-Ala-Asp) box polypeptide 23	2.11
FLJ30838	uncharacterized LOC400955	2.11
GFPT2	glutamine-fructose-6-phosphate transaminase 2	2.11
HBP1	HMG-box transcription factor 1	2.11
LAIR1	leukocyte-associated immunoglobulin-like receptor 1	2.11
LRPAP1	low density lipoprotein receptor-related protein associated protein 1	2.11
LRRK2	leucine-rich repeat kinase 2	2.11
NEFL	neurofilament, light polypeptide	2.11
NTRK3	neurotrophic tyrosine kinase, receptor, type 3	2.11
PTCH1	patched 1	2.11
RWDD2B	RWD domain containing 2B	2.11
RWDD3, TMEM56	RWD domain containing 3, TMEM56-RWDD3 readthrough, transmembrane protein 56	2.11

SLC9A3R1, MIR3615	solute carrier family 9, subfamily A, member 3 regulator 1, microRNA 3615	2.11
STRADB	STE20-related kinase adaptor beta	2.11
UGCG	UDP-glucose ceramide glucosyltransferase	2.11
UTRN	utrophin	2.11
ZNF143	zinc finger protein 143	2.11
ACSBG1	acyl-CoA synthetase bubblegum family member 1	2.1
ATIC	5-aminoimidazole-4-carboxamide ribonucleotide formyltransferase/IMP cyclohydrolase	2.1
ATP6V1A	ATPase, H+ transporting, lysosomal 70kDa, V1 subunit A	2.1
DOPEY1	dopey family member 1	2.1
DZIP1L	DAZ interacting protein 1-like	2.1
ETV2	ets variant 2	2.1
FAM83A	family with sequence similarity 83, member A	2.1
HERC5	HECT and RLD domain containing E3 ubiquitin protein ligase 5	2.1
IFT140	intraflagellar transport 140 homolog (Chlamydomonas)	2.1
METTL7A	methyltransferase like 7A	2.1
MICALL1	MICAL-like 1	2.1
MIR548AK	microRNA 548ak	2.1
MVD	mevalonate (diphospho) decarboxylase	2.1
NBN	nibrin	2.1
NCAPD3	non-SMC condensin II complex, subunit D3	2.1
NF1	neurofibromin 1	2.1
PEX5L	peroxisomal biogenesis factor 5-like	2.1
PLK4	polo-like kinase 4	2.1
PNPLA6	patatin-like phospholipase domain containing 6	2.1
PSEN2	presenilin 2 (Alzheimer disease 4)	2.1
RAPGEF6	Rap guanine nucleotide exchange factor (GEF) 6	2.1
SCG5	secretogranin V (7B2 protein)	2.1
SCUBE3	signal peptide, CUB domain, EGF-like 3	2.1
SLC9A6	solute carrier family 9, subfamily A (NHE6, cation proton antiporter 6), member 6	2.1
SYCP2	synaptonemal complex protein 2	2.1
ZFAND1	zinc finger, AN1-type domain 1	2.1
ZNF250	zinc finger protein 250	2.1
ZNF527	zinc finger protein 527	2.1
ACIN1	apoptotic chromatin condensation inducer 1	2.09
ADCY4	adenylate cyclase 4	2.09
AOX1	aldehyde oxidase 1	2.09
APOL2	apolipoprotein L, 2	2.09
C6orf70	chromosome 6 open reading frame 70	2.09
CCDC91	coiled-coil domain containing 91	2.09
CMAS	cytidine monophosphate N-acetylneuraminic acid synthetase	2.09
DKFZp686O1327	uncharacterized LOC401014	2.09

DLST	dihydrolipoamide S-succinyltransferase (E2 component of 2-oxo-glutarate complex)	2.09
EPB41L4A	erythrocyte membrane protein band 4.1 like 4A	2.09
GORASP2	golgi reassembly stacking protein 2, 55kDa	2.09
HSPG2	heparan sulfate proteoglycan 2	2.09
JHDM1D	jumonji C domain containing histone demethylase 1 homolog D (S. cerevisiae)	2.09
JPH1	junctophilin 1	2.09
KIF15	kinesin family member 15	2.09
LOC283050	uncharacterized LOC283050	2.09
MAGEA3	melanoma antigen family A, 3	2.09
MCOLN2	mucolipin 2	2.09
MGEA5	meningioma expressed antigen 5 (hyaluronidase)	2.09
PDILT	protein disulfide isomerase-like, testis expressed	2.09
PTCH1	patched 1	2.09
RBBP9	retinoblastoma binding protein 9	2.09
RGS18	regulator of G-protein signaling 18	2.09
SH3GLB2	SH3-domain GRB2-like endophilin B2	2.09
ST14	suppression of tumorigenicity 14 (colon carcinoma)	2.09
STAM2	signal transducing adaptor molecule (SH3 domain and ITAM motif) 2	2.09
UTS2D	urotensin 2 domain containing	2.09
ZFP106	zinc finger protein 106 homolog (mouse)	2.09
ZNF451	zinc finger protein 451	2.09
AGL	amylo-alpha-1, 6-glucosidase, 4-alpha-glucanotransferase	2.08
ASUN	asunder, spermatogenesis regulator homolog (Drosphila)	2.08
CCDC66	coiled-coil domain containing 66	2.08
CYP2C18, CYP2C19	cytochrome P450, family 2, subfamily C, polypeptide 18 & 19	2.08
DGKB	diacylglycerol kinase, beta 90kDa	2.08
DGKH	diacylglycerol kinase, eta	2.08
DLG5	discs, large homolog 5 (Drosophila)	2.08
DMXL2	Dmx-like 2	2.08
DPP10	dipeptidyl-peptidase 10 (non-functional)	2.08
ETV6	ets variant 6	2.08
EXD2	exonuclease 3'-5' domain containing 2	2.08
FAM65A	family with sequence similarity 65, member A	2.08
HMGA2	high mobility group AT-hook 2	2.08
KCNAB2	potassium voltage-gated channel, shaker-related subfamily, beta member 2	2.08
KCNU1	potassium channel, subfamily U, member 1	2.08
KRT25	keratin 25	2.08
MAP4K5	mitogen-activated protein kinase kinase kinase kinase 5	2.08
NIPBL	Nipped-B homolog (Drosophila)	2.08
PDE4DIP	phosphodiesterase 4D interacting protein, myomegalin-like	2.08
PDZRN3	PDZ domain containing ring finger 3	2.08
PSME4	proteasome (prosome, macropain) activator subunit 4	2.08

SLC25A22	solute carrier family 25 (mitochondrial carrier: glutamate), member 22	2.08
SLCO1C1	solute carrier organic anion transporter family, member 1C1	2.08
SLIT2	slit homolog 2 (Drosophila)	2.08
SMTN	smoothelin	2.08
SNX2	sorting nexin 2	2.08
SRPK1	SRSF protein kinase 1	2.08
TSPAN12	tetraspanin 12	2.08
TTC8	tetratricopeptide repeat domain 8	2.08
VAV3	vav 3 guanine nucleotide exchange factor	2.08
ALDOA	aldolase A, fructose-bisphosphate	2.07
BMS1P4	BMS1 pseudogene 4	2.07
BPTF	bromodomain PHD finger transcription factor, Rho GTPase activating protein 27 pseudogene	2.07
CBFA2T2	core-binding factor, runt domain, alpha subunit 2; translocated to, 2	2.07
CHAF1B	chromatin assembly factor 1, subunit B (p60)	2.07
CISD1	CDGSH iron sulfur domain 1	2.07
CLPB	ClpB caseinolytic peptidase B homolog (E. coli)	2.07
CLVS2	clavesin 2	2.07
DBR1	debranching enzyme homolog 1 (S. cerevisiae)	2.07
DDX58	DEAD (Asp-Glu-Ala-Asp) box polypeptide 58	2.07
EIF2B2	eukaryotic translation initiation factor 2B, subunit 2 beta, 39kDa	2.07
FAM48A	family with sequence similarity 48, member A	2.07
GPCPD1	glycerophosphocholine phosphodiesterase GDE1 homolog (S. cerevisiae)	2.07
HIPK3	homeodomain interacting protein kinase 3	2.07
ITCH	itchy E3 ubiquitin protein ligase	2.07
KDM6A	lysine (K)-specific demethylase 6A	2.07
LRRC41	leucine rich repeat containing 41	2.07
LTA	lymphotoxin alpha (TNF superfamily, member 1)	2.07
LTA	lymphotoxin alpha (TNF superfamily, member 1)	2.07
LTA	lymphotoxin alpha (TNF superfamily, member 1)	2.07
LTA	lymphotoxin alpha (TNF superfamily, member 1)	2.07
LTA	lymphotoxin alpha (TNF superfamily, member 1)	2.07
LTA	lymphotoxin alpha (TNF superfamily, member 1)	2.07
LTA	lymphotoxin alpha (TNF superfamily, member 1)	2.07
MAP3K6	mitogen-activated protein kinase kinase kinase 6	2.07
PAPSS2	3'-phosphoadenosine 5'-phosphosulfate synthase 2	2.07
PCMTD1	protein-L-isoaspartate (D-aspartate) O-methyltransferase domain containing 1	2.07
PDZD8	PDZ domain containing 8	2.07
PLA2G6	phospholipase A2, group VI (cytosolic, calcium-independent)	2.07
PNPO	pyridoxamine 5'-phosphate oxidase	2.07
PSME4	proteasome (prosome, macropain) activator subunit 4	2.07
RB1CC1	RB1-inducible coiled-coil 1	2.07
RRAGB	Ras-related GTP binding B	2.07

SCML1	sex comb on midleg-like 1 (Drosophila)	2.07
SLC9A9	solute carrier family 9, subfamily A (NHE9, cation proton antiporter 9), member 9	2.07
SUPT6H	suppressor of Ty 6 homolog (S. cerevisiae)	2.07
SYT1	synaptotagmin I	2.07
THRA, NR1D1	thyroid hormone receptor, alpha, nuclear receptor subfamily 1, group D, member 1	2.07
UNC79	unc-79 homolog (C. elegans)	2.07
ZNF227	zinc finger protein 227	2.07
ZNF765	zinc finger protein 765	2.07
ACSM3	acyl-CoA synthetase medium-chain family member 3	2.06
AMN1	antagonist of mitotic exit network 1 homolog (S. cerevisiae)	2.06
ANKRD49	ankyrin repeat domain 49	2.06
ARHGEF26	Rho guanine nucleotide exchange factor (GEF) 26	2.06
CDC14A	CDC14 cell division cycle 14 homolog A (S. cerevisiae)	2.06
CNKSR1	connector enhancer of kinase suppressor of Ras 1	2.06
DHTKD1	dehydrogenase E1 and transketolase domain containing 1	2.06
FAM149B1	family with sequence similarity 149, member B1	2.06
GON4L	gon-4-like (C. elegans)	2.06
HLA-F	major histocompatibility complex, class I, F	2.06
IMMP2L	IMP2 inner mitochondrial membrane peptidase-like (S. cerevisiae)	2.06
KLHL18	kelch-like 18 (Drosophila)	2.06
LOC283682	uncharacterized LOC283682	2.06
LRIG3	leucine-rich repeats and immunoglobulin-like domains 3	2.06
NFATC3	nuclear factor of activated T-cells, cytoplasmic, calcineurin-dependent 3	2.06
NLRP4	NLR family, pyrin domain containing 4	2.06
PDE9A	phosphodiesterase 9A	2.06
PHF15	PHD finger protein 15	2.06
PPIA	peptidylprolyl isomerase A (cyclophilin A), peptidyl-prolyl cis-trans isomerase A-like	2.06
PSMD11	proteasome (prosome, macropain) 26S subunit, non-ATPase, 11	2.06
RELB	v-rel reticuloendotheliosis viral oncogene homolog B	2.06
TRRAP	transformation/transcription domain-associated protein	2.06
VRK3	vaccinia related kinase 3	2.06
ZDHHC23	zinc finger, DHHC-type containing 23	2.06
ZFAT	zinc finger and AT hook domain containing	2.06
AGER, PBX2	advanced glycosylation end product-specific receptor, pre-B-cell leukemia homeobox 2	2.05
BBX	bobby sox homolog (Drosophila)	2.05
BTBD9	BTB (POZ) domain containing 9	2.05
C20orf112	chromosome 20 open reading frame 112	2.05
CAPN11	calpain 11	2.05
CCP110	centriolar coiled coil protein 110kDa	2.05
CHCHD7	coiled-coil-helix-coiled-coil-helix domain containing 7	2.05
CSTF3	cleavage stimulation factor, 3' pre-RNA, subunit 3, 77kDa	2.05
DNAH2	dynein, axonemal, heavy chain 2	2.05

DYRK4	dual-specificity tyrosine-(Y)-phosphorylation regulated kinase 4	2.05
DYX1C1-CCPG1	DYX1C1-CCPG1 readthrough (non-protein coding), cell cycle progression 1	2.05
ECI2	enoyl-CoA delta isomerase 2	2.05
EFCAB8	EF-hand calcium binding domain 8	2.05
FKBP15	FK506 binding protein 15, 133kDa	2.05
GMPS	guanine monphosphate synthetase	2.05
IDH3G	isocitrate dehydrogenase 3 (NAD+) gamma	2.05
IFT122	intraflagellar transport 122 homolog (Chlamydomonas)	2.05
LARP6	La ribonucleoprotein domain family, member 6	2.05
MAN2A2	mannosidase, alpha, class 2A, member 2	2.05
MAN2C1	mannosidase, alpha, class 2C, member 1	2.05
MANBA	mannosidase, beta A, lysosomal	2.05
MAPKBP1	mitogen-activated protein kinase binding protein 1	2.05
MYO3A	myosin IIIA	2.05
NCOA3	nuclear receptor coactivator 3	2.05
NKTR	natural killer-tumor recognition sequence	2.05
NOP9	NOP9 nucleolar protein homolog (yeast)	2.05
OXNAD1	oxidoreductase NAD-binding domain containing 1	2.05
PDCD10	programmed cell death 10	2.05
PDGFRB	platelet-derived growth factor receptor, beta polypeptide	2.05
PLCG2	phospholipase C, gamma 2 (phosphatidylinositol-specific)	2.05
PPP1R13B	protein phosphatase 1, regulatory subunit 13B	2.05
RAB28	RAB28, member RAS oncogene family	2.05
RORA	RAR-related orphan receptor A	2.05
SP110	SP110 nuclear body protein	2.05
SRRT	serrate RNA effector molecule homolog (Arabidopsis)	2.05
TRIM36	tripartite motif containing 36	2.05
TRPM3	transient receptor potential cation channel, subfamily M, member 3	2.05
TSGA13, COPG2	testis specific, 13, coatomer protein complex, subunit gamma 2	2.05
ZNF568	zinc finger protein 568	2.05
ADPRHL1	ADP-ribosylhydrolase like 1	2.04
C1RL-AS1	C1RL antisense RNA 1 (non-protein coding)	2.04
CDNF	cerebral dopamine neurotrophic factor	2.04
CLN5	ceroid-lipofuscinosis, neuronal 5	2.04
CRISPLD2	cysteine-rich secretory protein LCCL domain containing 2	2.04
DCAF5	DDB1 and CUL4 associated factor 5	2.04
DDR2	discoidin domain receptor tyrosine kinase 2	2.04
DHX35	DEAH (Asp-Glu-Ala-His) box polypeptide 35	2.04
DPYSL3	dihydropyrimidinase-like 3	2.04
EIF2C3	eukaryotic translation initiation factor 2C, 3	2.04
FAM175A	family with sequence similarity 175, member A	2.04
FBXL13	F-box and leucine-rich repeat protein 13	2.04
HDAC3	histone deacetylase 3	2.04

HUWE1	HECT, UBA and WWE domain containing 1, E3 ubiquitin protein ligase	2.04
KDM5D	lysine (K)-specific demethylase 5D	2.04
KIAA0100	KIAA0100	2.04
KIFAP3	kinesin-associated protein 3	2.04
KTN1	kinectin 1 (kinesin receptor)	2.04
LAMA1	laminin, alpha 1	2.04
LGMN	legumain	2.04
LNX1	ligand of numb-protein X 1, E3 ubiquitin protein ligase	2.04
MLL3	myeloid/lymphoid or mixed-lineage leukemia 3	2.04
MPP4	membrane protein, palmitoylated 4 (MAGUK p55 subfamily member 4)	2.04
MS4A12	membrane-spanning 4-domains, subfamily A, member 12	2.04
NBN	nibrin	2.04
NID1	nidogen 1	2.04
NUP205	nucleoporin 205kDa	2.04
PCLO	piccolo (presynaptic cytomatrix protein)	2.04
PPP1R12B	protein phosphatase 1, regulatory subunit 12B	2.04
RBM48	RNA binding motif protein 48	2.04
RP1	retinitis pigmentosa 1 (autosomal dominant)	2.04
SDHAF2	succinate dehydrogenase complex assembly factor 2	2.04
SENP1	SUMO1/sentrin specific peptidase 1	2.04
SERINC5	serine incorporator 5	2.04
SLC25A19	solute carrier family 25 (mitochondrial thiamine pyrophosphate carrier), member 19	2.04
TACO1	translational activator of mitochondrially encoded cytochrome c oxidase I	2.04
VPS41	vacuolar protein sorting 41 homolog (S. cerevisiae)	2.04
WNK3	WNK lysine deficient protein kinase 3	2.04
ZFAND4	zinc finger, AN1-type domain 4	2.04
ZNF569	zinc finger protein 569	2.04
ZNF609	zinc finger protein 609	2.04
ADCY5	adenylate cyclase 5	2.03
AKAP13	A kinase (PRKA) anchor protein 13	2.03
ATAD5	ATPase family, AAA domain containing 5	2.03
C14orf166B	chromosome 14 open reading frame 166B	2.03
C7orf10	chromosome 7 open reading frame 10	2.03
CDADC1	cytidine and dCMP deaminase domain containing 1	2.03
FAM194B	family with sequence similarity 194, member B	2.03
FAM49A	family with sequence similarity 49, member A	2.03
FMNL2	formin-like 2	2.03
FRA10AC1	fragile site, folic acid type, rare, fra(10)(q23.3) or fra(10)(q24.2) candidate 1	2.03
KCNT2	potassium channel, subfamily T, member 2	2.03
KIAA1045	KIAA1045	2.03
KIF9	kinesin family member 9	2.03
LINC00266-1	long intergenic non-protein coding RNA 266-1	2.03
NOL4	nucleolar protein 4	2.03

PCGF5	polycomb group ring finger 5	2.03
PCSK6	proprotein convertase subtilisin/kexin type 6	2.03
PIEZO2	piezo-type mechanosensitive ion channel component 2	2.03
POLQ	polymerase (DNA directed), theta	2.03
PPP1R9B	protein phosphatase 1, regulatory subunit 9B	2.03
PVR	poliovirus receptor	2.03
RAB11FIP2	RAB11 family interacting protein 2 (class I)	2.03
RASGEF1A	RasGEF domain family, member 1A	2.03
SLC12A1	solute carrier family 12 (sodium/potassium/chloride transporters), member 1	2.03
SLC43A2	solute carrier family 43, member 2	2.03
STRBP	spermatid perinuclear RNA binding protein	2.03
SUCLA2	succinate-CoA ligase, ADP-forming, beta subunit	2.03
TEF	thyrotrophic embryonic factor	2.03
TG	thyroglobulin	2.03
TRIM6-TRIM34	TRIM6-TRIM34 readthrough, tripartite motif containing 34, tripartite motif containing 6	2.03
TULP3	tubby like protein 3	2.03
ZER1	zer-1 homolog (C. elegans)	2.03
ABCA4	ATP-binding cassette, sub-family A (ABC1), member 4	2.02
ALX1	ALX homeobox 1	2.02
ATP8A2	ATPase, aminophospholipid transporter, class I, type 8A, member 2	2.02
C12orf52	chromosome 12 open reading frame 52	2.02
CCNT2	cyclin T2	2.02
CENPO	centromere protein O	2.02
DENND5B	DENN/MADD domain containing 5B	2.02
DOCK2	dedicator of cytokinesis 2	2.02
FAM115A, B	family with sequence similarity 115, member A & B, protein FAM115A-like	2.02
FOXRED1	FAD-dependent oxidoreductase domain containing 1	2.02
KHK	ketohexokinase (fructokinase)	2.02
KIAA1009	KIAA1009	2.02
MAP3K2	mitogen-activated protein kinase kinase kinase 2	2.02
MGAT4B	mannosyl (alpha-1,3-)-glycoprotein beta-1,4-N-acetylglucosaminyltransferase, isozyme B	2.02
NEB	nebulin	2.02
NEK11	NIMA (never in mitosis gene a)- related kinase 11	2.02
RAD9B	RAD9 homolog B (S. pombe)	2.02
RBL2	retinoblastoma-like 2 (p130)	2.02
RHBDF2	rhomboid 5 homolog 2 (Drosophila)	2.02
SIAE	sialic acid acetylesterase	2.02
SLC12A8	solute carrier family 12 (potassium/chloride transporters), member 8	2.02
SLC37A1	solute carrier family 37 (glycerol-3-phosphate transporter), member 1	2.02
ST3GAL6	ST3 beta-galactoside alpha-2,3-sialyltransferase 6	2.02
TMCO5B	transmembrane and coiled-coil domains 5B, pseudogene	2.02
TTC8	tetratricopeptide repeat domain 8	2.02

TTTY14	testis-specific transcript, Y-linked 14 (non-protein coding), non-protein coding RNA 185	2.02
USO1	USO1 vesicle docking protein homolog (yeast)	2.02
ZNF625-20	ZNF625-ZNF20 readthrough, zinc finger protein 20, zinc finger protein 625	2.02
ALS2CR11	amyotrophic lateral sclerosis 2 (juvenile) chromosome region, candidate 11	2.01
BICD1	bicaudal D homolog 1 (Drosophila)	2.01
C6orf58	chromosome 6 open reading frame 58	2.01
CC2D1B	coiled-coil and C2 domain containing 1B	2.01
CENPK	centromere protein K	2.01
CLGN	calmegin	2.01
DAB2	disabled homolog 2, mitogen-responsive phosphoprotein (Drosophila)	2.01
DCT	dopachrome tautomerase (dopachrome delta-isomerase, tyrosine-related protein 2)	2.01
EIF2AK2	eukaryotic translation initiation factor 2-alpha kinase 2	2.01
ERCC6L2	excision repair cross-complementing rodent repair deficiency, complementation group 6-like 2	2.01
EXOC6	exocyst complex component 6	2.01
EXPH5	exophilin 5	2.01
GINS4	GINS complex subunit 4 (Sld5 homolog)	2.01
GPCPD1	glycerophosphocholine phosphodiesterase GDE1 homolog (S. cerevisiae)	2.01
IL18RAP	interleukin 18 receptor accessory protein	2.01
JAK3	Janus kinase 3	2.01
KDM2B	lysine (K)-specific demethylase 2B	2.01
KIAA0895	KIAA0895	2.01
LRP4	low density lipoprotein receptor-related protein 4	2.01
LRRC16A	leucine rich repeat containing 16A	2.01
MAN1A1	mannosidase, alpha, class 1A, member 1	2.01
MAPKBP1	mitogen-activated protein kinase binding protein 1	2.01
MEF2A	myocyte enhancer factor 2A	2.01
MFSD11	major facilitator superfamily domain containing 11	2.01
MGAT4A	mannosyl (alpha-1,3-)-glycoprotein beta-1,4-N-acetylglucosaminyltransferase, isozyme A	2.01
MYO1B	myosin IB	2.01
PHF15	PHD finger protein 15	2.01
PMPCA	peptidase (mitochondrial processing) alpha	2.01
RHOT1	ras homolog family member T1	2.01
RUNDC3B	RUN domain containing 3B	2.01
SHCBP1	SHC SH2-domain binding protein 1	2.01
SLC16A14	solute carrier family 16, member 14 (monocarboxylic acid transporter 14)	2.01
SLC24A6	solute carrier family 24 (sodium/lithium/calcium exchanger), member 6	2.01
SLC26A4	solute carrier family 26, member 4	2.01
SLC30A6	solute carrier family 30 (zinc transporter), member 6	2.01
STK24	serine/threonine kinase 24	2.01
TBL1X	transducin (beta)-like 1X-linked	2.01
TEX9	testis expressed 9	2.01
TRPM4	transient receptor potential cation channel, subfamily M, member 4	2.01

UCHL1	ubiquitin carboxyl-terminal esterase L1 (ubiquitin thiolesterase)	2.01
UNC119	unc-119 homolog (C. elegans)	2.01
USP34	ubiquitin specific peptidase 34	2.01
WASF2	WAS protein family, member 2	2.01
WDR7	WD repeat domain 7	2.01
B4GALT3	UDP-Gal:betaGlcNAc beta 1,4- galactosyltransferase, polypeptide 3	-2.01
CD3D	CD3d molecule, delta (CD3-TCR complex)	-2.01
EOMES	eomesodermin	-2.01
EXD1	exonuclease 3'-5' domain containing 1	-2.01
FXR1	fragile X mental retardation, autosomal homolog 1	-2.01
GLT1D1	glycosyltransferase 1 domain containing 1	-2.01
KIF15	kinesin family member 15	-2.01
KLRF1	killer cell lectin-like receptor subfamily F, member 1	-2.01
NELL1	NEL-like 1 (chicken)	-2.01
NFKBIA	nuclear factor of kappa light polypeptide gene enhancer in B-cells inhibitor, alpha	-2.01
PLA2G6	phospholipase A2, group VI (cytosolic, calcium-independent)	-2.01
SFMBT2	Scm-like with four mbt domains 2	-2.01
SH2D2A	SH2 domain containing 2A	-2.01
THSD7B	thrombospondin, type I, domain containing 7B	-2.01
TMEM74B	transmembrane protein 74B	-2.01
TMOD2	tropomodulin 2 (neuronal)	-2.01
TSPAN2	tetraspanin 2	-2.01
TUBB3	tubulin, beta 3 class III	-2.01
WDFY4	WDFY family member 4	-2.01
ADCY5	adenylate cyclase 5	-2.02
ADIPOQ	adiponectin, C1Q and collagen domain containing	-2.02
ATP8B4	ATPase, class I, type 8B, member 4	-2.02
C1orf141	chromosome 1 open reading frame 141	-2.02
C9orf57	chromosome 9 open reading frame 57	-2.02
CA5A	carbonic anhydrase VA, mitochondrial	-2.02
FAM107A	family with sequence similarity 107, member A	-2.02
KLHL32	kelch-like 32 (Drosophila)	-2.02
LOC285423	uncharacterized LOC285423	-2.02
LOC388276	hCG2045437	-2.02
MRPS18C	mitochondrial ribosomal protein S18C, 28S ribosomal protein S18c, mitochondrial-like	-2.02
NIT1	nitrilase 1	-2.02
RHCE	Rh blood group, CcEe antigens	-2.02
RNF183	ring finger protein 183	-2.02
SATB2	SATB homeobox 2	-2.02
SF3B1	splicing factor 3b, subunit 1, 155kDa	-2.02
SLC22A31	solute carrier family 22, member 31	-2.02
SLC26A4	solute carrier family 26, member 4	-2.02

TCN2	transcobalamin II	-2.02
AP1M2	adaptor-related protein complex 1, mu 2 subunit	-2.03
ASB14	ankyrin repeat and SOCS box containing 14	-2.03
C20orf152	chromosome 20 open reading frame 152	-2.03
CCDC144NL	coiled-coil domain containing 144 family, N-terminal like	-2.03
CNTN6	contactin 6	-2.03
FAM206A	family with sequence similarity 206, member A	-2.03
ISLR2	immunoglobulin superfamily containing leucine-rich repeat 2	-2.03
LOC100505875	uncharacterized LOC100505875	-2.03
LOC100653273	uncharacterized LOC100653273	-2.03
LOC400541	uncharacterized LOC400541	-2.03
MFAP5	microfibrillar associated protein 5	-2.03
MYT1	myelin transcription factor 1	-2.03
NPR3	natriuretic peptide receptor C/guanylate cyclase C (atrionatriuretic peptide receptor C)	-2.03
PTPRT	protein tyrosine phosphatase, receptor type, T	-2.03
RNASE1	ribonuclease, RNase A family, 1 (pancreatic)	-2.03
RYR3	ryanodine receptor 3	-2.03
SKIV2L2	superkiller viralicidic activity 2-like 2 (S. cerevisiae)	-2.03
SLIT2	slit homolog 2 (Drosophila)	-2.03
TMEM155	transmembrane protein 155	-2.03
ACSBG2	acyl-CoA synthetase bubblegum family member 2	-2.04
AKR1B1	aldo-keto reductase family 1, member B1 (aldose reductase)	-2.04
CCDC129	coiled-coil domain containing 129	-2.04
CDH16	cadherin 16, KSP-cadherin	-2.04
DPEP1	dipeptidase 1 (renal)	-2.04
FPGS	folylpolyglutamate synthase	-2.04
HSD11B1	hydroxysteroid (11-beta) dehydrogenase 1	-2.04
NHP2L1	NHP2 non-histone chromosome protein 2-like 1 (S. cerevisiae)	-2.04
PARP15	poly (ADP-ribose) polymerase family, member 15	-2.04
PURG	purine-rich element binding protein G	-2.04
RGS5	regulator of G-protein signaling 5	-2.04
SCNN1B	sodium channel, non-voltage-gated 1, beta subunit	-2.04
SLC8A2	solute carrier family 8 (sodium/calcium exchanger), member 2	-2.04
SYCE1	synaptonemal complex central element protein 1	-2.04
TMCO5A	transmembrane and coiled-coil domains 5A	-2.04
AP5Z1, MIR4656	adaptor-related protein complex 5, zeta 1 subunit, microRNA 4656	-2.05
ARMCX2	armadillo repeat containing, X-linked 2	-2.05
HOXA7	homeobox A7	-2.05
HOXC4,5, 6	homeobox C4, homeobox C5, homeobox C6	-2.05
LOC100506030	uncharacterized LOC100506030	-2.05
SCNN1A	sodium channel, non-voltage-gated 1 alpha subunit	-2.05
SH3GL3	SH3-domain GRB2-like 3	-2.05

TG	thyroglobulin	-2.05
TG	thyroglobulin	-2.05
WDR63	WD repeat domain 63	-2.05
ANKRD44	ankyrin repeat domain 44	-2.06
CDT1	chromatin licensing and DNA replication factor 1	-2.06
COA1	cytochrome C oxidase assembly factor 1 homolog (S. cerevisiae)	-2.06
HK2	hexokinase 2	-2.06
KIRREL2	kin of IRRE like 2 (Drosophila)	-2.06
LRBA	LPS-responsive vesicle trafficking, beach and anchor containing	-2.06
NADSYN1	NAD synthetase 1	-2.06
PKMYT1	protein kinase, membrane associated tyrosine/threonine 1	-2.06
PPP4R4	protein phosphatase 4, regulatory subunit 4	-2.06
ANKRD24	ankyrin repeat domain 24	-2.07
ARFGAP2	ADP-ribosylation factor GTPase activating protein 2	-2.07
C14orf164	chromosome 14 open reading frame 164	-2.07
CFB	complement factor B	-2.07
CLSTN2	calsyntenin 2	-2.07
DCHS2	dachsous 2 (Drosophila)	-2.07
DNAH5	dynein, axonemal, heavy chain 5	-2.07
IFT80	intraflagellar transport 80 homolog (Chlamydomonas)	-2.07
KLHL28	kelch-like 28 (Drosophila)	-2.07
LOC100130348	uncharacterized LOC100130348, uncharacterized LOC399904	-2.07
NDUFB2	NADH dehydrogenase (ubiquinone) 1 beta subcomplex, 2, 8kDa	-2.07
SH3KBP1	SH3-domain kinase binding protein 1	-2.07
SLC22A12	solute carrier family 22 (organic anion/urate transporter), member 12	-2.07
TKTL1	transketolase-like 1	-2.07
CPA1	carboxypeptidase A1 (pancreatic)	-2.08
EGR1	early growth response 1	-2.08
ENO1	enolase 1, (alpha)	-2.08
ENPP3	ectonucleotide pyrophosphatase/phosphodiesterase 3	-2.08
FLJ13197	uncharacterized FLJ13197	-2.08
MAFF	v-maf musculoaponeurotic fibrosarcoma oncogene homolog F (avian)	-2.08
MRPS18C	mitochondrial ribosomal protein S18C, 28S ribosomal protein S18c, mitochondrial-like	-2.08
PKHD1L1	polycystic kidney and hepatic disease 1 (autosomal recessive)-like 1	-2.08
PTPRN2	protein tyrosine phosphatase, receptor type, N polypeptide 2	-2.08
SCN4A	sodium channel, voltage-gated, type IV, alpha subunit	-2.08
SEC62	SEC62 homolog (S. cerevisiae)	-2.08
TPK1	thiamin pyrophosphokinase 1	-2.08
UBE2G2, SUMO3	ubiquitin-conjugating enzyme E2G 2, SMT3 suppressor of mif two 3 homolog 3	-2.08
UNG	uracil-DNA glycosylase	-2.08
ZMYM4-AS1	ZMYM4 antisense RNA 1 (non-protein coding)	-2.08
ZNF609	zinc finger protein 609	-2.08

ADORA1	adenosine A1 receptor	-2.09
BEST3	bestrophin 3	-2.09
C1orf198	chromosome 1 open reading frame 198	-2.09
C4A, C4B	complement component 4A (Rodgers blood group), complement component 4B	-2.09
C4A, C4B, STK19	complement component 4A (Rodgers blood group), complement component 4B	-2.09
C4B, C4A	complement component 4B (Chido blood group), complement component 4A	-2.09
C4B, C4A	complement component 4B (Chido blood group)	-2.09
C4B, C4A	complement component 4B (Chido blood group)	-2.09
C4B, C4A	complement component 4B (Chido blood group)	-2.09
C4B, C4A	complement component 4B (Chido blood group)	-2.09
CD163	CD163 molecule	-2.09
CDC14B	CDC14 cell division cycle 14 homolog B (S. cerevisiae)	-2.09
CYP11A1	cytochrome P450, family 11, subfamily A, polypeptide 1	-2.09
DSCAM	Down syndrome cell adhesion molecule	-2.09
GTF3C4	general transcription factor IIIC, polypeptide 4, 90kDa	-2.09
HEATR8-TTC4	HEATR8-TTC4 readthrough, HEAT repeat containing 8, tetratricopeptide repeat domain 4	-2.09
LZTR1	leucine-zipper-like transcription regulator 1	-2.09
NDUFB2	NADH dehydrogenase (ubiquinone) 1 beta subcomplex, 2, 8kDa	-2.09
RBPJ	recombination signal binding protein for immunoglobulin kappa J region	-2.09
RNF32	ring finger protein 32	-2.09
SSPN	sarcospan	-2.09
TESC	tescalcin	-2.09
TNK2	tyrosine kinase, non-receptor, 2	-2.09
ABCD4	ATP-binding cassette, sub-family D (ALD), member 4	-2.1
ANHX	anomalous homeobox	-2.1
CAMK4	calcium/calmodulin-dependent protein kinase IV	-2.1
CFLAR-AS1	CFLAR antisense RNA 1 (non-protein coding)	-2.1
DPF3	D4, zinc and double PHD fingers, family 3	-2.1
ENGASE	endo-beta-N-acetylglucosaminidase	-2.1
PLAT	plasminogen activator, tissue	-2.1
PRKCZ	protein kinase C, zeta	-2.1
SLC12A9	solute carrier family 12 (potassium/chloride transporters), member 9	-2.1
SLFNL1	schlafen-like 1	-2.1
TTC29	tetratricopeptide repeat domain 29	-2.1
ACSL6	acyl-CoA synthetase long-chain family member 6	-2.11
C20orf112	chromosome 20 open reading frame 112	-2.11
COL1A1	collagen, type I, alpha 1	-2.11
DNAH11	dynein, axonemal, heavy chain 11	-2.11
FAM131A	family with sequence similarity 131, member A	-2.11
FANCC	Fanconi anemia, complementation group C	-2.11
HIAT1	hippocampus abundant transcript 1	-2.11
INF2	inverted formin, FH2 and WH2 domain containing	-2.11

KRT15	keratin 15	-2.11
LOC100507308	uncharacterized LOC100507308	-2.11
LOC400940	uncharacterized LOC400940	-2.11
PIP5KL1	phosphatidylinositol-4-phosphate 5-kinase-like 1	-2.11
SKIV2L	superkiller viralicidic activity 2-like (S. cerevisiae)	-2.11
SKIV2L	superkiller viralicidic activity 2-like (S. cerevisiae)	-2.11
SKIV2L	superkiller viralicidic activity 2-like (S. cerevisiae)	-2.11
SKIV2L	superkiller viralicidic activity 2-like (S. cerevisiae)	-2.11
SKIV2L	superkiller viralicidic activity 2-like (S. cerevisiae)	-2.11
SKIV2L	superkiller viralicidic activity 2-like (S. cerevisiae)	-2.11
SLC7A13	solute carrier family 7 (anionic amino acid transporter), member 13	-2.11
VAV3	vav 3 guanine nucleotide exchange factor	-2.11
ZP1	zona pellucida glycoprotein 1 (sperm receptor)	-2.11
B4GALNT1	beta-1,4-N-acetyl-galactosaminyl transferase 1	-2.12
CHRD	chordin	-2.12
COL14A1	collagen, type XIV, alpha 1	-2.12
DCP1B	DCP1 decapping enzyme homolog B (S. cerevisiae)	-2.12
DGKK	diacylglycerol kinase, kappa	-2.12
DMD	dystrophin	-2.12
DNAH10	dynein, axonemal, heavy chain 10	-2.12
HEATR2	HEAT repeat containing 2	-2.12
MECOM	MDS1 and EVI1 complex locus	-2.12
PLEKHM1	pleckstrin homology domain containing, family M (with RUN domain) member 1	-2.12
PREX2	phosphatidylinositol-3,4,5-trisphosphate-dependent Rac exchange factor 2	-2.12
RDH12	retinol dehydrogenase 12 (all-trans/9-cis/11-cis)	-2.12
ADCY6, MIR4701	adenylate cyclase 6, microRNA 4701	-2.13
BEST2	bestrophin 2	-2.13
C10orf112	chromosome 10 open reading frame 112	-2.13
CAPZA1	capping protein (actin filament) muscle Z-line, alpha 1	-2.13
ENPP2	ectonucleotide pyrophosphatase/phosphodiesterase 2	-2.13
GPR89A, GPR89B	G protein-coupled receptor 89A, G protein-coupled receptor 89B	-2.13
HLA-DPB1	major histocompatibility complex, class II, DP beta 1	-2.13
HLA-DPB1	major histocompatibility complex, class II, DP beta 1	-2.13
HLA-DPB1	major histocompatibility complex, class II, DP beta 1	-2.13
HLA-DPB1	major histocompatibility complex, class II, DP beta 1	-2.13
HLA-DPB1	major histocompatibility complex, class II, DP beta 1	-2.13
HLA-DPB1	major histocompatibility complex, class II, DP beta 1	-2.13
HLA-DPB1	major histocompatibility complex, class II, DP beta 1	-2.13
HN1	hematological and neurological expressed 1	-2.13
ITK	IL2-inducible T-cell kinase	-2.13
KLC2	kinesin light chain 2	-2.13
LONRF3	LON peptidase N-terminal domain and ring finger 3	-2.13

NRAP	nebulin-related anchoring protein	-2.13
PI4KB	phosphatidylinositol 4-kinase, catalytic, beta	-2.13
SERINC4	serine incorporator 4	-2.13
TMPRSS2	transmembrane protease, serine 2	-2.13
ZNF692	zinc finger protein 692	-2.13
ALPL	alkaline phosphatase, liver/bone/kidney	-2.14
B3GNT5	UDP-GlcNAc:betaGal beta-1,3-N-acetylglucosaminyltransferase 5	-2.14
CCL14-CCL15	CCL14-CCL15 readthrough, chemokine (C-C motif) ligand 14 & 15	-2.14
MGST3	microsomal glutathione S-transferase 3	-2.14
MYCBPAP	MYCBP associated protein	-2.14
NFRKB	nuclear factor related to kappaB binding protein	-2.14
OVGP1	oviductal glycoprotein 1, 120kDa	-2.14
PCDH12	protocadherin 12	-2.14
RASGRP3	RAS guanyl releasing protein 3 (calcium and DAG-regulated)	-2.14
ZP1	zona pellucida glycoprotein 1 (sperm receptor)	-2.14
C20orf152	chromosome 20 open reading frame 152	-2.15
CCDC164	coiled-coil domain containing 164	-2.15
COL24A1	collagen, type XXIV, alpha 1	-2.15
CYFIP2	cytoplasmic FMR1 interacting protein 2	-2.15
DOCK2	dedicator of cytokinesis 2	-2.15
FGR	Gardner-Rasheed feline sarcoma viral (v-fgr) oncogene homolog	-2.15
FMO1	flavin containing monooxygenase 1	-2.15
HSD17B1	hydroxysteroid (17-beta) dehydrogenase 1	-2.15
OR13A1	olfactory receptor, family 13, subfamily A, member 1	-2.15
PLXND1	plexin D1	-2.15
RUSC1-AS1	RUSC1 antisense RNA 1 (non-protein coding)	-2.15
TATDN1	TatD DNase domain containing 1	-2.15
TRPM8	transient receptor potential cation channel, subfamily M, member 8	-2.15
WDFY4	WDFY family member 4	-2.15
BAZ2A	bromodomain adjacent to zinc finger domain, 2A	-2.16
COL16A1	collagen, type XVI, alpha 1	-2.16
DNAH3	dynein, axonemal, heavy chain 3	-2.16
IDH1	isocitrate dehydrogenase 1 (NADP+), soluble	-2.16
LOC732275	uncharacterized LOC732275	-2.16
NDRG2	NDRG family member 2	-2.16
NME1-NME2	NME1-NME2 readthrough, NME/NM23 nucleoside diphosphate kinase 1 & 2	-2.16
PDCD6IP	programmed cell death 6 interacting protein	-2.16
RYR3	ryanodine receptor 3	-2.16
TTN-AS1	TTN antisense RNA 1 (non-protein coding)	-2.16
ARHGAP4	Rho GTPase activating protein 4	-2.17
ATAD1	ATPase family, AAA domain containing 1	-2.17
COL4A6	collagen, type IV, alpha 6	-2.17
CSMD1	CUB and Sushi multiple domains 1	-2.17

DDB1	damage-specific DNA binding protein 1, 127kDa	-2.17
MEPE	matrix extracellular phosphoglycoprotein	-2.17
PADI1	peptidyl arginine deiminase, type I	-2.17
PDE3A	phosphodiesterase 3A, cGMP-inhibited	-2.17
PMEL	premelanosome protein	-2.17
SLC22A24	solute carrier family 22, member 24	-2.17
SNORD32B	small nucleolar RNA, C/D box 32B	-2.17
USP13	ubiquitin specific peptidase 13 (isopeptidase T-3)	-2.17
C12orf51	chromosome 12 open reading frame 51	-2.18
CCDC39	coiled-coil domain containing 39	-2.18
CSMD3	CUB and Sushi multiple domains 3	-2.18
FGF21	fibroblast growth factor 21	-2.18
FLJ20444	uncharacterized protein FLJ20444	-2.18
FN3K	fructosamine 3 kinase	-2.18
NMD3	NMD3 homolog (S. cerevisiae)	-2.18
PDE6C	phosphodiesterase 6C, cGMP-specific, cone, alpha prime	-2.18
POTEB	POTE ankyrin domain family, member B, POTE ankyrin domain family member B-like	-2.18
POTEB	POTE ankyrin domain family, member B, POTE ankyrin domain family member B-like	-2.18
RIN3	Ras and Rab interactor 3	-2.18
ZNF575	zinc finger protein 575	-2.18
ABHD6	abhydrolase domain containing 6	-2.19
ART4	ADP-ribosyltransferase 4 (Dombrock blood group)	-2.19
CA5BP1	carbonic anhydrase VB pseudogene 1	-2.19
CXCL12	chemokine (C-X-C motif) ligand 12	-2.19
CYB5R2	cytochrome b5 reductase 2	-2.19
DNAJB5	DnaJ (Hsp40) homolog, subfamily B, member 5	-2.19
DNAJC9-AS1	DNAJC9 antisense RNA 1 (non-protein coding), chromosome 10 open reading frame 103	-2.19
IPO7	importin 7	-2.19
KIAA0101	KIAA0101	-2.19
PLA2G6	phospholipase A2, group VI (cytosolic, calcium-independent)	-2.19
RNF166	ring finger protein 166	-2.19
SBF2	SET binding factor 2	-2.19
SCN3A	sodium channel, voltage-gated, type III, alpha subunit	-2.19
SLC24A5	solute carrier family 24, member 5	-2.19
TFAP2D	transcription factor AP-2 delta (activating enhancer binding protein 2 delta)	-2.19
WHSC1	Wolf-Hirschhorn syndrome candidate 1	-2.19
BCL6B	B-cell CLL/lymphoma 6, member B	-2.2
BMP5	bone morphogenetic protein 5	-2.2
CACNA1E	calcium channel, voltage-dependent, R type, alpha 1E subunit	-2.2
CACNA1I	calcium channel, voltage-dependent, T type, alpha 1I subunit	-2.2
MIR943, WHSC2	microRNA 943, Wolf-Hirschhorn syndrome candidate 2	-2.2
MS4A8B	membrane-spanning 4-domains, subfamily A, member 8B	-2.2

NR2C2	nuclear receptor subfamily 2, group C, member 2	-2.2
NSMAF	neutral sphingomyelinase (N-SMase) activation associated factor	-2.2
SYNJ2	synaptojanin 2	-2.2
TEX26-AS1	TEX26 antisense RNA 1 (non-protein coding)	-2.2
TRIM39-RPP21	TRIM39-RPP21 readthrough, tripartite motif containing 39	-2.2
TRIM39-RPP21	TRIM39-RPP21 readthrough, tripartite motif containing 39	-2.2
TRIM39-RPP21	TRIM39-RPP21 readthrough, tripartite motif containing 39	-2.2
TRIM39-RPP21	TRIM39-RPP21 readthrough, tripartite motif containing 39	-2.2
AGAP2	ArfGAP with GTPase domain, ankyrin repeat and PH domain 2	-2.21
ARID4A	AT rich interactive domain 4A (RBP1-like)	-2.21
CCDC153	coiled-coil domain containing 153	-2.21
CFTR	cystic fibrosis transmembrane conductance regulator (ATP-binding cassette sub-family C, member 7)	-2.21
IQCJ, SCHIP1	IQ motif containing J, schwannomin interacting protein 1, IQCJ-SCHIP1 readthrough	-2.21
LOC348817	uncharacterized LOC348817, CCDC13 antisense RNA 1 (non-protein coding)	-2.21
PDE10A	phosphodiesterase 10A	-2.21
RALYL	RALY RNA binding protein-like	-2.21
TATDN1	TatD DNase domain containing 1	-2.21
TFEB	transcription factor EB	-2.21
TMEM14B	transmembrane protein 14B	-2.21
ABCA9	ATP-binding cassette, sub-family A (ABC1), member 9	-2.22
CSNK2B	casein kinase 2, beta polypeptide	-2.22
FAM65B	family with sequence similarity 65, member B	-2.22
PNCK	pregnancy up-regulated non-ubiquitously expressed CaM kinase	-2.22
PSAP	prosaposin	-2.22
SNORD32B	small nucleolar RNA, C/D box 32B	-2.22
SNORD32B	small nucleolar RNA, C/D box 32B	-2.22
SNORD32B	small nucleolar RNA, C/D box 32B	-2.22
SNORD32B	small nucleolar RNA, C/D box 32B	-2.22
SNORD32B	small nucleolar RNA, C/D box 32B	-2.22
SNORD32B	small nucleolar RNA, C/D box 32B	-2.22
SSBP1, MIR5096	single-stranded DNA binding protein 1, mitochondrial, microRNA 5096	-2.22
TBC1D5	TBC1 domain family, member 5	-2.22
AHNAK2	AHNAK nucleoprotein 2	-2.23
ARHGEF3	Rho guanine nucleotide exchange factor (GEF) 3	-2.23
C1orf51	chromosome 1 open reading frame 51	-2.23
CAB39L	calcium binding protein 39-like	-2.23
CBR3-AS1	CBR3 antisense RNA 1 (non-protein coding)	-2.23
ENOSF1	enolase superfamily member 1	-2.23
FUT8	fucosyltransferase 8 (alpha (1,6) fucosyltransferase)	-2.23
GRID1	glutamate receptor, ionotropic, delta 1	-2.23
NUAK1	NUAK family, SNF1-like kinase, 1	-2.23
PARVB	parvin, beta	-2.23

RBFOX1	RNA binding protein, fox-1 homolog (C. elegans) 1	-2.23
SLC27A1	solute carrier family 27 (fatty acid transporter), member 1	-2.23
TAB1	TGF-beta activated kinase 1/MAP3K7 binding protein 1	-2.23
TMC5	transmembrane channel-like 5	-2.23
ADCYAP1	adenylate cyclase activating polypeptide 1 (pituitary)	-2.24
C3	complement component 3	-2.24
CFP	complement factor properdin	-2.24
FBXO18	F-box protein, helicase, 18	-2.24
GAB1	GRB2-associated binding protein 1	-2.24
LILRA6	leukocyte immunoglobulin-like receptor, subfamily A (with TM domain), member 6	-2.24
LINC00499	long intergenic non-protein coding RNA 499	-2.24
ODZ4	odz, odd Oz/ten-m homolog 4 (Drosophila)	-2.24
PDE4DIP	phosphodiesterase 4D interacting protein, myomegalin-like	-2.24
PPEF1	protein phosphatase, EF-hand calcium binding domain 1	-2.24
RHOU, DUSP5P	ras homolog family member U, dual specificity phosphatase 5 pseudogene	-2.24
STAC3	SH3 and cysteine rich domain 3	-2.24
SUSD4	sushi domain containing 4	-2.24
TTBK1	tau tubulin kinase 1	-2.24
BZRAP1	benzodiazapine receptor (peripheral) associated protein 1	-2.25
CAPRIN1	cell cycle associated protein 1	-2.25
CCR8	chemokine (C-C motif) receptor 8	-2.25
PCOLCE-AS1	PCOLCE antisense RNA 1 (non-protein coding)	-2.25
TYRP1	tyrosinase-related protein 1	-2.25
AATK	apoptosis-associated tyrosine kinase	-2.26
C10orf112	chromosome 10 open reading frame 112	-2.26
DMBT1	deleted in malignant brain tumors 1	-2.26
FER1L6	fer-1-like 6 (C. elegans)	-2.26
GABRA2	gamma-aminobutyric acid (GABA) A receptor, alpha 2	-2.26
HERC5	HECT and RLD domain containing E3 ubiquitin protein ligase 5	-2.26
NAAA	N-acylethanolamine acid amidase	-2.26
PPP1R16A	protein phosphatase 1, regulatory subunit 16A	-2.26
SPTBN4	spectrin, beta, non-erythrocytic 4	-2.26
SSPN	sarcospan	-2.26
ZBTB8OS	zinc finger and BTB domain containing 8 opposite strand	-2.26
ATP6V1G2	ATP6V1G2-DDX39B readthrough (non-protein coding)	-2.27
C4orf17	chromosome 4 open reading frame 17	-2.27
CATSPERB	catsper channel auxiliary subunit beta	-2.27
DEK	DEK oncogene	-2.27
GAL3ST4	galactose-3-O-sulfotransferase 4	-2.27
HMGCLL1	3-hydroxymethyl-3-methylglutaryl-CoA lyase-like 1	-2.27
SNORD84	small nucleolar RNA, C/D box 84, DEAD (Asp-Glu-Ala-Asp) box polypeptide 39B	-2.27
TTN	titin	-2.27

ZNF799	zinc finger protein 799	-2.27
ABCB11	ATP-binding cassette, sub-family B (MDR/TAP), member 11	-2.28
CD36	CD36 molecule (thrombospondin receptor)	-2.28
EYS	eyes shut homolog (Drosophila)	-2.28
IL17D	interleukin 17D	-2.28
REC8	REC8 homolog (yeast)	-2.28
SH3D21	SH3 domain containing 21, uncharacterized	-2.28
TTC37	tetratricopeptide repeat domain 37	-2.28
ZDHHC17	zinc finger, DHHC-type containing 17	-2.28
ZNF497	zinc finger protein 497	-2.28
FEZ1	fasciculation and elongation protein zeta 1 (zygin I)	-2.29
FRY	furry homolog (Drosophila)	-2.29
POR	P450 (cytochrome) oxidoreductase	-2.29
PYHIN1	pyrin and HIN domain family, member 1	-2.29
SLC12A9	solute carrier family 12 (potassium/chloride transporters), member 9	-2.29
TACC2	transforming, acidic coiled-coil containing protein 2	-2.29
ACE2	angiotensin I converting enzyme (peptidyl-dipeptidase A) 2	-2.3
ARC	activity-regulated cytoskeleton-associated protein	-2.3
CCDC155	coiled-coil domain containing 155	-2.3
GATA4	GATA binding protein 4	-2.3
IL24	interleukin 24	-2.3
LOC340515	uncharacterized LOC340515	-2.3
LPA	lipoprotein, Lp(a)	-2.3
MLXIPL	MLX interacting protein-like	-2.3
RUNDC3B	RUN domain containing 3B	-2.3
SCN1A	sodium channel, voltage-gated, type I, alpha subunit	-2.3
SYT9	synaptotagmin IX	-2.3
TLE3	transducin-like enhancer of split 3 (E(sp1) homolog, Drosophila)	-2.3
Mar-10	membrane-associated ring finger (C3HC4) 10, E3 ubiquitin protein ligase	-2.31
ESRP1	epithelial splicing regulatory protein 1	-2.31
GAGE1-13/A-H	G antigen 1-12/A-I	-2.31
ITGB1BP1	integrin beta 1 binding protein 1	-2.31
JAKMIP1	janus kinase and microtubule interacting protein 1	-2.31
KAZN	kazrin, periplakin interacting protein	-2.31
LOC387895	uncharacterized LOC387895	-2.31
MASP2	mannan-binding lectin serine peptidase 2	-2.31
PAX8	paired box 8	-2.31
RNF216	ring finger protein 216	-2.31
SHC4	SHC (Src homology 2 domain containing) family, member 4	-2.31
USP50	ubiquitin specific peptidase 50	-2.31
ZACN	zinc activated ligand-gated ion channel	-2.31
ANKHD1-EIF4EBP3	ankyrin repeat and KH domain containing 1, eukaryotic translation initiation factor 4E binding protein 3	-2.32
CHODL	chondrolectin	-2.32

EMC1	ER membrane protein complex subunit 1	-2.32
ESR2	estrogen receptor 2 (ER beta)	-2.32
IL23R	interleukin 23 receptor	-2.32
LILRA4	leukocyte immunoglobulin-like receptor, subfamily A (with TM domain), member 4	-2.32
MYO15B	myosin XVB pseudogene	-2.32
NXPE2	neurexophilin and PC-esterase domain family, member 2	-2.32
PGA3	pepsinogen 3, group I (pepsinogen A)	-2.32
PTPRO	protein tyrosine phosphatase, receptor type, O	-2.32
TAF6	TAF6 RNA polymerase II, TATA box binding protein (TBP)-associated factor, 80kDa	-2.32
ACPL2	acid phosphatase-like 2	-2.33
ATP13A4	ATPase type 13A4	-2.33
BIVM-ERCC5	BIVM-ERCC5 readthrough, complementation group 5	-2.33
C12orf35	chromosome 12 open reading frame 35	-2.33
CCDC78	coiled-coil domain containing 78	-2.33
CRTAC1	cartilage acidic protein 1	-2.33
DNAH12	dynein, axonemal, heavy chain 12	-2.33
DNAH9	dynein, axonemal, heavy chain 9	-2.33
FAM98B	family with sequence similarity 98, member B	-2.33
FBN2	fibrillin 2	-2.33
GUCY2GP	guanylate cyclase 2G homolog (mouse), pseudogene	-2.33
USP3	ubiquitin specific peptidase 3	-2.33
ZNF470	zinc finger protein 470	-2.33
AMOT	angiomotin	-2.34
CYP4F12	cytochrome P450, family 4, subfamily F, polypeptide 12	-2.34
HAL	histidine ammonia-lyase	-2.34
MARK2	MAP/microtubule affinity-regulating kinase 2	-2.34
PLCB1	phospholipase C, beta 1 (phosphoinositide-specific)	-2.34
PXDN	peroxidasin homolog (Drosophila)	-2.34
RPS4Y2	ribosomal protein S4, Y-linked 2	-2.34
AFF3	AF4/FMR2 family, member 3	-2.35
DNAH11	dynein, axonemal, heavy chain 11	-2.35
EML5	echinoderm microtubule associated protein like 5	-2.35
GART	phosphoribosylglycinamide formyltransferase, phosphoribosylglycinamide synthetase	-2.35
PADI4	peptidyl arginine deiminase, type IV	-2.35
RPS6KL1	ribosomal protein S6 kinase-like 1	-2.35
TIAM1	T-cell lymphoma invasion and metastasis 1	-2.35
ACADM	acyl-CoA dehydrogenase, C-4 to C-12 straight chain	-2.36
ENPEP	glutamyl aminopeptidase (aminopeptidase A)	-2.36
GRINA	glutamate receptor, ionotropic, N-methyl D-aspartate-associated protein 1 (glutamate binding)	-2.36
HMCN1	hemicentin 1	-2.36
PPFIA1	protein tyrosine phosphatase, receptor type, f polypeptide (PTPRF), interacting protein (liprin), alpha 1	-2.36

SYCP2L	synaptonemal complex protein 2-like, transmembrane protein 14B	-2.36
A2ML1	alpha-2-macroglobulin-like 1	-2.37
COBL	cordon-bleu homolog (mouse)	-2.37
IL13RA2	interleukin 13 receptor, alpha 2	-2.37
RP1	retinitis pigmentosa 1 (autosomal dominant)	-2.37
STX5	syntaxin 5	-2.37
DDHD2	DDHD domain containing 2	-2.38
KIF1A	kinesin family member 1A	-2.38
LOC100131825	uncharacterized LOC100131825	-2.38
MOK	MOK protein kinase	-2.38
PDGFC	platelet derived growth factor C	-2.38
SOD2	superoxide dismutase 2, mitochondrial	-2.38
TRPA1	transient receptor potential cation channel, subfamily A, member 1	-2.38
TTC40	tetratricopeptide repeat domain 40	-2.38
AKR1B15	aldo-keto reductase family 1, member B15	-2.39
ANKRD55	ankyrin repeat domain 55	-2.39
BPIFB1	BPI fold containing family B, member 1	-2.39
COL25A1	collagen, type XXV, alpha 1	-2.39
DNAH11	dynein, axonemal, heavy chain 11	-2.39
GAL3ST1	galactose-3-O-sulfotransferase 1	-2.39
KRTAP5-10	keratin associated protein 5-10	-2.39
TMPRSS3	transmembrane protease, serine 3	-2.39
TRPC6	transient receptor potential cation channel, subfamily C, member 6	-2.39
UNC80	unc-80 homolog (C. elegans)	-2.39
CLEC2B	C-type lectin domain family 2, member B	-2.4
DLG4	discs, large homolog 4 (Drosophila)	-2.4
ECE2	endothelin converting enzyme 2	-2.4
ELP4	elongation protein 4 homolog (S. cerevisiae)	-2.4
GAS8	5-hydroxyisourate hydrolase pseudogene, growth arrest-specific 8	-2.4
PDE1B	phosphodiesterase 1B, calmodulin-dependent	-2.4
PROL1	proline rich, lacrimal 1	-2.4
BPIFB6	BPI fold containing family B, member 6	-2.41
CMYA5	cardiomyopathy associated 5	-2.41
DUOX1	dual oxidase 1	-2.41
FAM13C	family with sequence similarity 13, member C	-2.41
FLJ46010	FLJ46010 protein	-2.41
IL16	interleukin 16	-2.41
PKHD1L1	polycystic kidney and hepatic disease 1 (autosomal recessive)-like 1	-2.41
RELN	reelin	-2.41
RENBP	renin binding protein	-2.41
RIPK3	receptor-interacting serine-threonine kinase 3	-2.41
RTDR1	rhabdoid tumor deletion region gene 1	-2.41
SAMD11	sterile alpha motif domain containing 11	-2.41

SSPO	SCO-spondin homolog (Bos taurus)	-2.41
TSLP	thymic stromal lymphopoietin	-2.41
VAV3	vav 3 guanine nucleotide exchange factor	-2.41
ZNF839	zinc finger protein 839	-2.41
DMTF1	cyclin D binding myb-like transcription factor 1	-2.42
ESR1	estrogen receptor 1	-2.42
IQGAP1	IQ motif containing GTPase activating protein 1	-2.42
KCNU1	potassium channel, subfamily U, member 1	-2.42
PIH1D2	PIH1 domain containing 2	-2.42
RNF175	ring finger protein 175	-2.42
SPHK2	sphingosine kinase 2	-2.42
VPS26B	vacuolar protein sorting 26 homolog B (S. pombe)	-2.42
WDR72	WD repeat domain 72	-2.42
ZNF3	zinc finger protein 3	-2.42
CES3	carboxylesterase 3	-2.43
FBXO9	F-box protein 9	-2.43
RAD1	RAD1 homolog (S. pombe)	-2.43
SPATA9	spermatogenesis associated 9	-2.43
ABCC6	ATP-binding cassette, sub-family C (CFTR/MRP), member 6	-2.44
BCL2L14	BCL2-like 14 (apoptosis facilitator)	-2.44
CCDC30	coiled-coil domain containing 30	-2.44
CCDC93	coiled-coil domain containing 93	-2.44
GTF2H3	general transcription factor IIH, polypeptide 3, 34kDa	-2.44
LILRA3	leukocyte immunoglobulin-like receptor, subfamily A, member 3	-2.44
MMD2	monocyte to macrophage differentiation-associated 2	-2.44
MYH14	myosin, heavy chain 14, non-muscle	-2.44
NRG3	neuregulin 3	-2.44
PDE4DIP	phosphodiesterase 4D interacting protein, myomegalin-like	-2.44
PMFBP1	polyamine modulated factor 1 binding protein 1	-2.44
SLC7A11-AS1	SLC7A11 antisense RNA 1 (non-protein coding)	-2.44
TANC1	tetratricopeptide repeat, ankyrin repeat and coiled-coil containing 1	-2.44
TRAF3IP3	TRAF3 interacting protein 3	-2.44
DHX16	DEAH (Asp-Glu-Ala-His) box polypeptide 16	-2.45
DHX16	DEAH (Asp-Glu-Ala-His) box polypeptide 16	-2.45
DHX16	DEAH (Asp-Glu-Ala-His) box polypeptide 16	-2.45
DHX16	DEAH (Asp-Glu-Ala-His) box polypeptide 16	-2.45
DHX16	DEAH (Asp-Glu-Ala-His) box polypeptide 16	-2.45
DLG2	discs, large homolog 2 (Drosophila)	-2.45
DSG4	desmoglein 4	-2.45
FRMPD4	FERM and PDZ domain containing 4	-2.45
GCLC	glutamate-cysteine ligase, catalytic subunit	-2.45
SDR16C5	short chain dehydrogenase/reductase family 16C, member 5	-2.45
TRPM3	transient receptor potential cation channel, subfamily M, member 3	-2.45

UNC80	unc-80 homolog (C. elegans)	-2.45
CCDC171	coiled-coil domain containing 171	-2.46
LOC284998	uncharacterized LOC284998	-2.46
NPHP4	nephronophthisis 4	-2.46
PITPNM1	phosphatidylinositol transfer protein, membrane-associated 1	-2.46
C12orf10	chromosome 12 open reading frame 10	-2.47
COX7B	cytochrome c oxidase subunit VIIb	-2.47
FAM227B	family with sequence similarity 227, member B	-2.47
FAM71D	family with sequence similarity 71, member D	-2.47
MX2	myxovirus (influenza virus) resistance 2 (mouse)	-2.47
OSGEPL1	O-sialoglycoprotein endopeptidase-like 1	-2.47
PRDM15	PR domain containing 15	-2.47
TEX29	testis expressed 29	-2.47
AMOT	angiomotin	-2.48
C22orf43	chromosome 22 open reading frame 43	-2.48
KAT7	K(lysine) acetyltransferase 7	-2.48
LYPLA1	lysophospholipase I	-2.48
MYH13	myosin, heavy chain 13, skeletal muscle	-2.48
NFKBIL1	nuclear factor of kappa light polypeptide gene enhancer in B-cells inhibitor-like 1	-2.48
NFKBIL1	nuclear factor of kappa light polypeptide gene enhancer in B-cells inhibitor-like 1	-2.48
PLA2G4E	phospholipase A2, group IVE	-2.48
PSMG4	proteasome (prosome, macropain) assembly chaperone 4	-2.48
RIMS2	regulating synaptic membrane exocytosis 2	-2.48
THOC2	THO complex 2	-2.48
C12orf56	chromosome 12 open reading frame 56	-2.49
E2F5	E2F transcription factor 5, p130-binding	-2.49
MMAB	methylmalonic aciduria (cobalamin deficiency) cblB type	-2.49
DAOA	D-amino acid oxidase activator	-2.5
FAM149A	family with sequence similarity 149, member A	-2.5
HERC2	HECT and RLD domain containing E3 ubiquitin protein ligase 2, putative HERC2-like protein 3-like	-2.5
LRIG1	leucine-rich repeats and immunoglobulin-like domains 1	-2.5
EYS	eyes shut homolog (Drosophila)	-2.51
LAMP3	lysosomal-associated membrane protein 3	-2.51
PLA2G4A	phospholipase A2, group IVA (cytosolic, calcium-dependent)	-2.51
SLC26A8	solute carrier family 26, member 8	-2.51
TDRD1	tudor domain containing 1	-2.51
ARSE	arylsulfatase E (chondrodysplasia punctata 1)	-2.52
HLF	hepatic leukemia factor	-2.52
RBCK1	RanBP-type and C3HC4-type zinc finger containing 1	-2.52
CASD1	CAS1 domain containing 1	-2.53
DLGAP4	discs, large (Drosophila) homolog-associated protein 4	-2.53
MPP2	membrane protein, palmitoylated 2 (MAGUK p55 subfamily member 2)	-2.53

SMPDL3B	sphingomyelin phosphodiesterase, acid-like 3B	-2.53
WDR7	WD repeat domain 7	-2.53
GUCY1A3	guanylate cyclase 1, soluble, alpha 3	-2.54
PPARGC1A	peroxisome proliferator-activated receptor gamma, coactivator 1 alpha	-2.54
SDK1	sidekick cell adhesion molecule 1	-2.54
TRAT1	T cell receptor associated transmembrane adaptor 1	-2.54
BMP7	bone morphogenetic protein 7	-2.55
C19orf45	chromosome 19 open reading frame 45	-2.55
IL7R	interleukin 7 receptor	-2.55
UNC80	unc-80 homolog (C. elegans)	-2.55
DIABLO	diablo, IAP-binding mitochondrial protein	-2.56
DKFZp686O1327	uncharacterized LOC401014	-2.56
FBLN1	fibulin 1	-2.56
BAIAP2L2	BAI1-associated protein 2-like 2	-2.57
COMTD1	catechol-O-methyltransferase domain containing 1	-2.57
JAKMIP3	Janus kinase and microtubule interacting protein 3	-2.57
LRP1B	low density lipoprotein receptor-related protein 1B	-2.57
GRM4	glutamate receptor, metabotropic 4	-2.58
MYO5B	myosin VB	-2.58
ZRANB3	zinc finger, RAN-binding domain containing 3	-2.58
CACNA1D	calcium channel, voltage-dependent, L type, alpha 1D subunit	-2.59
CSMD3	CUB and Sushi multiple domains 3	-2.59
GLYATL1	glycine-N-acyltransferase-like 1	-2.59
IGKV1-5	immunoglobulin kappa variable 1-5	-2.59
LOC100287562	uncharacterized LOC100287562	-2.59
MCOLN3	mucolipin 3	-2.59
NECAB1	N-terminal EF-hand calcium binding protein 1	-2.59
OTOGL	otogelin-like	-2.59
PDE11A	phosphodiesterase 11A	-2.59
THAP9	THAP domain containing 9	-2.59
ARAP2	ArfGAP with RhoGAP domain, ankyrin repeat and PH domain 2	-2.6
CDK2	cyclin-dependent kinase 2	-2.6
CHEK2	checkpoint kinase 2	-2.6
ITGA4	integrin, alpha 4 (antigen CD49D, alpha 4 subunit of VLA-4 receptor)	-2.6
PDGFRA, FIP1L1	platelet-derived growth factor receptor, alpha polypeptide, FIP1 like 1 (S. cerevisiae)	-2.6
SEL1L2	sel-1 suppressor of lin-12-like 2 (C. elegans)	-2.6
TDP1	tyrosyl-DNA phosphodiesterase 1	-2.6
UOX	urate oxidase, pseudogene	-2.6
C17orf57, ITGB3	chromosome 17 open reading frame 57, integrin, beta 3 (platelet glycoprotein IIIa, antigen CD61)	-2.61
COX4I2	cytochrome c oxidase subunit IV isoform 2 (lung)	-2.61
DDX18	DEAD (Asp-Glu-Ala-Asp) box polypeptide 18	-2.61
FAM205B	family with sequence similarity 205, member B	-2.61

HTN3	histatin 3	-2.61
MCTP1	multiple C2 domains, transmembrane 1	-2.61
MKNK1	MAP kinase interacting serine/threonine kinase 1	-2.61
MYCBPAP	MYCBP associated protein	-2.61
SMARCB1	SWI/SNF related, matrix associated, actin dependent regulator of chromatin, subfamily b, member 1	-2.61
LRP1B	low density lipoprotein receptor-related protein 1B	-2.62
MYD88	myeloid differentiation primary response gene (88)	-2.62
PIK3C2G	phosphoinositide-3-kinase, class 2, gamma polypeptide	-2.62
POLR2F	polymerase (RNA) II (DNA directed) polypeptide F	-2.62
POLR2F	polymerase (RNA) II (DNA directed) polypeptide F	-2.62
RIMS1	regulating synaptic membrane exocytosis 1	-2.62
FRAS1	Fraser syndrome 1	-2.63
GDPD2	glycerophosphodiester phosphodiesterase domain containing 2	-2.63
KALRN	kalirin, RhoGEF kinase	-2.63
MIR4273	microRNA 4273	-2.63
SPAG1	sperm associated antigen 1	-2.63
TRPA1	transient receptor potential cation channel, subfamily A, member 1	-2.63
C11orf10	chromosome 11 open reading frame 10	-2.64
KIAA1875	KIAA1875	-2.64
TRIM66	tripartite motif containing 66	-2.64
ADCY2	adenylate cyclase 2 (brain)	-2.65
ATP8B5P	ATPase, class I, type 8B, member 5, pseudogene	-2.65
FGD3	FYVE, RhoGEF and PH domain containing 3	-2.65
LINC00571	long intergenic non-protein coding RNA 571	-2.65
PKLR	pyruvate kinase, liver and RBC	-2.65
SLAIN2	SLAIN motif family, member 2	-2.65
TDRD9	tudor domain containing 9	-2.65
TRIM29	tripartite motif containing 29	-2.65
VRK2	vaccinia related kinase 2	-2.65
C10orf129	chromosome 10 open reading frame 129	-2.66
COL6A6	collagen, type VI, alpha 6	-2.66
MTFP1	mitochondrial fission process 1	-2.66
MYO1G	myosin IG	-2.66
SORBS1	sorbin and SH3 domain containing 1	-2.66
TRIM29	tripartite motif containing 29	-2.66
ZFYVE28	zinc finger, FYVE domain containing 28	-2.66
CHI3L2	chitinase 3-like 2	-2.67
NBLA00301	Nbla00301	-2.67
NRBP1	nuclear receptor binding protein 1	-2.67
RIMBP2	RIMS binding protein 2	-2.67
SNORD97	small nucleolar RNA, C/D box 97	-2.67
SPG11	spastic paraplegia 11 (autosomal recessive)	-2.67
DNAH11	dynein, axonemal, heavy chain 11	-2.68

DNHD1, FXC1	dynein heavy chain domain 1, fracture callus 1 homolog (rat)	-2.68
KIAA1967	KIAA1967	-2.68
MIR4462	microRNA 4462	-2.68
OSTalpha	organic solute transporter alpha	-2.68
ABCC4	ATP-binding cassette, sub-family C (CFTR/MRP), member 4	-2.69
CERS2	ceramide synthase 2	-2.69
FLJ46906	uncharacterized LOC441172	-2.69
SPATA20	spermatogenesis associated 20	-2.69
EPB41L3	erythrocyte membrane protein band 4.1-like 3	-2.7
HTR3D	5-hydroxytryptamine (serotonin) receptor 3D, ionotropic	-2.7
PDZD2	PDZ domain containing 2	-2.7
PSMB9	proteasome (prosome, macropain) subunit, beta type, 9 (large multifunctional peptidase 2)	-2.7
PSMB9	proteasome (prosome, macropain) subunit, beta type, 9 (large multifunctional peptidase 2)	-2.7
PSMB9	proteasome (prosome, macropain) subunit, beta type, 9 (large multifunctional peptidase 2)	-2.7
PSMB9	proteasome (prosome, macropain) subunit, beta type, 9 (large multifunctional peptidase 2)	-2.7
SPPL2A	signal peptide peptidase like 2A	-2.7
TRO	trophinin	-2.7
C3P1	complement component 3 precursor pseudogene	-2.71
POTEB	POTE ankyrin domain family, member B, POTE ankyrin domain family member B-like	-2.71
POTEB	POTE ankyrin domain family, member B, POTE ankyrin domain family member B-like	-2.71
SLC35C2	solute carrier family 35, member C2	-2.71
FBXO32	F-box protein 32	-2.72
TMCO6	transmembrane and coiled-coil domains 6	-2.72
WDR52-AS1	WDR52 antisense RNA 1 (non-protein coding)	-2.72
ZMAT1	zinc finger, matrin-type 1	-2.72
MAST4	microtubule associated serine/threonine kinase family member 4	-2.73
SEC14L2	SEC14-like 2 (S. cerevisiae)	-2.73
SNCAIP	synuclein, alpha interacting protein	-2.73
ABCB6, ATG9A	ATP-binding cassette, sub-family B (MDR/TAP), member 6, autophagy related 9A	-2.74
MFSD6	major facilitator superfamily domain containing 6	-2.74
MYH7B	myosin, heavy chain 7B, cardiac muscle, beta	-2.74
PPARGC1B	peroxisome proliferator-activated receptor gamma, coactivator 1 beta	-2.74
TEX11	testis expressed 11	-2.74
TPM3	tropomyosin 3	-2.74
WAC	WW domain containing adaptor with coiled-coil	-2.74
CLPTM1L	CLPTM1-like	-2.75
FAM208A	family with sequence similarity 208, member A	-2.75
GPR160	G protein-coupled receptor 160	-2.75
HEATR8-TTC4	HEATR8-TTC4 readthrough, HEAT repeat containing 8, tetratricopeptide repeat domain 4	-2.75
TRIO	triple functional domain (PTPRF interacting)	-2.76

ZC3H14	zinc finger CCCH-type containing 14	-2.76
ANKZF1	ankyrin repeat and zinc finger domain containing 1	-2.77
CADPS	Ca++-dependent secretion activator	-2.77
HECTD2	HECT domain containing E3 ubiquitin protein ligase 2	-2.77
FAM65C	family with sequence similarity 65, member C	-2.78
GPT	glutamic-pyruvate transaminase (alanine aminotransferase)	-2.78
HIBCH	3-hydroxyisobutyryl-CoA hydrolase	-2.78
NAV3	neuron navigator 3	-2.78
RANBP17	RAN binding protein 17	-2.78
CDH16	cadherin 16, KSP-cadherin	-2.79
COPB1, PSMA1	coatomer protein complex, subunit beta 1, proteasome (prosome, macropain) subunit, alpha type, 1	-2.79
ACAT1	acetyl-CoA acetyltransferase 1	-2.8
CCDC108	coiled-coil domain containing 108	-2.8
CYP3A4	cytochrome P450, family 3, subfamily A, polypeptide 4	-2.8
MUC6	mucin 6, oligomeric mucus/gel-forming	-2.8
TMPPE, GLB1	transmembrane protein with metallophosphoesterase domain, galactosidase, beta 1	-2.8
C20orf112	chromosome 20 open reading frame 112	-2.81
CASP8	caspase 8, apoptosis-related cysteine peptidase	-2.81
RAPGEF5	Rap guanine nucleotide exchange factor (GEF) 5	-2.81
C12orf63	chromosome 12 open reading frame 63, chromosome 12 open reading frame 55	-2.82
CELSR3, MIR4793	cadherin, EGF LAG seven-pass G-type receptor 3 (flamingo homolog, Drosophila), microRNA 4793	-2.82
FHAD1	forkhead-associated (FHA) phosphopeptide binding domain 1	-2.82
IQCH	IQ motif containing H	-2.82
LOC100508781	protein FAM115A-like	-2.82
ANXA4	annexin A4	-2.83
DHRS12	dehydrogenase/reductase (SDR family) member 12	-2.83
FPGS	folylpolyglutamate synthase	-2.83
GPR18	G protein-coupled receptor 18	-2.83
PEX5	peroxisomal biogenesis factor 5	-2.83
PIP5K1B	phosphatidylinositol-4-phosphate 5-kinase, type I, beta	-2.83
VWA3B	von Willebrand factor A domain containing 3B	-2.83
CD96	CD96 molecule	-2.84
CPAMD8	C3 and PZP-like, alpha-2-macroglobulin domain containing 8	-2.84
SLC22A10	solute carrier family 22, member 10	-2.84
VARS2	valyl-tRNA synthetase 2, mitochondrial (putative)	-2.84
VARS2	valyl-tRNA synthetase 2, mitochondrial (putative)	-2.84
VARS2	valyl-tRNA synthetase 2, mitochondrial (putative)	-2.84
VARS2	valyl-tRNA synthetase 2, mitochondrial (putative)	-2.84
VARS2	valyl-tRNA synthetase 2, mitochondrial (putative)	-2.84
ZNF503-AS1	ZNF503 antisense RNA 1 (non-protein coding)	-2.84
DDX47	DEAD (Asp-Glu-Ala-Asp) box polypeptide 47	-2.86
BLNK	B-cell linker	-2.87

CLDN12	claudin 12	-2.87
GNRHR2	gonadotropin-releasing hormone (type 2) receptor 2	-2.87
MEGF6	multiple EGF-like-domains 6	-2.87
SPATA7	spermatogenesis associated 7	-2.87
USP20	ubiquitin specific peptidase 20	-2.88
AVIL	advillin	-2.89
CCDC33	coiled-coil domain containing 33	-2.89
CCND3	cyclin D3	-2.89
SFPQ	splicing factor proline/glutamine-rich	-2.89
VEPH1	ventricular zone expressed PH domain homolog 1 (zebrafish)	-2.89
ZNF660	zinc finger protein 660, zinc finger protein 197	-2.89
POU2F2	POU class 2 homeobox 2	-2.9
CSMD1	CUB and Sushi multiple domains 1	-2.91
INPP5D	inositol polyphosphate-5-phosphatase, 145kDa	-2.91
LOC100507431	uncharacterized LOC100507431	-2.91
PPP1R7	protein phosphatase 1, regulatory subunit 7	-2.91
LOC100124692	maltase-glucoamylase (alpha-glucosidase) pseudogene	-2.92
SGK1	serum/glucocorticoid regulated kinase 1	-2.92
NFE2L2	nuclear factor (erythroid-derived 2)-like 2	-2.93
MYOM3	myomesin family, member 3	-2.93
ACPP	acid phosphatase, prostate	-2.94
BBS1	Bardet-Biedl syndrome 1	-2.94
FGF13	fibroblast growth factor 13	-2.94
GRIK1	glutamate receptor, ionotropic, kainate 1	-2.94
KAZALD1	Kazal-type serine peptidase inhibitor domain 1	-2.94
MYEOV	myeloma overexpressed (in a subset of t(11;14) positive multiple myelomas)	-2.94
RYR3	ryanodine receptor 3	-2.94
SERPINF2	serpin peptidase inhibitor, clade F (alpha-2 antiplasmin, pigment epithelium derived factor)	-2.94
TRAK2	trafficking protein, kinesin binding 2	-2.94
WNK2	WNK lysine deficient protein kinase 2	-2.94
CCDC146	coiled-coil domain containing 146	-2.95
CCDC171	coiled-coil domain containing 171	-2.95
RYR2	ryanodine receptor 2 (cardiac)	-2.95
SPAG17	sperm associated antigen 17	-2.95
TMEM134	transmembrane protein 134	-2.96
FAM118A	family with sequence similarity 118, member A	-2.97
INADL	InaD-like (Drosophila)	-2.97
RC3H1	ring finger and CCCH-type domains 1	-2.97
MAPK10	mitogen-activated protein kinase 10	-2.98
OVGP1	oviductal glycoprotein 1, 120kDa	-2.98
RNF17	ring finger protein 17	-2.98
LOC100507206	uncharacterized LOC100507206	-2.99

PAOX, MTG1	polyamine oxidase (exo-N4-amino), mitochondrial GTPase 1 homolog (S. cerevisiae)	-2.99
RYR3	ryanodine receptor 3	-2.99
ATP8A2	ATPase, aminophospholipid transporter, class I, type 8A, member 2	-3
LEF1	lymphoid enhancer-binding factor 1	-3
LINC00313	long intergenic non-protein coding RNA 313	-3.02
MDC1	mediator of DNA-damage checkpoint 1	-3.02
MDC1	mediator of DNA-damage checkpoint 1	-3.02
MDC1	mediator of DNA-damage checkpoint 1	-3.02
MDC1	mediator of DNA-damage checkpoint 1	-3.02
MDC1	mediator of DNA-damage checkpoint 1	-3.02
MDC1	mediator of DNA-damage checkpoint 1, MDC1 antisense RNA 1 (non-protein coding)	-3.02
MDC1-AS1	MDC1 antisense RNA 1 (non-protein coding)	-3.02
MTMR7	myotubularin related protein 7	-3.02
MUC19	mucin 19, oligomeric	-3.02
TDRD1	tudor domain containing 1	-3.02
COL4A3	collagen, type IV, alpha 3 (Goodpasture antigen)	-3.03
HEPH	hephaestin	-3.03
SCN3A	sodium channel, voltage-gated, type III, alpha subunit	-3.03
ABTB1	ankyrin repeat and BTB (POZ) domain containing 1	-3.04
PTPRK	protein tyrosine phosphatase, receptor type, K	-3.04
USP20	ubiquitin specific peptidase 20	-3.04
ATXN7L1	ataxin 7-like 1	-3.06
KALRN	kalirin, RhoGEF kinase	-3.06
ZNF827	zinc finger protein 827	-3.06
GRIA2	glutamate receptor, ionotropic, AMPA 2	-3.08
MFSD4	major facilitator superfamily domain containing 4	-3.08
SACM1L	SAC1 suppressor of actin mutations 1-like (yeast)	-3.08
GARNL3	GTPase activating Rap/RanGAP domain-like 3	-3.09
PIGQ	phosphatidylinositol glycan anchor biosynthesis, class Q	-3.09
SLC26A7	solute carrier family 26, member 7	-3.09
COL3A1	collagen, type III, alpha 1, microRNA 3606	-3.1
LOC100506950	uncharacterized LOC100506950	-3.1
ACSS3	acyl-CoA synthetase short-chain family member 3	-3.11
GTPBP10	GTP-binding protein 10 (putative), claudin 12	-3.11
MUC2	mucin 2, oligomeric mucus/gel-forming	-3.11
TXNDC12	thioredoxin domain containing 12 (endoplasmic reticulum)	-3.11
C1QTNF5	C1q and tumor necrosis factor related protein 5, membrane frizzled-related protein	-3.12
MAP7D2	MAP7 domain containing 2	-3.12
VWA7	von Willebrand factor A domain containing 7	-3.12
VWA7	von Willebrand factor A domain containing 7	-3.12
VWA7	von Willebrand factor A domain containing 7	-3.12
VWA7	von Willebrand factor A domain containing 7	-3.12

VWA7	von Willebrand factor A domain containing 7	-3.12
Mar-01	membrane-associated ring finger (C3HC4) 1, E3 ubiquitin protein ligase	-3.13
ANAPC1	anaphase promoting complex subunit 1	-3.13
CFP	complement factor properdin	-3.13
GNB1L	guanine nucleotide binding protein (G protein), beta polypeptide 1-like	-3.13
USH2A	Usher syndrome 2A (autosomal recessive, mild)	-3.13
OTUD3	OTU domain containing 3	-3.14
PLSCR4	phospholipid scramblase 4	-3.14
SEPP1	selenoprotein P, plasma, 1	-3.14
TRPA1	transient receptor potential cation channel, subfamily A, member 1	-3.14
TBC1D5	TBC1 domain family, member 5	-3.15
ASIC4	acid-sensing (proton-gated) ion channel family member 4	-3.16
C2orf88	chromosome 2 open reading frame 88	-3.16
EFCAB6	EF-hand calcium binding domain 6	-3.16
NPC1L1	NPC1 (Niemann-Pick disease, type C1, gene)-like 1	-3.16
VAV3	vav 3 guanine nucleotide exchange factor	-3.16
C3orf24	chromosome 3 open reading frame 24	-3.17
KRTAP15-1	keratin associated protein 15-1	-3.17
ERBB3	v-erb-b2 erythroblastic leukemia viral oncogene homolog 3 (avian)	-3.18
LONRF1	LON peptidase N-terminal domain and ring finger 1	-3.18
PTPRO	protein tyrosine phosphatase, receptor type, O	-3.18
LMO7	LIM domain 7	-3.19
ROS1, GOPC	c-ros oncogene 1 , receptor tyrosine kinase	-3.19
DNAH11	dynein, axonemal, heavy chain 11	-3.2
PTPRD	protein tyrosine phosphatase, receptor type, D	-3.2
WRAP73	WD repeat containing, antisense to TP73	-3.2
EXOC1	exocyst complex component 1	-3.21
ADAM32	ADAM metallopeptidase domain 32	-3.24
CPVL	carboxypeptidase, vitellogenic-like	-3.24
GCGR	glucagon receptor	-3.24
TDRD12	tudor domain containing 12	-3.24
ACSM1	acyl-CoA synthetase medium-chain family member 1	-3.25
CATSPERB	catsper channel auxiliary subunit beta	-3.25
GPR112	G protein-coupled receptor 112	-3.26
COQ6	coenzyme Q6 homolog, monooxygenase (S. cerevisiae)	-3.27
PCDH15	protocadherin-related 15	-3.27
RAD18	RAD18 homolog (S. cerevisiae)	-3.27
GLDN	gliomedin	-3.28
TMX4	thioredoxin-related transmembrane protein 4	-3.28
GNGT1	guanine nucleotide binding protein (G protein), gamma transducing activity polypeptide 1	-3.29
INADL	InaD-like (Drosophila)	-3.29
JAKMIP3	Janus kinase and microtubule interacting protein 3	-3.29
MIR3929	NLR family, CARD domain containing 3, microRNA 3929	-3.29

ZBTB22	zinc finger and BTB domain containing 22	-3.3
ZBTB22	zinc finger and BTB domain containing 22	-3.3
ZBTB22	zinc finger and BTB domain containing 22	-3.3
ZBTB22	zinc finger and BTB domain containing 22	-3.3
ZBTB22	zinc finger and BTB domain containing 22	-3.3
CDC123	cell division cycle 123 homolog (S. cerevisiae)	-3.31
MYH8	myosin, heavy chain 8, skeletal muscle, perinatal	-3.31
EYS	eyes shut homolog (Drosophila)	-3.33
SMTN	smoothelin	-3.33
MECOM	MDS1 and EVI1 complex locus	-3.34
SPEG	SPEG complex locus	-3.34
TNXB	tenascin XB	-3.34
TNXB	tenascin XB	-3.34
TNXB	tenascin XB	-3.34
TNXB	tenascin XB	-3.34
TNXB, TNXA	tenascin XB, tenascin XA (pseudogene)	-3.34
TNXB, TNXA	tenascin XB, tenascin XA (pseudogene)	-3.34
SERPINE3	serpin peptidase inhibitor, clade E (nexin, plasminogen activator inhibitor type 1), member 3	-3.35
TRBV5-1	T cell receptor beta variable 5-1	-3.35
TTF2	transcription termination factor, RNA polymerase II	-3.35
CASQ1	calsequestrin 1 (fast-twitch, skeletal muscle)	-3.36
EPB41L3	erythrocyte membrane protein band 4.1-like 3	-3.37
GAS6-AS1	GAS6 antisense RNA 1 (non-protein coding)	-3.37
SIDT2	SID1 transmembrane family, member 2	-3.37
CCDC84	coiled-coil domain containing 84	-3.38
CREB3L3	cAMP responsive element binding protein 3-like 3	-3.39
KCNAB1	potassium voltage-gated channel, shaker-related subfamily, beta member 1	-3.39
FER1L5	fer-1-like 5 (C. elegans)	-3.4
KIAA1456	KIAA1456	-3.4
FANK1	fibronectin type III and ankyrin repeat domains 1	-3.43
RPH3A	rabphilin 3A homolog (mouse)	-3.43
DNAH10	dynein, axonemal, heavy chain 10	-3.45
ZBED3-AS1	ZBED3 antisense RNA 1 (non-protein coding)	-3.45
APLP2	amyloid beta (A4) precursor-like protein 2	-3.46
ETV6	ets variant 6	-3.47
GGCT	gamma-glutamylcyclotransferase	-3.47
ABCA4	ATP-binding cassette, sub-family A (ABC1), member 4	-3.48
PPP2R5B	protein phosphatase 2, regulatory subunit B', beta	-3.51
VPS33A	vacuolar protein sorting 33 homolog A (S. cerevisiae)	-3.51
ZNF704	zinc finger protein 704	-3.51
COG2	component of oligomeric golgi complex 2	-3.52
FRY	furry homolog (Drosophila)	-3.52
APOB	apolipoprotein B (including Ag(x) antigen)	-3.53

DNAH11	dynein, axonemal, heavy chain 11	-3.53
CATSPERD	catsper channel auxiliary subunit delta	-3.55
CPA1	carboxypeptidase A1 (pancreatic)	-3.55
LAMA2	laminin, alpha 2	-3.55
MFAP5	microfibrillar associated protein 5	-3.55
C4orf45	chromosome 4 open reading frame 45	-3.56
LOC100132815	importin 5 pseudogene	-3.56
PLRG1	pleiotropic regulator 1	-3.56
FOXN3	forkhead box N3	-3.57
PPFIBP1	PTPRF interacting protein, binding protein 1 (liprin beta 1)	-3.57
CALCOCO2	calcium binding and coiled-coil domain 2	-3.58
FGD2	FYVE, RhoGEF and PH domain containing 2	-3.58
KLHL24	kelch-like 24 (Drosophila)	-3.58
SORCS3	sortilin-related VPS10 domain containing receptor 3	-3.58
DDX4	DEAD (Asp-Glu-Ala-Asp) box polypeptide 4	-3.59
NELL1	NEL-like 1 (chicken)	-3.59
C4orf37	chromosome 4 open reading frame 37	-3.6
FHAD1	forkhead-associated (FHA) phosphopeptide binding domain 1	-3.61
CUBN	cubilin (intrinsic factor-cobalamin receptor)	-3.62
PSEN1	presenilin 1	-3.62
BRSK2	BR serine/threonine kinase 2	-3.63
C14orf38	chromosome 14 open reading frame 38	-3.63
SCML4	sex comb on midleg-like 4 (Drosophila)	-3.63
STAMBPL1	STAM binding protein-like 1	-3.63
ACAN	aggrecan	-3.64
SP140	SP140 nuclear body protein	-3.64
SMCR7L	Smith-Magenis syndrome chromosome region, candidate 7-like	-3.66
PSME4	proteasome (prosome, macropain) activator subunit 4	-3.69
UTP20	UTP20, small subunit (SSU) processome component, homolog (yeast)	-3.69
C3orf24	chromosome 3 open reading frame 24	-3.7
SLC4A5	solute carrier family 4, sodium bicarbonate cotransporter, member 5	-3.7
DCTN2	dynactin 2 (p50)	-3.72
SLIRP	SRA stem-loop interacting RNA binding protein	-3.73
UNC5C	unc-5 homolog C (C. elegans)	-3.73
ABCB5	ATP-binding cassette, sub-family B (MDR/TAP), member 5	-3.75
C9orf43	chromosome 9 open reading frame 43	-3.75
PVRL4	poliovirus receptor-related 4	-3.75
ALDH1L1	aldehyde dehydrogenase 1 family, member L1	-3.76
STK11IP	serine/threonine kinase 11 interacting protein	-3.77
CYP4V2	cytochrome P450, family 4, subfamily V, polypeptide 2	-3.79
IKZF1	IKAROS family zinc finger 1 (Ikaros)	-3.82
LYPD6B	LY6/PLAUR domain containing 6B	-3.82
OTX2-AS1	OTX2 antisense RNA 1 (non-protein coding)	-3.85

RAB3GAP2	RAB3 GTPase activating protein subunit 2 (non-catalytic), aurora kinase A pseudogene 1	-3.85
DAOA	D-amino acid oxidase activator	-3.86
TAF1	TAF1 RNA polymerase II, TATA box binding protein (TBP)-associated factor, 250kDa	-3.89
RPUSD4	RNA pseudouridylate synthase domain containing 4	-3.9
RNH1	ribonuclease/angiogenin inhibitor 1	-3.92
SPTB	spectrin, beta, erythrocytic	-3.92
ARMCX4	armadillo repeat containing, X-linked 4	-3.93
DOCK2	dedicator of cytokinesis 2	-3.94
DNAH1	dynein, axonemal, heavy chain 1	-3.95
GTF2H1	general transcription factor IIH, polypeptide 1, 62kDa	-3.95
ACAT1	acetyl-CoA acetyltransferase 1	-3.98
KDM3B	lysine (K)-specific demethylase 3B	-3.98
UNC80	unc-80 homolog (C. elegans)	-4.02
CTSB	cathepsin B	-4.03
KIAA1731	KIAA1731	-4.03
GRAMD1C	GRAM domain containing 1C	-4.07
CEP192	centrosomal protein 192kDa	-4.08
C3orf32	chromosome 3 open reading frame 32	-4.09
PDE4B	phosphodiesterase 4B, cAMP-specific	-4.09
SLC44A5	solute carrier family 44, member 5	-4.09
METAP1D	methionyl aminopeptidase type 1D (mitochondrial)	-4.1
PPARGC1A	peroxisome proliferator-activated receptor gamma, coactivator 1 alpha	-4.12
ATP1A4	ATPase, Na+/K+ transporting, alpha 4 polypeptide	-4.14
BNIPL	BCL2/adenovirus E1B 19kD interacting protein like	-4.17
EAF2	ELL associated factor 2	-4.17
KLHL7	kelch-like 7 (Drosophila)	-4.17
ATP2A3	ATPase, Ca++ transporting, ubiquitous	-4.18
NUP205	nucleoporin 205kDa	-4.18
CHRNA9	cholinergic receptor, nicotinic, alpha 9 (neuronal)	-4.19
PTPRC	protein tyrosine phosphatase, receptor type, C	-4.19
MS4A4A	membrane-spanning 4-domains, subfamily A, member 4A	-4.2
PTGER3	prostaglandin E receptor 3 (subtype EP3)	-4.23
USH1C	Usher syndrome 1C (autosomal recessive, severe)	-4.23
NALCN	sodium leak channel, non-selective	-4.25
SYNE1	spectrin repeat containing, nuclear envelope 1	-4.27
STK31	serine/threonine kinase 31	-4.28
HIF3A	hypoxia inducible factor 3, alpha subunit	-4.29
USP53	ubiquitin specific peptidase 53	-4.31
GLUD1	glutamate dehydrogenase 1	-4.33
TANK	TRAF family member-associated NFKB activator	-4.33
DDX10	DEAD (Asp-Glu-Ala-Asp) box polypeptide 10	-4.37
ANKAR	ankyrin and armadillo repeat containing	-4.38

SRPK2	SRSF protein kinase 2	-4.4
CACNA1S	calcium channel, voltage-dependent, L type, alpha 1S subunit	-4.42
IL17RE	interleukin 17 receptor E	-4.43
PPFIBP2	PTPRF interacting protein, binding protein 2 (liprin beta 2)	-4.43
LY9	lymphocyte antigen 9	-4.44
ADAM29	ADAM metallopeptidase domain 29	-4.45
GNL3	guanine nucleotide binding protein-like 3 (nucleolar), small nucleolar RNA, C/D box 19B	-4.45
GCOM1-2	GRINL1A complex locus 1-2	-4.5
MASP1	mannan-binding lectin serine peptidase 1 (C4/C2 activating component of Ra-reactive factor)	-4.51
FHAD1	forkhead-associated (FHA) phosphopeptide binding domain 1	-4.52
STAC3	SH3 and cysteine rich domain 3	-4.53
TF	transferrin	-4.55
DDX10	DEAD (Asp-Glu-Ala-Asp) box polypeptide 10	-4.6
ANTXRL	anthrax toxin receptor-like	-4.61
KRT24	keratin 24	-4.61
CACNA1I	calcium channel, voltage-dependent, T type, alpha 1I subunit	-4.62
ECT2L	epithelial cell transforming sequence 2 oncogene-like	-4.64
MIPOL1	mirror-image polydactyly 1	-4.64
IL1RAPL1	interleukin 1 receptor accessory protein-like 1	-4.7
KANSL1L	KAT8 regulatory NSL complex subunit 1-like	-4.75
SYCP2	synaptonemal complex protein 2	-4.75
MSR1	macrophage scavenger receptor 1	-4.84
ANAPC11	anaphase promoting complex subunit 11	-4.89
ABCF1	ATP-binding cassette, sub-family F (GCN20), member 1	-4.97
ABCF1	ATP-binding cassette, sub-family F (GCN20), member 1	-4.97
ABCF1	ATP-binding cassette, sub-family F (GCN20), member 1	-4.97
ABCF1	ATP-binding cassette, sub-family F (GCN20), member 1	-4.97
ABCF1	ATP-binding cassette, sub-family F (GCN20), member 1	-4.97
ABCF1	ATP-binding cassette, sub-family F (GCN20), member 1	-4.97
ABCF1	ATP-binding cassette, sub-family F (GCN20), member 1	-4.97
CDHR2	cadherin-related family member 2	-5.01
RABGAP1L	RAB GTPase activating protein 1-like	-5.07
EIF5	eukaryotic translation initiation factor 5	-5.08
CD8A	CD8a molecule	-5.09
EMCN	endomucin	-5.09
C17orf70	chromosome 17 open reading frame 70	-5.1
KCNQ5	potassium voltage-gated channel, KQT-like subfamily, member 5	-5.12
ZRANB3	zinc finger, RAN-binding domain containing 3	-5.14
SEMA5A	sema domain, seven thrombospondin repeats (type 1 and type 1-like),semaphorin 5A	-5.16
USP40	ubiquitin specific peptidase 40	-5.16
TMEM108	transmembrane protein 108	-5.17
ZBED3-AS1	ZBED3 antisense RNA 1 (non-protein coding)	-5.2

DNAH2	dynein, axonemal, heavy chain 2	-5.22
MIR3661	microRNA 3661	-5.22
SLC6A1	solute carrier family 6 (neurotransmitter transporter, GABA), member 1	-5.27
PKHD1L1	polycystic kidney and hepatic disease 1 (autosomal recessive)-like 1	-5.31
NUP188	nucleoporin 188kDa	-5.33
NXF2B, NXF2	nuclear RNA export factor 2B, nuclear RNA export factor 2	-5.33
NXF2B, NXF2	nuclear RNA export factor 2B, nuclear RNA export factor 2	-5.33
SPNS2	spinster homolog 2 (Drosophila)	-5.43
TACC2	transforming, acidic coiled-coil containing protein 2	-5.52
PIP5K1B	phosphatidylinositol-4-phosphate 5-kinase, type I, beta	-5.53
EP400NL	EP400 N-terminal like	-5.57
MYO1D	myosin ID	-5.58
SGCD	sarcoglycan, delta (35kDa dystrophin-associated glycoprotein)	-5.65
CGNL1	cingulin-like 1	-5.71
HK1	hexokinase 1	-5.9
TNIP1	TNFAIP3 interacting protein 1	-5.9
ALPK1	alpha-kinase 1	-6.06
RHCG	Rh family, C glycoprotein	-6.08
RSPH10B	radial spoke head 10 homolog B (Chlamydomonas)	-6.11
OPRM1	opioid receptor, mu 1	-6.23
DNAH3	dynein, axonemal, heavy chain 3	-6.38
PZP	pregnancy-zone protein	-6.55
TIE1	tyrosine kinase with immunoglobulin-like and EGF-like domains 1	-6.62
SNAP91	synaptosomal-associated protein, 91kDa homolog (mouse)	-6.77
EMC1	ER membrane protein complex subunit 1	-7.06
CNTN4	contactin 4	-7.47
DCC	deleted in colorectal carcinoma	-7.55
SELENBP1	selenium binding protein 1	-8.25
LOC285857	uncharacterized LOC285857	-9.33
CR1	complement component (3b/4b) receptor 1 (Knops blood group)	-9.7